METEOR-Berichte

Mid-Atlantic Expedition 2003-2004

Cruise No. 60, Leg 1 – 5

November 11., 2003 – April 15., 2004
Kiel (Germany) –Funchal - Fort-de-France - Lisbon (Portugal)

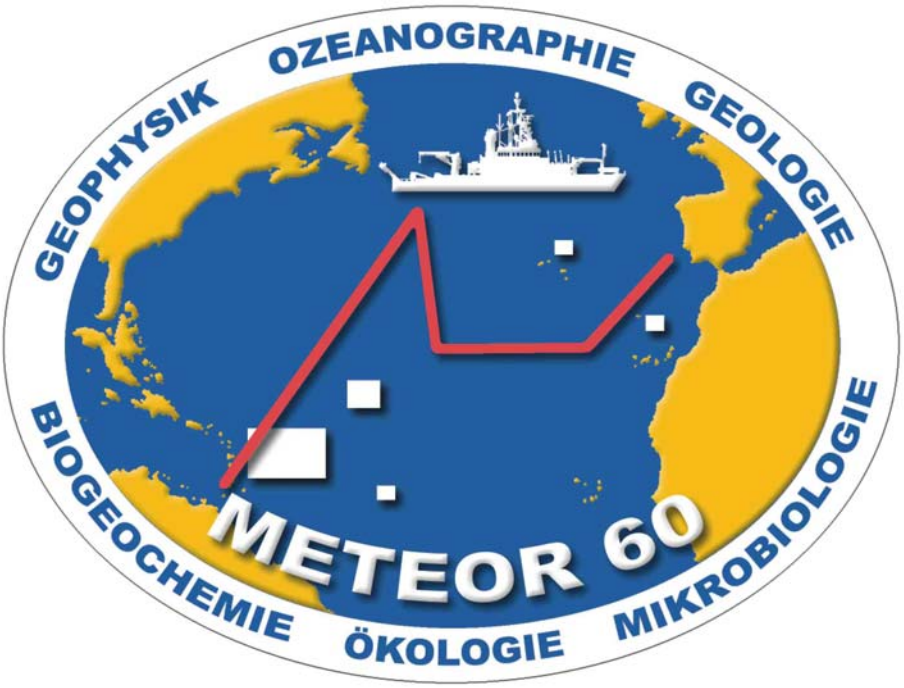

Autoren:
D. Wallace, B. Christansen, J. Phipps-Morgan, Th. Kuhn, U. Send,

Editorial Assistance:

Senatskommission für Ozeanographie der Deutschen Forschungsgemeinschaft
MARUM – Zentrum für Marine Umweltwissenschaften der Universität Bremen

Leitstelle Deutsche Forschungsschiffe
Institut für Meereskunde der Universität Hamburg

2011

The METEOR-Berichte are published at irregular intervals. They are working papers for people who are occupied with the respective expedition and are intended as reports for the funding institutions. The opinions expressed in the METEOR-Berichte are only those of the authors.

The METEOR expeditions are funded by the *Deutsche Forschungsgemeinschaft (DFG)* and the *Bundesministerium für Bildung und Forschung (BMBF)*.

The reports are available in PDF format from http://www.dfg-ozean.de/.

Editor:
DFG Senatskommission für Ozeanographie
c/o MARUM – Zentrum für Marine Umweltwissenschaften
Universität Bremen
Leobener Strasse
28359 Bremen

Authors:
Dr. Bernd Christiansen
Universität Hamburg
Institut für Hydrobiologie und
Fischereiwissenschaft
Zeiseweg 9,
D-22765 Hamburg / Germany
Telefon: +49(0)40-42838-6670
Telefax: +49(0)40-42838-6696
e-mail: bchristiansen@uni-hamburg.de

Prof. Dr. Jason Phipps Morgan
GEOMAR
Forschungszentrum für
Marine Geowissenschaften
Abt. Marine Umweltgeologie
Wischhofstr. 1-3
24148 Kiel / Germany
Telefon: +49(0)431-600 2272
Telefax: +49(0)431-600 2922
e-mail: jmorgan@geomar.de

Dr. Thomas Kuhn
Department of Economic Geology and
Leibniz Lab. for Applied Marine Research
Institute of Mineralogy Freiberg University of Mining and Technology
Brennhausgasse 14
D-09596 Freiberg / Germany
Telefon: +49/(0)3731-393398
Telefax: +49/(0)3731-392610
e-mail: kuhnto@mineral.tu-freiberg.de

Prof. Dr. Uwe Send
Institut für Meereskunde
FB1 – Ozeanzirkulation + Klima
- Physikalische Ozeanographie II -
Düsternbrooker Weg 20
24105 Kiel / Germany
Telefon: +49-431-600 4150
Telefax: +49-431-600 4152
e-mail: usend@ifm.uni-kiel.de

Prof. Dr. D.W.R. Wallace
Institut für Meereskunde
FB2 – Marine Biogeochemie
- Chemische Ozeanographie -
Düsternbrooker Weg 20
24105 Kiel / Germany
Telefon: +49-431-600 4200
Telefax: +49-431-600 4202
e-mail: dwallace@ifm.uni-kiel.de

Citation: Bernd Christiansen, Jason Phipps Morgan, Thomas Kuhn, Uwe Send, D.W.R. Wallace, RV METEOR, Cruise Report M60/L1, M60/L2, M60/L3, M60/L4, M60/L5, Mid-Atlantic Expedition 2003/2004, M60/1-5, 212 pp., DFG Senatskommission für Ozeanographie

ISSN 2195-8475

Table of Contents; Introduction

Table of Contents; Leg 1

Table of Contents; Leg 2

Table of Contents; Leg 3

Table of Contents; Leg 4

Table of Contents; Leg 5

Abstract

The Meteor 60 expedition started in Kiel on 11 November 2003 and ended in Lisbon on 15 April 2004. The expedition comprised 5 separate legs and covered a large region of the sub-tropical North Atlantic from the Azores and Madeira to the tropical western Atlantic. Leg 1 focussed on the ecology and biogeochemistry of seamounts in the eastern Atlantic in the context of the EU program OASIS (OceAnic Seamounts: an Integrated Study). Leg 2 comprised a detailed seismic and geophysical investigation of a propagating ridge segment at the Mid-Atlantic Ridge in cooperation with French scientists. Leg 3 was a multidisciplinary (geological, biological and chemical) investigation of the effects of hydrothermal circulation at the Mid-Atlantic ridge in support of the DFG SPP 1144 “From Mantle to Ocean: Energy, Material and Life Cycles at Spreading Axes”. Leg 4 was a physical oceanographic study of long-term variation of the thermohaline circulation in the western basin of the Atlantic in the context of the BMBF-CLIVAR program MOVE (Meridional Overturning Variability Experiment). Together with US investigators, calibration work was also conducted for GRACE (Gravity Recovery and Climate Experiment); and Leg 5 was a multidisciplinary (chemical/biological) investigation of CO_2 uptake and the biological pump in the water column of the North Atlantic sub-tropical gyre (DFG Collaborative Research Project SFB 460 “Dynamik Thermohaliner Zirkulationsschwankungen”).

Zusammenfassung

Die Expedition Meteor 60 begann am 11. November 2003 in Kiel und endete am 14. April 2004 in Lissabon. Die Expedition bestand aus 5 Fahrtabschnitten und deckte weite Teile der Region des subtropischen Nordatlantiks von den Azoren und Madeira bis zum tropischen Westatlantik ab. Fahrtabschnitt 1 beschäftigte sich mit der Ökologie und Biogeochemie von unterseeischen Bergen („Seamouts“) im östlichen Atlantik im Rahmen des EU-Programms OASIS (OceAnic Seamounts: an Integrated Study). Fahrtabschnitt 2 führte, in Kooperation mit französischen Wissenschaftlern, eine detailierte seismische und geophysikalische Untersuchung eines „propagating“ Rückensegments am Mittelatlantischen Rückens durch. Der Fahrtabschnitt 3 war eine multidisziplinäre (geologisch, biologisch und chemisch) Untersuchung des Effekts der hydrothermalen Zirkulation am Mittelatlantischen Rückens zur Unterstützung des DFG SSP 1144 “From Mantle to Ocean: Energy, Material and Life Cycles at Spreading Axes”. Fahrabschnitt 4 stand im Kontext des BMBF-CLIVAR Programms MOVE (Meridional Overturning Variability Experiment) und war eine physikalische Studie zu den längerfristigen Veränderungen der thermohalinen Zirkulation im westlichen Becken des Atlantiks. Darüber hinaus wurden zusammen mit amerikanischen Forschern Kalibrationsarbeiten für GRACE (Gravity Recovery and Climate Experiment) durchgeführt. Fahrtabschnitt 5 war eine multidisziplinäre (chemisch/biologisch) Untersuchung der CO2-Aufnahme und der biologischen Pumpe in der Wassersäule des subtropischen „Gyre“ im Nordatlantik (DFG Collaborative Research Project SFB 460 “Dynamik Thermohaliner Zirkulationsschwankungen”).

Organisation of the Cruise

R/V METEOR cruise No. 60 was divided into five individual legs (see Table I, Figure I), each of these with its own scientific focus. The grouping of the 5 separate legs into one expedition was more for geographical and logistical reasons associated with ports-of-call and associated transits. Each of these legs is the subject of a full report, and each individual report contains a detailed explanation of the research objectives for that particular leg.

Leg	Period	Ports	Chief Scientists
M60/1	11.11.2003 – 06.12.2003	Kiel (Germany) Funchal (Madeira)	Dr. B. Christensen
M60/2	09.12.2003 – 12.01.2004	Funchal (Madeira) Fort-de-France (Martinique)	Prof. Dr. J. Phipps Morgan
M60/3	14.01.2004 – 14.02.2004	Fort-de-France (Martinique) Fort-de-France (Martinique)	Dr. T. Kuhn
M60/4	16.02.2004 – 06.03.2004	Fort-de-France (Martinique) Fort-de-France (Martinique)	Prof. Dr. U. Send
M60/5	09.03.2004 – 15.04.2004	Fort-de-France (Martinique) Lisbon	Prof. Dr. D. Wallace

Table 0.1: Legs, Ports-of-Call and Chief Scientists of R/V METEOR cruise 60.

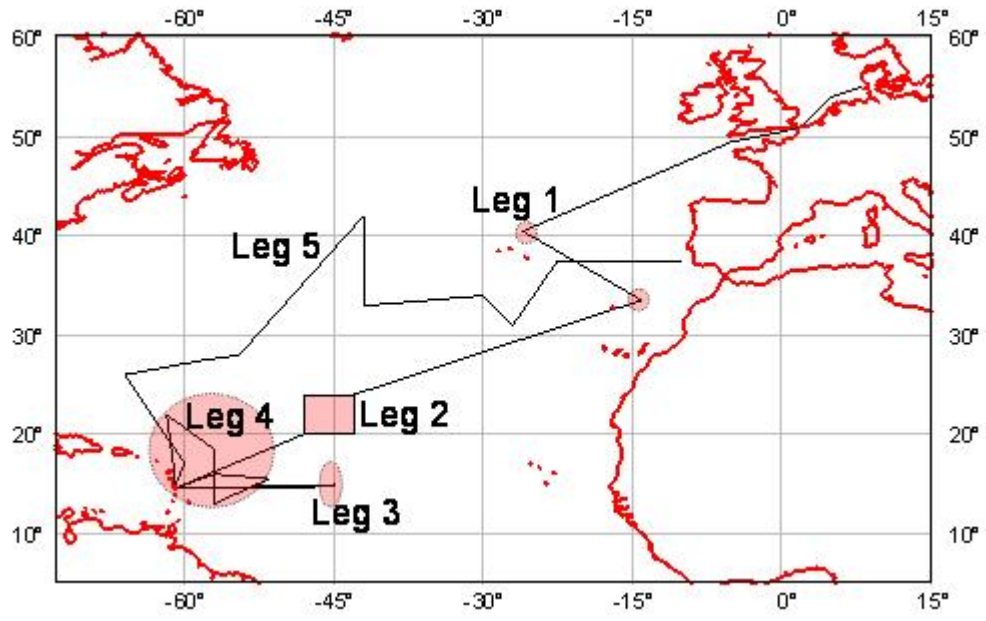

Figure 0.1 Overall schematic of the areas covered by the 5 Legs of Meteor Cruise 60.

METEOR-Berichte

OASIS

Oceanic Seamounts: an Integrated Study

Cruise No. 60, Leg 1

November 11 - December 06, 2003, Kiel - Funchal

B. Christiansen, T. Beck, B. Bett, D. Billett, M. Emelianov, M. Espino Caballero, T. Furey, K.-H. George, C. Gutiérrez Lobato, A. Henche, S. Hirch, B. Holscher, T. Horton, C. Joppich, F. José, K. Kiriakoulakis, R. Koppelmann, S. Laakmann, A. Lübben, L. Maçedo, D. Maier, B. Martin, A. Mendonça, S. Ruseler, P. Simonelli, T. Truscheit, R. Turnewitch, J. Ullgren, J. C. Vilas Español, S. Werk

Table of Contents; Leg 1

1.1 Participants M 60/1

Name	Task	Institution
Christiansen, Bernd, Dr.	chief scientist, zooplankton	UHH-IHF
Beck, Tim	macrofauna	FAU
Bett, Brian, Dr.	megafauna	SOC
Billett, Dave, Dr.	megafauna	SOC
Emelianov, Mikhail, Dr.	physical oceanography	ICM
Espino Caballero, Minerva	primary production, fluxes	ULPGC
Furey, Tom	moorings	NUIG
George, Kai-Horst, Dr.	meiofauna	DZMB
Gutiérrez Lobato, Carlos	primary production, fluxes	ULPGC
Henche, Annika	meiofauna	DZMB
Hirch, Stefanie	zooplankton	UHH-IHF
Holscher, Boris	hyperbaric experiments	TUHH
Horton, Tammy, Dr.	scavengers	SOC
José, Felix	physical oceanography	IMAR
Kiriakoulakis, Kostas, Dr.	biogeochemistry	ULIV
Koppelmann, Rolf, Dr.	zooplankton, hyperbaric experiments	UHH-IHF
Laakmann, Silke	benthos/lipids	UHB
Lübben, Andrea	biogeochemistry	URO
Maçedo, Luis, Dr.	physical oceanography	IMAR
Maier, Dominique	zooplankton	UHH-IHF
Martin, Bettina	zooplankton	UHH-IHF
Mendonça, Ana	primary production, fluxes	IMAR
Ruseler, Silke	biochemistry	UHH-IHF
Simonelli, Paolo	zooplankton	UHH-IHF
Turnewitch, Robert, Dr.	biogeochemistry	SOC
Ullgren, Jenny	physical oceanography	NUIG
Vilas Español, Juán Carlos	primary production, fluxes	ULPGC
Werk, Stephan	biogeochemistry	URO
Joppich, Christoph	meteorology	DWD
Truscheit, Thorsten	meteorology	DWD

Participating institutions

DZMB	Deutsches Zentrum für Marine Biodiversität, Südstrand 44, 26382 Wilhelmshaven, Germany
FAU	Friedrich-Alexander Universität Erlangen, Institut für Paläontologie, Loewenichstr. 28, 91054 Erlangen, Germany
ICM	Institut de Ciencies del Mar, CMIMA - CSIC, Grup d'Oceanografia Fisica, Passeig Maritim de la Barceloneta, 37-49, 08003 Barcelona, Spain
IMAR	IMAR/DOP, Departamento de Oceanografia e Pescas, Universidade dos Açores, 9901-862 Horta, Portugal
NUIG	National University of Ireland, Galway, Department of Oceanography, Newcastle Road, Galway, Ireland
SOC	Southampton Oceanography Centre, George Deacon Division for Ocean Processes, Waterfront Campus, European Way, Southampton SO14 3ZH, UK
TUHH	Technische Universität Hamburg-Harburg, Arbeitsbereich Meerestechnik 1, Laemmersieth 72, 22305 Hamburg, Germany

UHB	Universität Bremen, Postfach 330440, Leobener Str., NW 2, 28334 Bremen, Germany
UHH-IHF	Universität Hamburg, Institut für Hydrobiologie und Fischereiwissenschaft, Zeiseweg 9, 22765 Hamburg, Germany
ULIV	University of Liverpool, Dept. of Earth Science, Oceanography Laboratories, Bedford Street North, Liverpool L69 7ZL, UK
DWD	Deutscher Wetterdienst, Postfach 301190, 20304 Hamburg, Germany
ULPGC	Universidad de Las Palmas de Gran Canaria, Facultad de Ciencias del Mar, Campus Universitario de Tarifa, 35017 Las Palmas de Gran Canaria, Spain
URO	Universität Rostock, Institut für Aquatische Ökologie - Meersbiologie, Albert-Einstein-Straße 3, 18059 Rostock, Germany

1.2 Research Programme

The first leg of cruise M 60 aimed at physical, biogeochemical and biological sampling in the framework of the EU project OASIS (OceAnic Seamounts: an Integrated Study). OASIS is an interdisciplinary project and comprises 9 partners from 5 European countries. The project studies the functional characteristics of seamount ecosystems. Based on two case studies, OASIS will yield an advanced mechanistic understanding of the processes characterizing seamount ecosystems, and their influence on the surrounding ocean. The scientific knowledge gained, condensed in a conceptual ecosystem model, will be applied to outline a model management plan as well as site-specific management plans for the seamounts investigated.

The primary goal of OASIS, to provide a holistic, integrated assessment of seamount ecology, will be achieved by addressing the following main objectives: a) To identify and describe the physical forcing mechanisms effecting seamount systems. b) To assess the origin, quality and dynamics of particulate organic material within the water column and surface sediment at seamounts. c) To describe aspects of the biodiversity and the ecology of seamount biota, to assess their dynamics and the maintenance of their production. d) Modelling the trophic ecology of seamount ecosystems. e) Application of scientific knowledge to practical conservation.

The scientific programme included three main objectives:
1. Physical oceanography - Under this objective, the hydrographic processes that control the circulation, mixing and exchange of fluid in the vicinity of seamounts are addressed. These are key requirements for an understanding of the biogeochemical and biological processes, and they are essential for the design of an effective biogeochemical and biological sampling strategy. The tasks within this objective include in particular the measurement and modelling of the 3D current system and of vertical diffusivity in the near-bottom water layer.
2. Biogeochemistry - The organisms below the euphotic zone depend, with a few exceptions, on (particulate) organic material that has been produced in the surface ocean. During its descent to the seafloor this material is altered in many ways, for example by ingestion and egestion by pelagic animals, by microbial degradation or aggregate formation. Within the benthic mixed

layer, sedimentation and resuspension will strongly influence the availability of this material. All these processes will affect the nutritional value of the organic matter for organisms living at or close to the seafloor. The tasks within this objective study primary production, the export flux of organic material to deeper water layers, the quality of organic particles, their origin and exchange processes between sediment and water column.
3. Biology - Seamounts often accommodate enhanced stocks of commercially valuable species. Several hypotheses exist regarding how these stocks are maintained, e.g. by trapping of particles in Taylor columns, by enhanced primary production due to upwelling, or by trapping of the vertically migrating deep scattering layer fauna. This objective addresses the major faunistic groups (zooplankton, micronekton, benthos and fish) at seamounts and their interactions, with special emphasis on the bottom mixed layer fauna and the deep scattering layer. The objective is achieved through traditional sampling with multiple closing nets, epibenthic sledge and trawls, and with photographic and acoustic methods.

The studies were performed at two seamounts in the northeast Atlantic (see Figure 1.1), with a focus on the Sedlo Seamount north of the Azores. This seamount has a summit depth of ca. 750 m. Principally all parts of the seamount were sampled, from the base to the summit including the overlying water column. For comparison, samples were taken at a reference station outside the influence of the seamount.

Seine Seamount northeast of Madeira rises up to 170 m below the sea surface. Here, a few selected samples were taken, supplementing material from a former cruise.

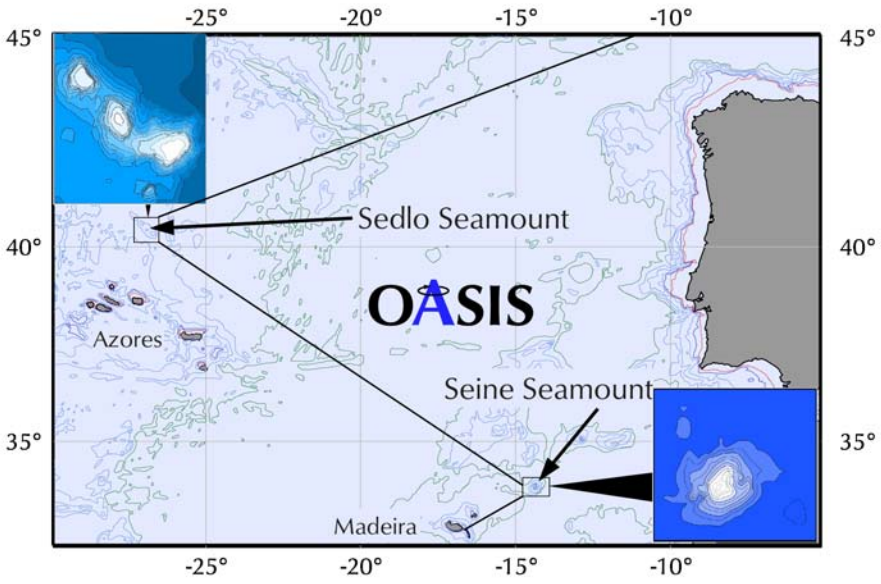

Figure 1.1: METEOR cruise M60/1: cruise track and study sites

A further goal of the cruise was to test a newly developed hyperbaric laboratory which is designed to study deep-sea organisms under in situ pressure.

1.3 Cruise narrative

After the last provisions were loaded, Meteor sailed from Kiel at noon on 11 November. We enjoyed the passage of Kiel Canal with cold, but sunny weather. The weather stayed calm in the North Sea, and all groups were busy to assemble their equipment and to set up the laboratories. At the western entrance of the English Channel a gale hit us with wind force 8 Bft and waves up to 8 m high which slowed our speed considerably. But the wind and the sea calmed down soon, and we could continue the preparations for the station work.

On 16 November a first series of test stations with the CTD was run which revealed some problems with the electrical connections. These could be fixed, and on 18 November Meteor arrived at our first study site, Sedlo Seamount. First, two CTD stations were run, and then a combined hydrographic/bathymetric survey was performed at the southeastern summit of the seamount which is the main area of interest for our studies. Parallel tracks were used for swath bathymetry with hydrosweep, and a grid of 5*3 CTD stations, each going to 1500 m depth, was used to sample hydrographic data and water for the analysis of particulate organic matter (Figure 1.2). During the survey, four moorings carrying current meters which had been deployed on a cruise with the Portuguese research vessel Arquipélago in summer 2003, were recovered successfully. A baited amphipod trap was deployed on the summit of Sedlo Seamount on 21 November.

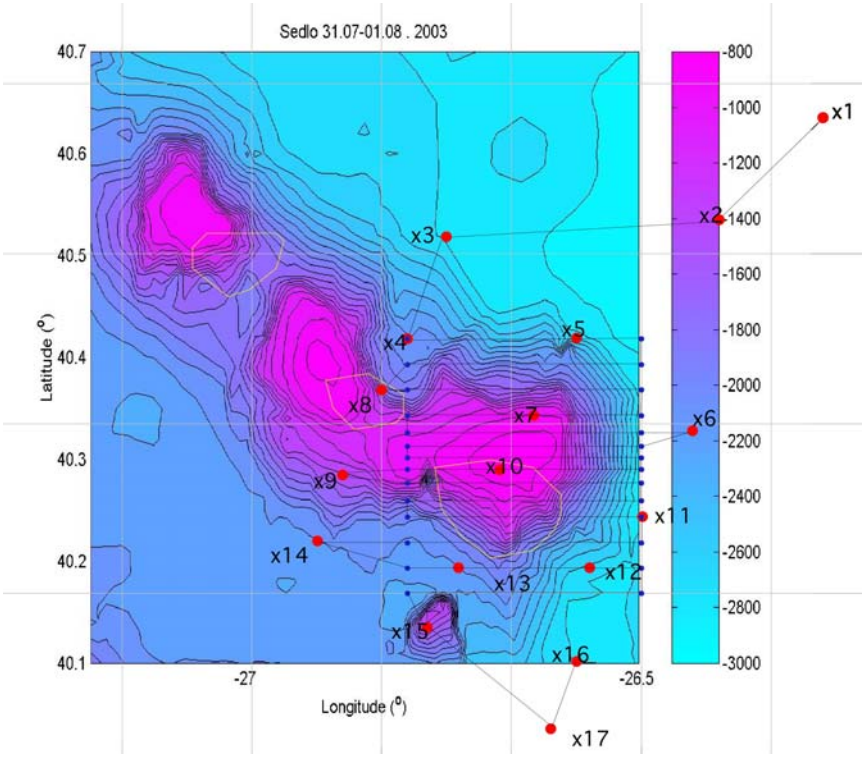

Figure 1.2: Meteor cruise M60/1: Bathymetric track and hydrography stations

The bathymetric survey which was sometimes impaired by high swell, was finished on 21 November in the evening, and a first haul with the 1m2-double-MOCNESS was conducted, yielding stratified samples from 1000 m water depth to the surface. Station work continued with further MOCNESS hauls and CTD-rosette casts, including SAPS (stand-alone pump systems), for the analysis of primary production, nutrients, dissolved and particulate organic matter. On 22 November the WASP (wide angle seabed photography) was lowered to the summit of Sedlo Seamount for the first time. The distance to the seafloor was kept at approximately 3 m and was monitored by an acoustic telemetry system. The system produced still images and one hour of digital video film. Surprisingly, the summit plateau showed bare rock in many places, with only a few patches of sediment in between, sometimes with bolders and gravel, all this pointing to strong currents sweeping over the top of the seamount. After the WASP, two multiple corer hauls were conducted, which both failed.

Two further WASP hauls on 23 November at ca 1000 m water depths similarly showed bare rock in most places.

On 23 November in the morning the amphipod trap was released and recovered. The catch was surprisingly small, with only a few amphipods, but several fishes. A fifth current meter mooring was successfully recovered after the amphipod trap.

Further CTD casts, MOCNESS tows with both the 10 m2 and the 1m2-double systems, and WASP transects were performed at different locations and depths in the area of Sedlo Seamount until 30 November. Benthic sampling during this time included multiple corer, box corer, amphipod trap, rock dredge and epibenthic sledge. The epibenthic sledge haul at the base of the seamount failed because both the epibenthic and the suprabenthic nets were damaged. The rock dredge, towed at the flank of the seamount, caught a few sessile organisms like crinoids and corals.

Station work at Sedlo Seamount was finished on 30 November, and Meteor sailed to our second study site, Seine Seamount, where we arrived on 2 December in the afternoon. Strong wind and high swell did not allow for using towed gear, so we started with several CTD/rosette casts. On the following day, the weather and sea conditions improved considerably, and one 10 m2-MOCNESS haul (down to 1000 m) and two hauls with the 1m2-double-MOCNESS (down to 4170 m) could be performed.

The remaining time at Seine Seamount was mainly used for benthic sampling, including WASP transects, multiple corer and box corer. The WASP videos showed that the summit plateau was

covered with sediment. At the edges, some patches with flat rock could be seen. An epibenthic sledge haul on the summit plateau of the seamount, at a water depth of 170-180 m, caught large numbers of megafaunal organisms, like sea urchins, sea stars, crustaceans, worms, but also benthopelagic fish like snipe fish, which are typical for seamounts.

Meteor left Seine Seamount on 5 December in the afternoon and sailed to Funchal, Madeira, where we arrived the next day in the morning.

1.4 Preliminary Results

1.4.1 Bathymetry and hydrography

(B. Christiansen, M. Emilianov, T. Furey, F. José, L. Macedo, J. Pelegri, M. White)

Bathymetry

In addition to existing maps, hydrosweep and parasound were used to gain topographic information of the two study sites. Both sites have been poorly studied in this respect. The detailed measurements focussed on the bottom topography in the vicinity of the sampling stations and are a prerequisite for sampling the benthos and the near-bottom water layer.

The hydrosweep track at Sedlo Seamount is shown in Fig. 1.2. We focused on the southeastern summit of the seamount, which is the main area of interest for the OASIS project. High swell sometimes impaired the survey. The resulting map is shown in Fig. 1.3, showing a rather flat summit plateau at ca 750 m and steep flanks to the north, east and south. Due to the unfavourable weather conditions at Seine Seamount, no hydrosweep data from this site could be used.

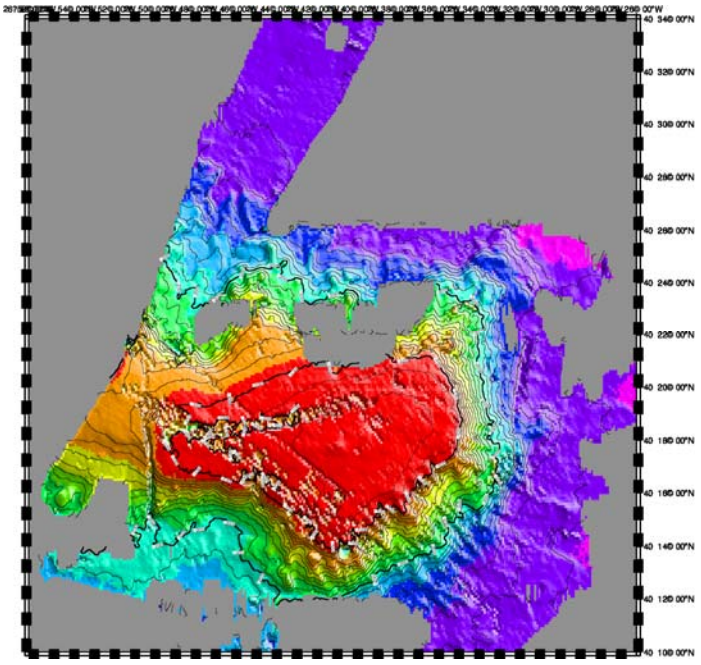

Figure 1.3: Bathymetric map of the Sedlo Seamount southeastern summit based on the hydrosweep survey during M 60/1.

Hydrography

Moored current meters and ADCP as well as CTD profiles of temperature and salinity were used to measure the flow field, the structure of the benthic mixed layer (BML) and the vertical diffusivity.

The main Sedlo mooring array, consisting of 5 moorings and 18 current meters (CMs), was recovered during cruise Meteor M60/1 (Figure 1.4 and Table 1.1). All but one of the CMs recorded data and generally the data quality was good. Target depths at the mid flank mooring sites (1400 m) were easily achieved due to the steep slopes of the seamount. A range of water depths from 1406-1548 m resulted and hence the CMs were not all at the same depth levels as would be hoped, but instead within a range of about 150 m. This would appear to be reasonable.

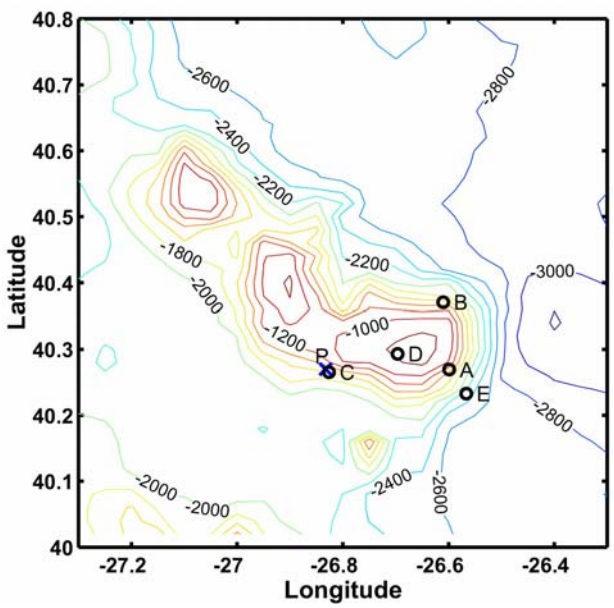

Figure 1.4: Location (o) of the CM moorings deployed on Sedlo seamount between July and December 2003. The cross (x) indicates the position of the Pilot mooring deployed between March and July 2003 close to location C in the main array.

Table 1.1: Location, water and CM depths for the main Sedlo mooring array. July-Dec, 2003.

	Latitude North	Longitude West	Depth (m)	Current meter Depths (m)
Moor E	40° 13‘ 58“	26° 34‘ 00“	2242	913, 2215, 2235
Moor D	40° 17‘ 35“	26° 41‘ 47“	780	773,753
Moor C	40° 15‘ 53“	26° 49‘ 34“	1548	885, 1445, 1521, 1541
Moor A	40° 16‘ 10“	26° 35‘ 56“	1406	840, 1404, 1463, 1483
Moor B	40 27‘ 14“	26° 36‘ 36“	1460	870, 1374, 1432, 1453

Some of the basic results shown by the measurements at Sedlo Seamount are detailed below.

Current measurements at Sedlo

Data return from the Sedlo array was good. Initial analysis suggests that a weak mean background flow impinging on the seamount chain was from the west or south-west. The stronger mean currents found to the north and SW of the SE summit (Figure 1.5) would support this view, given that local acceleration of a steady flow would be to the left of the seamount looking downstream. This steady flow, together with any trapping and intensification of diurnal

tides, would drive an anti-cyclonic (clockwise) flow around the seamount. The very weak mean flows found at the SE flank might correspond to a stagnant region expected from the formation of a Taylor Column over the seamount due to a westward impinging flow. Theoretical considerations have suggested a Taylor Column might form over Sedlo seamount. This was also confirmed from vorticity measurements based on the triangle of 3 mid flank moorings at a level close to the summit depth. Daily mean vorticity estimates showed negative values for most of the measurement period (Figure1.6).

Currents at the depth level of the summit were moderate in strength at all moorings, but with large mesoscale variability present. At the summit mooring, however, the currents close to the summit depth were stronger and more polarised, suggesting that some bottom trapped residual motion was present. Tidal analysis suggested that there was some intensification of tidal motions, particularly at the sub inertial diurnal period. This amplification (by a factor of 4), however, was an increase from a very small background value f less than 1 cms-1. Flows below 1370 m depth are extremely weak, surprisingly so. For a large part of the time (~40 %) the currents were below the threshold of the current meter rotors, even for the CMs close (7 m) from the seabed.

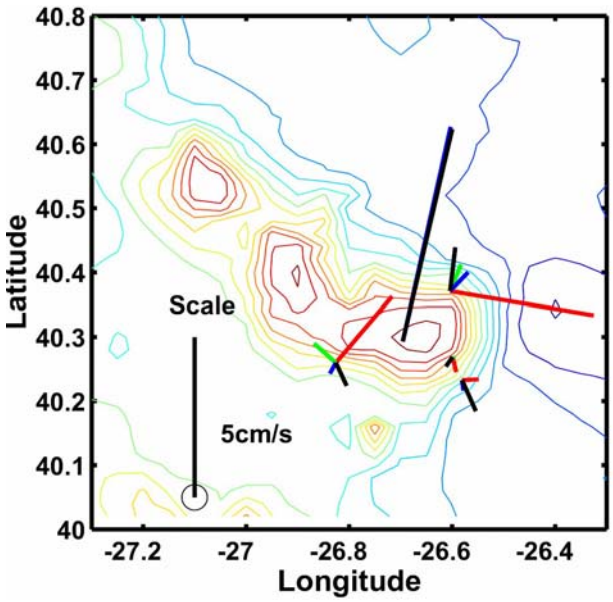

Figure 1.5: Mean current vectors for measurements between July and December 2003. Vector colours represent particular levels – Black – 8 mab, Blue – 30 mab, Green – CMs between 1370-1540 m depth and Red – CMs between 800 - 900 m depth.

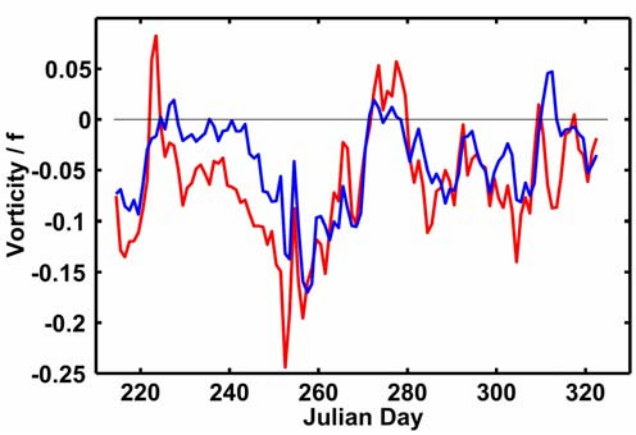

Figure 1.6: Time series of daily mean vorticity (normalised by f) estimated for the triangle of CMs at the level just below the summit depth (840-920 m) using (red) moorings A, B and C (all mid flank) and (blue) using deep mooring E instead of mooring A.

Water masses and flow from CTD and ADCP data.

Figure 1.7 shows the location of the hydrographic stations taken over the Sedlo seamount during the R/V Meteor M60/1 cruise (18 to 21 November 2003), superimposed on the bathymetry. A total of 17 Conductivity-Temperature-Depth (CTD) stations were taken, from deep waters relatively far from the seamount (stations 1 and 2) to the area surrounding the seamount's eastern summit (stations 3 through 17). At each station temperature, salinity, depth, and dissolved oxygen were measured down to near the sea floor.

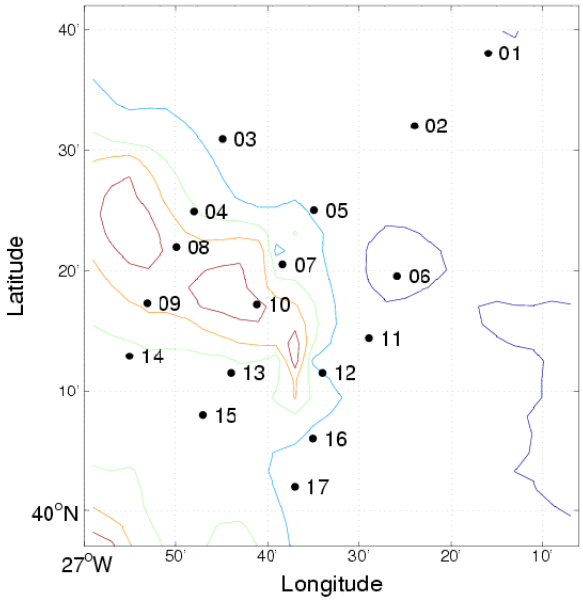

Figure 1.7: Location of hydrographic stations over Sedlo seamount during R/V Meteor M60/1 cruise.

The temperature and salinity data from all stations is presented as a T-S diagram in Figure 1.8

(left), with density lines superimposed. North Atlantic Central Water (NACW) is present down to densities of 27.3 (at approximately 700 m) and further deep we find North Atlantic Deep Water (NADW) in all stations. We also found the existence of Mediterranean Water (MW) in most stations, though it was absent in the westernmost stations (3, 4, 8, 9, and 14). This is clear from the T-S diagrams for each individual station shown in Figure 1.8 (right), where MW clearly shows up as a subsurface salinity maximum. The blocking of MW flow by the seamount is a remarkable feature that, to our knowledge, has not been previously reported.

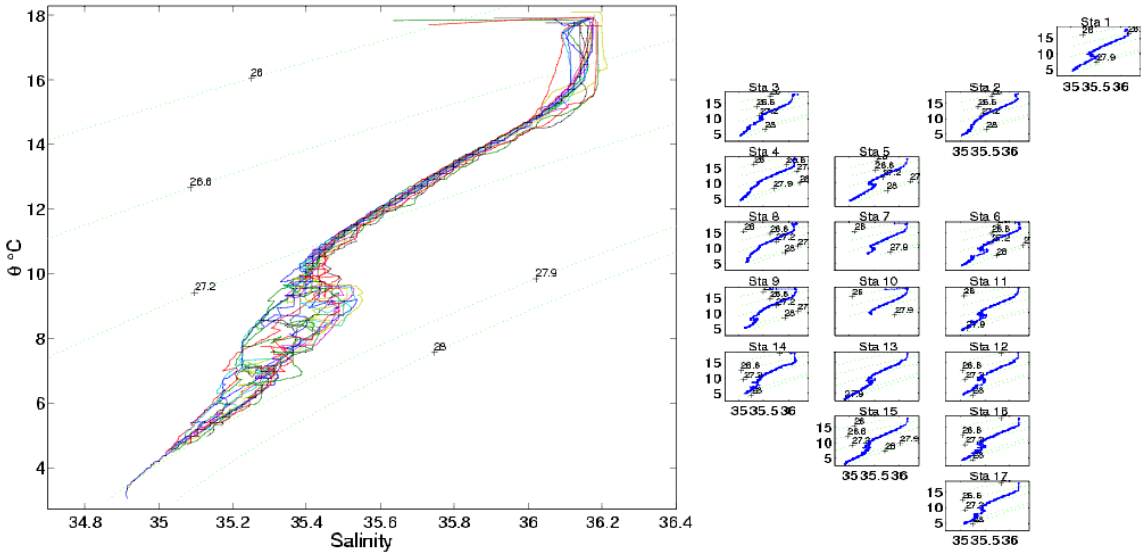

Figure 1.8: Left: T-S diagram for all stations. Right: Individual T-S diagrams per station.

The data obtained from the CTD stations is used to view the distribution of the measured/inferred variables both on horizontal and vertical sections. Figures 1.9-1.11 illustrate the distribution of temperature, salinity, potential density, dissolved oxygen, buoyancy frequency, and dynamic height (relative to 1400 m) at 50 m, 400 m, and 1400 m depths. All properties exhibit alternating bands with maximum/minimm values around the seamount summit, that may be indicative of some seamount control. From the dynamic heights we may calculate the geostrophic velocity fields, these being of order 0.1 m s-1 at 50 m depth, and one order of magnitude less at 400 m depth.

At 1400 m depths, which is the main level of MW propagation for the area (Mauritzen et al., 2001), there appears to be a east-west separation that may be related of the observed blocking of MW propagation by the seamount. This is also the depth of the seamount summit so its effects may be more noticeable.

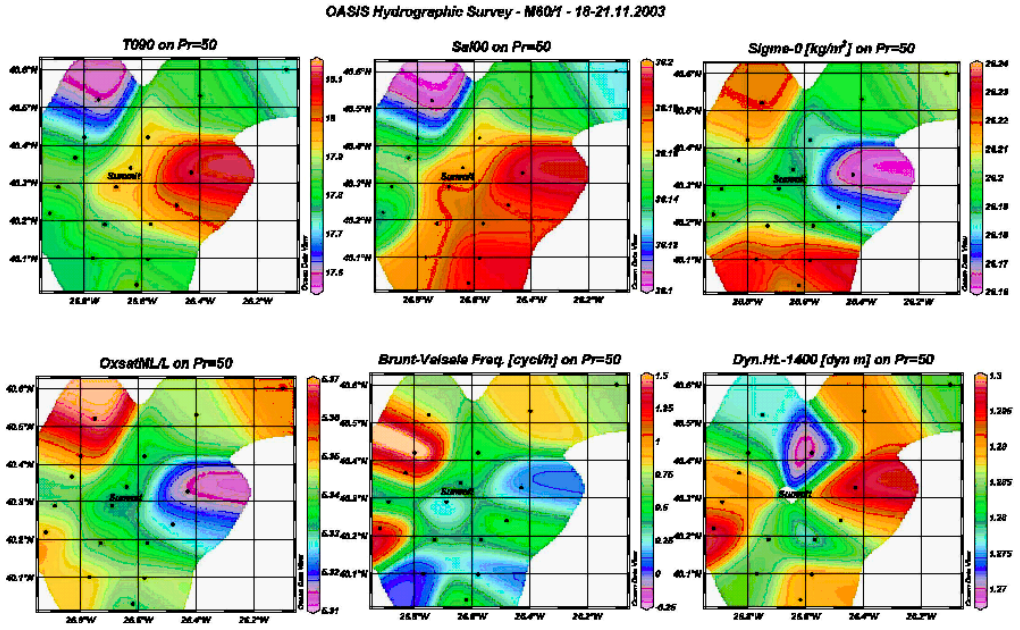

Figure 1.9: Temperature, salinity, sigma-theta, dissolved oxygen, buoyancy frequency, and dynamic height (relative to 1400 m) at 50 m depth during the M60/1 cruise.

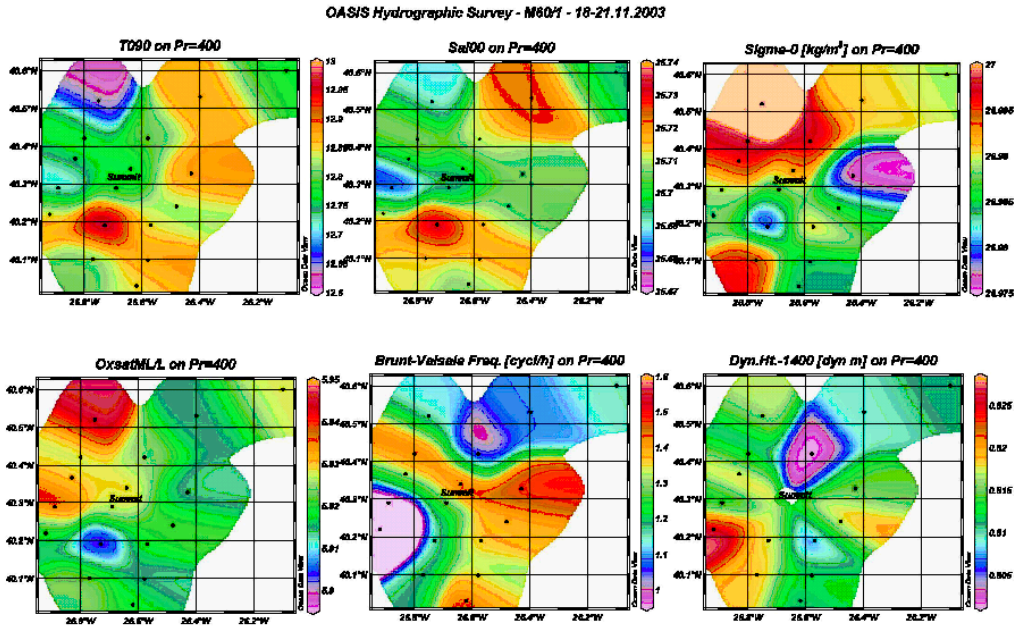

Figure 1.10: Temperature, salinity, sigma-theta, dissolved oxygen, buoyancy frequency, and dynamic height (relative to 1400 m) at 400 m depth during the M60/1 cruise.

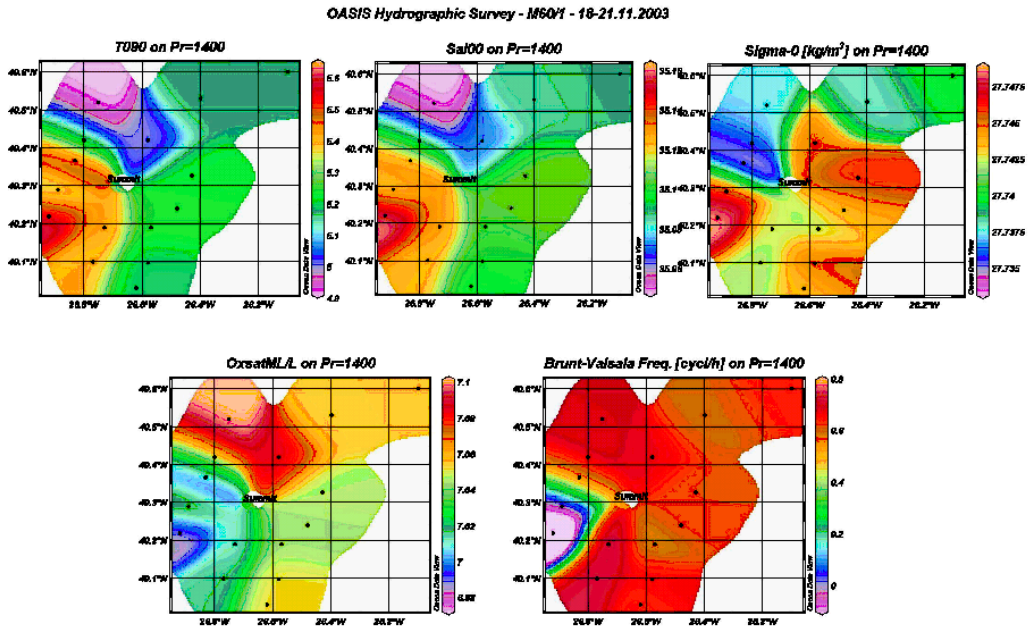

Figure 1.11: Temperature, salinity, sigma-theta, dissolved oxygen, and buoyancy frequency at 1400 m depth during the M60/1 cruise.

During the cruise we also measured the horizontal velocity field with the ship's Acoustic Doppler Current Profiler (ADCP). Figure 1.12 illustrates the path followed by the ship (dashed white line) and, as an example, the near-surface (24 m depth) velocity field interpolated over a regular grid. The color code corresponds to the bottom depths. The velocity field is available down to the sea floor although our analysis shows that it becomes less accurate with depth.

The surface flow pattern is quite complex, with a remarkable southward flow in the western portion and some significant northward flow in the southeastern corner. Within the domain there appear to be alternating bands of flow with different directions that may, or may not, be associated to the presence of the seamount. Further research is necessary to find out if these bands result from the interaction of the background flow (including the tide) with the seamount.

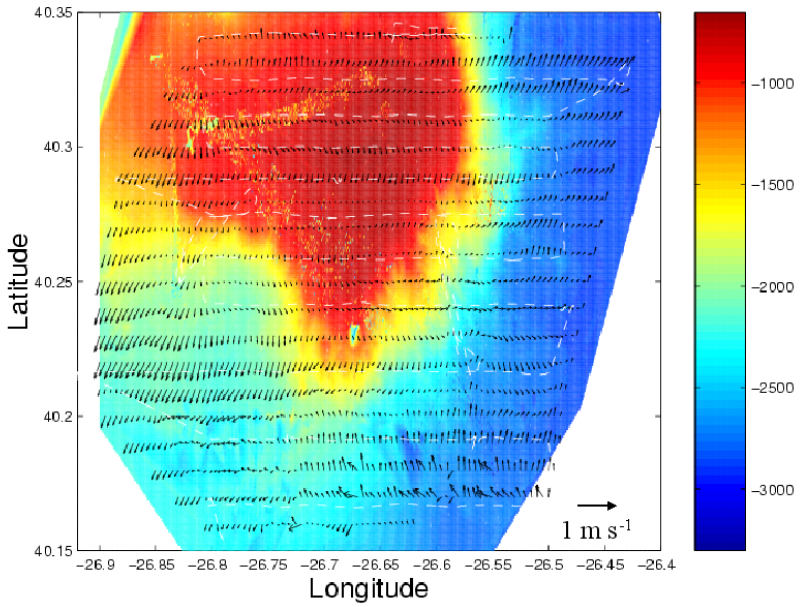

Figure 1.12: Velocity field at 24 m depth as obtained from the ADCP on board the R/V Meteor during the M60/1 cruise.

1.4.2 Biogeochemistry

(J. Aristegui, J.C. Vilas Español, K. Kiriakoulakis, A. Mendonça, S. Werk)

Filter samples were taken for SPM, POC, PN, chlorophyll and 234Th-analyses from the CTD. In general 7 depths of each station were sampled, 4 in the upper water layer down to 300 meters depth, and 3 in the mid water-layer and near the bottom. At the Sedlo seamount stations A, B, C, D, F, X3 and X13, (see station plan and Figure 1.2) and at Seine seamount one station located between stations F and E was sampled (water depth 3500 m). For primary production measurement, water samples were incubated for 24 h under ambient light conditions representing different depths.

Particulate material has also been collected on pre-combusted (400°C; >4 h) GF/F filters (293mm diameter) using SAPS (Stand-Alone Pumping Systems; Challenger Oceanic). During Meteor 60/1, five stations were at (or close to) the Sedlo Seamount (summit, slopes, between the peaks and far away; Fig. 1.13) and there was one station sampled at the Seine Seamount (SW slope; Fig. 1.14). The sampling depths were at 50 m (in the photosynthetic layer) at 15-20 m above bottom (mab; in the benthic boundary layer) and at various intermediate depths (200-1200 m). Most of these intermediate stations were close or within the Mediterranean Outflow Water (MOW) as determined from previous CTD profiles. The objective of sampling MOW was not always met, as its depth varied at each station and it was not was not always present.

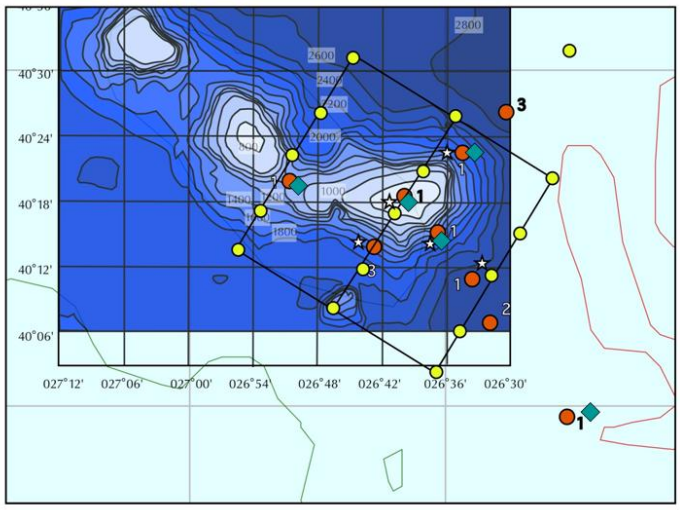

Fig. 1.13: Sampling of the Sedlo Seamount. Green diamonds indicate the major stations sampled using SAPS during cruise Meteor 60/1.

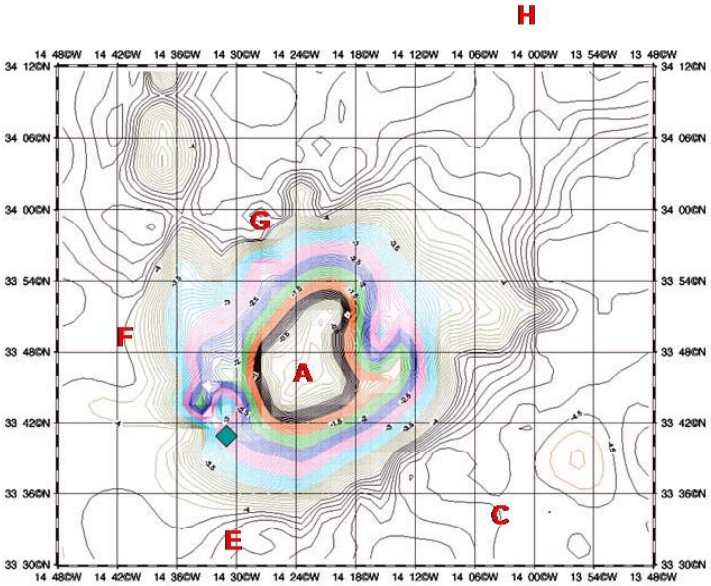

Fig. 1.14: Sampling of the Seine Seamount. The green diamond indicates the SAPS station sampled during cruise Meteor 60/1 (Nov-Dec 2003).

The pumps were deployed on the CTD wire, together with the CTD and were operated at the chosen depths for two hours. On recovery, the SAPS filters were partitioned for measurement of 234Th (URO; ~25% of filter) organic matter (POC, TN, lipid, pigment) and isotopic composition (□13C and □15N). CTD water from the same deployment was collected and filtered (GF/F; 25mm diameter) from the comparable depths to the SAPS. In all cases but one the SAPS pumps functioned correctly, however during the last deployment of the Meteor 60/12 cruise on the slope of the Seine Seamount, the drift of the ship led the shallow (50 m) pump to exit the water prior to the completion of the two-hour sampling period. Fragments of the deep-sea coral Madrepora oculata were collected from a dredge at the Sedlo Seamount. All samples were stored at -80° C.

Community Production (Pg, Pc) and Respiration (R)

Figure 1.15 illustrates the vertical distribution of gross production (Pg), net community production (Pn) and dark community respiration (Rd) around Sedlo seamount. Very low Pn (negative values) were measured, as expected, during winter time in Sedlo. For comparison, during a summer cruise on Discovery, Pn was near metabolic equilibrium (Pn in the water column close to 0). Rd presented de highest values in Sedlo during winter.

No evidence of Chl-a accumulation was observed around Sedlo Seamont (Figure 1.16). Seamount effects are, however, difficult to identify, since the seasonal or regional variability, may mask the mesoscale variability induced by the seamounts.

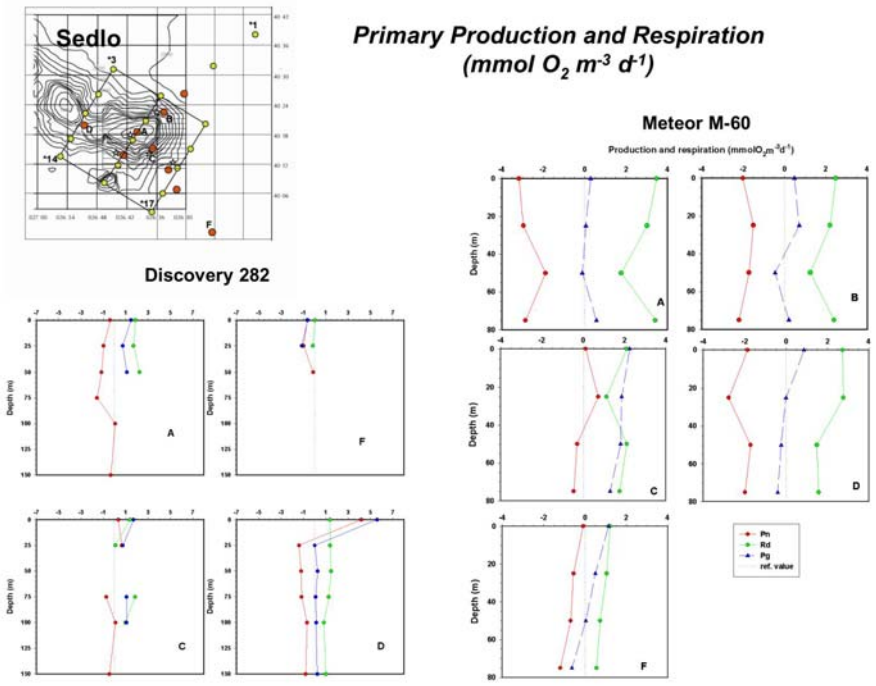

Figure 1.15: Primary production and respiration (ULPGC) at Sedlo seamount from M60 and D282.

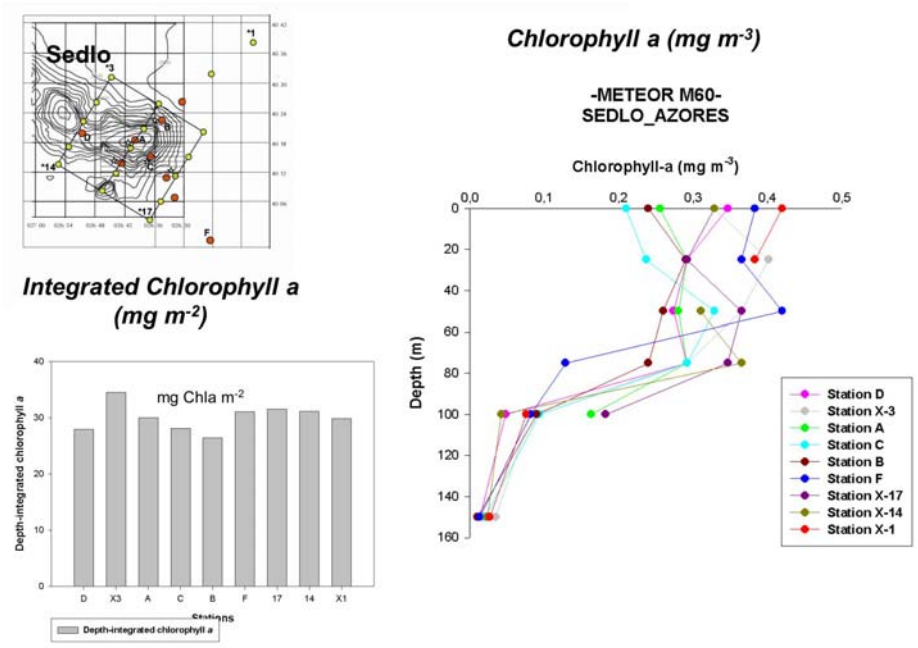

Figure 1.16: Chlorophyll a at Sedlo from M60 (ULPGC).

Preliminary lipid results of SAPS filters

Some preliminary results from lipid analyses at Sedlo are presented here. Specifically, the 23 most abundant lipids (> 90% of total extractable lipids) have been quantified in the shallow (50 m) samples from selected sites of the Sedlo Seamounts (Figure 1.17). These include a range of saturated, mono-unsaturated and poly-unsaturated fatty acids (PUFAs) of carbon number C14 to C22, sterols (C27 to C30) and C37 alkenones. In all samples the C14 and C16 fatty acids were the most abundant compounds and sterols were dominated by the C28□5,22 and C27□5 homologues. Sedlo (Autumn/Winter 2003) site C (edge of SE slope) had no PUFAs when compared with the summit (Figure 1.17). In Sedlo the concentrations of lipids were very similar between the two sites.

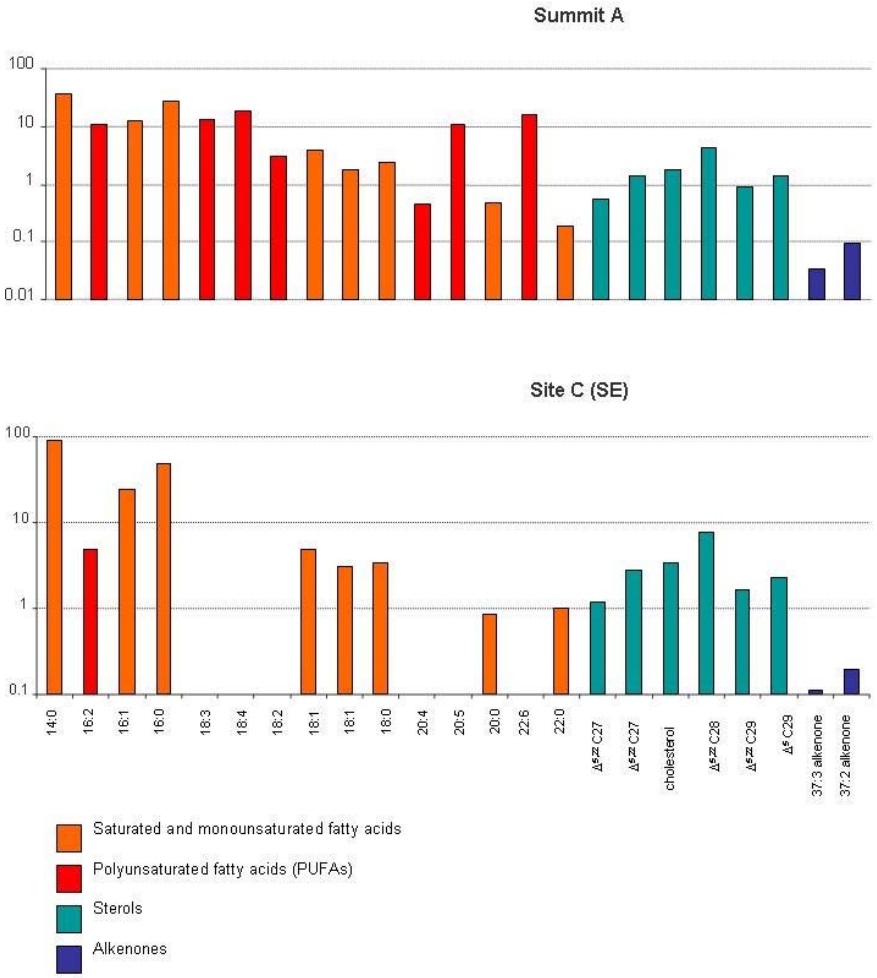

Figure 1.17: Preliminary lipid results from Sedlo Seamount (M60, autumn/winter 2004; 50 m).

234Th/238U results

CTD data during November-December 2004 showed a surface mixed layer in the top 100 m. Below there was a decrease in temperature and salinity. As in spring 2003 there was a signal of Mediterranean water, which was more pronounced at Seine Seamount at a depth of about 1200 m, but less clear on Sedlo. Initial 234Th/238U results from Seine Seamount (M60/1) showed a disequilibrium in the surface water column which seems to last for more than 1000 m (Figure 1.18h). Usually 234Th and 238U gain equilibrium between 200 – 300 m. A disequilibrium in the deep water column could not be seen with the same clarity as on on a previous cruise (Poseidon 295 in spring 2003). On Sedlo Seamount the summit shows a 234Th/238U disequilibrium from the surface down to about 200 m (Figure 1.18c). Interestingly, disequilibrium occurs again 150 m above bottom (water depth ~600 m). At the surrounding sites surface disequilibria have their maximum at a depth of about 50 m. Once again radioactive disequilibria can be found in the deep water column at several locations (Figures 1.18 b,d,e,f,g). This effect seems to focus on the base around the southeastern summit. This might be generated by resuspended material from the slopes of the seamount.

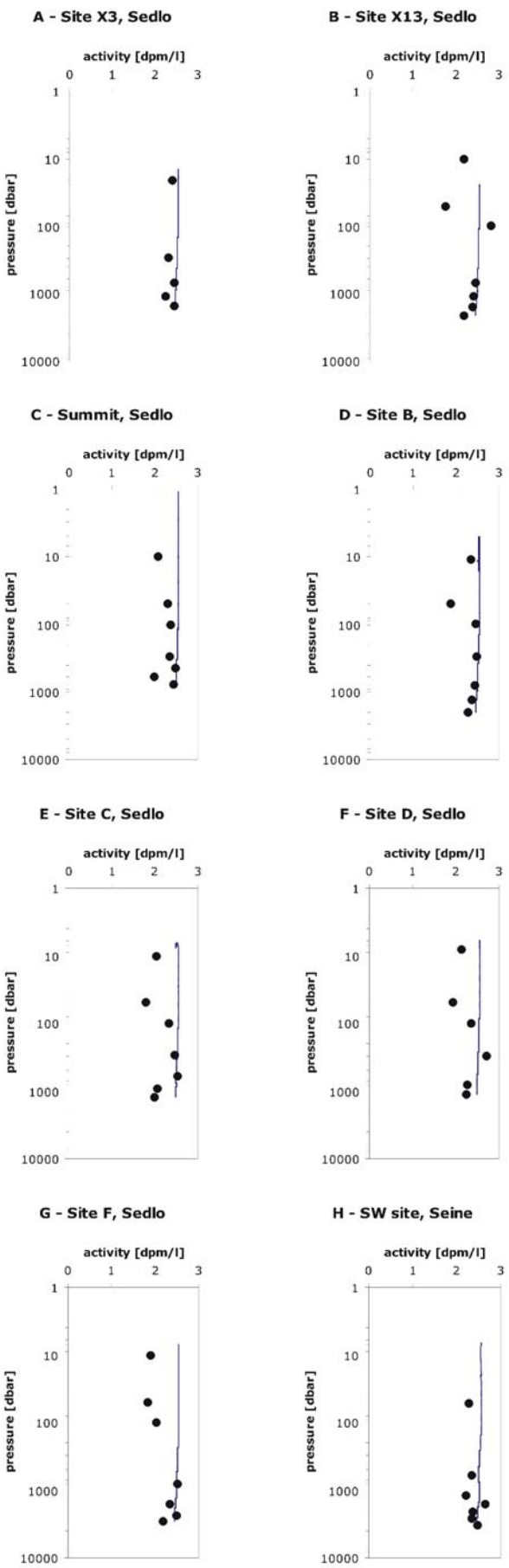
A - Site X3, Sedlo
B - Site X13, Sedlo
C - Summit, Sedlo
D - Site B, Sedlo
E - Site C, Sedlo
F - Site D, Sedlo
G - Site F, Sedlo
H - SW site, Seine
activity [dpm/l]
0
1
2
3
pressure [dbar]
1
10
100
1000
10000

Figure 1.18: Profiles of activity of total thorium at the different locations above and around Sedlo and Seine Seamount in November/December 2003. The solid lines show the distribution of uranium activity.

1.4.3 Biology

(T. Beck, B. Bett, B. Christiansen, K.-H. George, S. Hirch, B. Martin)

Zooplankton distribution at two seamounts in the NE Atlantic

Introduction

The maintenance of enriched biomass of benthopelagic fish at seamounts, and the concentration of commercially used fish around seamounts has been reported frequently (Hubbs, 1959; Parin et al., 1997; Rogers, 1994; Uiblein et al., 1999). However, the origin of available food to sustain the seamount-associated communities in the inherently nutrient impoverished surrounding open ocean is still in discussion (Nellen, 1973; Parin et al., 1997).

Two hypotheses for this question can be found in the recent literature:
1.) Due to the increased biomass of planktonic organisms found over several seamounts an enhanced primary production as a result of upwelling has been postulated. But direct evidence of this causal connection is weak (Dower and Mackas, 1996; Genin and Boehlert, 1985; Mouriño et al., 2001).
2.) An alternate hypothesis to explain the maintenance of seamount-bounded benthos organisms and fish populations is the nutritional input from the surrounding open ocean. The mechanism for that can be advection and retention of organisms due to altered flow field in the vicinity of elevated bottom topography, as well as interception with the vertically migrating sound-scattering layer (SSL) (Hesthagen, 1970; Rogers, 1994).

Our former studies at the Great Meteor Seamount support the latter theory that diurnally migrating zooplankton is getting trapped over shallow topography. We found out that especially euphausiids and calanoid copepods of the genus Pleuromamma constituted the main part of the bottom-near zooplankton above the summit (Martin and Nellen, 2004). These organisms could also be detected in the stomachs of seamount associated benthopelagic fish (Fock et al., 2002)

The study will be based on the hydrographical data gathered during the cruise concerning the main current directions and the possible existence of Taylor columns as well as potential upwelling. Moreover, it will take into consideration the 'Meteor Seamount Model' (Beckmann and Mohn, 2002), which describes the behaviour of passive particles as well as vertically migrating organisms in the flow field of the Taylor column over the summit at the Great Meteor

Seamount. The development of a similar model for the 2 mounts under investigation is planned by the participating oceanographers.

To understand the planktonic community structure as well as trophic processes in seamount-biocoenoses it is essential to determine whether there exists (A) an autochthonous plankton community or whether the occurring plankton is of (B) oceanic origin. Consequently, it is to analyse whether the food web on the seamount is controlled by (A) or (B).

For that purpose our sampling was designed to cover oceanic stations on the luff-side, and seamount-influenced stations above the summits, and above the lee-ward slopes of the mounts. Special attention is paid to the role of the DSL as a link between the euphotic zone and the seamounts. The influence of the DSL is assumed to vary between the areas under investigation because of the different summit heights of the mounts. To detect vertical migration and trapping effects the sampling has been carried out at night as well as at daytime. It is known that scattering layers over seamounts show significant diel variations that suggest changes in biological activity (Wilson and Boehlert, 1990). To detect the dynamics as well as the relative biomass of sonic scatterers acoustic devices like echo sounder and ADCP have been employed throughout the cruises.

Methods

During the cruise on R.V. Meteor in November/December 2003 to Sedlo and Seine seamount zooplankton was sampled at 12 stations with a 1m2-Double- MOCNESS (Wiebe et al., 1985) and at 3 stations with a 10m2-MOCNESS (Table 1.2). The 1m2-Double-MOCNESS was equipped with 19 nets of 0.333 mm mesh size and one net of 0.100 mm, the 10 m2 MOCNESS with 6 nets of 1.6 mm mesh size. The nets can be opened and closed sequentially. Environmental data as temperature, conductivity, and pressure were contiually sent to the ship and recorded. The water column was traversed by stratified tows. For biochemical analyses, discrete layers were fished horizontally in 50 and 300m depth, and above the bottom. The filtered volume was calculated by a flow-meter. To investigate diel vertical migrations, i.e. the movement of the DSL, hauls with the 1m2-Double-MOCNESS from the upper 1000 m were performed during day and night. At Sedlo seamount stations above the eastern summit, east and west of this summit (Figure 1.19) as well as out of the influence of the seamount (far field) were sampled. The 10m2-MOCNESS was used to sample micronekton at the eastern and western slopes.

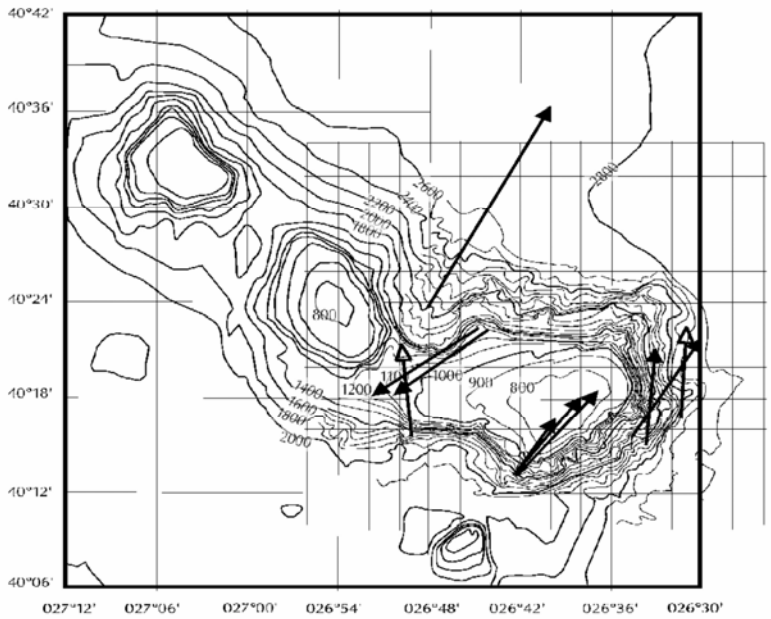

Fig. 1.19: MOCNESS stations at Sedlo seamount (the far field stations are not shown). Arrows with black arrowheads show the tracks of 1m^2-Double-MOCNESS, white arrowheads show the tracks of 10m^2-MOCNESS.

At Seine seamount a haul with the 10m2-net was performed at the western slope (Fig. 1.20). A day haul above the summit as well as a night haul at the south-western slope were conducted with the 1m2-Double-MOCNESS (Fig. 1.20). The latter partially failed due to entangling of most of the nets. The samples to be used for determination of wet weight and taxonomic composition were fixed in 4% formaldehyde-in-seawater on board the ship. At the university's laboratory biomass was measured as wet weight standardized to gram per 100m2 water volume. The organisms are going to be identified according to taxonomical classes, crustaceans to orders, some taxa to species level, and subsequently enumerated.

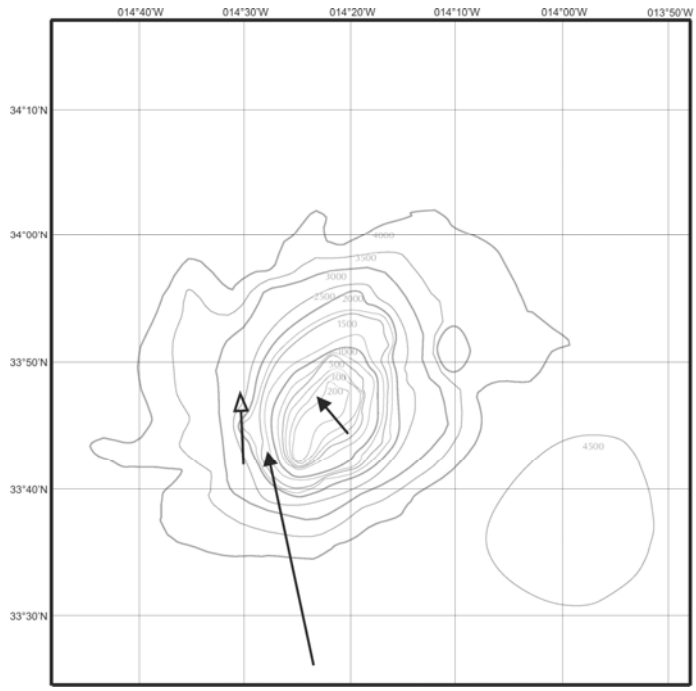

Fig. 1.20: MOCNESS stations at Seine seamount. Arrows with black arrowheads show the tracks of 1m2-Double-MOCNESS, white arrowheads show the tracks of 10m2-MOCNESS.

For further analyses of the scattering layers the data of the ship mounted 38 kHz ADCP and the echo sounder were recorded. Due to a breakdown of the 75 kHz ADCP data of this device cannot be used.

First results

The biomass of the organisms smaller 2 cm which were caught with the 1m2-double-MOCNESS are shown in Figure 1.21. Comparing the day and night samples, a reallocation of zooplankton, which would point to diel vertical migration of animals of this size could not be detected. At Sedlo highest biomass was found at the far field station at night time, lowest above the summit. The amount of zooplankton caught during day time above Seine was even lower, which points to an impoverished zooplankton fauna above the summits of the two seamounts. It has to be studied whether these incidences are caused by physical processes like strong currents associated to a Taylor column. Predation by fish could be an additional explanation for this phenomenon.

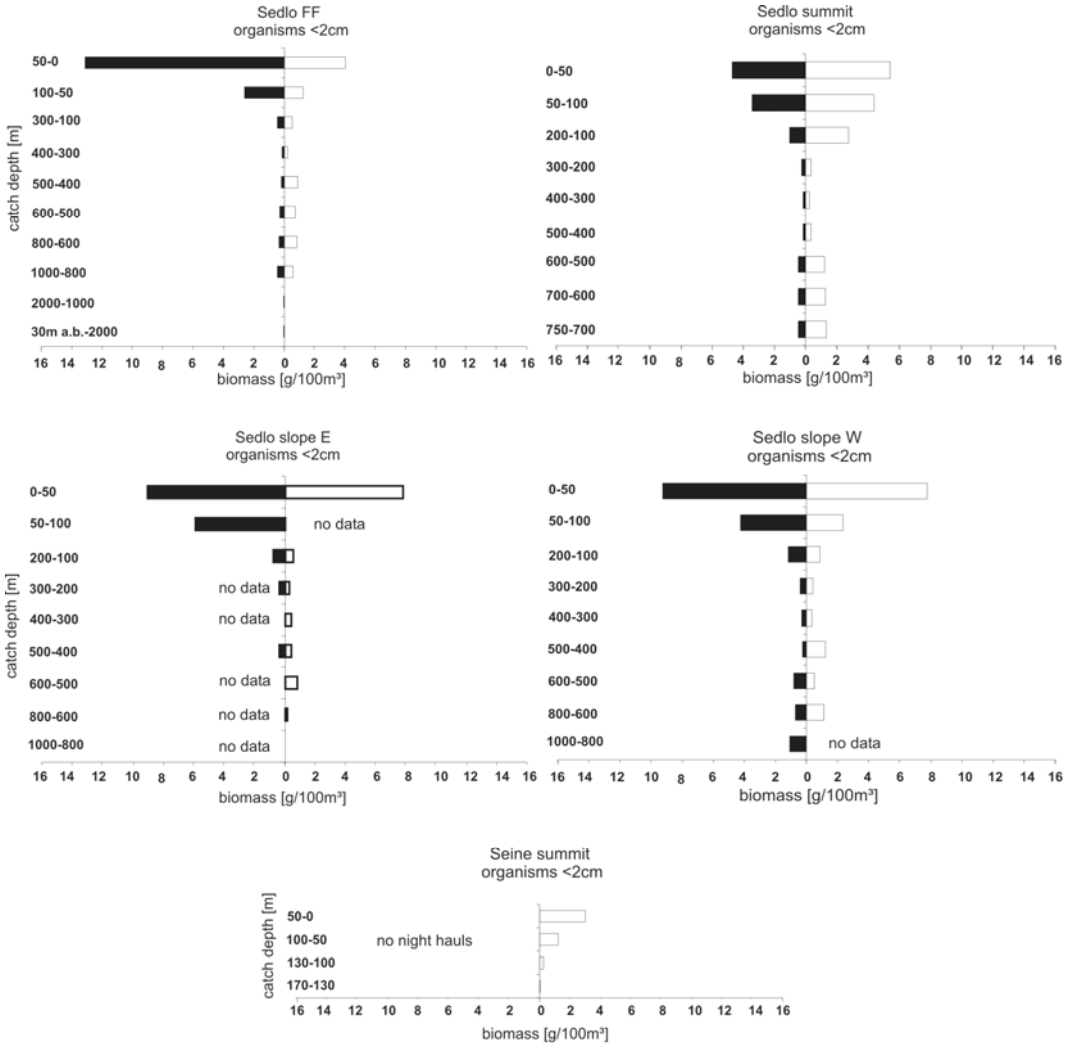

Fig. 1.21: Biomass at different stations at Sedlo and Seine seamount. Black bars represent night time hauls, white bars day time hauls.

Table 1.2: MOCNESS haul data.

Haul #	Date	Sampling time UTC		Coordinates Start		Coordinates End		Water depth/m	Sampling Depth	daytime D: day N: night
		Start	End	Latitude	Longitude	Latitude	Longitude	max.		
MOC-D-01	21.11.03	22:05	2:38	40°15.5‘ N	26°34.0‘ W	40°23.1‘ N	26°29.7‘ W	2697	0-1000 m	N
MOC-D-02	22.11.03	12:30	16:47	40°15.2‘ N	26°33.1‘ W	40°22.9‘ N	26°33.6‘ W	1963	0-1000 m	D
MOC-D-03	23.11.03	14:45	18:10	40°12.9‘ N	26°43.2‘ W	40°18.2‘ N	26°36.5‘ W	837	0-30 mab	D
MOC-D-04	23.11.03	23:46	03:22	40°12.8‘ N	26°42.9‘ W	40°17.8‘ N	26°37.0‘ W	800	0-30 mab	N
MOC-D-05	24.11.03	11:32	13:15	40°13.1‘ N	26°42.9‘ W	40°16.1‘ N	26°39.0‘ W	865	0-500 m	D
MOC-D-06	25.11.03	12:54	17:02	40°22.2‘ N	26°44.4‘ W	40°18.1‘ N	26°50.9‘ W	1183	0-100 mab	D
MOC-D-07	26.11.03	01:13	04:41	40°20.0‘ N	26°45.5‘ W	40°17.9‘ N	26°53.1‘ W	989	0-50 mab	N
MOC-D-08	26.11.03	11:53	19:15	40°23.8‘ N	26°48.2‘ W	40°36.4‘ N	26°39.1‘ W	2693	0-100 mab	D
MOC-D-09	29.11.03	00:00	05:25	39°50.5‘ N	26°18.2‘ W	39°43.7‘ N	26°32.7‘ W	2850	0-30 mab	N
MOC-D-10	29.11.03	09:34	17:30	39°50.4‘ N	26°16.7‘ W	40°06.3‘ N	26°16.4‘ W	3796	0-200 mab	D
MOC-D-11	03.12.03	15:36	17:21	33°41.1‘ N	14°20.5‘ W	33°47.0‘ N	14°23.2‘ W	190	0-20 mab	D
MOC-D-12	03.12.03	21:44	04:15	33°27.7‘ N	14°23.9‘ W	33°43.1‘ N	14°28.6‘ W	3991	0-10 mab	N
MOC-10-01	27.11.03	11:45	15:05	40°15.9‘ N	26°31.5‘ W	40°22.7‘ N	26°30.8‘ W	2700	0-1000 m	D
MOC-10-02	27.11.03	18:41	21:45	40°15.1‘ N	26°49.9‘ W	40°20.8‘ N	26°50.2‘ W	1195	0-1000 m	N
MOC-10-03	03.12.03	10:09	12:33	33°42.1‘ N	14°30.1‘ W	33°47.4‘ N	14°30.5‘ W	1195	0-1000 m	D

Trophic interactions in the water column

The trophic pathways of seamount communities will be investigated using biochemical analysis of stable Isotope ratios (δ15N, δ13C) and fatty acid biomarkers from specimen material collected during the cruise.

The ratio of stable isotopes of nitrogen (δ15N) can be used to estimate trophic position as the δ15N of a consumer is typically enriched by 3-4‰ relative to its diet. In contrast, the ratio of carbon isotopes (δ13C) changes little (less than 1 ‰) as carbon moves through food webs and, therefore, can be used to evaluate the ultimate sources of carbon for an organism (DeNiro and Epstein, 1978; DeNiro and Epstein, 1981; Michener and Schell, 1994; Peterson and Fry, 1987). The isotopic composition reflects an organisms assimilated diet over a period of time determined by the turnover rate of the tissues (Davenport and Bax, 2002).

Lipids are essential for energy storage, buoyancy and as membrane components. Their fatty acids can be used as qualitative markers to trace predator-prey relationships based on the observation that certain fatty acid patterns can be transferred conservatively from primary producers to their consumers and among consumers (Dalsgaard et al., 2003/ and references therein).

Sampling

Water samples for suspended particulate organic matter (sPOM), which is assumed to represent the trophic base of the ecosystem, were taken with a CTD rosette from 50 m depth at seamount and farfield stations on all cruises. The sampled water was poured through a 300 µm mesh-size sieve and vacuum filtered on pre-combusted GF/C filters. The filters were stored at -20 °C for δ13C and δ15N determination and at –80 °C for fatty acid analysis.

Zooplankton samples for trophic investigations (δ13C and δ15N stable isotope determination and lipid analysis) were taken from oblique MOCNESS hauls at discrete depth layers (50-100 m, 200-300 m, 500-600 m and 800-1000 m). The different zooplankton taxa were sorted immediately in the cooling laboratory at 4°C (Table 3.6). The samples for stable isotope analysis were stored at -20 °C and the samples for lipid analysis at -80 °C.

Benthos and bentho-pelagic fish samples for δ13C and δ15N stable isotope determination and lipid analysis were taken from hauls with the dredge and the epibenthic sledge on the R.V. Meteor cruise (Table 3.7). Animals were either frozen whole or a piece of their muscle tissue

dissected and frozen until biochemical analysis.

Table 3.6: Zooplankton samples for δ13C and δ15N stable isotope determination and lipid analysis from MOCNESS hauls during Meteor (M60/1) cruise.

Group	Species	Sampling location		
Decapods	*Acanthephyra purpurea*	Sedlo		
	Acanthephyra spec.		Farfield	Seine
Euphausiids	*Euphausia hemigibba*	Sedlo		
	Euphausia eximia/krohni	Sedlo		
	Meganyctiphanes norvegica	Sedlo	Farfield	
Mysids	*Gnathophausia zoea*	Sedlo		
Copepods	*Pleuromamma xiphias*	Sedlo		
	Lucicutia spec	Sedlo		Seine
	Euchaeta spec.	Sedlo	Farfield	
	Neocalanus spec. juv.	Sedlo		
	Calanus spec.	Sedlo	Farfield	
	Clausocalanus spec.	Sedlo		
	Oncaea spec.	Sedlo		
Ostracods	*Ostracoda spec.*	Sedlo		Seine
Chaetognaths	*Eukrohnia fowleri*	Sedlo	Farfield	Seine
	Eukrohnia hamata	Sedlo		
	Pterosagitta draco	Sedlo		Seine
	Sagitta hexaptera	Sedlo		Seine
	Sagitta planctonis	Sedlo		
	Sagitta serratodentata	Sedlo		
	Sagitta zetesios	Sedlo		
Pteropods	*Cavolinia inflexa*	Sedlo	Farfield	Seine
	Cavolinia inflexa eggs	Sedlo	Farfield	
Amphipods	*Phronima spec*.	Sedlo		
	Hyperiidae spec.			Seine
Pisces	*Cyclothone spec.1*	Sedlo		Seine
	Cyclothone spec.2	Sedlo		
	Myctophidae spec.1	Sedlo		
	Myctophidae spec.2			Seine
	Argyropelecus hemigymnus	Sedlo		Seine
	Melanostomiidae spec.1	Sedlo		
	Melamphaidae spec.1	Sedlo		
	Melamphaidae spec.2		Farfield	
	Eurypharynx pelecanoides		Farfield	

Table 3.7: Benthic and bentho-pelagic samples from Sedlo and Seine Seamount for δ13C and δ15N stable isotope determination and lipid analysis from epibenthic sledge and dredge sampling during the Meteor (M60/1) cruise. * denominates samples taken from animals preserved in buffered formalin. ** denominates samples from the amphipod trap.

Group	Species	Sampling location	
Amphipods	*Eurythenes gryllus juv.***	Sedlo	
Cniderians	*Madrepora occulata*	Sedlo	
Echinoderms	*Asteroida spec.1*		Seine
	Asteroida spec.2		Seine
	Asteroida spec.3		Seine
	Asteroida spec.4		Seine
	Asteroida spec.5		Seine
	Asteroida spec.6		Seine
	Ophiuroid spec.1	Sedlo	
	Ophiuroid spec.2		Seine
	Echinoid spec.		Seine
	Benthodytes spec.	Sedlo	
Polychaets	*Eunice spec.*	Sedlo	
	Polychaet spec.		Seine
Pisces	*Simenchelys parasitica***	Sedlo	
	*Synaphobranchus kaupi***	Sedlo	
	Arnoglossus rueppelli		Seine
	Gadella maraldi		Seine
	Macroramphosus scolopax		Seine
	Anthias anthias		Seine*
	Callanthias ruber		Seine*
	Capros aper		Seine*

The frozen (-20 °C) samples for the measurement of δ13C and δ15N stable isotope ratios will be freeze dried and, except for the filter samples, pulverised using pestle and mortar. The material will then be analysed by an isotope mass spectrometer.

To determine the fatty acid composition of single taxa and sPOM samples, the frozen (-80 °C) samples will be freeze dried, their lipids extracted and methylated and these fatty acid methyl esters determined using gas chromatography.

Zooplankton respiration derived from ETS activity
Methodology

The Electron Transport System (ETS) activity is used, according to the method of Packard (1971), modified by Kenner and Ahmed(1975), to determine zooplankton community respiration at discrete depth layers as well as respiration rates of individuals of selected taxa. The biochemical method estimates, under substrate saturation, the maximum overall activity of the enzymes associated with the respiratory electron transport systems, which can be converted to

potential respiration rates of organisms (Packard, 1985). The enzymatic activity was recalculated for in-situ temperature using the Arrhenius equation and an activation energy of 15.2 kcal mol–1 (Packard et al., 1975). A respiration/ETS ratio of 0.5 will be used to transform potential oxygen consumption (µlO2 g wet wg-1d-1) measured by the ETS method to respiration (R) (Hernández-León and Gómez, 1996; King and Packard, 1975a; King and Packard, 1975b).

Zooplankton samples for respiration measurements were fished horizontally at discrete depth layers (50 m, 300 m, 500 m and 1000 m depth and above the bottom at the seamount summits) with the 1m2 -Double-MOCNESS (Table 3.8). The zooplankton samples were fractioned over a 5mm sieve and the sieve fraction smaller than 5 mm was split in half with the Folsom plankton splitter. One half of each sample was frozen immediately at –80°C and its ETS activity was measured either directly on board or as soon as possible at a land based laboratory. The other half of the sample was stored at -20°C for reference biomass determination at the home laboratory. Additionally, the ETS activity of abundant single taxa was measured (Table 3.9). The single taxa samples were taken from the same oblique MOCNESS hauls, from which stable isotope and lipid samples were taken. Directly upon recovery of the system, the taxa were sorted in the cooling laboratory at 4°C and stored at -80 °C until ETS analyses.

Table 3.8: Zooplankton samples from MOCNESS hauls for ETS activity analysis of community respiration.

Haul	Date	Time	Station	Seamount	net number	Sampling depths
D-MOC1	22.11.2003	night	700	Sedlo slope	R9,R5, R2, L5	50, 300, 500, 1000m
D-MOC2	22.11.2003	day	702	Sedlo slope	R9,R5, R2, L5	50, 300, 500, 1000m
D-MOC3	23.11.2003	day	710	Sedlo summit	L5	750m
D-MOC4	24.11.2003	night	712	Sedlo summit	R9,R5, R2, L5	50, 300, 500, 750m
D-MOC5	24.11.2003	day	715	Sedlo summit	R9,R5, R2	50, 300, 500m
D-MOC6	25.11.2003	day	722	Sedlo canyon	R9,R5, R2	50, 300, 500m
D-MOC7	26.11.2003	night	724	Sedlo canyon	R9,R5, R2, L5	50, 300, 500, 900m
D-MOC9	29.11.2003	night	737	Sedlo farfield	R9, R2	50, 500m
D-MOC10	29.11.2003	day	740	Sedlo farfield	R9,R5	50m, 400-300m
D-MOC11	03.12.2003	day	750	Seine summit	R9, L4+R4	50m, 160m (10m.a.b.)

Table 3.9: Single species samples from MOCNESS hauls for ETS activity analysis.

Group	Species	Station No	Sample depth /m
Decapods	*Acanthephyra spec.*	749	600-450
Euphausiids	*Nematoscelis atlantica*	702	1000
	Euphausia hemigibba	700	100-50
	Euphausia eximia/krohni	702	600-500
Mysids	*Gnathophausia zoea*	710	800
Copepods	*Pleuromamma xiphias*	702	600-500
	Lucicutia spec.	749	1000-600
	Euchaeta spec.	702	1000
	Neocalanus spec. juv.	702	100-50
Chaetognaths	*Sagitta hexaptera*	749	450-300
Pteropods	*Cavolinia inflexa*	700	100-50

Preliminary results

Zooplankton community ETS (µlO2 m-3h-1) showed its highest activity in the euphotic zone at 50 m depth and strongly decreased values at the sampled depths below the euphotic zone from 300 m to 1000 m depth (Figure 1.22), which might be due to the decrease of biomass, temperature and, probably food availability with depth. This result has been reported in previous studies of zooplankton ETS activities in the upper 1000 m (Hernándes-León et al., 2001; King et al., 1978; Packard et al., 1974).

Community ETS activity at 50m depth is highly variable. Most night hauls revealed higher ETS activity values than the respective day hauls which is probably caused by diurnal zooplankton migration (Hernándes-León et al., 2001). At Sedlo seamount ETS activity varied between a maximum value of 7.58 and a minimum value of 0.73. This variability in ETS activity could be due to increased patchiness of zooplankton distriburtion caused by seamount specific currents, trapped migrating zooplankton and predation of seamount associated fauna (Genin, 2004).

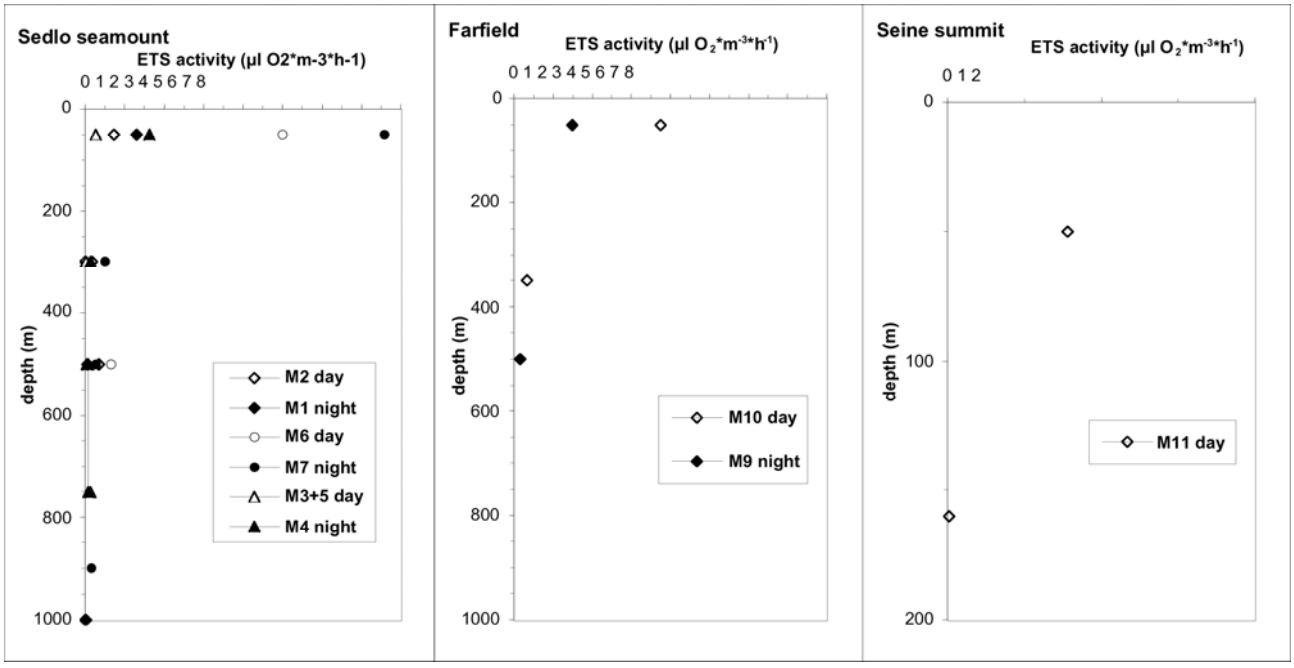

Figure 1.22: Vertical profiles of ETS activity during day and night samplings at the different sites. The farfield site includes the Seine and Sedlo farfield sites.

Megafauna, macrofauna and benthopelagic fauna

The benthic studies focus on the megafauna (those specimens which can be identified with

optical methods). The British WASP system (WASP=wide angle seafloor photography), an altimeter-controlled camera sled with downward looking still camera and video camera was used for photographic and video transects. A total of 12 WASP transects were performed, 9 at Sedlo and 3 at Seine Seamount (Table 1.7). One haul had to be stopped because the gear struck a rock and was damaged. However, the gear could be repaired and used for further hauls. Another haul was cancelled due to problems with the acoustics. Figure 1.23 presents an example of a still image from a video taken at the flank of Sedlo Seamount, depth 2350 m.

Table 1.7: Positions of WASP hauls

Station #	date	latitude		longitude		water depth
703	22.11.2003	40°17.9	N	26°39.1	W	725-750
704	22.11.2003	40°19.1	N	26°38	W	755-763
706	23.11.2003	40°18.5	N	26°48	W	935
707	23.11.2003	40°19.9	N	26°51	W	973
711	23.11.2003	40°21.1	N	26°36	W	1003-1012
716	24.11.2003	40°12.9	N	26°35.9	W	2352
725	26.11.2003	40°15.9	N	26°53.9	W	1676
733	27.11.2003	40°11	N	26°33	W	2706-2714
741	29.11.2003	39°50	N	26°18	W	2875
752	04.12.2003	33°46	N	14°22	W	178
753	04.12.2003	33°49	N	14°22.1	W	215
761	05.12.2003	33°42.9	N	14°18.3	W	1660

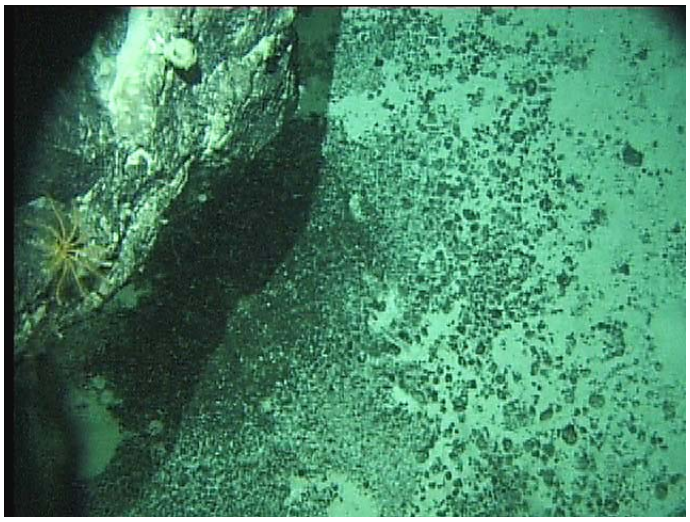

Figure 1.23: Still image from WASP video, Sedlo Seamount, lower flank, 2350 m

Additionally, megafauna was sampled with a rock dredge and with an epibenthic sledge. Two dredge hauls were performed at the flanks of Sedlo Seamount, revealing small samples of crinoids, gorgonarians and corals. During one haul of the epibenthic sledge on the abyssal plain next to Sedlo Seamount the net was lost. Another haul on the summit plateau of Seine Seamount

was successful. The sample included several benthopelagic and benthic fish species (Table 1.8). The most abundant fish was the snipefish, Macroramphosus sp. Megafauna included echinoderms (Asteroidea, Echinoidea), a large number of as yet unidentified worms, a large hermit crab and other crustaceans.

Table 1.8: Catch composition of benthic and benthopelagic fishes from the epibenthic sledge

Order	Family	Species
Perciformes	Labridae	*Lappanella fasciata*
Scorpaeniformes	Scorpaenidae	*Pontinus kuhlii*
Perciformes	Serranidae	*Anthias anthias*
Perciformes	Serranidae	*Callanthias ruber*
Zeiformes	Caproidae	*Capros aper*
Pleuronectiformes	Bothidae	*Arnoglossus rueppeli*
Anguilliformes	Congridae	*Gnathophis mystax*
Gadiformes	Moridae	*Gadella maraldi*
Syngnathiformes	Centriscidae	*Macroramphosus gracilis/scolopax*

Macrofauna samples were taken using a box corer. Due to the very difficult sampling situation on both study sites it was not possible to cover the whole depth-range of the planned sampling scheme. Nearly all samples from Seine Bank are limited to the summit plateau. From Sedlo Seamount only 2 samples could be taken. Both samples are of very restricted size, less than 100 g each. Comparison of the two study sites was not directly possible. The limited number of samples available and the small sample size from Sedlo Seamount as well as the important difference in water-depth makes new samplings necessary in order to improve the database for a reliable comparison of both seamount settings.

Taxonomy and community analysis of the harpacticoid fauna (Crustacea, Copepoda) of Sedlo and Seine seamount (north-eastern Atlantic)

Objective:

The aim of the investigation is to compare the summit harpacticoid fauna of two Atlantic seamounts, Sedlo and Seine, with associations of the surrounding deep sea, adjacent geographical areas, and the plateau harpacticoid fauna of the Great Meteor Seamount, which was the object of a former investigation. Similarity and diversity analyses will elucidate whether the two seamounts sampled during M60/1 of R.V. Meteor in November/December 2003 act as “stepping stones” or “isolated submerged islands” for the distribution of Harpacticoida. Moreover, they will provide information about bathymetrical and geographical exchange of the summit Harpacticoida with neighbouring areas.

Sampling stations and treament of material

Totally, 14 hauls distributed over 11 stations were taken for meiofauna. Sampling was realized using a Multiple Corer (MUC) and a Giant Box Corer (GKG). The material was fixed immediately on board in 5% formalin. Later on, meiofauna was extracted via centrifugation using Levasil. Meiofauna was sorted out, and Harpacticoida were separated for further analyses at species level. Table 1 lists the stations which provided material for further faunistic analyses.

Tab. 1.9: List of stations/hauls used for further faunistic analyses.

	Station	Gerät	Datum	Tiefe	Position
Sedlo-Seamount	# 705	MUC	23.11.03	774m	40°19.0'N/26°40.0'W
	# 717	GKG	24.11.03	2.721m	40°11.0'N/26°33.1'W
	# 728	GKG	26.11.03	856m	40°18,6'N/26°42,0'W
	# 742 a	MUC	29.11.03	2.875m	39°50,0'N/26°17,9'W
	# 742 b	GKG	30.11.03	2.873m	39°50,0'N/26°17,9'W
Seine-Seamount	# 754	MUC	04.12.03	210m	33°49,1'N/14°21,9'W
	# 755	MUC	04.12.03	235m	33°48,0'N/14°22,0'W
	# 756 a	MUC	04.12.03	179m	33°46,0'N/14°21,9'W
	# 756 b	MUC	04.12.03	178m	33°46,0'N/14°22,0'W
	# 759	GKG	04.12.03	178m	33°45,9'N/14°21,8'W
	# 760	GKG	04.12.03	180m	33°46,2'N/14°23,0'W

State of the art

All stations/hauls listed in Tab. 1 were centrifugated. Sorting of meiobenthic major groups is almost finished. The following 22 major taxa have been recorded so far: Acari, Amphipoda, Annelida, Bivalvia, Coelenterata, Copepoda, Gastrotricha, Isopoda, Kinorhyncha, Loricifera, Mysidacea, Nematoda, Ophiurida, Ostracoda, Pantopoda, Porifera, Rotatoria, Solenogastres, Tanaidacea, Tantulocarida, Tardigrada, and Turbellarimorpha.
The collected Copepoda distribute over 5 orders: Calanoida, Cyclopoida, Harpacticoida, Misophrioida, and Siphonostomatoida.

Sorting and assignment of Harpacticoida is still in process. Within Harpacticoida, 23 suprageneric taxa have been sorted out: Ameirinae, Ancorabolidae, Argestidae, Canuellidae, Cerviniidae, Cletodidae, Cletopsyllidae, Cylindropsyllinae, Diosaccinae, Ectinosomatidae, Harpacticidae, Laophontidae, Leptopontiidae, Paramesochridae, Peltidiidae, "Pseudotachidiinae", Superornatiremidae, Tegastidae, Tetragonicipitidae, Tisbidae, and Zosimidae.

Ongoing investigation deals with the identification of Harpacticoida at generic and species level to provide data for further detailed similarity and diversity analyses at species level.

1.4.4 Hyperbaric experiments

(B. Holscher, R. Koppelmann)

A pilot study of hyperbaric experiments on metazoan plankton was performed using the pressurized experimental chamber A-PROACH. A-PROACH stands for adaptive pressurised ocean analysis chamber. It has been designed for performing general deep-sea experiments in a laboratory. It provides simultaneous simulation of hydrostatic pressure (< 50 MPa), temperature (-2..50 °C), current (laminar and turbulent flow) and fluid composition (salinity, oxygen concentration, etc.). It provides access to the sample by sub-sampling, substance insertion, optical windows and electric sensor measurements. The experimental volume is 24 l, maximum solid sample size < 9 mm.

Transporter Vessel

The transporter vessel is used to transfer samples under in situ pressure from a collecting device to the experimental chamber. Main part of the transporter vessel is a cylindrical tube with two symmetric end caps. Valves are integrated in the end caps and operated by pivoting a lever. The tube is situated in a block of syntactic foam, which serves for temperature insulation and buoyancy. A deep-sea servo motor is used for operating the valves. It is necessary to create a flow to fill the vessel with water, this can either be done by a pump or by connecting the vessel to a collection device that offers flowing water as output. It is also thinkable to use the vessel as baited trap. In this case, flow is not necessary; the vessel is baited to attract actively moving animals.

The transporter vessel has a capacity of 400 ml and its valves allow to enter particles of a diameter < 9 mm. The pressure loss during ascent is minimal due to a pressure compensating cartridge inside the vessel. Temperature conservation depends on the speed of ascend and the surrounding temperature.

Operation on cruise M60/1

Deep-sea crustaceans depend vitally on the thermodynamic characteristics of their environment. Therefore, observing living deep-sea crustaceans on the surface requires isobar and isotherm transport and maintenance. This has been accomplished by Yayanos (1978): His collection

vessel was capable of maintaining in-situ pressure and offered a window for observation. Here, the crustaceans are collected in the transportation device and, once on the surface, transferred into A-PROACH for long-term observation and measurements, e.g. oxygen consumption. Due to the bigger chamber, the artificial environment resembles closer the in-situ conditions than Yayanos' device; due to the manifold cognition access, more analysis methods can be applied.

For transport and handling, A-PROACH was installed into a standard open-top container, where it was bolted to the bottom and additionally lashed during truck transfer and storm. A-PROACH in its current state is not fully seaworthy: It is not possible to open the pressure cylinder at ship movement, because when lifted off the bottom end-cap, it is not impeded from swinging horizontally, e.g. by means of a rail.

Additionally to the standard equipment of A-PROACH, a deep-sea video camera was installed inside the pressure tank to better observe and record any captured life. The camera was a development of the Department of Ocean Engineering 1. It used a colour CCD as sensor and was complemented by a white LED as light source. The output signal went via the standard electrical duct of A-PROACH to the video-in of a TV-video-combination.

The experimental setup inside the laboratory was completed while still on land to avoid the necessity to lift off the pressure cylinder on the ship. The experiment was thus prepared in a way that all necessary operations inside the laboratory could take place through the top end-cap of the tank.

The inner setup of A-PROACH was prepared with little deviation from standard operation mode: The Microcosm Flux Chamber was used, a single bag served for pressure equalisation, since chemical manipulation of the chamber water was not necessary for the planned experiment. The pumping circuit of the Microcosm Flux Chamber was extended to create a flow through the external transportation device. This allows to actively transport the contents of the transportation device into the chamber. To avoid the escape of particles of interest (diameter > 1 mm), a fine mesh was placed in front of the suction nozzle inside the chamber.

Thus, A-PROACH offered simulation of pressure, temperature and controlled laminar or turbulent current, cognition by means of video camera and eye observation, real-time pressure, temperature and oxygen measurement, sub-sampling of the overall chamber contents, and repetitive introduction of fluid and particles of up to 9 mm diameter.

The laboratory system was completed by the transporter vessel, which was adapted to connect to a MOCNESS as one of its collection cups. To this end, the transportation device had to obtain neutral buoyancy in sea water. The high density of the pressure-bearing steel parts was counter-

balanced by an appropriate amount of syntactic foam. The syntactic foam served at the same time as temperature insulating material. This lead to a corpus with a frontal area of 500 mm2 and a drag which is significantly larger than the drag of a standard collection cup. This required adaptation of the MOCNESS, too: ropes were installed leading from the net‘s frame to the mouth, where the transportation device was tied to. To work like a collection cup, a fine mesh (mesh size 0.05 mm) was placed inside the cylindrical vessel at the back end allowing to escape water and particles smaller than mesh diameter.

For the co-ordination of MOCNESS and the transporter vessel, it was not possible to access or manipulate the controls of the former. The electronics housing of the transportation device was installed next to the one of MOCNESS, but both were working independently. For their co-ordination, a deep-sea capable hall sensor was used, which detected the opening of one of the nets. This was realised by connecting a magnet, which was primarily held in front of the hall sensor, to the net‘s frame bar. When the net opened, the frame bar fell and consequently tore the magnet off its initial position. This was detected by the hall sensor and transmitted to the control, which could then react appropriately. Furthermore, as a backup, a pressure sensor was installed into the wall of the housing. Its signals could be used in case the hall sensor failed.

The position of the electronics housing on the MOCNESS main frame required energy and signal transmission to the transporter vessel, where the actuator for valve operation was located, realised in form of a deep-sea cable leading alongside the corresponding net. To avoid tangling with other nets, it was taped to one of the ropes supporting the transportation device
The electronics housing did not provide a power switch. It was therefore necessary to open the housing just before beginning of the experiment to connect the batteries. Furthermore, for a program start, a serial connection to a computer was necessary: A serial cable connected temporarily to the appropriate connector on the housing. This connection provided a computer terminal operation of the device‘s processor. By means of a simple menu and parameter input, the initial experiment data could be programmed, before the cable was disconnected and the further operation continued autonomously.

During sinking of MOCNESS to its operation depth, premature battery depletion was prevented by putting the processor into „deep sleep“ mode for the estimated sinking time. In this mode, no hall sensor change nor pressure sensor information was gathered.

The MOCNESS provided online data to the ship‘s control via a coaxial cable link. Its depth could be controlled by the ship‘s speed and the length change of the cable. During the tows, nets were closed and opened by the operator on the ship.

Initially, the valves of the transporter vessel were set to "open" position. When the appropriate

net (the one where the device was connected to) opened, a signal to the control was given via the hall sensor. An electronic timer was then started. At the end of the pre-set time, the valves of the device were closed by giving power to the actuator for some time. After that, synchronised on board by simple clock timing, the net was closed and the experiment continued with the further nets.

During this cruise, five MOCNESS casts with the transporter vessel took place. Three of the five experiments delivered a sample at circa in situ pressure. The temperature of the vessel after recovery was measured once and deviated far from the in situ temperature. None of the samples contained visible crustaceans.

To particularise: At the first experiment, the pressure sensor delivered wrong data, which caused the control to close the chamber prematurely. Furthermore, the second valve did not close completely, so that the vessel was not securely closed. As a consequence, the software was changed to improve the pressure sensor data acquisition and the closing time for the valves was readjusted to make sure that both valves would completely close.

The second experiment delivered a sample at 7 MPa. The sample was transferred into A-PROACH, after connection and adjusting the pressure of the laboratory. No objects could be detected by observation through the windows while stirring the sample to move otherwise invisible sample volume below the window. The sample was then withdrawn from the AV module and carefully sieved. No objects were found.

At the third experiment, the pressure sensor again delivered wrong data, leading to premature closing of the chamber. No sample could be collected. The pressure sensor was deactivated from now on. Its data was still collected, but did not influence the control anymore.

At the fourth experiment, a sample was collected at 25 MPa. All further proceedings were equivalent to the second experiment. At the fifth experiment, a sample was collected at 30 MPa. All further proceedings were equivalent to the second and fourth experiment.

Additionally, the temperature of the vessel was measured with a digital thermometer, which showed 15 °C. The in situ temperature at the collection depth is < 5 °C, thus the insulation of the vessel was by no means sufficient for the procedure of this experiment, which may be explained as follows: The MOCNESS has a total number of 20 nets, which can be opened and closed consecutively. During the experiment, the instrument is brought to its greatest depth first. Since collections with the isobaric transportation device is most interesting at greatest depth, the appropriate net with the installed vessel is opened here. The following nets are opened consecutively at lesser depths each. After completion, the device is brought to the surface and

recovered. The procedure implies thus a residence of the device of several hours in relatively warm water closer to the surface. As a consequence from the long exposure to warm water, the transporter vessel, in spite of its insulation, is heated up. Thus, even in the case of a successful capture of deep-sea crustaceans, these would not have survived such high temperatures.

1.5 Station list M60/1

Station No M	Date	Time UTC	Latitude	Longitude	Water depth m	Gear
675	16.11.03	10:38	45° 43.7 N	15° 45.0 W	4711	CTD
676	16.11.03	13:46	45° 30.2 N	16° 18.6 W	4071	CTD
677	16.11.03	15:34	46° 23.5 N	16° 34.3 W	3581	CTD
678	18.11.03	15:52	40° 38.0 N	26° 16.0 W	2895	CTD
679	18.11.03	18:55	40° 32.0 N	26° 24.0 W	2887	CTD
680	18.11.03	21:40	40° 31.0 N	26° 45.0 W	2741	CTD
681	18.11.03	23:52	40° 24.9 N	26° 48.1 W	2164	CTD
682	19.11.03	3:16	40° 25.0 N	26° 35.0 W	2653	CTD
683	19.11.03	7:45	40° 22.0 N	26° 50.0 W	1423	CTD
684	19.11.03	10:54	40° 22.1 N	26° 36.8 W	1298	CMM recovery
685	19.11.03	15:33	40° 20.5 N	26° 38.3 W	891	CTD
686	19.11.03	21:03	40° 19.6 N	26° 25.9 W	2873	CTD
687	19.11.03	4:10	40° 17.2 N	26° 41.2 W	757	CTD
688	20.11.03	6:25	40° 17.3 N	26° 53.1 W	1395	CTD
689	20.11.03	8:50	40° 15.1 N	26° 49.8 W	1465	CMM recovery
690	20.11.03	12:04	40° 15.7 N	26° 35.3 W	1535	CMM recovery
691	20.11.03	13:54	40° 13.1 N	26° 33.9 W		CMM recovery
692	20.11.03	21:28	40° 14.4 N	26° 29.0 W	2818	CTD
693	21.11.03	1:56	40° 13.0 N	26° 55.0 W	2150	CTD
694	21.11.03	4:30	40° 11.5 N	26° 44.0 W	2176	CTD
695	21.11.03	7:30	40° 11.6 N	26° 34.0 W	2600	CTD
696	21.11.03	9:09	40° 11.4 N	26° 34.0 W	2682	A-Trap deployment
697	21.11.03	12:52	40° 8.0 N	26° 46.5 W	2379	CTD
698	21.11.03	16:00	40° 2.0 N	26° 37.0 W	2618	CTD
699	21.11.03	18:24	40° 5.9 N	26° 35.0 W	2707	CTD
700	21.11.03	22:16	40° 15.5 N	26° 34.0 W	2000	D-MOC
701	22.11.03	4:30	40° 15.3 N	26° 37.0 W	1222	3 CTD
702	22.11.03	12:30	40° 15.2 N	26° 33.1 W	2040	D-MOC
703	22.11.03	18:30	40° 17.9 N	26° 39.1 W	725	WASP
704	22.11.03	20:40	40° 19.1 N	26° 38.0 W	763	WASP
705	22.11.03	23:34	40° 19.0 N	26° 40.0 W	773	MUC
706	23.11.03	3:38	40° 18.5 N	26° 48.0 W	935	WASP
707	23.11.03	6:00	40° 19.9 N	26° 51.0 W	973	WASP
708	23.11.03	9:56	40° 11.0 N	26° 33.9 W	2693	A-Trap recovery
709	23.11.03	12:51	40° 17.1 N	26° 42.3 W		CMM recovery
710	23.11.03	14:45	40° 12.9 N	26° 43.2 W	837	D-MOC
711	23.11.03	20:00	40° 21.1 N	26° 36.0 W 26°.	1003	WASP
712	23.11.03	23:46	40° 12.8 N	26° 0 W	1750	D-MOC
713	24.11.03	4:10	40° 19.0 N	26° 40.0 W	774	3 CTD
714	24.11.03	10:26	40° 19.0 N	26° 39.9 W	772	A-Trap deployment
715	24.11.03	11:32	40° 13.1 N	26° 42.9 W	1660	D-MOC
716	24.11.03	15:45	40° 12.9 N	26° 35.9 W	2352	WASP
717	24.11.03	19:25	40° 11.0 N	26° 33.1 W	2719	GKG
718	24.11.03	23:25	40° 11.1 N	26° 33.1 W	2718	MUC
719	25.11.03	3:44	40° 19.9 N	26° 50.6 W	1123	RD
720	25.11.03	6:43	40° 20.0 N	26° 51.0 W	1110	RD
721	25.11.03	9:41	40° 19.1 N	26° 39.3 W	775	A-Trap recovery
722	25.11.03	12:54	40° 22.2 N	26° 44.4 W	1240	D-MOC

723	25.11.03	18:00	40° 20.1	N	26° 50.2	W	1134	3 CTD
724	26.11.03	1:13	40° 20.0	N	26° 45.5	W	1033	D-MOC
725	26.11.03	6:10	40° 15.9	N	26° 53.9	W	1676	WASP
726°	26.11.03	11:53	40° 23.8	N	26° 48.2	W	2029	D-MOC
727	26.11.03	21:13	40° 20.0	N	26° 50.7	W	1123	A-Trap deployment
728	26.11.03	22:35	40° 18.3	N	26° 42.1	W	786	2 GKG
729	27.11.03	2:52	40° 22.4	N	26° 34.4	W	1746	3 CTD
730	27.11.03	11:45	40° 15.9	N	26° 31.5	W	2687	MOC 10
731	27.11.03	17:06	40° 19.5	N	26° 50.7	W	1179	A-Trap recovery
732	27.11.03	18:41	40° 15.1	N	26° 49.9	W	1888	MOC 10
733	27.11.03	23:34	40° 11.0	N	26° 33.0	W	2714	WASP
734	28.11.03	5:18	40° 14.8	N	26° 28.1	W	2720	EBS
735	28.11.03	13:22	39° 50.1	N	26° 17.9	W	2872	A-Trap deployment
736	28.11.03	13:47	39° 50.4	N	26° 17.9	W	2872	3 CTD
737	29.11.03	0:00	39° 50.5	N	26° 18.2	W	2877	D-MOC
738	29.11.03	6:47	39° 50.0	N	26° 17.9	W	2876	CTD
739	29.11.03	7:30	39° 50.0	N	26° 17.2	W	2835	A-Trap recovery
740	29.11.03	9:34	39° 50.4	N	26° 16.7	W	2890	D-MOC
741	29.11.03	19:05	39° 50.0	N	26° 18.0	W	2815	WASP
742	30.11.03	23:09	39° 49.9	N	26° 18.0	W	2871	MUC
743	02.12.03	15:50	33° 48.0	N	14° 40.1	W	4008	CTD
744	02.12.03	17:42	33° 30.5	N	14° 31.5	W	3395	CTD
745	02.12.03	22:09	33° 52.0	N	14° 30.1	W	3489	CTD
746	03.12.03	2:18	33° 52.0	N	14° 14.0	W		CTD
747	03.12.03	5:24	33° 42.0	N	14° 13.8	W	3382	CTD
748	03.12.03	8:38	33° 46.0	N	14° 22.0	W	178	CTD
749	03.12.03	10:09	33° 42.1	N	14° 30.1	W	2388	MOC 10
750	03.12.03	15:36	33° 44.1	N	14° 20.5	W	607	D-MOC
751	03.12.03	21:44	33° 27.7	N	14° 23.9	W	4272	D-MOC
752	04.12.03	8:08	33° 46.0	N	14° 22.0	W	178	WASP
753	04.12.03	9:40	33° 49.0	N	14° 22.1	W	215	WASP
754	04.12.03	10:50	33° 49.1	N	14° 21.9	W	209	MUC
755	04.12.03	11:55	33° 48.0	N	14° 22.0	W	207	MUC
756	04.12.03	12:52	33° 46.1	N	14° 22.0	W	178	2 MUC
757	04.12.03	16:45	33° 49.0	N	14° 22.0	W	206	A-Trap deployment
758	04.12.03	17:33	33° 45.5	N	14° 21.3	W	186	EBS
759	04.12.03	20:42	33° 46.0	N	14° 21.9	W	177	GKG
760	04.12.03	22:00	33° 46.2	N	14° 23.0	W	180	GKG
761	05.12.03	0:30	33° 42.9	N	14° 18.3	W	1700	WASP + Fisch z.W.
762	05.12.03	3:55	33° 36.3	N	14° 11.7	W	4412	MUC
763	05.12.03	8:35	33° 48.4	N	14° 21.9	W	204	A-Trap recovery
764	05.12.03	10:39	33° 40.5	N	14° 31.3	W	3270	CTD
765	05.12.03	16:53	33° 49.0	N	14° 21.9	W	222	GKG

CTD	Seabird CTD with 24 bottle rosette
CMM	current meter mooring
A-Trap	amphipod trap
D-MOC	$1m^2$-double-MOCNESS
WASP	camera sled (wide angle seafloor photography)
MUC	multiple corer
GKG	giant box corer
MOC 10	$10m^2$-MOCNESS
RD	rock dredge
EBS	epibenthic sledge

1.6 Acknowledgements

We would like to thank Captain Kull and his crew for the excellent cooperation and their skilled work during cruise M 60/1. The pleasant atmosphere on board contributed significantly to the success of the cruise. The expedition was funded by the Deutsche Forschungsgemeinschaft. The project OASIS is funded by the European Commission under the Fifth Framework Programme and contributing to the implementation of the Key Action 'Sustainable Marine Ecosystems' within the Specific Programme 'Energy, Environment and Sustainable Development', contract No EVK3-CT-2002-00073-OASIS.

1.7 References

Beckmann, A. and C. Mohn (2002). The upper ocean circulation at Great Meteor Seamount. Part II: Retention potential of the seamount induced circulation. Ocean Dynamics 52: 194-204.

Dalsgaard, J., M. St. John, G. Kattner, D. Muller-Navarra and W. Hagen (2003). Fatty acid trophic markers in the pelagic marine environment Advances in Marine Biology 46: 225-340.

Davenport, S.R. and N.J. Bax (2002). A trophic study of a marine ecosystem off southeastern Australia using stable Isotopes of carbon and nitrogen Canadian Journal of Fisheries and Aquatic Sciences 59: 514-530.

DeNiro, M.J. and S. Epstein (1978). Influence of diet on the distribution of carbon isotopes in animals Geochimica et Cosmochimica Acta 42: 495-506.

DeNiro, M.J. and S. Epstein (1981). Influence of diet on the distribution of nitrogen isotopes in animals Geochimica et Cosmochimica Acta 45: 341-351.

Dower, J.F. and D.L. Mackas (1996). "Seamount effects" in the zooplankton community near Cobb Seamount. Deep-Sea Res. I 43(6): 837-858.

Fock, H., F. Uiblein, F. Köster and H.v. Westernhagen (2002). Biodiversity and species-environment relationships of the demersal fish assemblage at the Great Meteor Seamount (subtropical NE Atlantic), sampled by different trawls. Mar. Biol. 141(1): 185-199.

Genin, A. (2004). Bio-physical coupling in the formation of zooplankton and fish aggregations over abrupt topographies J. Mar. Syst. 50(1-2): 3-20.

Genin, A. and G.W. Boehlert (1985). Dynamics of temperature and chlorophyll structures above a seamount: An oceanic experiment J. Mar. Res. 43: 907-924.

Hernándes-León, S., M. Gómez, M. Pagazaurtundua, A. Portillo-Hahnefeld, I. Montero and C. Almeida (2001). Vertical distribution of zooplankton in Canary Island waters: implications for export flux Deep-Sea Res. 48(I): 1071-1092.

Hernández-León, S. and M. Gómez (1996). Factors affecting the respiration/ETS ratio in marine zooplankton J. Plankton Res. 18: 239-255.

Hesthagen, I.H. (1970). On the near-bottom plankton and benthic invertebrate fauna of the Josephine Seamount and the Great Meteor Seamount. Meteor Forsch. Ergebn. (D) 8: 61-70.

Hubbs, C.L. (1959). Initial discoveries of fish faunas on seamounts and offshore banks in the eastern Pacific. Pacific Science 13: 26-33.

Kenner, R.A. and S.I. Ahmed (1975). Measurement of electron transport activities in marine phytoplankton Mar. Biol. 33: 119-128.

King, F.D., A.H. Devol and T.T. Packard (1978). Plankton metabolic activity in the eastern tropical North Pacific Deep-Sea Res. 25: 689-704.

King, F.D. and T.T. Packard (1975a). The effect of hydrostatic pressure on respiratory electron

transport system activity in marine zooplankton Deep-Sea Res. 22: 99-105.
King, F.D. and T.T. Packard (1975b). Respiration and the activity of the respiratory electron transport system in marine zooplankton Limnological Oceanography 20: 849-854.
Martin, B. and W. Nellen (2004). Composition and vertical distribution of zooplankton at the Great Meteor Seamount, subtropical NE Atlantic. Archive of Fishery and Marine Research 51(1-3): 89-100.
Mauritzen, C., Y. Morel and J. Paillet (2001). On the influence of Mediterranean water on the central waters of the North Atlantic Ocean. Deep-Sea Res. I 48: 347-381.
Michener, R.M. and D.M. Schell (1994). Stable isotope ratios as tracers in marine aquatic food webs In: R.H. Michener and K. Lajtha, eds., Stable isotopes in ecology and environmental science Blackwell, Oxford, 138-157.
Mouriño, B., E. Fernández, P. Serret, D. Harbout, B. Sinaha and R. Pingree (2001). Variability and seasonality of physical and biological fields at the Great Meteor Tablemount (subtropical NE Atlantic). Oceanol. Acta 24(2): 167-185.
Nellen, W. (1973). Untersuchung zur Verteilung von Fischlarven und Plankton im Gebiet der Großen Meteorbank. Meteor Forsch. Ergebn. (D) 13: 47-69.
Packard, T.T. (1971). The measurement of respiratory electron transport activity in marine phytoplankton. J. Mar. Res. 29: 235-244.
Packard, T.T. (1985). Measurement of electron transport activity of marine microplankton Advances in Aquatic Microbiology: 207-261.
Packard, T.T., A.H. Devol and F.D. King (1975). The effect of temperature on the respiratory electron transport system in marine plankton Deep-Sea Res. 22: 237-249.
Packard, T.T., D. Harmon and J. Boucher (1974). Respiratory electron transport activity in plankton from upwelled waters Tethys 6: 213-222.
Parin, N.V., A.N. Mironov and K.N. Nesis (1997). Biology of the Nazca and Sala y Gomez Submarine Ridges, an Outpost of the Indo-West Pacific Fauna in the Eastern Pacific Ocean: Composition and Distribution of the Fauna, its Communities and History. Advances in Marine Biology 32: 147-228.
Peterson, B.J. and B. Fry (1987). Stable isotopes in ecosystem studies Annual Revue of Ecology and Systematics 18: 239-320.
Rogers, A.D. (1994). The biology of seamounts Advances in Marine Biology 30: 305-350.
Uiblein, F., A. Geldmacher, F. Köster, W. Nellen and G. Kraus (1999). Species composition and depth distribution of fish species collected in the area of the Great Meteor Seamount, eastern central Atlantic, during cruise M 42/3, with seventeen new records. Informes Tecnicos del Instituto Canario de Ciencias Marinas 5: 1-77.
Wiebe, P.H., A.W. Morton, A.M. Bradley, R.H. Backus, J.E. Craddock, V. Barber, T.J. Cowles and G.R. Flierl (1985). New developments in the MOCNESS, an apparatus for sampling zooplankton and micronekton. Mar. Biol. 87: 313-323.
Wilson, C. and G. Boehlert (1990). Acoustic measurements of micronekton distribution over Southeast Hancock Seamount, Central Pacific Ocean. In: S.P. Singal, ed., Acoustic Remote Sensing: Proceedings of the Fifth International Symposium on Acoustic Remote Sensing of the Atmosphere and Oceans. Tata-McGraw Hill, New Dehli, 222-229.
Yayanos, A.A. (1978). Recovery and maintenance of live amphipods at a pressure of 580 bars from an ocean depth of 5700 meters. Science 200: 1056-1059.

METEOR-Berichte

TITLE

Part 3

Cruise No. 60, Leg 2

December 9, 2003 - January 12, 2004, Funchal - Martinique

Chief Scientist: Prof. Dr. J. Phipps Morgan (IFM-GEOMAR)

Table of Contents; Leg 2

2.1 Participants M 60/2

Name	Task	Institution
Phipps Morgan, Jason	chief scientist	IFM-GEOMAR
Gente, Pascal	tectonics	CNRS
Kahle, Richard	Data processing	UC
Klein, Gerald	Data processing	IFM-GEOMAR
Landschoff, Torsten	Seismics	IFM-GEOMAR
Maia, Marcia	Tectonics / magnetics	CNRS
Noeske, Martina	Seismics	IFM-GEOMAR
Noeske, Carl	Seismics	IFM-GEOMAR
Pierre, Virginie	Seismics	IFM-GEOMAR
Ranero, Cesar	Geophysics	IFM-GEOMAR
Soares, Valentina	Seismics	UL
Steffen, Klaus	Seismics	IFM-GEOMAR
Tilmann, Frederik	Seismics	UC

Participating institutions

IFM-GEOMAR	Leibniz-Institut für Meereswissenschaften, Wischhofstr. 1-3 24148 Kiel / Germany
CNRS	CNRS UMR 6538 and Universite de Bretagne Occidentale, 6 Av. Le Gorgeu, 29200 Brest / France
UC	Bullard Laboratory, Dep. Earth Sciences, University of Cambridge, Maddingley Rd., Cambridge, CB3 OEZ / UK
UL	Departamento de Geologia, Faluldade de Ciencias da Universidade de Lisboa, Campo Grande, Edificio C2, 1749-016, Lisboa / Portugal

2.2 Research Programme

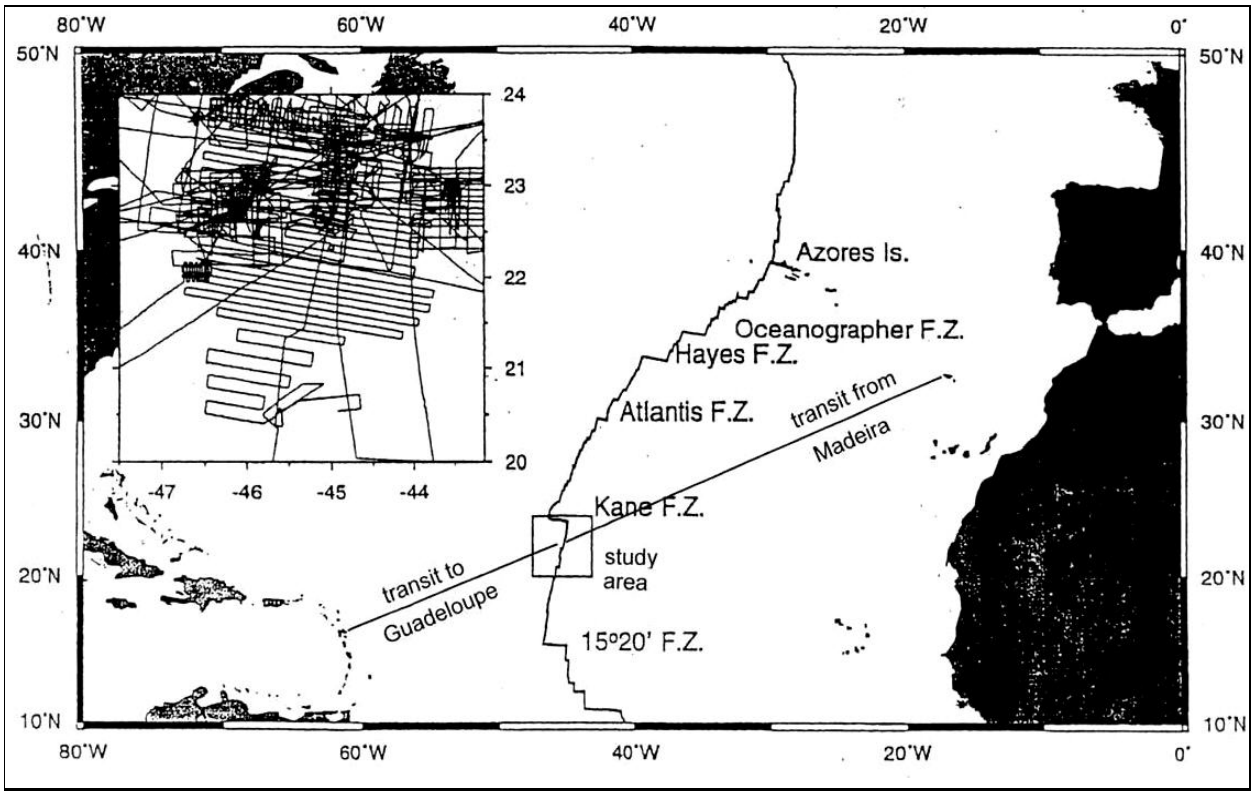

Figure 2.1 Proposed cruise track for Meteor 60 Leg 2.

Scientific Programme

The objective of Leg 2 of Meteor 60 was to use active seismic refraction and passive microearthquake and teleseismic imaging methods to study the crust, uppermost mantle, and deformation associated with active ridge propagation in a median valley environment, studying the actively propagating ridge segment from 21.2-22°S along the Mid-Atlantic Ridge. The active seismic experiment used 4 18-instrument, 120-km-long refraction lines, two in the across-axis direction, two in the along-axis direction, to determine the crustal thickness and velocity structure along and across this median valley segment of the spreading centre. The seismic source was two 32-liter airguns. The passive experiment redeployed these 18 instruments at the end of the field program to record 6 months of local microseismic (and global teleseismic) activity – also shooting to this array to better constrain the crustal structure beneath each station. The data collected will be used for two different passive seismic investigations with different goals; a local microseismicity study to study lithospheric deformation processes within this region, and a regional tomographic-type study to image along-axis changes in the structure of mantle upwelling beneath this section of the ridge.

Active seismic refraction experiment:

Specific goals/ geologic targets of the seismic refraction part of the research program were:

(1) NNE-SSW Profiles

(A) Along-axis crustal structure of the active spreading segment

- possible active magma chamber at segment center (beneath along-axis high)
- relation of axial crustal velocities to gravity, microseismicity, and the development of new magmatic activity at the growing propagating ridge tip's southern extension

(B) Crustal structure along an isochron that has experienced shear-zone deformation in its southern, but not its northern half

- changes in seismic velocity structure(& density?) between sheared and unsheared crust
- possible role of serpentinization in shear zone deformation?
- changes in seismic velocity structure as a function of crustal age and median-valley wall deformation (compare to 'A')
- what are gravitational effects of crustal/lithospheric mantle density variations within the sheared zone?

(2) E-W Profiles

(C) Across-axis crustal structure through the shallowest part of segment center (with smallest median valley relief)

- differences between median valley and fossil shear zone fault-zone velocities
- crustal thickness/velocity variations + gravity $\wedge$ mantle density structure beneath this region (i.e. regional mantle 'Bouguer' anomaly)

(D) Across-axis profile crossing near active PR tip and shearing zone

- origin/compensation of shear-zone uplift
- seismic velocity structure of shear zone crust

ALL PROFILES: local crustal thickness/seismic velocity information needed for passive microseismicity and subaxial tomography experiments.

Passive seismic experiments:

The passive experiment was to redeploy the 18 instruments at the end of the field program to record 6 months of local microseismic (and global teleseismic) activity – also shooting to this array to better constrain the crustal structure beneath each station. This array would be recovered after 6 months by the Meteor. To best take advantage of the enormous amount of prior French bathymetric, gravity, and magnetic mapping in this area, a collaboration with French colleagues (Gente and Maia) on the local tectonic and regional seismic interpretation of the study area was initiated. The data collected will be used for two different passive seismic investigations with different goals; a local microseismicity study to study lithospheric deformation processes within this region, and a regional tomographic-type study to image along-axis changes in the structure of mantle upwelling beneath this section of the ridge.

(1) Goals of the Microseismicity Study*:*

Seismotectonics of a propagating spreading segment

- delineation of active faults along the spreading axis
- active faulting associated with the growing propagating ridge tip's southern extension (diffuse or concentrated?)

Seismotectonics of active deformation in the shear zone

- distribution of microseismic faulting associated with the zone of active shearing (transform-like or diffuse?)
- focal mechanisms of shearing-zone faulting (bookshelf with NNW-SSE slip-planes, or transform-like with E-W slip planes?)

(2) Goals of the Passive Teleseismic Study:

Structure of mantle upwelling and melting beneath a propagating spreading segment

- is there a slow-velocity anomaly from mantle melting concentrated beneath the axial high?
- what are the lengthscales of along-axis to across-axis mantle seismic variation?

Lithospheric/mantle structure beneath the shearing zone

- is there a slow-velocity anomaly beneath the uplifted shearing/sheared zone, or is this uplift dynamically compensated?
- is there unusual shear-wave splitting beneath the uplifted shearing/sheared zone? (diagnostic of deep serpentinization / regional deformation?)

2.3 Cruise narrative

Week 1

The Meteor left Funchal, Madeira at ~1600, 9 Dec, slightly delayed in order to test the faulty winch computer that had been repaired during the port stop in Madeira. Good weather allowed Meteor to make up for this delay during the transit to the study area, which was reached on the afternoon of 15 Dec.. The transit-week was spent preparing and testing equipment.

Week 2

During the 2nd week, two seismic refraction profiles were completed: one along the axis of the propagating ridge at 21°30'N along the Mid-Atlantic Ridge, the other crossing the sheared zone created between the growing and retreating ridge segments. Each profile involved the deployment of 15 Ocean Bottom Hydrophones (OBHs), then shooting a roughly 200-km-long acoustic (air-gun) track, then collecting the instruments and recovering their stored data. The pace of work has been quick and several significant problems were overcome. Shortly after the start of the first air-gun deployment, the compressor failed, yet within 10 hours the major problem had been isolated and repaired. Unfortunately, two instruments failed in a crucial part of the first profile. An initial look at the data from the first profile suggests that significant changes

in crustal thickness exist along-axis, with the thinnest crust found near the tip of the propagating ridge axis and the deep at the other end of this segment.
The presence of swell combined with the track of the second profile, which had been chosen for geological reasons, made Meteor susceptible to significant rolls (in spite of generally excellent weather conditions). The slow 4 knot speed used for air-gun profiles limited the utility of the ship's stabilizers.

3rd Week

The 3rd week was used to collect seismic refraction profiles across the most volcanically active section of the growing ridge axis at 21°45'N along the Mid-Atlantic Ridge. Two profiles were shot to record the time-variation of crustal production along this section of the ridge. In addition a further axial profile was collected to fill a critical data gap (caused by multiple recorder failures) in our initial profile. This profile was combined with a partial 'tomographic' shooting strategy to better constrain upper crustal structure in this region, which is a promising site to be underlain by an active magma chamber, and a 3 day passive microearthquake deployment (over Christmas) to image the depth-extent of seismic activity in this region. After recovery of the instruments, swath-bathymetry data was collected over an incompletely mapped shallow region that was presumed to be a 'peridotite massif complex'. This mapping continued for 6 hours and was followed by deployment of another seismic profile that should better constrain crustal magmatism and the possible volume-extent of non-magmatic mantle peridotite outcropping at the largely amagmatic northern end of the propagating ridge segment. Ultimately these seismic data will be merged with gravity and bathymetry data collected on previous French cruises to the region in order to constrain the magmatic patterns associated with the onset and continuation of ridge propagation.
Calm seas and lots of sun permitted Christmas to be celebrated with a Caribbean barbecue on the heli-deck, complete with peach-colored sky, and a Plattdeutsch Christmas Story.

4th Week

At the beginning of the 4th week, bad weather slowed the progress of the seismic work; the air-guns were taken out of the water for 15 hours until the seas calmed. Following the storm the weather became excellent. After completion of a last seismic profile just before Sylvester (New Year's Eve) which focused on the imaging of the crustal and mantle structures, there was a pause in the seismic work which allowed for bathymetric mapping of a further propagating ridge segment at 19° 50' S. A total of 3 days were used to fill small but significant gaps in previously available Simrad-based bathymetric maps of this section of the ridge-axis. During this mapping work, the sea conditions were almost perfect which allowed a few significant problems with the Meteor's Hydrosweep mapping system to be identified (e.g. software errors and problems associated with noise from sea conditions). These problems restricted the range of ship's headings that could be used for the mapping work and therefore reduced the measurement

possibilities of the system. Despite this, good luck with the weather allowed for mapping of most of the regions of missing data with the results that a high-resolution map is available for a 2nd propagating ridge system in a spreading centre with a median valley. Following the mapping, Meteor returned to the main research area in order to set out the equipment for the last passive seismic experiment conducted prior to starting the transit to Fort-de-France on 8 January.

2.4 Preliminary Results

(No preliminary results section was provided for this Leg).

2.5 Station list M60/2

(No station list was provided for this Leg).

Meteor 60 Leg 3

Mineralogical, geochemical, and biological investigations of hydrothermal systems on the Mid-Atlantic Ridge between 14°45‘N and 15°05‘N (HYDROMAR I)

14 January - 14 February 2004, Fort-de-France - Fort-de-France (Martinique)

T. Kuhn, B. A lexander, N. Augustin, D . Birgel, C. Borowsk i, L.M. de Carv alho, G. Engemann, S. Ertl, L. Franz, C. Grech, R. Hekinian, J.F. Imhoff,. T Jellinek, S. Klar, A. Koschinsky, J. Kuever, F. Kulescha, K. Lackschewitz, S. Petersen, V. Ratmeyer, J. Renken, G. Ruhland, J. Scholten, K. Schreiber, R. Seifert, J. Süling, M. Türkay, U. Westernströer, F. Zielinski

Project Leader: Peter M. Herzig

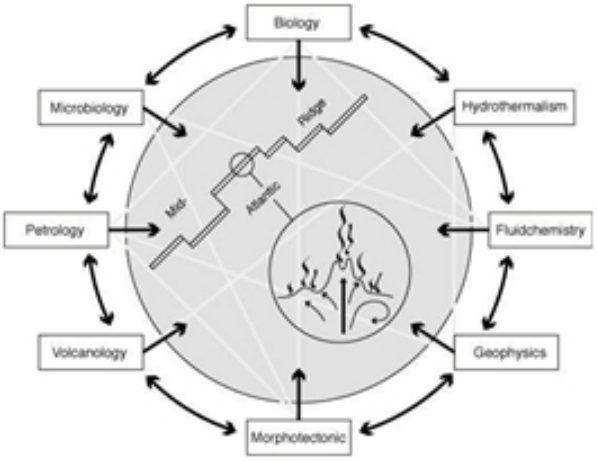

Leitstelle Meteor
Institut für Meereskunde der Universität Hamburg

2012

Table of Contents; Leg 3

Summary

The R/V METEOR cruise M60/3 took place from January 13 through February 14, 2004 from/to Fort-de-France (Martinique) and led to the Logatchev hydrothermal fields situated on the Mid-Atlantic Ridge (MAR) at 14°45‘N and 44°59‘W as well as to a working area II at 14°55‘N and 44°55‘W. The main mapping and sampling tool used during the cruise was the ROV (Remotely Operated Vehicle) QUEST provided by the University of Bremen.

The active Logatchev hydrothermal field lies on a small plateau on the eastern flank of the inner rift valley in 2900 m to 3060 m water depth. It is characterized by sites of active, high-T fluid emanation and sulfide precipitation as well as by inactive sites. Extensive bathymetric and video mapping during the M60/3 cruise revealed three factors which appear to control the location of the Logatchev hydrothermal field: (1) cross-cutting faults, (2) young basaltic volcanism, and (3) slump structures forming probably thick talus deposits. Furthermore a new, but inactive hydrothermal field (Logatchev-4 at 14°42.38‘N / 44°54.50‘W) was discovered during M60/3. Our investigations show that hydrothermal circulation may have taken place through talus material and has altered peridotite debris. The heat is probably supplied from magmatic bodies associated with basaltic melts localized underneath the adjacent rift valley and/or off-axis volcanic structures. Heat could also be provided by localized intrusion of melts (probably focussed along faults) into the peridotite. To date, a situation similar to that of the Logatchev area has only been found at 14°54‘N / 44°55‘W (Eberhardt et al., 1988). The similarity of the local geological setting to that of the Logatchev area indicates that this region has hydrothermal potential.

Mapping and sampling with ROV QUEST and the TV-grab revealed that the active Logatchev-1 hydrothermal field is larger than previously described. It extends at least 800 m in a NW-SE and probably more than 400 m in a SW-NE direction. Two main areas of high-temperature (high-T) hydrothermal activity make up the central part of the field: an area of at least three „smoking craters“ (ANNA-LOUISE, IRINA and SITE „B“) and the large mound of IRINA II with black smoker chimneys at its top as well as the newly discovered QUEST smoking crater. The smoking craters consist of a rampart-like rim that is 1-2 m high and a 2-3 m deep central depression. Dense mussel beds were absent in these environments, macrofauna was generally sparce. However, abundant microbial mats were seen at locations where the black smoke emanating from the sea floor passes over rock surfaces. IRINA II consists of a mound (basal diameter of about 60 m) with steep slopes rising about 15 m above the surrounding seafloor. Four vertical chimneys, a couple of meters high, mark the top of the mound. In contrast to the smoking craters they are densely overgrown with and surrounded by mussels. QUEST is a newly discovered high-T, black smoke venting site situated about 130 m WNW (in 330° direction) of the active chimneys of IRINA II.

Hydrothermal fluids (both high- and low-T) display similar patterns of their chemical composition suggesting the presence of a single fluid type. The emanating high-T fluids are strongly reducing have high methane and hydrogen contents and low sulfide concentrations. Iron is the dominant dissolved and particle-bound metal. However, all hydrothermal fluid samples were diluted by seawater and the results presented here are not yet recalculated to endmember compositions. Methane and hydrogen but also metal sulfides are considered to be the major energy sources for the development of life in the Logatchev field.

Host rocks of the Logatchev field sampled by TV-grab and ROV were mainly serpentinized peridotites while basalts and gabbros (sometimes in magmatic contact with peridotite) occurred subordinately. Remarkable were samples of coarse-grained websterites, orthopyroxenites and orthopyroxene-rich, pegmatoidal norites, which were interpreted as magmatic cumulates from the crust/mantle transition zone. A large variety of hydrothermal precipitates was recovered including chalcopyrite chimneys, massive pyrite crusts, silicified breccias, abundant secondary Cu-sulfides (including native copper), red jaspers, abundant FeMn-oxyhydroxides as well as atacamite and Mn-oxides. The occurrence of massive sulfides as crusts overlying altered host rock material along the flanks of the deposit suggests that they might only be a thin veneer directly at or below the seafloor.

We are grateful to captain M. Kull, the officers and the crew of the R/V METEOR as well the ROV crew for their excellent performance and co-operation which was primordial for the success of the cruise. We are also thankful to G. Cherkashov for providing Russian data and maps prior to the HYDROMAR cruise. The German Research Foundation (DFG) funded this cruise which was carried out within the framework of the DFG Priority Program 1144: From Mantle to Ocean: Energy-, Material- and Life-cycles at Spreading Axes.

3.1 Participants

	Name	Discipline	Institution
1.	Kuhn, Thomas, Dr. / Chief Scientist	Geochemistry	TUBAF/ IfM-GEOMAR
2.	Alexander, Brian	Fluid Chemistry	IUB
3.	Augustin, Nico	Petrology	GeoB
4.	Birgel, Daniel	Biogeochemistry	RCOM
5.	Borowski, Christian, Dr.	Microbiology	MPI-Bremen
6.	de Carvalho, L.M., Dr.	Fluid Chemistry	UFSM
7.	Engemann, Greg	ROV	ASR
8.	Ertl, Siegmund, Dr.	Gas Chemistry	IfBM
9.	Franz, Leander, PD Dr.	Petrology	TUBAF
10.	Grech, Chris	ROV	MBARI
11.	Hekinian, Roger Dr.	Geochemistry	IGW
12.	Imhoff, Johannes, Prof. Dr.	Microbiology	IfM-GEOMAR
13.	Jellinek, Thomas, Dr.	Zoology	Senckenberg
14.	Koschinsky-Fritsche, Andrea, PD Dr.	Fluid Chemistry	IUB
15.	Klar, Steffen	ROV	GeoB/MARUM
16.	Küver, Jan, Dr.	Microbiology	MPA
17.	Kulescha, Friedhelm	Technician	Oktopus
18.	Lackschewitz, Klas, Dr.	Petrology	GeoB
19.	Petersen, Sven, Dr.	Geochemistry	TUBAF
20.	Ratmeyer, Volker, Dr.	ROV	MARUM
21.	Renken, Jens	ROV	MARUM
22.	Ruhland, Götz	ROV	MARUM
23.	Scholten, Jan, Dr.	Geochemistry	IGW
24.	Schreiber, Kerstin	Geochemistry	TUBAF
25.	Seifert, Richard, Dr.	Gas Chemistry	IfBM
26.	Süling, Jörg, Dr.	Microbiology	IfM-GEOMAR
27.	Truscheit, Torsten	Meteorology	DWD
28.	Türkay, Michael, Dr.	Zoology	Senckenberg
29.	Westernströer, Ulrike	Fluid Chemistry	IGW
30.	Zielinski, Frank	Microbiology	MPI-Bremen

ASR	Alstom Schilling Robotics 201 Cousteau Place Davis, CA 95616 / USA
DWD	Deutscher Wetterdienst Geschäftsfeld Seeschifffahrt Bernhardt Nocht Str. 76 20359 Hamburg / Germany
GeoB	Universität Bremen FB Geowissenschaften Postfach 330440 28334 Bremen / Germany

IfBM	Universität Hamburg Institut für Biogeochemie und Meereschemie Bundesstr. 55 D-20146 Hamburg / Germany
IfM-GEOMAR	Leibniz-Institut für Meereswissenschaften Düsternbrooker Weg 20 D- 24105 Kiel / Germany Wischhofstr. 1-3 D-24148 Kiel / Germany
IGW	Universität Kiel Institut für Geowissenschaften Olshausenstr. 40 D-24098 Kiel / Germany
IUB	International University Bremen Geosciences and Astrophysics P.O. Box 750561 D-28725 Bremen / Germany
MARUM	Zentrum für Marine Umweltwissenschaften Universität Bremen Klagenfurter Str. D-28359 Bremen / Germany
MBARI	Monterey Bay Aquarium Research Institute 7700 Sandthold Road Moss Landing, CA 95039-9644 / USA
MPA	Amtliche Materialprüfungsanstalt Bremen Paul Feller Str. 1 28199 Bremen / Germany
MPI-Bremen	Max-Planck-Institut für Marine Mikrobiologie Celsiusstr. 1 D-28359 Bremen / Germany
Oktopus GmbH	Kieler Str. 51 D-24594 Hohenwestedt / Germany
RCOM	Forschungszentrum Ozeanränder an der Universität Bremen Postfach 330440 D-28334 Bremen / Germany
Senckenberg	Forschungsinstitut Senckenberg Senckenberganlage 25 D-60325 Frankfurt a. M. / Germany
TUBAF	TU Bergakademie Freiberg Institut für Mineralogie Lehrstuhl für Lagerstättenlehre und Leibniz-Labor für Angewandte Meeresforschung Brennhausgasse 14 D-09596 Freiberg / Germany
UFSM	Universidade Federal de Santa Maria Caixa Postal 5051 97110-970 Santa Maria-RS / Brasil

3.2 Research Program

(Thomas Kuhn)

The principal scientific aim of leg M60/3 was to investigate the relationship of geological and biological processes in active, ultramafic-hosted hydrothermal systems on the Mid-Atlantic Ridge (MAR) between 14°45‘N and 15°05‘N. Two different sample locations were targeted: (i) the active Logatchev hydrothermal field at 14°45‘N which hosts massive sulfides and (ii) the area at 14°55‘N where a hydrothermal field was described from photo sled investigations and where outcropping oceanic mantle rocks were sampled during previous cruises. The main tools for seafloor investigations and sampling were the new 4000m workclass ROV QUEST provided by the University of Bremen (c/o Prof. G. Wefer, Dr. V. Ratmeyer, MARUM) and the TV-grab. Special tools were adapted to the ROV for biological and fluid sampling.

The research objectives focused on the chemistry of hydrothermal fluids and minerals in relation to the tectonic activity, the composition of the oceanic lithosphere, and the activity of hydrothermal biota. An important question is, whether there is a genetic link between the hydrothermally active Logatchev field and the ultramafic rocks which host the hydrothermal precipitates. The results of these investigations will also improve our understanding of the formation processes of massive sulfide deposits on land which are hosted by ultramafic rocks. Geochemical and biological work focused on the interaction of hydrothermal fluids and biota in hydrothermal systems. Major objectives are the analyses of chemical species in the hydrothermal fluids (both, gaseous species and metals) and their interaction with the colonization patterns, the functional roles and the activity patterns of hydrothermal bacteria, archaea and fauna. A central issue in these investigations is the transition of inorganic and organic compounds and energy that is provided by electron donating reduced gases (i.e. diluted H_2, H_2S, CH_4) from the geochemical level to the biological level of the hydrothermal communities. The influence of supercritical phase separation on the fluid chemistry, mineral precipitation and the structure of hydrothermal communities are also addressed.

Hydrothermal systems hosted by ultramafic rocks, which are characterized by active hydrothermalism as well as active serpentinization, are especially suitable for combined research on the above-mentioned scientific objectives. The research cruise M60/3 was carried out within the frame of the DFG-Priority Program 1144 “From Mantle to Ocean: Energy-, Material- and Life-cycles at Spreading Axes”.

3.3 Narrative of the Cruise

(Thomas Kuhn)

Cruise M60/3 started on January 13, 2004 in Fort-de-France (Martinique) with loading the scientific equipment onboard R/V METEOR, the built-up of the ROV QUEST as well as a harbour test of a new deployment frame for the ROV. The scheduled departure on January 15 had to be postponed for 33 hours due to a faulty acoustic array of the POSIDONIA navigation system. Since the exact positioning of the ROV was an essential part of the scientific work, we decided to wait for a spare one which was sent from France. On January 16, at 21:20 LT

R/V METEOR departed from Fort-de-France and started its transit to the Logatchev hydrothermal field at 14°45'N and 44°59'W.

The working area was reached on January 20 at 20:00 LT. Scientific work started with the deployment of a reference station for the POSIDIONIA ROV navigation. During the night HYDROSWEEP mapping, a CTD station as well as the calibration of the reference station kept the vessel busy.

Due to two crossing swells which caused strong rolling vessel movements the first ROV station could not be carried out on January 21. Instead, the HYDROSWEEP mapping was continued. During the night a long TV-sled (st. 22, Fig. 3.1) track was run over the eastern rift valley flank crossing the Logatchev-1 hydrothermal field down to the central valley floor.
Since the weather and sea conditions improved on January 22 the first ROV station could be carried out. The swell still was about 2-3 m and both the ROV and the ship's crew made a very good job to deploy the ROV QUEST. In the course of this first ROV station the northwestern part of the Logatchev-1 hydrothermal field was mapped and sampled in 3060 m to 3050 m water depth. A previously unknown site with diffuse venting hydrothermal fluids, a mussel field and wide-spread bacterial mats were discovered south of ANYA'S GARDEN. A temperature logger was deployed and fluid measurements carried out. After the investigation of this diffuse venting site, QUEST moved to the IRINA II complex about 100 m ESE (Fig. 3.2). This complex consists of a mound structure of about 60 m diameter at its base and 15 m height. Active black smoker chimneys, 2-4 m high, are situated on its top. The chimneys are densely overgrown by hydrothermal fauna and are surrounded by mussel fields. A temperature logger and a homer beacon were placed close to a marker of the French-Russian campaign MICROSMOKE. All ROV systems worked well and the video data were of excellent quality.

HYDROSWEEP mapping was carried out during the night. On January 23 a first TV-grab station in the Logatchev-1 field was unseccussful due to a technical failure of the grab. The following TV-sled transect (st. 27) from the rift mountains at 1600 m water depth to the socalled Logatchev-2 field in 2650 m water depth discovered a new hydrothermal field. Since three hydrothermal fields called Logatchev-1 to Logatchev-3 were previously known in this area, we called the new one Logatchev-4 (Fig. 3.1). It is an inactive field with beds of empty shells and is about 90 m long. It was found about 50 m below a ENE-WSW ridge. It seems that the shells were displaced from the ridge. The exact position of the TV-sled on the seafloor was calculated using the POSIDONIA system (with a transponder mounted on the sled). HYDROSWEEP mapping was continued during the night.

During station 29ROV on January 24 the area between IRINA II and IRINA was mapped (Fig. 3.2). Two so-called smoking craters (site "B" and IRINA) were investigated and fluid samples were taken. Due to a drop of oil pressure the station had to be aborted and no sulfide samples could be taken. HYDROSWEEP mapping was continued during the night.

Three TV-grab stations were carried out on January 25 (32, 33, 35GTV; Fig. 3.2). Numerous samples of massive sulfides and crusts, vein quartz, mussel beds on silicified hydrothermal crusts, atacamite as well as ultramafic rocks with different degrees of serpentinization were sampled. Two hydrocast profiles were carried out north of and within the Logatchev-1 field.

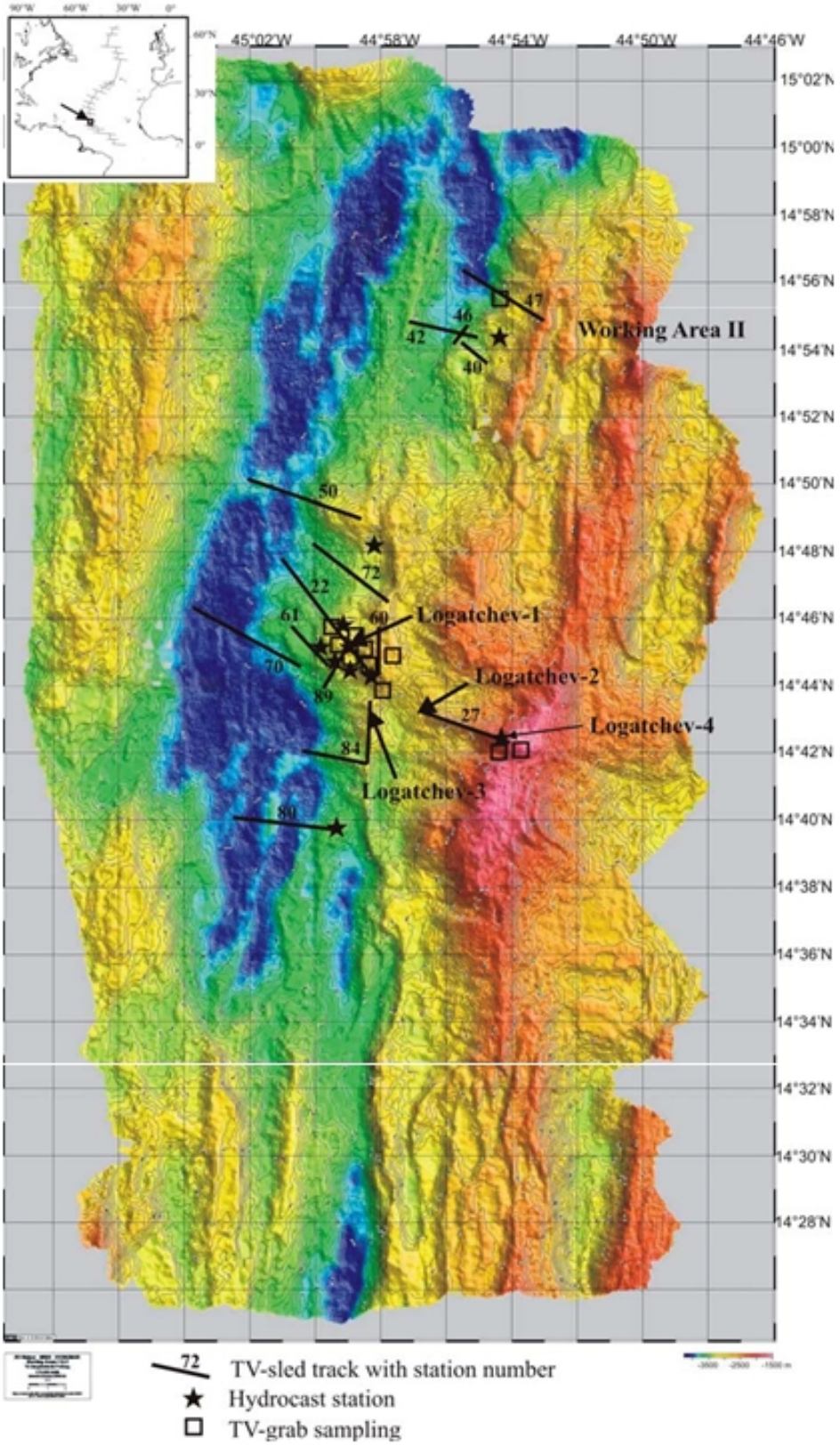

Fig. 3.1: Bathymetric map of the working area produced with HYDROSWEEP during M60/3. TV-sled, hydrocast (CTD/Ro.) and TV-grab sampling stations are also shown. All ROV operations were carried out in the Logatchev-1 hydrothermal field. Insert: Location of the working area on the MAR

On January 26 station 38ROV was reserved for biological and fluid-chemical work at the IRINA II complex. At the beginning of the station two baited traps were deployed on the mussel beds near the chimney complex. They were recovered at the end of the station. Diffusely venting fluids were sampled for geochemical and microbiological investigations, hydrothermal fauna was collected for taxonomic and molecular research. Detailed video images of the habitat of shrimps and mussels were recorded. The total duration of the station (from deck to deck) was 14 hours. It started with technical checks at 8:00 a.m. which took about 1 hour, lowering and hieving through the water column took 4 hours in total, therefore time for the work at the seafloor was 8-9 hours.

The Russian R/V PROFESSOR LOGATCHEV arrived at the working area on the evening of January 26. Captain (M. Kull), the chief scientist (T. Kuhn) and two other scientists (K. Lackschewitz and R. Hekinian) went over to the Russian vessel to discuss and organize the research work of the coming days. After a two hours visit they returned to the R/V METEOR. A two hours transit to working area II at 14°55'N and 44°55'W was followed by two TV-sled tracks (st. 40, 42; Fig. 3.1) interrupted by HYDROSWEEP mapping on January 27. The objective of these tracks was to map the area and to relocate a hydrothermal field which was suggested by other workers (Eberhardt et al., 1988). Rather young basalts, small pillow mounds and ridges, some larger scarps and crosscutting faults were observed, but no hydrothermal activity was found. Unfortunately two attempts of ROV deployment failed due to bad sea conditions and a winch problem. A hydrocast station (st. 44 on January 28) close to a station of Charlou et al. (1993) detected strong methane and hydrogen anomalies in the water column at least suggesting strong serpentinization in this area (Fig. 3.1). Two mor TVsled tracks (st. 46, 47; Fig. 3.1) on January 29 were conducted to map the contact between ultramafics and basalts in working area II above the suggested hydrothermal field. According to the results of station 47 a TV-grab taken right beneath a scarp sampled ultramafic rocks which, in one case, showed mylonitic textures, in another a magmatic contact between ultramafics and basalts (see Chapter 3.4.6). HYDROSWEEP mapping carried out on January 28 and 29 filled gaps in the bathymetric map. Another TV-sled station (st. 50) carried out along the eastern flank of the rift valley between working area I and II revealed only ultramafic rocks even in the rift valley. The rift axis area consists of a succession of undulating hills. Three fissures most likely mark the current rift axis.

During the night between January 29 and 30, R/V METEOR returned to working are I (Logatchev fields). Two hydrocast stations south of the Logatchev-1 hydrothermal field investigated the hydrothermal plume dispersal in the water column. On January 30 sea conditions made the next ROV station (53ROV) possible. This geological dive aimed at detailed mapping and sampling of the smoking craters IRINA and ANNA-LOUISE (Fig. 3.2). The general dimension and structure of the smoking craters was mapped and video-recorded, active and inactive chimneys were sampled using both manipulators. Fluid samples from black smokers on the rim of the smoking craters were also taken. Another TV-grab (54GTV) was taken on a small mound about 100 m to the east of the smoking crater area in order to sample the periphery of the Logatchev-1 field (Fig. 3.2). The samples consist of secondary Cu-sulfides with carbonate veins, silica and grains of native copper suggesting that this area also was a site of high-temperature precipitation in the past which is now in a state of oxidation. During the night HYDROSWEEP mapping was continued.

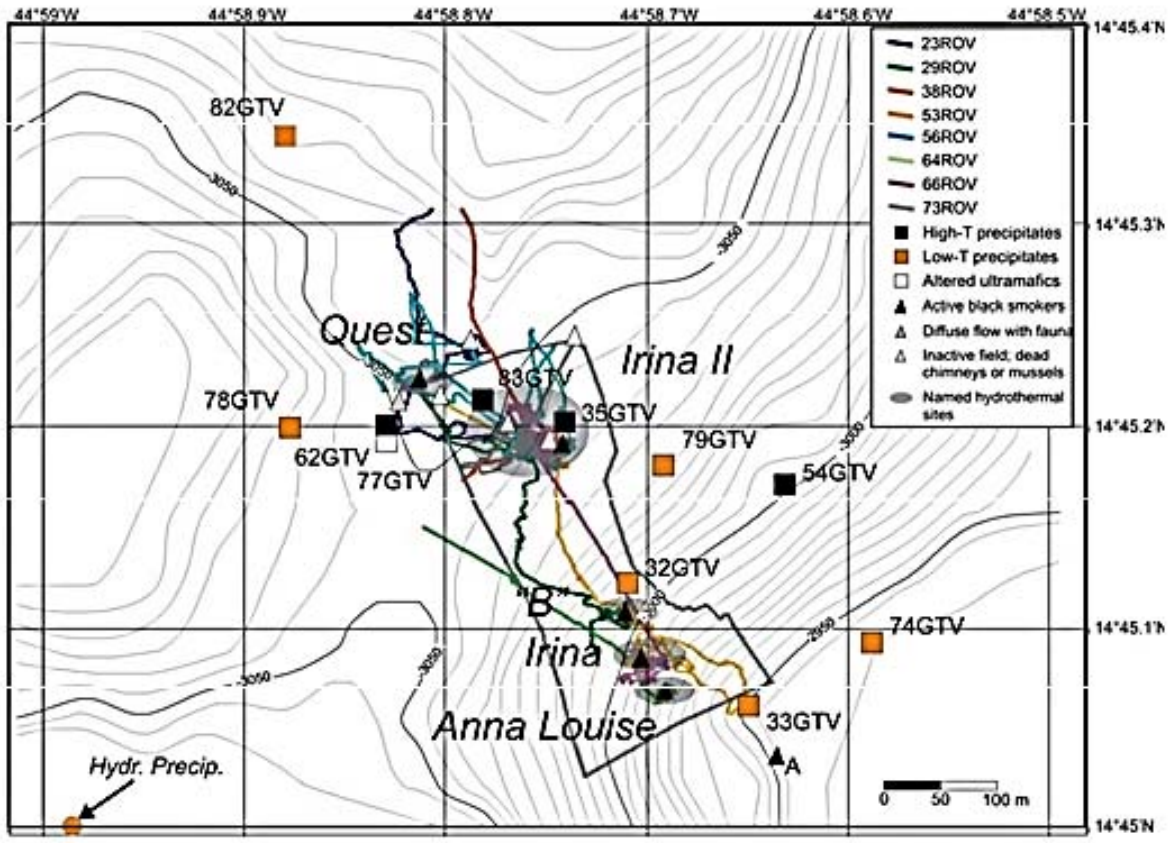

Fig. 3.2: Logatchev-1 hydrothermal field with ROV tracks and TV-grab stations carried out during M60/3. QUEST is a newly discovered site venting high-temperature black smoke. Site"A" was not obserevd during M60/3 but described in literature (Gebruk et al., 2000). Hydrothermal precipitates (but no current hydrothermal activity) were also observed during station 89OFOS about 500 m to the SW of the Logatchev-1 field.

During dive 56ROV on January 31 biological and fluid samples were taken from IRINA II and ANYA'S GARDEN (Fig. 3.2). A special objective was the investigation of ANYA'S GARDEN since this site was described as a place where species of Calyptogena should occur. This species is specialized in H_2S-rich fluids and therefore this site should be different from other sites of the Logatchev-1 field where CH_4- and H_2-rich fluids emanate. However, no field with live Calyptogena could be found, neither at the location of the marker ANYA (this marker was not in the place where it should be according to literature; Gebruk et al., 2000) nor at the location described by other authors. However, during dive 56ROV a new black smoker venting site was detected and named after the ROV as QUEST site (Fig. 3.2). At this site but also at the smoker complex of IRINA II samples of Bathymodyolus and Calyptogena (a few specimen of Calyptogena occurred) together with shrimps (Rimicaris exoculata) and accompanying fauna (crabs, polychaets etc.) were taken. At QUEST bacterial mats were sampled with a special shovel adapted to the ROV. Directly above the mats fluid samples were also taken and fluid parameters (T, O_2, Redox, H_2S) were measured with an in-situ fluid measuring system (PROFILUR). Station 56ROV ended at 21:00 on January 31. The following night and during February 1 a TV-grab station on the shallowest point of the eastern valley walls (1600 m water depth; Fig. 3.1) and two hydrocast stations to the west and southwest of

the Logatchev-1 field were carried out. The TV-grab sampled different types of serpentinized ultramafic rocks, basalts and one amphibolite. The hydrocast revealed several methane and hydrogen anomalies in different water depths. Later this day two TV-sled tracks (st. 60, 61; Fig. 3.1) were run in the areas east and west of Logatchev-1. The objective of st. 60 was to map the plateau above the Logatchev-1 field and of st. 61 to map the contact between ultramafics and basalts and to investigate the round-shaped feature close to the central valley floor (Fig. 3.1).

The night to February 2 was filled with another TV-grab station (62GTV) to sample an area west of the main active zone of the Logatchev-1 field. This grab sampled serpentinized and mineralized ultramafics, pyroxenites, scoriaceous black breccia and also sulfide-rich material. After two HYDROSWEEP profiles, the next ROV QUEST station (64ROV) was aimed at mapping and sampling the smoking crater ANNA LOUISE for geological and geochemical investigations (Fig. 3.2). Apart from this work, temperature loggers were recovered from IRINA which measured diffusely venting hydrothermal fluids for 3.5 days. February 2 was completed by HYDROSWEEP profiles.

QUEST station 66ROV on February 3 again concentrated on biological and fluid-chemical sampling and experiments at sites IRINA and IRINA II. Microbial mats were sampled at locations where black smoke emanating from the sea floor was in contact with rock surfaces close to an old marker at IRINA (FIG. 3.2). Temperature measurements were carried out and fluid samples taken immediately above these bacterial mats. At the northwestern slope of the IRINA II mound only empty shells of Calyptogena but living ones of Bathymodiolus were found. At this site of diffuse venting living mussels were sampled. The sampling was completed by fluid samples and measurements of fluid parameters with PROFILUR.

On February 4 one TV-grab station (67GTV), three hydrocast stations and one TV-sled track (st. 70) were carried out. The TV-grab was aimed at sampling the Logatchev-4 hydrothermal field (Fig. 3.1). However, due to the very steep morphology it was only possible to take samples about 50 m below the field. The samples consisted of coarse-grained pyroxenits, peridotites and metabasalts in direct contact with ultramafics and one empty shell of Bathymodiolus. The hydrocast stations were carried out in the N, S, and E of Logatchev-1. A transponder was mounted on the hydrocast frame for exact positioning using the POSIDONIA system. The objective of these stations was to investigate the hydrothermal plume structure of the Logatchev-1 field. Mapping of the central valley floor close to the Logatchev-1 field was the objective of the TV-sled station.

February 5 started with another TV-sled (st. 72) which investigated steep morphological structures at the eastern rift flank north of the Logatchev-1 field and mapped the contact between ultramafics and basalt. It turned out that the seafloor consists of several nearly vertical escarpments which may mark young fault zones along which mantle material was tectonically emplaced. After this TV-sled track another ROV station (73ROV) explored the immediate surroundings of the Logatchev-1 field in order to map possible fault planes, to map the arial extension of the currently hydrothermally active area and to add information about how far hydrothermal precipitates reach away from the current active zone (Fig. 3.2). It could be shown during this station that the Logatchev-1 field extends far mor to the N and SW than previously known. Some samples from inactive chimneys at IRINA II were also sampled

using the manipulators of the ROV and two baited traps were deployed at a mussel field close to the smoker complex of IRINA II. Station 73ROV was followed by another TV-grab (74GTV) which sampled the mound that was mapped east of the smoking craters during the previous ROV station.

February 6 was used for hydrocast, TV-grab and TV-sled stations. A ROV deployment was not possible due to increasing and crossing swells from E and NNW. The hydrocast stations (75, 76 CTD/Ro) sampled the hydrothermal plumes to the SSW of the Logatchev-1 field. Three TV-grab stations (st. 77, 78, 79; Fig. 3.2) were aimed at sampling the periphery to the E and W of the Logatchev-1 field and also to get rock samples from the surrounding of the field. All three stations were successfull and recovered low-T hydrothermal precipitates which mark the distal part of the hydrothermal field were strong dilution of hydrothermal fluids by entraining seawater prevails. During the TV-sled track of st. 80 an area about 5 nm to the south of the Logatchev-1 field was mapped where a distinct methane anomaly (but only a weak hydrogen anomaly) was found in 2800 m water depth (Fig. 3.1). The track started at the eastern flank of the rift valley, crossed the position of the methane anomaly and was continued over most parts of the central valley mapping a pillow basalt ridge.

The wind continously increased to Bft. 8 on February 7 and the sea swell also gradually built up. Therefore, a ROV station was still impossible on this day. We continued our geological and geochemical program with two hydrocasts in the area SE of Logatchev-1, one TV-grab and one TV-sled station. The hydrocast stations should further improve our understanding of the hydrothermal plume structure around Logatchev-1. Station 83GTV (Fig. 3.2) aimed at sampling a mussel bed for a statistical analysis of the size distribution of species Bathymodiolus. The TV-sled track (st. 84) was run over Logatchev-3 to map the hydrothermal precipitates and the distribution of ulramafics and basalts in this area (Fig. 3.1).

The bad weather with heavy sea and wind continued on February 8 and therefore no ROV deployment was possible. Instead, the geological and geochemical program was continued as on February 7 with two hydrocast stations, one directly over Logatchev-1 and one to the SSW, one TV-grab and one TV-sled. The objective of the TV-grab (st. 87) was to sample large-sized ultramafic rock samples close to Logatchev-1 for separating zircon for age dating. The TV-sled track (st. 89) was carried out from the Logatchev-1 field to the SSW in order to map fault structures and the contact between ultramafics and basalt. During this station hydrothermal precipitates were discovered about 600 m WSW of ANNA LOUISE (Fig. 3.2). If there is a connection between Logatchev-1 and these precipitates, this hydrothermal field would be much larger than previously known. The recovery of the reference station was also realized on February 8.

The station work was finished on February 9 at 03:35 LT and R/V METEOR started its transit to Fort-de-France. Arrival in FdF was on February 13 at 08:00 LT. Container were unloaded from the vessel on this day and the cruise M60/3 ended on February 14 with the disembarkation of the scientific crew.

The original scientific program included a third working area at 15°05'N/44°58'W (20 nm north of the Logatchev field) to be investigated with the ROV QUEST. However, the main working area was the Logatchev-1 hydrothermal field. Especially, the biological and fluid chemistry groups concentrated on this working area. They needed a minimum number of 10

ROV stations for their experiments and sampling. Since we could carry out only 9 successful ROV stations in the entire Logatchev field we had to stay there in order to get another chance if the weather increased. However, the bad weather conditions also stayed during the last days of the cruise and made another ROV deployment impossible. Therefore, we decided to do more geological (TV-sled and -grab) and water-chemical work (hydrocast) in the Logatchev field for a better understanding of this area instead of going to working area III where gathering new knowledge on top of what was already known would have been impossible without the ROV.

3.4 Preliminary Results

3.4.1 Seafloor mapping and structural geology

(R. Hekinian, T. Kuhn)

3.4.1.1 Introduction

In contrast to the fast spreading East Pacific Rise (EPR), the Mid-Atlantic Ridge (MAR) with its low spreading rates (< 3 cm/yr, total rate) consist of ridge segments with a more discontinuous and irregular shaped structure. These ridge segments away from the influence of large mantle plume upwelling zone such the Azores and Iceland show also thinner crust gashed by a deep (>3000m) central rift valley. Thin crust suggests a low rate of magmatism and the eventual exposure of lower and upper mantle material, such as ultramafics and gabbro. Thus magma-starved segments of the MAR are found in the equatorial region between 12ºN and 16ºN. These areas are also characterized by short ridge segments interrupted by non-transform discontinuities as well as closely spaced major fracture zones such as those located between 5ºN and 5ºS which extend from African to Brazilian coasts.

In 1993-1994 the Russian scientific team aboard the R/V PROFESSOR LOGATCHEV has found a hydrothermal field which they called the " Logatchev field" located on the eastern rift mountain of the MAR south of the "Fifteen-Twenty fracture zone and near 14º45'N (Batuyev et al., 1994). The main characteristic of the spreading ridge segment at 14º45' N is the presence of important serpentinized peridotite outcropping on the rift valley floor as well as on the eastern and western walls of the ridge axis.

Also, during previous exploration along the MAR it was found that the rift valley flanks are sometimes the main location for hydrothermalism associated with ultramafics as well as with MORB. This was observed for example at 26º00'N-26º13'N in the TAG and at 14º-15ºN on step faulted terrains of the rift valley eastern marginal walls (Batuyev et al., 1994; Rona et al., 1992). Although most hydrothermal sites are associated with basaltic lavas erupted in the axial valley, two areas of the MAR which were studied in detail are known to have been the sites of hydrothermal activities forming sulfide deposits on top of ultramafic rocks. These areas are the Rainbow hydrothermal field near 36º14'N/33º54.12'W (German et al., 1998) and the Logatchev fields near 14º45'N-45º00'W (Batuyev et al., 1994).

The origin of these hydrothermal deposits constructed on top of ultramafics is not well assessed and controversial. Are these hydrothermal deposits directly connected with the leaching of ultramafic complexes of lower crust-upper mantle composition? Or are they, instead, related to the leaching of the mafic components (basalt-dolerite-gabbro) intruded into

the lithosphere? If the hydrothermal precipitates originated from the basalic and/or mafic intrusive dolerite than it is likely that hydrothermal circulation would take place within basaltic basement formed at the ridge axis. Another alternative to this hypothesis is that the off-axis hydrothermal venting and the associated ultramafics are underlain by basaltic units. This implies that the ultramafic complex on which the hydrothermal deposits are formed represent large mass-wasted material covering the basaltic basement. This is further discussed below.

3.4.1.2 Rift valley

The rift valley floor at 3900-4200 m depth consists of a moderately (< 30%) sedimented area with isolated volcanic constructions forming small mounds and elongated ridges often with step faulted outcrops. The previous sampling of the rift valley, mainly in the northern part (north of 14º50'N), showed the presence of both ultramafics and basaltic rocks. The present study confirms this finding and shows that basaltic outcrops are prominent in the rift valley deeper than 3900 m (Fig. 3.3). It was also found that the spreading is taking place in a narrow zone (< 1 km) with active fault scarps and recent fissures oriented N010º. The younger flows observed are tubular and bulbous lava with preserved small protrusions extruded from the larger pillows. Sheet flows in the form of lobated, flat and ropy surfaces were observed during deep-towed bottom camera stations. The sheet flows often show collapse features of drained lava.

3.4.1.3 Rift mountains

The eastern and the western wall of the rift mountains axis are dissymmetrical with respect to the axis of the MAR spreading center near 14º45'N. In the explored area, the summits of the east and west walls culminate at 1600 meters and 2900 meters, respectively. These contour lines are located at about 10 km and 4 km from the MAR axis. Also the east rift mountain is characterized by several cross-cutting faults. The main orientation of the fault scarps is N010º which also corresponds to the general spreading direction. The other direction of faulting is to N270º-280º which is transverse to the other main fault structures.

The rift mountains region located to the east of the rift valley at 14º45'N and along longitudes 45°00'W and 44º52'W constitutes the prominent features of ridge crest marginal highs oriented to N013º as the MAR axis (Fig. 3.3). The summit of the first discontinuous set of the rift mountain consists of a plateau culminating at about 2900 m water depth that is about 1000 meters above the rift valley floor (4100 m). The eastern wall at the 3050 m contour line shows a narrow, "sliver-like" linear structure oriented to N013º representing the summit of the first rift flank. The top of the rift mountain there is a narrow, " sliver-like" structure (<300 m wide) which has a small east facing depression (<300 m depth). A bottom video camera station (60OFOS) along this plateau near 2970 m depths showed abundant sediment cover and horizontal ledges of ultramafic outcrops associated with patches of inactive hydrothermal fields made up of empty clam shells. This newly discovered field was named Logatchev-4 hydrothermal field according to the already known Logatchev-1 to -3 fields in this area

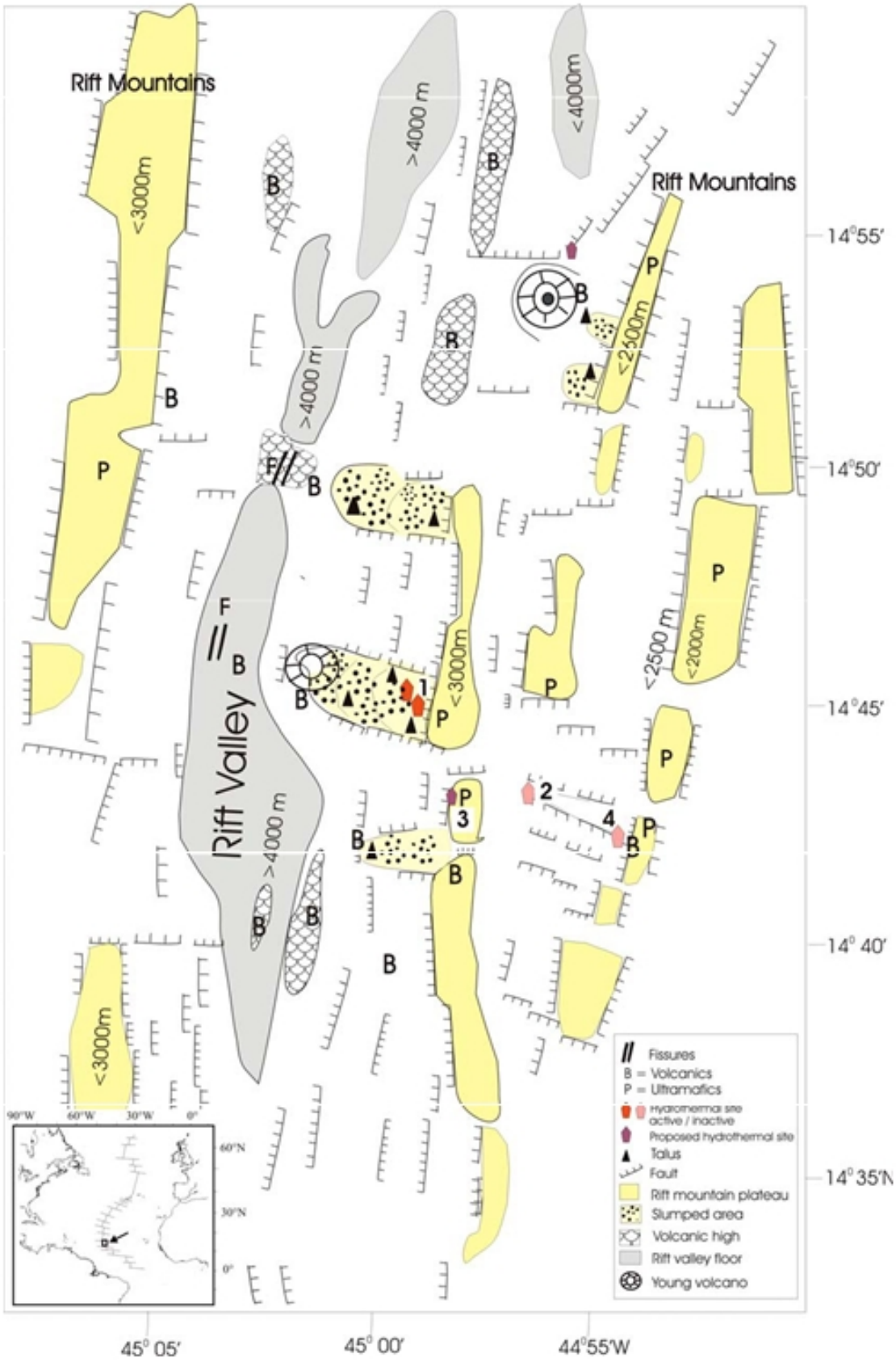

Fig. 3.3: Sketched structural interpretation drawn after multichannel (HYDROSWEEP) bathymetric data of the MAR segment near 14º45'N - 45º00'W obtained during M60/3. Note the cro ss-cutting faults and the fault-related occurrence of hydrothermal fields. 1, 2, 3, and 4 are separate hydrothermal fields (Logatche v 1-4). Sma ll figure: locati on of the working area at the MAR.

(Fig. 3.3). The west facing flank of this east rift mountain wall between 2950 m and 3600 m depths consists of several small staircase scarps representing normal faults that are also oriented N013º (Fig. 3.1 and 3.3). Several (3) of these scarps are covered with large „land slides“ forming poorly sorted talus made up of large blocks consisting of mafic and ultramafic rocks (Fig. 3.3 and 3.4). Another OFOS station (84OFOS) carry out along a N-S track on top of the plateau near 14º43’N/44º58.50’W at about 3020 m water depth shows in situ massive ultramafic outcrops. These outcrops extend few hundreds of meters along faulted scarps. Further to the south near 14º41.70’N/44º58’W a volcanic construction made up of pillow lava was seen at about 3000 m water depth.

The rift mountain becomes shallower (1600-2400 m) further to the east with steep faulted scarp culminating with a plateau along longitude 44º52’W (Fig. 3.3). When extrapolating from a TV station (27OFOS), several of these scarps, near 14º42’N/44º52’W at 2700 and at about 2500 m depth, show in situ outcrops of serpentinized peridotite alternated with basaltic flows. This is inferred from the altered debris of metabasalts and other basaltic rocks and serpentinized peridotite recovered at 1608m and 1950 m depths near 14º42.3’N and 44º51.87’W (stations 57 and 63GTV).

The rift mountain walls going from the summit (plateau 2900m depth) of first rift mountain down to the intersection with the rift valley at 3850 m depths consists of several step faulted structures with small relief which are often buried by slumped material. However, during two video camera stations (84- and 89OFOS) large ultramafic blocks were observed and it is not clear weather these large blocks are in place or if they represent down slope transported debris.

3.4.1.4 Off-axis volcanoes

Two off-axis volcanoes of less than 500 m height were detected during multichannel bathymetric survey (HYDROSWEEP) and observed during deep towed camera stations. They are located on the eastern margin of the rift valley at the intersection with the rift flank located near 14º45’N and 14º55’. They consist of basaltic flows and show recent faulting and collapsed features.

3.4.1.5 Slumped structures

The presence of irregular bulged features bounded by E-W oriented transverse faults on the eastern rift flank are believe to represent slumped structures as defined from the concentric oval shaped contour lines observed from bathymetry (Fig. 3.3 & 3.4). These features are bounded by “en echelon” faults and form several “step like” terraces bounded by west facing small and semi-circular scarps (<100 m relief) covered with talus material. The terrace and steps extend down to the western slope at the intersection with the rift valley floor. The sizes of these slumped structures vary from about 1 - 4 km in length and 1-2 km in width. The mass-waste forming these slumped structures extends more than 4 km down slope of the eastern wall between 3100 and 3400 m depths (Fig. 3.3 & 3.4). They are covered by pelagic and hydrothermal sediments, with some isolated patches of loose tabular and irregular shaped blocks of ultramafics. The irregular distribution of the sediment and the avalanche debris indicates that the slumping is still an on-going process, probably as the result of major

tectonic events that must have taken place during the uplift of the rift mountains forming the rift valley walls. The ultramafics are believed to represent debris of dislocated material from the rift flank plateau shallower than 3000 m depths bounding the rift valley to the East immediately above the Logachev hydrothermal field.
Hydrothermal circulation taking place throughout the talus debris has possibly reworked and altered the serpentinized rock fragments. Indeed, sulfur-bearing ultramafic fragments found underneath the hydrothermal chimneys and the surrounding area were collected during several ROV and television grab-sampling stations.

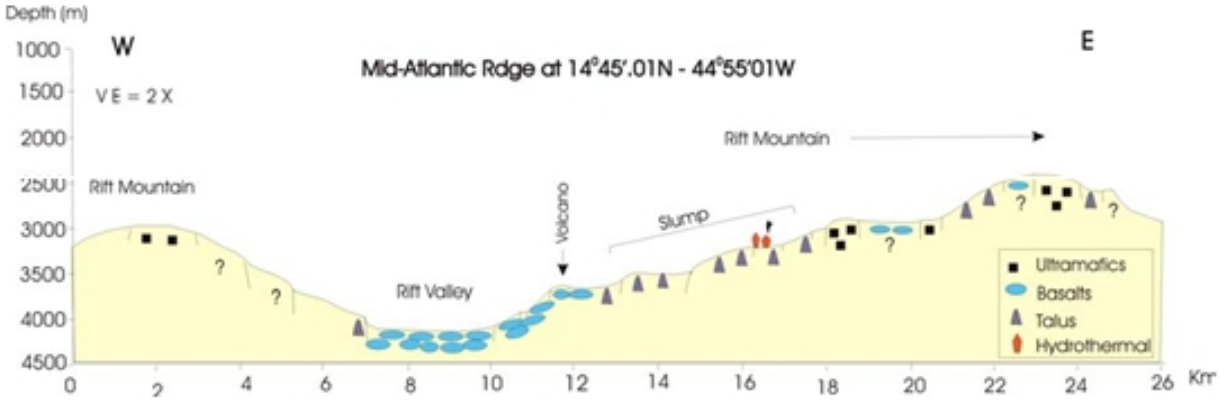

Fig. 3.4 Geological profile (East-West) constructed from bathymetric contour lines at latitudes 14°45.01'N. The geology is inferred from seafloor obs ervations and sampling d uring cruise M60/03. VE = vertical exaggeration.

3.4.1.6 The formation of the Logatchev hydrothermal field

The formation of hydrothermal deposit on top of serpentinized peridotite is believed to result from the circulation of hot fluids through fissured and faulted terrain associated with avalanche debris forming a porous medium (Fig. 3.5). The heat is probably supplied from magma cooling associated with basaltic melts localized underneath the adjacent rift valley and/or off-axis volcanic structures. Also it is not excluded that heat could be provided by localized intrusion of magmatic melts into the peridotite during partial melting. The presence of gabbroic and dolerite fragments with magmatic contacts to the ultramafic rocks indicates late intrusion of magma post dating the emplacement of the serpentinized ultramafics.

3.4.2 Geology and morphology of the Logatchev-1 hydrothermal field

(T. Kuhn, K. Schreiber)

The Logatchev-1 hydrothermal field is situated on a plateau right below a 350 m high cliff at a water depth of 3060 m to 2900 m. Mapping and sampling with ROV QUEST and the TV-grab revealed that the field is larger than previously described (Mozgova et al., 1999;
Cherkashev et al., 2000; Gebruk et al., 2000). It extends at least 800 m in a NW-SE and 400 m in a SW-NE direction (Fig. 3.2). Even about 600 m to the SW of the main mound hydrothermal precipitates have been detected during a TV-sled track (st. 89; Fig. 3.2 & 3.6). Two main areas of high-temperature hydrothermal activity make up the central part of the

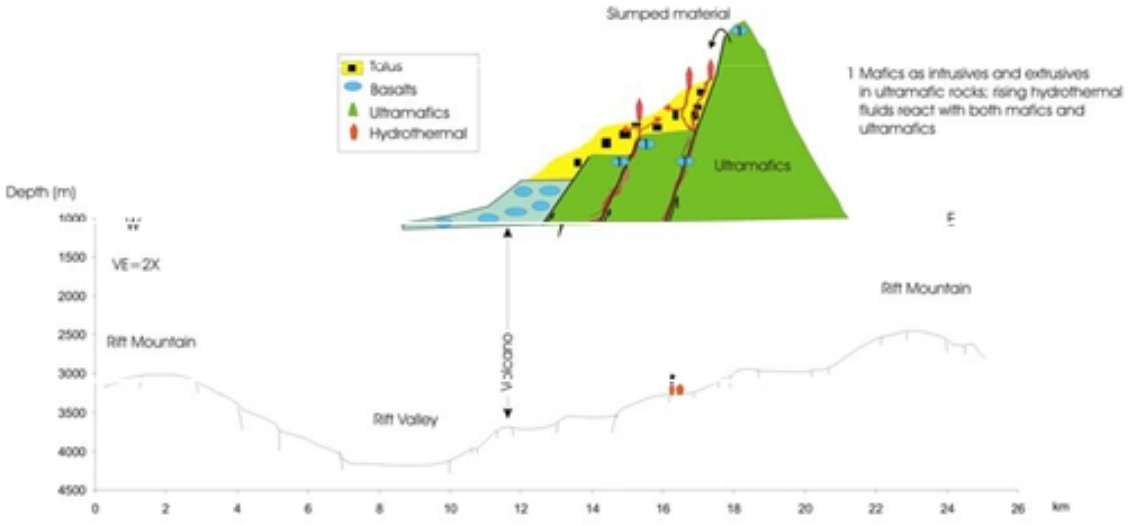

Fig. 3.5 Model for the formation of the Logatchev hydrothermal fields near 14°45‘N. The rise of hydrothermal fluids may be partly co ntrolled by fault structures at depth. Fluid-rock reactions may take place within ultramafic and b asaltic/gabbroic rocks. Porous talus material formed from large slumpings may provide pathways for large-scale hydrothermal precipitation at and beneath the seafloor. VE= vertical exaggeration.

field: an area of at least three „smoking craters“ (ANNA-LOUISE, IRINA and SITE „B“) and the large mound of IRINA II with black smoker chimneys at its top as well as the newly discovered QUEST smoking crater (Fig. 3.2). The smoking craters show a rim that is 1-2 m high and a 2-3 m deep central depression. ANNA-LOUISE seems to be the largest crater observed having a diameter of about 10 m, whereas IRINA and „B“ have distinctly smaller craters. Up to 2 m high, delicate chimneys are situated on the crater rims. They immediately broke when touched by the ROV manipulators. Black smoke was intensely venting at all three sites, either from the chimneys on the crater rim or from holes in the ground within the craters. At one chimney (the so-called “Candelabrum” at the rim of ANNA-LOUISE) black smoke with both a strong bouyancy but also with nearly no bouyancy (being horizontally dispersed) were observed. Strong bottom currents which changed direction during individual ROV dives resulted in almost horizontal plume dispersal for some black smokers. Dense mussel beds were absent in these environments, and first inspections of the video material revealed that conspicuous hydrothermal fauna was largely restricted to alvinocarid shrimps occuring in moderate numbers, a few crabs (Segonzacia), unidentified actinians, the hydrozoan Candelabrum and several species of fish (Fig. 3.7). Abundant microbial mats were seen at locations where the black smoke emanating from the sea floor was in regular contact with the surfaces. First inspections of a 3d-model of the seafloor morphology based on ROV depth data suggest that the smoking craters are not sitting on top of a large mound structure but that they rather form single uprisings on the seafloor causing a terrace-like appaerance of an otherwise steep slope (Fig. 3.6).

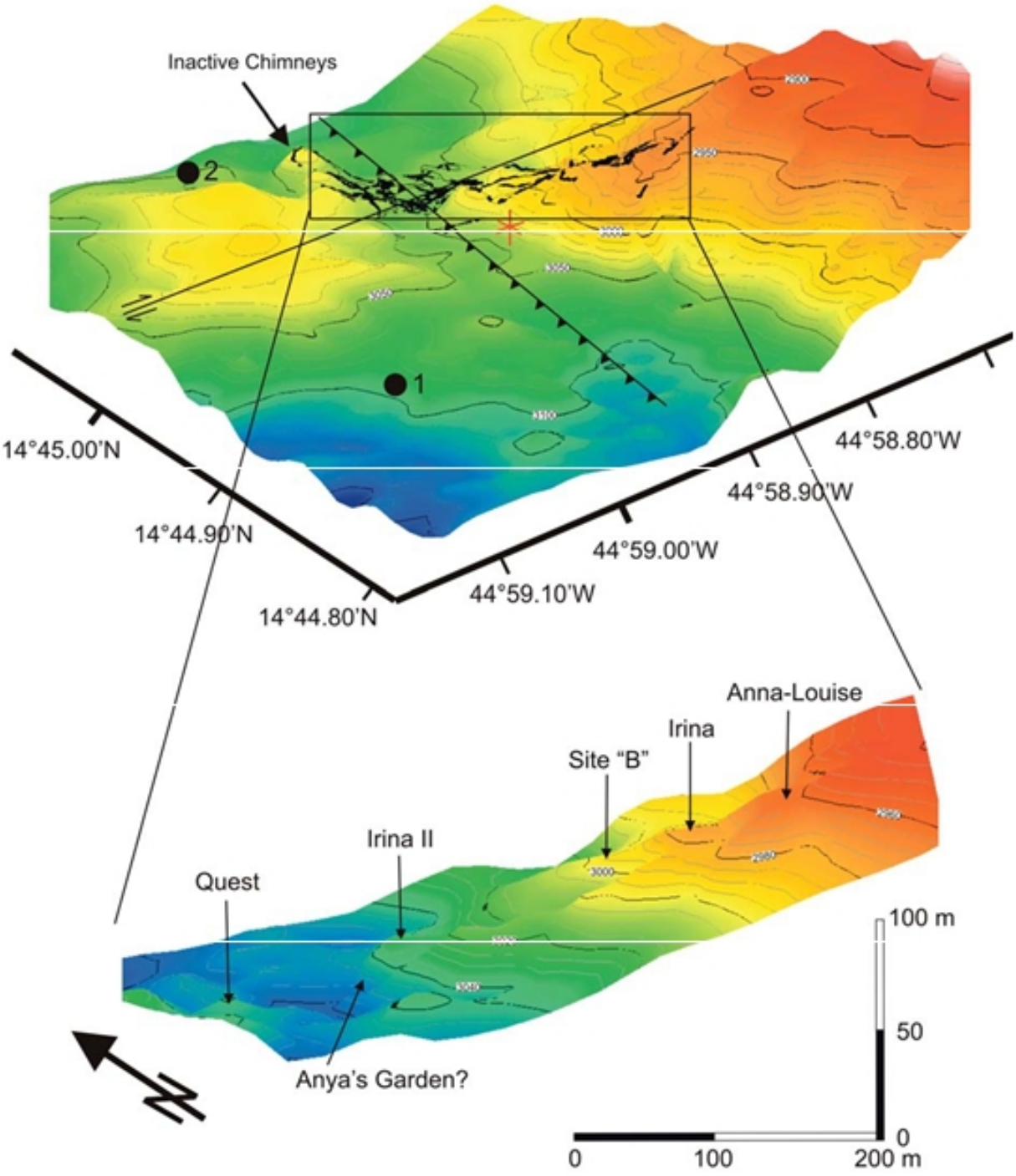

Fig. 3.6 Perspective view of the bathymetry in the vicinity of the Logatchev-1 hydrothermal field based on HYDROSWEEP and ROV data (upper figure). The rectangle marks the outline of the field as known before the cruise M60/3 (Mozgova et al., 1999). Point "1" marks hydrothermal precipitates detected during a TV-sled station, "2" marks low-T precipitates sampled by TV-grab station 82. At this site a T-anomaly of 0.12°C in the near-bottom water was also detected during TV-sled station 22. The normal and transverse faults are interpreted structures (see Fig. 3.3); black lines are ROV dives. The lower picture displays details of the Logatchev field based on ROV depth data. Note that the smoking craters (Anna-Louise, IRINA and Site "B") occur on top of a terrace-like morphology rather than a mound. Both figures are 1.5x vertically exaggerated.

IRINA II consists of a mound with steep slopes rising about 15 m above the surrounding seafloor. The round to elongate structure has a basal diameter of about 60 m. Four vertical chimneys, a couple of meters high, mark the top of the mound. The chimneys are densely overgrown with mussels (Bathymodiolus cf. puteoserpentis; Fig. 3.7). Shrimps (Rimicaris exoculata) gather in large numbers over low-T fluid vents along the sides of the chimneys. The chimneys are surrounded by densely populated mussel beds and also by inactive chimneys and empty mussel shells further down the slope. The Marker ANYA was found on the NW base of the IRINA II slope surrounded by diffuse fluid venting with loosely aggregated mussels, a Thyasira-species living in the sediment, and dense clusters of empty vesicomyid shells. Living vesicomyid specimens were not encountered. However, we doubt that this site is identical to the ANYA'S GARDEN locality described in the literature, because its position and distance from IRINA II does not correspond to the published data (Gebruk et al., 2000). ROV and TV-grab samples revealed that the populations of mussels, crabs and shrimps contained animals of all body sizes, which indicates continuous recruitment of these species rather than recruitment in discrete events, which would produce similar size cohorts.

QUEST is a newly discovered high-T, black smoke venting site situated about 130 m WNW (circa in 330° direction) of the active chimneys of IRINA II (Figs. 3.2 & 3.6). The formation of a depression, small chimneys and smoking pipes emanating black smoke make the QUEST site comparable to the smoking craters on the main mound (Fig. 3.7). However, QUEST does not show the typical circular crater rim and therefore may represent a younger structure, possibly an early state of a developing smoking crater. While the faunal composition grossly corresponded to that found at the smoking craters on the main mound, QUEST additionally harboured scattered clusters of mussels.

Dead mussel beds and/or inactive sulfide structures were mapped about 50 m to the north of the QUEST site, approximately 80 m north of IRINA II, and about 80 m WSW of ANNA-LOUISE. A temperature anomaly of 0.12°C was detected in bottom water during a TV-sled operation close to sampling station 82GTV (Fig. 3.6). The samples recovered from this station contained low-temperature hydrothermal precipitates (Fe-Mn oxides) similar to those generally found in the surroundings of the high-T areas of Logatchev-1.

The position of the Logatchev-1 field may be controlled by two crossing fault structures as suggested by bathymetric and video data (Figs. 3.3 & 3.6). If the seafloor is in fact largely covered by slumped material, the mineralization at Logatchev-1 may form a large stockwork or replacement zone beneath the seafloor (Fig. 3.5). The widespread ocurrence of both low-T and high-T precipitates at the seafloor supports this hypothesis which can only be further tested by geophysical investigation (geoelectrics) and by drilling.

Detailed maps of the different hydrothermal structures of the Logatchev-1 field based on ROV tracks are given in Appendix 2.

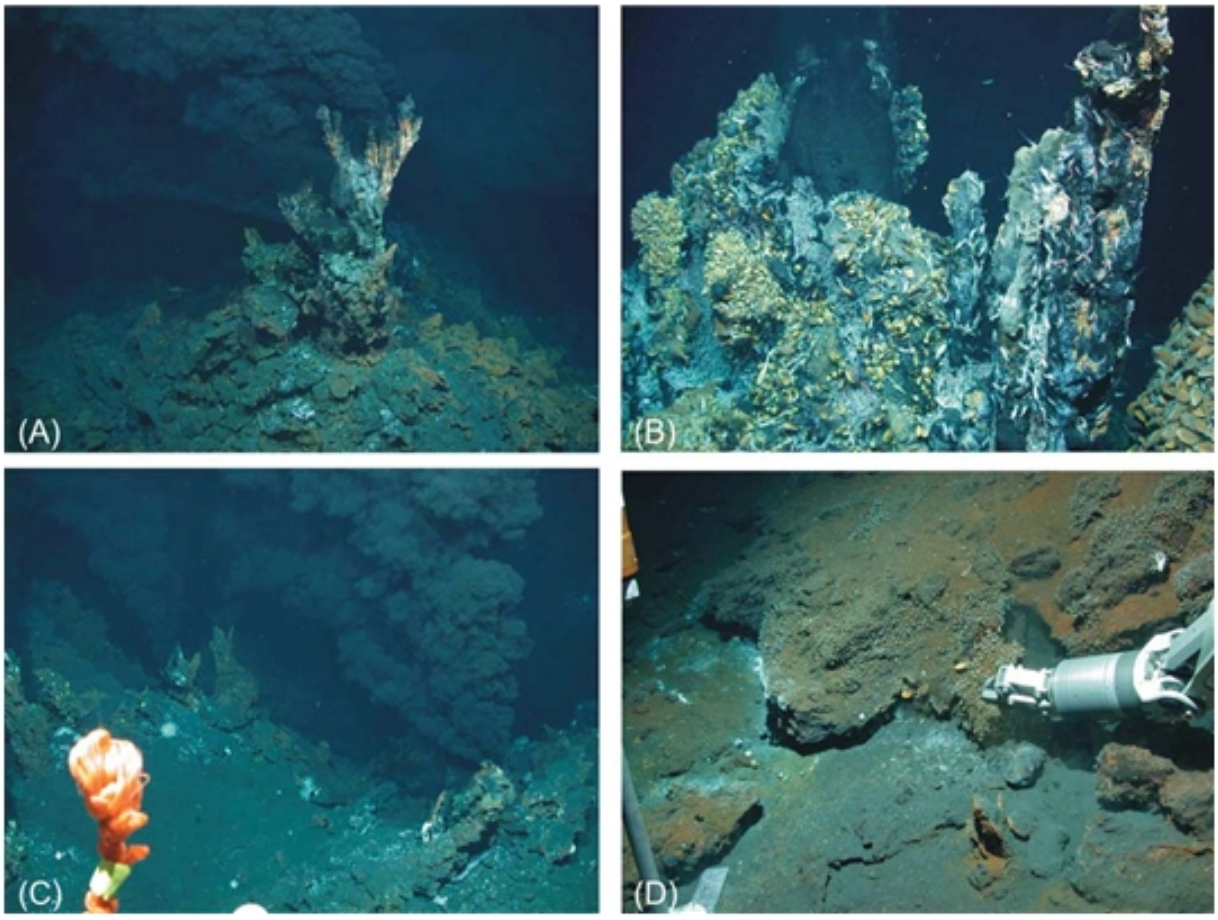

Fig. 3.7 Seafloor photographs from Logatchev-1 field taken with a SCORPIO still camera mounted on the ROV QUEST. (A): The "Candelabrum" chimney on the rim of smoking crater ANNALOUISE. (B) Chimney complex at IRINA II. Note the abundant vent fauna compared to (A). (C) Small chimneys in a depression marking the newly discoverd QUEST site. (D) Sulfide-rich crusts covering the seafloor near QUEST site. Such crusts were observed all over the Logatchev-1 field.

3.4.3 ROV deployments

(T. Kuhn, V. Ratmeyer, C. Borowski, A. Koschinsky)

The Remotely Operated Vehicle (ROV) QUEST was provided by the University of Bremen (MARUM, Prof. Dr. G. Wefer, Dr. V. Ratmeyer) for cruise M60/3. This cruise was the first one during which the ROV QUEST was exclusively used for scientific purposes. Only two test cruises preceded M60/3 and one major task of this cruise therefore was to check the ROV's ability to meet scientific requirements.

The QUEST system comprises the ROV itself, a control container, a workshop container, a mobile winch with 5000 m 18 mm steal-armored, optical cable for data and energy transmission and a deployment frame. All of these system components were installed on the afterdeck of R/V METEOR (Fig. 3.8).

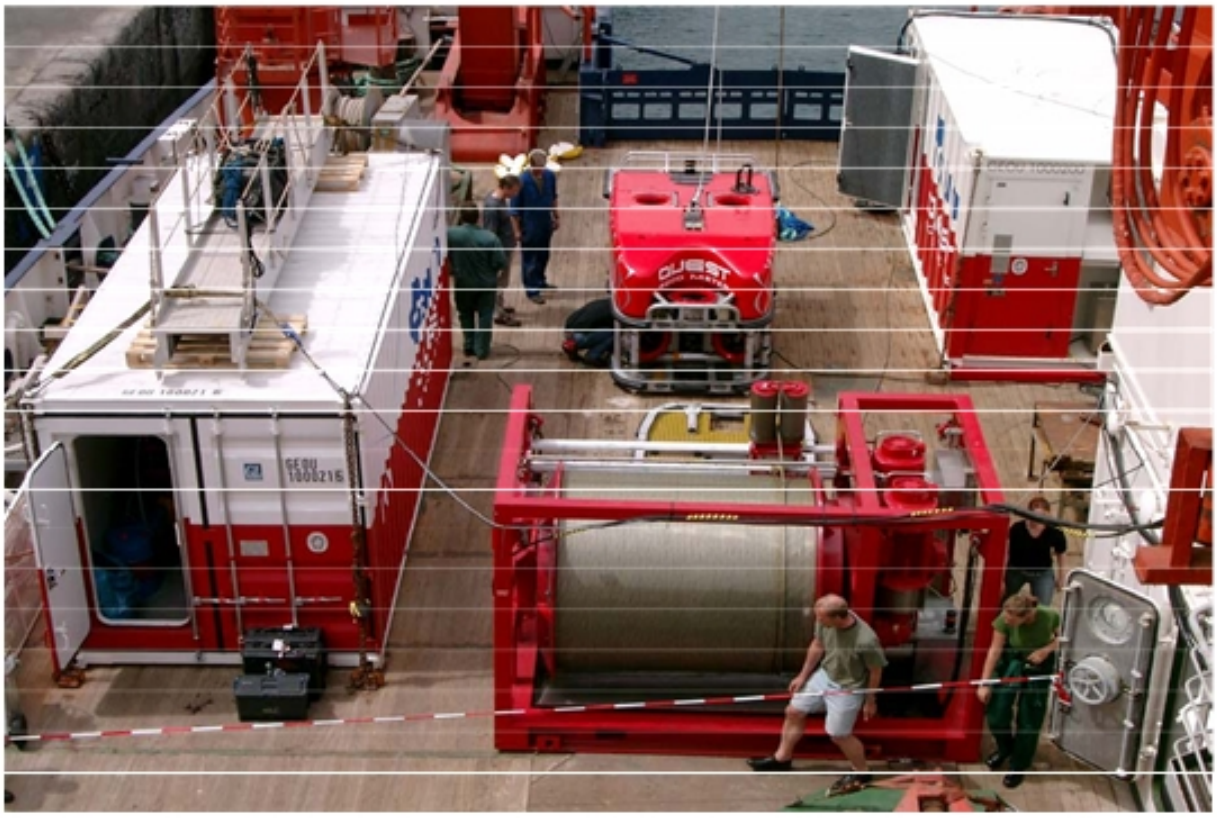

Fig. 3.8: The ROV QUEST system on the afterdeck of R/V METEOR consists of the ROV itself (middle), a control container (right side), a workshop container (left side) and a mobile winch (front).

QUEST was deployed over the A-frame with a special deployment frame. However, this frame did not effectively prevent the ROV from swinging to the side during deployment. Once the QUEST is in the water it is free-flowing, i.e., it moves independently from the cable which only transmits energy and data. Five to six bouyancy spheres were fixed on the cable at the first 30 m above the device in order to keep the cable upwards away from the ROV. It is only after the fixation of the bouyancy spheres that the ROV starts diving. Therefore, these spheres had to be removed before the ROV can be recovered. This procedure together with the fact that the vessel was not fully manoeuverable during the last about 100 m of emerging of the ROV to the surface, were the limiting factors for the deployment of the ROV under different sea states. We could deploy the ROV at a swell up to 2-2.5 m. However, our situation was complicated by a crossing swell of about 90° and 340° which caused strong rolling of R/V METEOR.

The ROV sinks with about 0.5 - 1 m/s. Together with the deployment/recovery procedure the submergence to the seafloor and the emergence back to the vessel took 2 hours each for a water depth of 3000 m.

We regularly started our ROV stations at 8:00 a.m. with checking of the system which took about 1 hour. After lowering the ROV to the seafloor at 3000 m water depth we started the work on the seafloor at about 11:00 a.m. and continued working until 17:00 to 21:00 p.m. Between 19:00 p.m. and midnight the ROV was back on deck, the subsamples were taken and the treatment of the samples started. Since most of the water and biological samples had to be worked with immediately after the dives, most of the scientists had to work all night after a ROV station. Routine technical checking was the work of the ROV team after each dive

which took about 1 hour if no technical problem had occurred. If all system components work reliably the next ROV station can start the next morning.

Based on our experience and on a ROV crew of 6 persons it is possible to have two ROV stations with bottom times of 5-7 hours on two successive days and one day for technical maintenance (provided the weather is ok). A careful planning of the ROV stations and of the sample treatment is as necessary as a complementary scientific program to fill the days during which the ROV cannot be deployed.

The navigation of ROV QUEST was realized by two systems: an USBL and a Doppler-Velocity-Log (DVL) navigation. The USBL was realized with the POSIDONIA system from IXSEA OCEANO (Brest, France). At the beginning of all station work a reference station (mooring with a transponder) was set on the seafloor. This station was calibrated by running an Eight over the station with R/V METEOR as requested by the POSIDONIA software. This way the position of the reference station could be calculated with an accuracy of 2-3 m in xy-direction and 1 m in z-direction. To navigate the ROV QUEST on the seafloor a responder was mounted on the frame of the ROV which was electrically triggered. Unfortunately, this responder had an electircal failure during the first dive and could no longer be used. Moreover, it was not possible to trigger the responder in transponder mode, i.e., acoustically through the water column, because the QUEST motors are too noisy. Therefore, a DVL navigation system was applied using a doppler log installed on the ROV. This way, two homer beacons were set on the seafloor and their exact position were calculated using the reference station as a fixed point. It was then possible to calculate every position on the seafloor either with respect to the reference station or to the homer beacons. Navigation within a range of about 500 m around the reference station or beacons was possible. Since we went to the same seafloor structures several times we could control the accuracy of this navigation which turned out to be within a few meters. Problems only occurred when the ROV was sitting on the seafloor for a longer time during experiments or sampling. During such situations a drift of position occurred which had to be recalculated.

Abb. 3.9 Two homer beacons used for ROV QUEST navigation during M60/3.

During each station different data accumulated, including navigation, heading, depth, height above seafloor, video, photo, in-situ sensors, protocols, sampling etc. All data were gathered during each dive in a data base provided by the ROV crew. The navigation data can be synchronized

with all other data via the time frame. This was done after each dive using the software ADELIE which consists of components for the synchronization of data as well as for GIS-based (ARCVIEW) display and analysis.

3.4.4 Low-temperature measurements in the Logatchev-1 hydrothermal field

(K.S. Lackschewitz, N. Augustin, H. Villinger)

During the FS Meteor cruise M60/3, first temperature measurements in the Logatchev hydrothermal field were performed. A miniaturized temperature data logger (MTL) was mounted on ROV QUEST to continuously record temperatures during every dive. Additionally, we deployed 4 data loggers at the ocean floor for monitoring temperatures in areas with diffuse fluid outflow and biological colonization. The MTLs were constructed to be extremely robust, small (16 cm long, Fig. 3.10) and easy to operate in water depths up to 6000 m (Pfender and Villinger, 2002). The temperature range extends from -5 to +60°C with an absolute accuracy of ± 0.1K and a relative temperature resolution of 0.001°C. We increased the absolute accuracy of the MTLs through a precise calibration by comparing the data logger measurements to a high precision thermometer mounted at a CTD. Therefore, we attached 7 MTLs at the CTD and measured a water profile down to 3200 m with the highest sample rate of 1s. The temperature measurement range was 26 to 3°C.

Fig. 3.10 Temperatur logger for low-T hydrothermal fluids used during M60/3.

We measured the temperature distribution in the Logatchev-Field 1 during 8 ROV dives. The data obtained from the MTLs show a background bottom water temperature of approximately 2.6°C which clearly increases in areas with active high-temperature black smokers and craters (Fig. 3.11). The highest measured temperature was 31°C in the nearbottom water close to high-T vents, whereas the average increased temperatures ranged between 2.7 and 3.5°C. In addition, numerous diffuse outflow sites were identified. One MTL, which we left for 3,5 days at the seafloor in an area with diffuse fluid-outflow and a colonization of mussels recorded temperature variations between 2.7 and 3.2°C (Fig. 3.12). One can clearly observe a periodic change in temperature which is most likely caused by the tidal influence on pressure and/or bottom currents. Temperature measurements on a diffuse vent at the crater rim of IRINA over 3 days revealed pulsating temperatures with variations over time periods of 1 to 2.5 hours. The longer a cycle lasted the higher the temperatures went within a range between 2.7°C and 8°C.

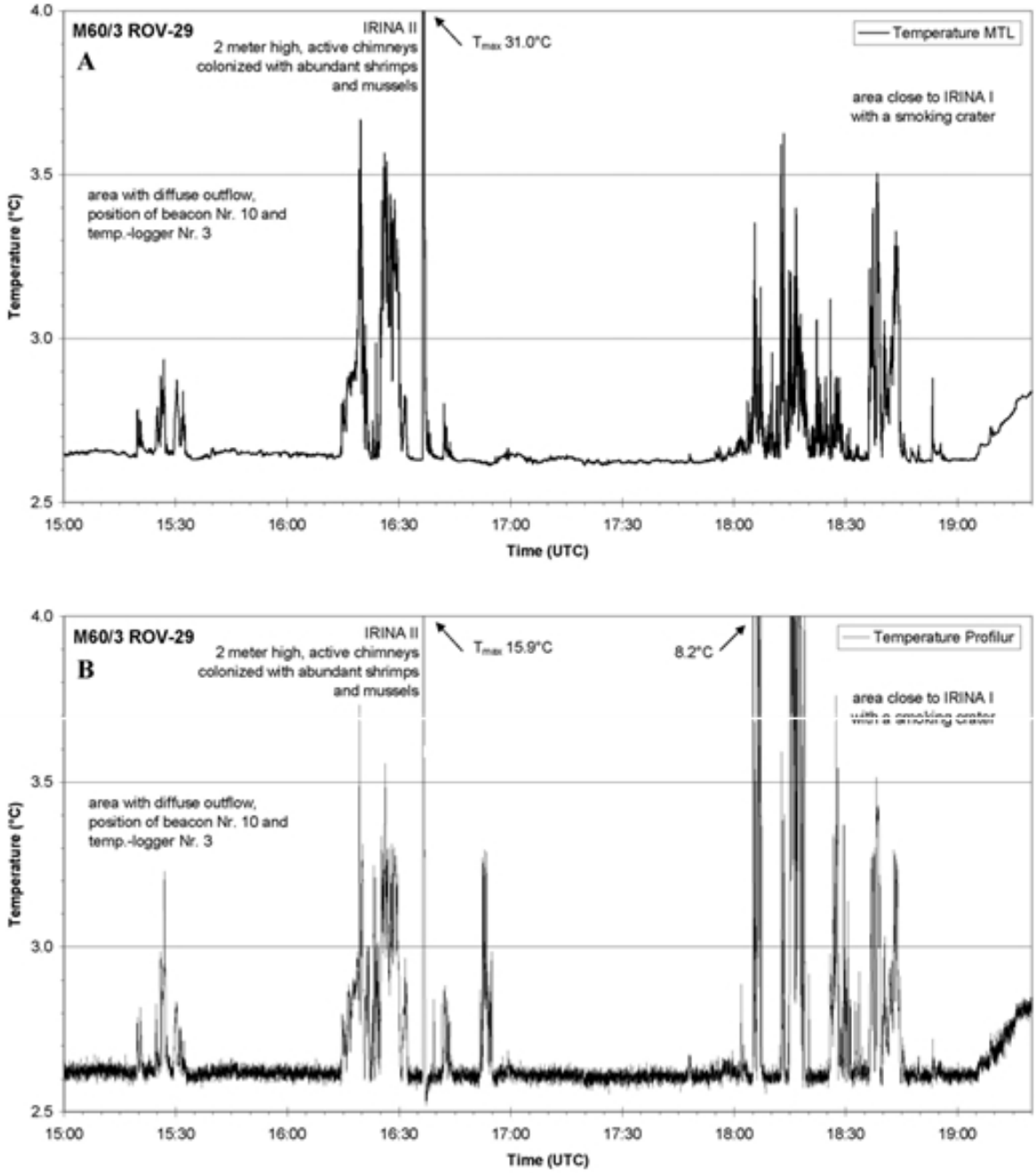

Fig. 3.11 Comparison of temperature profiles recorded during dive 29ROV (see Fig. 3.2). A: Miniaturized Data Logger (MTL). B: PROFILUR, Pt100 sensor. Both sensors were mounted on the tool sled of ROV QUEST.

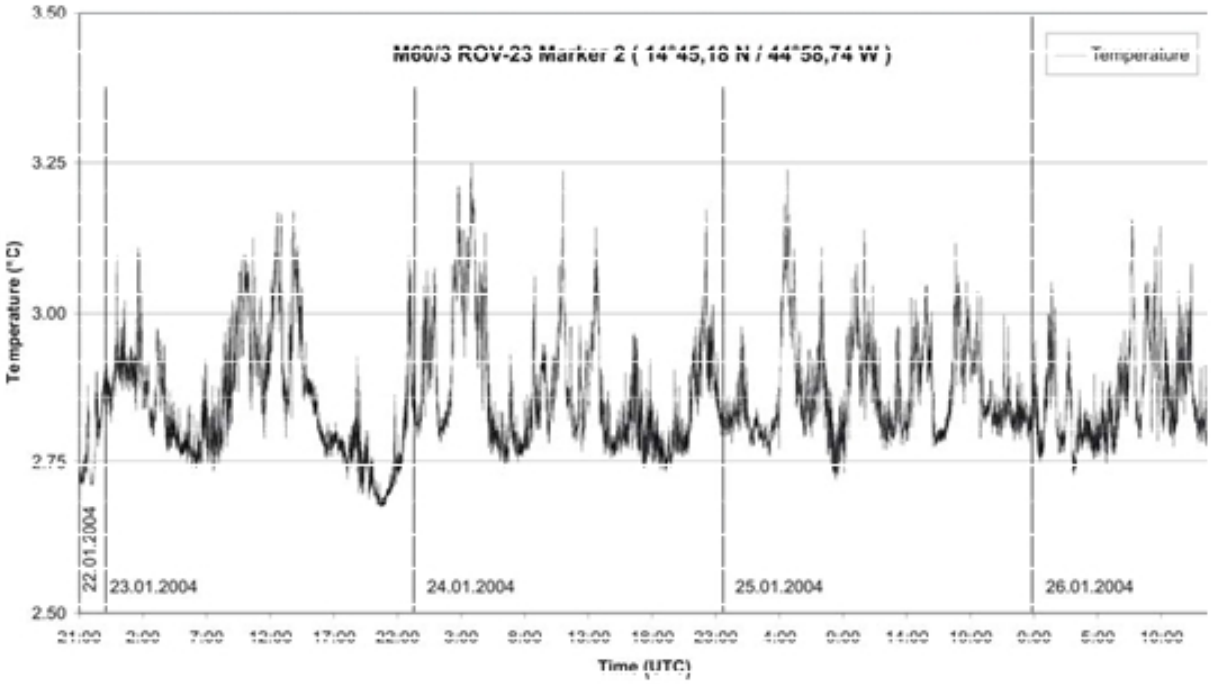

Fig. 3.12 Temperature measurements of a diffuse, low-T emanation site at the mussel bed close to the high-T chimney complex at IRINA II using a miniaturized temperature logger. The logger was placed on top of the mussel bed.

3.4.5 In situ measurements of biogeochemical parameters: temperature, oxygen, hydrogen sulfide, pH and conductivity

(F. Zielinski, C. Borowski, N. Dubilier)

The mussel Bathymodiolus puteoserpentis harbors sulfide- and methane-oxidizing bacteria in its gills and occurs in large quantities at the Logatchev 1 hydrothermal vent field. To obtain a better understanding of the environment of these mussels and how it affects their productivity we collected in situ measurements of temperature, oxygen, hydrogen sulfide, pH, and conductivity in the waters surrounding the mussels (Fig. 3.13). The data were gained using sensors and microsensors connected to the PROFILUR, a custom-built pressure- and water resistant titanium cylinder (525 x 145 mm) which houses the electronics for signal- and A/D-conversion. The PROFILUR was tested to withstand pressures up to 4000 m depth and was thus well suited for the demands of the M60/3 cruise. The following sensors were employed: Pt100 temperature sensors, (UST Umweltsensortechnik GmbH, Geschwenda, Germany), Clark type O_2 microsensors (Revsbech 1989), amperometric H_2S microsensors (Jeroschewski et al. 1996, Kühl et al. 1998), glass pH microelectrodes (Revsbech & Jørgensen 1986) and conductivity sensors. Except for the Pt100 temperature sensor all microsensors were manually produced at the MPIMM, in the Department of Biogeochemistry, Group of Microsensors.

Before each ROV dive the sensors were connected to the PROFILUR electronics by inserting them in plastic holders filled with paraffin oil for pressure compensation. After extended calibrations of all sensors, the PROFILUR was fastened to an extendable drawer underneath the ROV, with the sensors tip protruding from the drawer (Fig. 3.14). All data were stored in the internal PROFILUR memory as well as in the central ROV database and downloaded for later

analysis at the end of the dive. In situ measurements with the PROFILUR were carried out on dives 29, 38, 56 and 66ROV. Temperature, H_2S and O_2 were measured on all 4 dives, pH on 3, and conductivity on 2 of the 4 dives.

Fig. 3.13 The PROFILUR measuring geochemical data at a Bathymodiolus mussel colony on the active vent structure of IRIN A II.

Temperature measurements were transmitted on board for online temperature tracking. Consistent with the data obtained from the MTL our sensor measured an average bottom water temperature of 2.6°C and an increase in temperature at diffuse outflow sites ranging from 2.7 to 3.5°C.

Fig. 3.14 The PROFILUR mounted on the extendable drawer underneath the ROV set up for the dive to come. The microsensors were protected by a cage.

The temperature profiles of the PROFILUR and MTL were also in good agreement, with both detection methods often showing similar temperature gradients at similar time points (Fig. 3.11). However, the absolute temperature measured at steep gradients often varied between the two methods. In some cases, the PROFILUR measured peak temperatures up to 10-times higher than the MTL. This is most likely due to the different positions of the devices on

the ROV. These were separated from each other by about 1 meter, a distance at which steep temperature gradients can occur at vents. For example, the PROFILUR registered a steep temperature increase while approaching a Bathymodiolus mussel colony on an active vent structure with 26.8°C being the highest temperature measured, while the MTL recorded the regular background temperature of 2.6°C at the same time point (Fig. 3.15). All other sensor data are in the process of being analyzed.

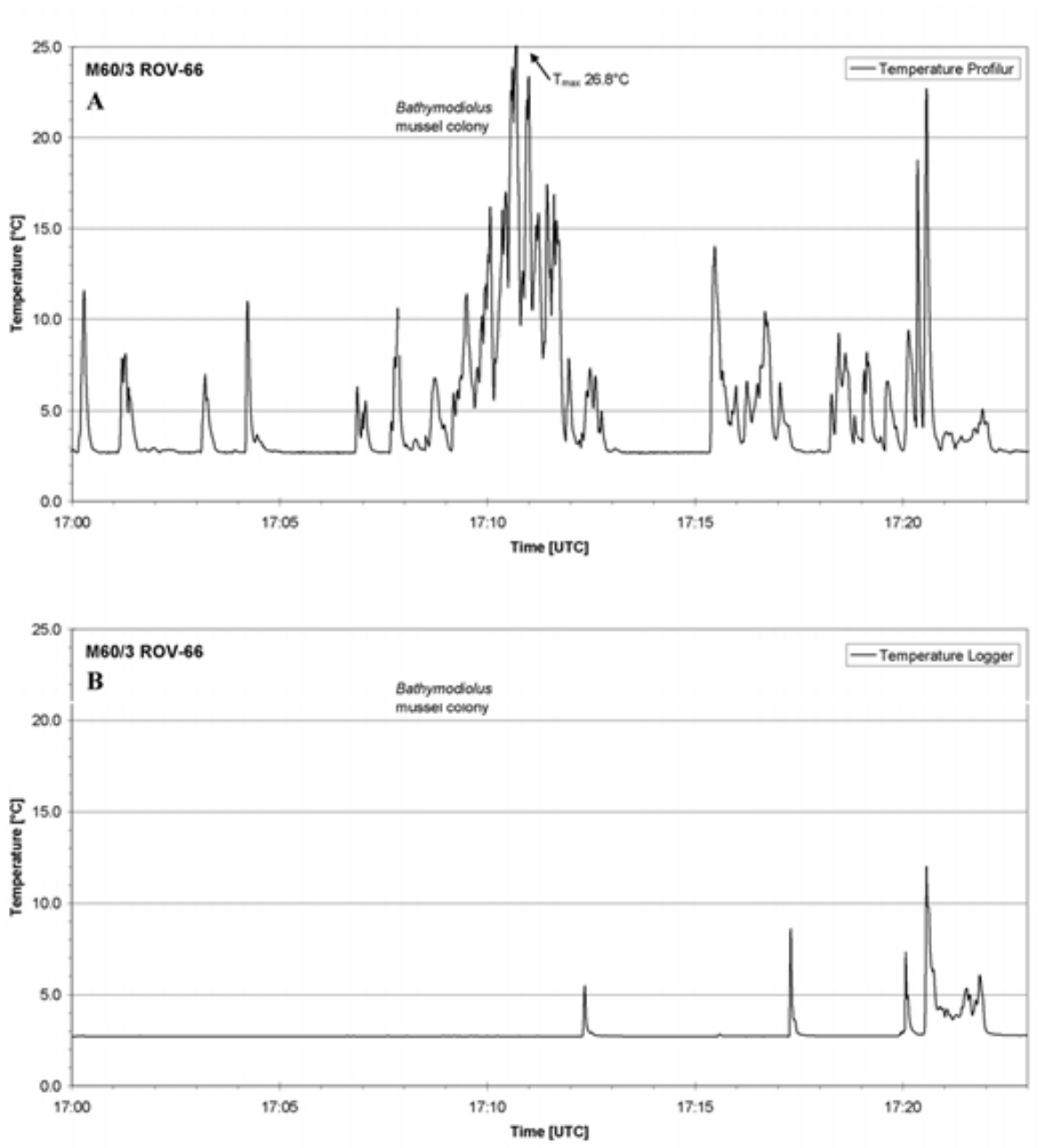

Fig. 3.15 Comparison of temperature profiles at a Bathymodiolus mussel colony recorded during dive 66ROV (see Fig. 3.2). A: PROFILUR Pt100 sensor. B: miniaturized data logger. For further explanation see text.

3.4.6 OFOS deployment

(T. Kuhn, S. Petersen, K. Schreiber, R. Hekinian)

A total of 14 TV-sled stations were carried out during M60/3 (Tab. 3.1), most of them in the vicinity of the Logatchev-1 hydrothermal field but also on top of the rift mountains, in the rift valley and in Working Area II (Fig. 3.1). The objectives of the OFOS stations were (i) to map the contact between ultramafic and mafic rocks and to recognize if this contact is stratigraphic or tectonic, (ii) to distinguish between talus and outcropping rocks, (iii) to map faults and fissures, and (iv) to measure the near-bottom water temperature in order to detect hydrothermal activity. The IFM-GEOMAR TV-sled was equipped with a BENTHOS photo camera and flash, a SONY digital camcorder and a FSI 3“ memory CTD probe. In order to get exact OFOS position data a POSIDONIA transponder was mounted on the TV-sled’s frame providing on-line navigation data of both the vessel and the OFOS.

Table: 3.1: OFOS stations during M60/3 (coordinates for the OFOS position at seafloor are given).

Station	Area	Location	Depth	Date	Objective & summary of results
22-OFOS	Logatchev 1	14° 46.61’ N 44° 58.23’ W to 14° 48.27’ N 45° 01.79’ W	2708 m to 3597 m	21.01.04	Profile over the Logatchev-1 hydrothermal field and structures along the inner rift valley flank. Talus and sediment mark the field and pillows appear at the flank of the rift valley.
27-OFOS	Logatchev 2	14° 42.30’ N 44° 53.87’ W to 14° 43.11’ N 44° 56.10’ W	1615 m to 2650 m	23.01.04	Transect along a WNW-ESE ridge. Ultramafic blocks (mainly talus) and sediments cover the ridge. An inactive mussel field was discovered (Logatchev-4).
40-OFOS	Working Area II	14° 53.43’ N 44° 55.04’ W to 14° 53.96’ N 44° 55.53’ W	3221 m to 3330 m	27.01.04	Mapping of Working Area II, search for hydrothermal activity. DVS failure, end of OFOS station due to winch problems.
42-OFOS	Working Area II	14° 54.02’ N 44° 55.41’ W to 14° 54.90’ N 44° 57.33’ W	3345 m to 3447 m	27.01.04	Continue mapping of station 40 OFOS in Working Area II, but on a more northerly course. Only basalt along the track, few sheet flows, talus very abundant; missing of the described hydrothermal site.
46-OFOS	Working Area II	14° 54.19’ N 44° 55.63’ W to 14° 54.43’ N 44° 55.62’ W	3462 m	28.01.04	Locate hydrothermal field in Working Area II. Only basalt noticed, small pillow mounds & ridges, some larger scarps, crosscutting faults but no hydrothermal activity.
47-OFOS	Working Area II	14° 54.99’ N 44° 55.15’ W to 14° 54.43’ N 44° 55.62’ W	2490 m to 3538 m	29.01.04	Investigation of the sea floor in Working Area II. Ultramafics all the way, heavily sedimented; discovery of one large scarp (30 m).
50-OFOS	Arrowhead Area	14° 48.99’ N 44° 58.37’ W to 14° 50.86’ N 45° 03.25’ W	2820 m to 3840 m	29.01.04	Mapping the contact of ultramafics to basalts. At the eastern flank of the rift valley, east of the rift, axis only ultramafics occur. Rift axis consists of a succession of undulating hills cut by 3 fissures.
60-OFOS	Logatchev 1	14° 44.38’ N 44° 58.30’ W to 14° 45.61’ N 45° 58.21’ W	2758 m to 2970 m	01.02.04	Mapping the plateau above Logatchev 1 field trying to locate areas of hydrothermal activity. The plateau consists of a highly sedimented area without any traces of hydrothermalism.
61-OFOS	Area W of	14° 45.10’ N	3049 m	01.02.04	Mapping the contact between basalts

Station	Area	Location	Depth	Date	Objective & summary of results
	Logatchev 1	44° 59.40' W to 14° 45.65' N 45° 01.35' W	to 3835 m		and ultramafics as well as a small volcanic feature west of Logatchev-1. The eastern valley wall consists of ultramafics, which is followed by talus. The volcano is made up of rather young pillow basalt.
70-OFOS	Central Valley	14° 44.63' N 44° 01.25' W to 14° 47.60' N 45° 03.55' W	3889 m to 3623 m	04.02.04	Mapping the Central Valley floor looking for tectonic/volcanic activity. Basalt crops out along the whole track with low sedimentation pointing to recent volcanic activity.
72-OFOS	Central Valley	14° 46.36' N 44° 57.80' W to 14° 49.02' N 45° 00.83' W	2770 m to 3946 m	05.02.04	Mapping the eastern wall of the rift valley. A large scarp > 100 m vertical offset in ultramafics. Ultramafics all along the track.
80-OFOS	Central Valley	14° 39.72' N 44° 59.48' W to 14° 40.71' N 45° 02.77' W	3481 m to 3976 m	06.02.04	Mapping the eastern flank of the Central Valley at station 17 CTD (prominent CH_4 anomaly) and across the axial valley. Young pillow basalts all the way along the track. Abundant fissures marking active tectonics at the western wall.
84-OFOS	Logatchev 1 and Central Valley	14° 43.48' N 44° 58.47' W to 14° 42.38' N 45° 59.91' W	2939 m to 3896 m	07.02.04	Mapping of the seafloor at Logatchev-3. No T anomaly found. Sharp contact between ultramafics and basalts close to the kink of the track (see Fig. 3.1)
89-OFOS	Area SW of Logatchev 1	14° 45.15' N 44° 58.84' W to 14° 44.91' N 45° 58.85' W	3011 m to 3090 m	08./09.02.04	Mapping of the area Southwest of Logatchev-1. Abundant scarps, fissures and only ultramafics along the whole track.

Most of the results of the OFOS deployment are already discussed in chapter 3.4.1. With respect to the main objectives given above, the following results can be stated:

(i) The central valley floor is mainly covered by rather young basaltic flows, whereas most of the eastern inner flanks of the rift valley are made up of ultramafic rocks. However, mafic rocks were also sampled from the flanks but seem to be of minor importance. Magmatic contacts were obserevd in some samples from the flanks (e.g., 49GTV-2; see chapter 3.4.7). Since the ultramafic rocks emplaced tectonically, there should be a tectonic contact between ultramafic and mafic rocks. This contact is mainly situated at the lower part of the inner flank close to the morphological transition from the slope to the rift valley floor. However, this contact is often blurred by talus material. Larger outcrops related to basaltic volcanism appear only at two locations higher up the flanks where young basalt volcanoes are located (see Fig. 3.3).

(ii) Large parts of the eastern valley flanks are covered by talus material. This is especially true in the vicinity of the Logatchev-1 hydrothermal field.

(iii) Sites of active tectonics may be characterized by open fissures, nearly vertical escarpments with no sediment coverage and tectonically deformed rocks. Open fissures were found in the middle of the central valley at the end of station 50OFOS in basaltic flows (at 14°50.1'N / 45°01.5'W, Fig. 3.1). This position may mark the current spreading axis which may be in a phase of tectonic spreading. Near vertical walls without sediment in ultramafic rocks were mapped in water depths between 3300 and

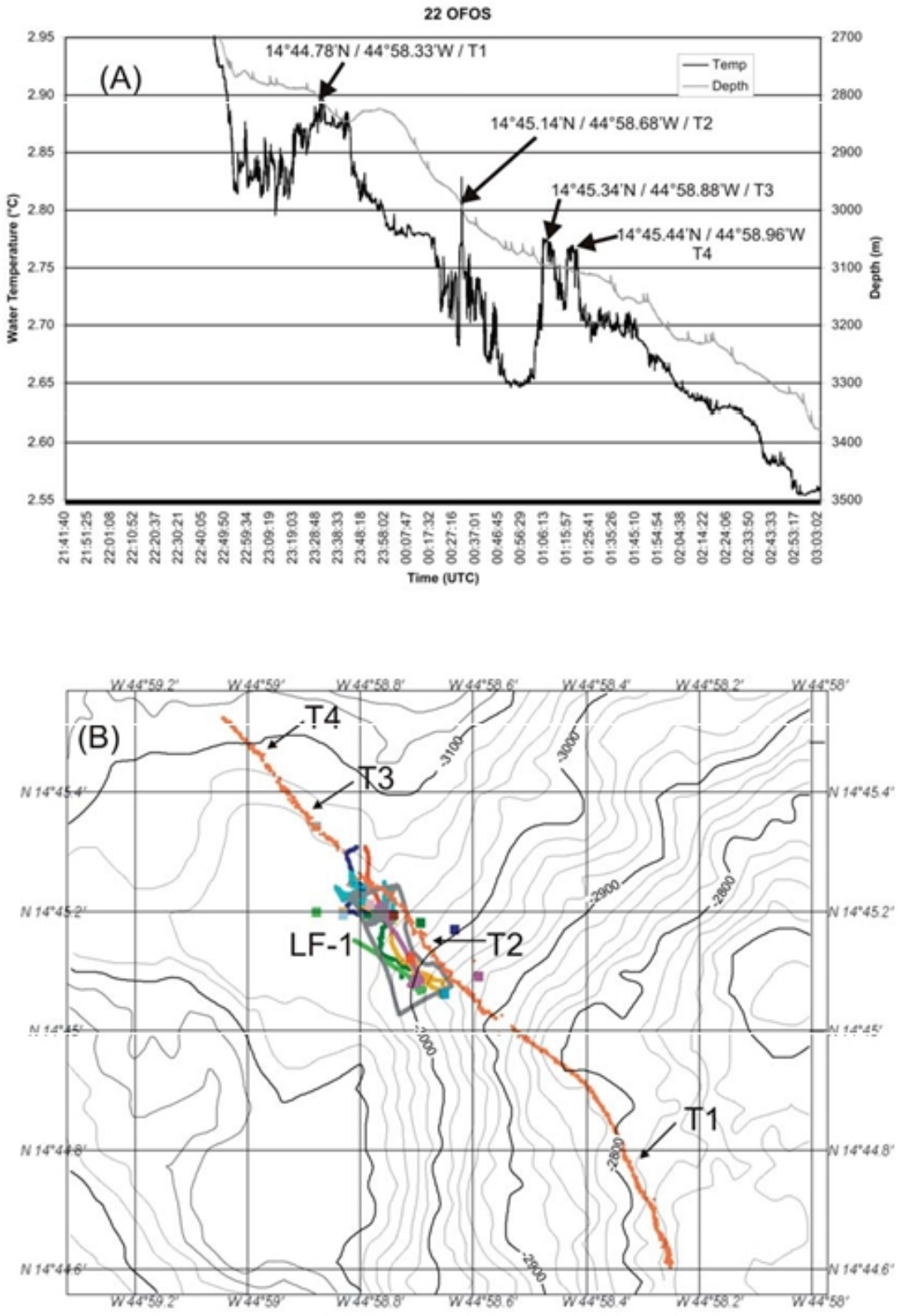

Fig. 3.16: A: Part of the water temperature and depth vs. time diagram of OFOS station 22 showing four distinct T anomalies between 0.07 and 0.13 °C. B: Track of 22OFOS in the vicinity of the active Logatchev-1 hydrothermal field (LF-1; see Fig. 3.2). Three T anomalies occur outside the LF-1 field. T 3 and 4 suggest that LF-1 may be distinctly larger than previously known, T1 may indicate another active hydrothermal field.

3600 m all along the inner eastern rift flank in stations 47, 72, 22, 61, 89 and 84 (Fig. 3.1). These steep slopes seem to mark the active tectonic emplacement of the mantle rocks. Indications of active tectonics were also mapped in working area II along stations 42 and 46OFOS. Tectonically deformed ultramafics with mylonitic textures were sampled in working area II (49GTV) at a position which is situated along the track of 47OFOS. OFOS station 27 was carried out on a WNW-ESE striking ridge, the southern slope of which is also characterized by almost vertical scarps of some tens of meters vertical offset. The Logatchev-4 hydrothermal field is situated on this tectonic structure (Figs. 3.1, 3.3).

(iv) Increased bottom water temperatures were only found during station 22OFOS which crossed the active Logatchev-1 hydrothermal field (Fig. 3.16). Four T anomalies occur close to the Logatchev-1 field, one marks the field itself whereas three others indicate either a considerable larger areal extent of the Logatchev-1 field or yet undiscovered new hydrothermal fields.

3.4.7 Sample description

(S. Petersen, K. Lackschewitz, N. Augustin, L. Franz, R. Hekinian, D. Birgel)

3.4.7.1 Summary

During cruise M60/ 3 a total of 5 ROV dives and 16 TV-grab stations recovered geological samples from the seafloor. Detailed information on the sampling stations are given in Table 3.2.

Host rocks of the Logatchev field are mainly serpentinized peridotites while basalts and gabbros (sometimes in magmatic contact with peridotite) occurred subordinately. Remarkable are samples of coarse grained websterites, orthopyroxenites and orthopyroxene-rich, pegmatoidal norites, which are interpreted as magmatic cumulates from the crust/mantle transition zone. A large variety of hydrothermal samples were recovered including active and inactive massive chalcopyrite chimneys, massive sulfides, silicified breccias and crusts, soft and indurated hydrothermal sediments, abundant secondary Cu-sulfides, red and orange jaspers, abundant Fe-Mn-oxyhydroxides as well as atacamite and Mn-oxides. Three grabs recovered silicified crusts that may act as a cap rock allowing for conductive cooling of the hydrothermal fluid. Sulfides are enriched immediately underneath this cap rock and usually contain a more pyrite-rich section at the top followed by more Cu-rich sulfides (chalcopyrite and isocubanite) underneath. The base of the grabs commonly contained large amounts of gray to green-gray indurated mud related to alteration of host rock material. This suggests that the massive sulfides along the flanks of the deposit might only be a thin veneer directly at or below the seafloor. The amount of sulfide talus, the state of oxidation and the widespread abundance of atacamite suggest an old active hydrothermal system. While oxidation is common, local reducing conditions result in the formation of secondary Cu-sulfides, mainly chalcocite and minor bornite and digenite, and rare native copper. Overall, the sulfides at the Logatchev 1 hydrothermal field are extremely enriched in Cu over Zn when compared to other seafloor hydrothermal systems.

3.4.7.2 Descriptions of individual stations

23ROV: During this dive silicified crusts with abundant pyrite were recovered from the northwestern end of the Logatchev 1 field (sample 23ROV-10) near the newly found Quest hydrothermal site. The sample is irregular in shape and consists of abundant amorphous silica with disseminated pyrite and white, angular, altered rock fragments. Later in the dive two pieces of a group of inactive black smoker type chimneys southwest of IRINA II were sampled in the vicinity of a mussel bed (samples 23ROV-12 and 23ROV-13). Piece 23ROV-12 consists of a 10 cm thick chalcopyrite core with a 1-7 cm rim of sphalerite-rich material. The outer crust is coated by Fe-Mn-oxyhydroxides. The whole sample seems to be silicified. Sample 23ROV-13 is a multi-spired chimney with a curved outline. At least three generations of chimney growth are visible. Two different sample groups were recovered on the sample tray or in the ROV frame and their sampling location is therefore uncertain. Samples 23ROV-14 are two pieces of light-brown Fe-oxyhydroxides with some black Mn-oxide layers. Samples of station 23ROV-15 are irregular dark-brown to red Fe-oxyhydroxides coating black to dark gray secondary Cu-sulfides, likely dominated by chalcocite.

Station 26GTV was attempted in the Logatchev 1 field, but failed, due to an electric failure. However, the grab recovered 5 small ultramafic samples in one of the pipes of the grab. These samples were slightly to almost completely serpentinized harzburgites (26GTV-1,-2,-3; 26GTV-5) and one coarse grained orthopyroxene-websterite (26GTV-4).

Station 32GTV was attempted on the northern flank of the main mound between the smoking craters to the south and the IRINA II site. The TV-grab recovered several 100 kg's of muddy material with abundant Fe-oxyhydroxides crusts and atacamite (32GTV-1; Fig. 3.17h) at the surface overlying mainly altered wallrock, i.e. strongly serpentinized peridotite (32GTV-3A), peridotite with quartz and sulfide impregnation (32GTV-3D) and orthopyroxene-websterite (32GTV-3B,-3C). Few pieces of massive, fractured quartz were found (32GTV-2) together with a single piece of fine-grained pyrite (32GTV-3E) and some sulfide mud (32GTV-5).

Another TV-grab was performed on the southeastern side of the main mound (station 33GTV) and recovered Fe-oxyhydroxides with abundant atacamite (33GTV-18) as well as a suite of relatively pristine ultramafics. These were medium- to coarse-grained harzburgites (33GTV-2,-3,-5,-9,-10,-12,-13,-14,-15), coarse-grained to pegmatoid orthopyroxene-websterites (33GTV-7,-8,-8A,-16; Fig. 3.18a,b), several serpentinized peridotites with random orientation of the minerals (33GTV-4,-17), one sheared peridotite mylonite (33GTV-11; Fig. 3.18d) and one medium-grained norite (33GTV-1; Fig. 3.18g). Individual orthopyroxene crystals of the pegmatoid samples reached up to 15 cm in size.

Station 35GTV was targeted on the large mussel bed in the vicinity of the IRINA II site. The TV-grab sampled abundant fauna including mussels, crabs, snails, and ophiruides. This faunal assemblage lived on a silicified crusts that protected them from the underlying hot fluids. The TV-grab broke this cap rock seal and all mussels were subsequently cooked during ascend. In situ temperatures measured in the mud underneath the crust ranged from 96-106°C. The geological samples recovered include the silicified cap rock (35GTV-1, up to 20 cm thick; Fig. 3.17d) which contains altered and fresh wallrock fragments and orthopyroxene crystal pieces as well as sulfide fragments. Underlying this crust is a section of porous to massive chalcopyrite and isocubanite (35GTV-2; Fig. 3.17e). Few pieces of pyrrhotite-rich

Table 3.2: Geological samples taken during cruise M60/3

Station	Date	Time	Lat. / Long.	Depth	Comment
23ROV-10	22.01.04	21:35	14°45.209'N/ 44°58.823'W	3038 m	siliceous cap rock with sulfides
23ROV-12	22.01.04	22:28	14°45.187'N/ 44°58.747'W	3036 m	inactive chimney
23ROV-13	22.01.04	22:28	14°45.187'N/ 44°58.747'W	3036 m	inactive chimney
23ROV-14	22.01.04	no data	location uncertain	no data	Fe-oxyhydroxide chips
23ROV-15	22.01.04	no data	location uncertain	no data	secondary Cu-sulfides, small bits
26GTV	23.01.04	13:13	14°45.19'N/ 44°58.77'W	3024 m	serpentinized harzburgite and Opx-websterite
32GTV	25.01.04	12:46	14°45.12'N/ 44°58.71'W	2982 m	Fe-oxyhydroxides, atacamite, sulfide sand, Opx-websterite and serpentinized peridotite
33GTV	25.01.04	17:28	14°45.06'N/ 44°58.65'W	2921 m	Fe-oxyhydroxides, atacamite, norite, harzburgite, websterite and peridotite
35GTV	25.01.04	23:38	14°45.19'N/ 44°58.74'W	3019 m	106°C on deck, mussel bed, massive sulfides, serpentinite, harzburgite
49GTV	29.01.04	16:25	14°55.48'N/ 44°54.34'W	3344 m	serpentinized dunite, harzburgite, microgabbro and basalt
53ROV-1	30.01.04	16:19	14°45.181'N/ 44°58.741'W	3033 m	black smoker chimney talus
53ROV-13	30.01.04	20:37	14°45.083'N/ 44°58.710'W	2959 m	black smoker chimney talus
53ROV-15	30.01.04	no data	location uncertain	no data	porous chalcopyrite/pyrrhotite
53ROV-16	30.01.04	no data	location uncertain	no data	red jasper
54GTV	31.01.04	02:39	14°45.17'N/ 44°58.63'W	2940 m	sulfide-carbonate breccias, jasper, atacamite, native copper
56ROV-1	31.01.04	no data	14°45.188'N/ 44°58.739'W	3034 m	pyrrhotite-rich chimney
57GTV	01.02.04	03:13	14°42.29'N/ 44°53.67'W	1608 m	serpentinized and brecciated peridotite, amphibolite and basalt
62GTV	02.02.04	02:07	14°45.20'N/ 44°58.83'W	3037 m	100°C on deck, silica crusts, sulfides, peridotite and pyroxenite
64ROV-1	02.02.04	17:22	14°45.065'N/ 44°58.691'W	2949 m	black smoker chimney talus
64ROV-2	02.02.04	17:40	14°45.065'N/ 44°58.689'W	2948 m	black smoker chimney talus
64ROV-10	02.02.04	18:38	14°45.068'N/ 44°58.688'W	2949 m	small bits taken with slurp gun
64ROV-11	02.02.04	18:55	14°45.065'N/ 44°58.692'W	2948 m	inactive chimney
67GTV	04.02.04	01:51	14°42.30'N/ 44°54.41'W	1967 m	serpentinized peridotite, orthopyroxenite and metabasalt
73ROV-1	05.02.04	18:30	14°45.197'N/ 44°58.774'W	3050 m	serpentinite and harzburgite
73ROV-2	05.02.04	19:02	14°45.190'N/ 44°58.755'W	3032 m	pyrrhotite-sphalerite chimney
74GTV	06.02.04	01:28	14°45.09'N/ 44°58.59'W	2882 m	carbonate mud with Fe-oxy-hydroxides, harzburgite, web-sterite &

Station	Date	Time	Lat. / Long.	Depth	Comment
					serpentinized peridotite
77GTV	06.02.04	14:27	14°45.18'N/ 44°58.80'W	3019 m	carbonate mud with Fe-oxyhydroxides, mylonitic serpentinite
78GTV	06.02.04	17:51	14°45.19'N/ 44°58.88'W	3005 m	abundant Mn-oxide crusts, ortho-pyroxenite, websterite, serpentinite
79GTV	06.02.04	20:48	14°45.18'N/ 44°58.69'W	3005 m	Fe-Mn-oxide crusts with atacamite in pelagic sediment
82GTV	07.02.04	13:36	14°45.34'N/ 44°58.88'W	3058 m	Mn-Fe-oxide layers and crusts, talc-bearing serpentinite
83GTV	07.02.04	17:15	14°45.21'N/ 44°58.78'W	3019 m	silica crusts, massive sulfides, Fe-oxyhydroxides serpentinite
87GTV	08.02.04	13:20	14°44.00'N/ 44°58.25'W	2967 m	gabbronorite, melanorite, serpentinized peridotite

material (35GTV-3), of anhydrite (35GTV-7), and of bornite/chalcocite-rich material likely replacing the massive chalcopyrite (35GTV-8) were also recovered. Host rocks include small, altered ultramafic rock chips (35GTV-4), however, larger samples of altered and pyritized harzburgite (35GTV-5) and serpentinite (35GTV-6, 35GTV-9) were also sampled. Remarkable was the presence of a mm-thick norite vein cutting through peridotite sample 35GTV-9. Fe-oxyhydroxide crusts are abundant (35GTV-10).

Station 49GTV aimed to sample the host rocks of working area II. The collected rocks were mainly ultramafics, which could be discriminated into 5 different groups. Most abundant were slightly serpentinized dunites and harzburgites with mylonitic textures (49GTV-3A to -3C) and with randomly oriented textures (49GTV-3D to -3P). Most of these samples were olivine-rich and display angular to rounded shapes classifying them as part of the talus. The second group is made up of ultramafics with low modal amounts of olivine and laminar to layered silicic melt intrusions (49GTV-4A to -4H; Fig. 3.18f). The third group is formed by distinctly serpentinized dunites and olivine-rich harzburgites with serpentine- and carbonatefilled fractures (49GTV-1A and 1B and 49GTV-5A to -5P). The fourth group consists of penetratively serpentinized peridotites (49GTV-6A to -6F). One rounded dunite sample with an orthogonal, serpentine-filled fracture system (49GTV-2) may be regarded as a magmatic cumulate. Furthermore, one small sample of vesicular basalt (49GTV-7), one basalt with magmatic contact to peridotite (49GTV-8) and one microgabbro (49GTV-9) were found. The matrix to these samples consists of grayish mud (49GTV-10).

53ROV: Sample 53ROV-1 is a piece of a chimney wall taken at the small, active black smoker a few meters south of IRINA II and consists of massive chalcopyrite with dots of hematite replacing chalcopyrite. Additionally, talus-like pieces of red jasper beneath a black smoker at the eastern rim of the smoking crater "B" (sample 53-ROV-2) were sampled. Sample 53ROV-13 is a talus piece of a chimney wall that was recovered beneath an active black smoker at IRINA (Fig. 3.17b). The chimney wall seems to be very young and consists entirely of chalcopyrite showing multiple layers resembling tree rings. Sample 53ROV-14 was taken at the base of the same black smoker in bright red Fe-oxyhydroxides. Two samples were recovered on the ROV frame and their sampling location is therefore uncertain. Sample 53ROV-15 is a piece of porous chalcopyrite/pyrrhotite, whereas sample 53ROV-16 is a red jasper.

Station 54GTV sampled 200 kg of breccia material on a hydrothermal mound to the east of IRINA II. The material consists of secondary Cu-sulfides with cm wide veins of white to brown carbonate + Fe-oxyhydroxides + atacamite + silica (54GTV-2; Fig. 3.17f). Chalcocite seems to be the dominant Cu-sulfide (54GTV-1), however, few relics of primary chalcopyrite are still present (54GTV-3). Native copper occurs as small (< 1mm) specs in the carbonate veins, but also in small late veins of quartz or amorphous silica. Partial oxidation results in the formation of porous, bright red Fe-oxides cementing and replacing chalcocite (54GTV-4; Fig. 3.17g). The surface material contains abundant Fe-oxyhydroxide mud (54GTV-7) and crusts with bright green atacamite (54GTV-6) as well as few large blocks of orange jasper (54GTV-5).

56ROV: During this dive a single small piece from an active chimney of IRINA II was accidentally recovered by the PROFILUR system. It consists of fine-grained chalcopyritepyrrhotite with a mm thin pyrite/marcasite crust.

Station 57GTV aimed to sample rocks at the shallowest position near the new Logatchev 4 field. About 50 % of the samples recovered were serpentinized peridotites, i.e. medium-grained dunites and harzburgites (57GTV-1A-1 to -5; Fig. 3.18c), cataclastic, medium-grained peridotite breccias (57GTV-1B-1 and -1B2) and one mylonitic peridotite (57GTV-1C). All these rocks yielded high amounts of relatively fresh olivine crystals. Mafic rocks of this station were pristine, gray-black as well as heavily weathered, brownish vesicular basalts with a dense matrix and mm-sized olivine phenocrysts (57GTV-3A to -3H). A remarkable finding of this grab was a fine-grained, greenish, schistose amphibolite consisting of distinctly aligned hornblende, olivine and plagioclase (57GTV-2). This rock exhibits a mm-sized alteration crust of limonite as well as limonite on fractures.

Station 62GTV sampled hydrothermal crusts in the Logatchev 1 field and almost exclusively grabbed scoriaceous, black, sulfide-cemented breccias (~100 kg; 62GTV-5). This material contained fragments of the wall-rock and abundant orthopyroxene crystals. The sulfides were predominantly pyrrhotite and subordinately pyrite/chalcopyrite. Ultramafic samples included serpentinized harzburgites with pyrrhotite mineralization on fractures and in the matrix (62GTV-1, -2, -4) and an almost totally serpentinized dunite with a thin sulfide crust (62GTV-3). Few pieces of pyrrhotite-rich material (62GTV-6) contained abundant barite and fragments of heavily altered orthopyroxene. Furthermore, one piece of vein quartz (62GTV-7), gray-green silicified clay (62GTV-8) and dark-brown to red globigerina clay (62GTV-9) were sampled.

64ROV: All samples taken during this dive were recovered from the rim of the ANNA LOUISE smoking crater. Sample 64ROV-1 is a massive, porous chalcopyrite-rich chimney with very small conduits and was taken from the talus pile between the active "Candelabrum" black smoker chimney and an inactive chimney next to it, both on the southern rim of the crater. The center of the chimney piece is slightly recrystallized. The outer surface is coated by a thin layer of Fe-oxyhydroxides. A second talus piece of massive, zoned chalcopyrite was recovered from the base of the "Candelabrum" chimney itself (64ROV-2) and shows bulbous chalcopyrite growth on the inside. The zonation is similar to that of sample 53ROV-13. Atacamite occurs on fractures. The middle part of the inactive chimney to the west of the "Candelabrum" black smoker was later recovered (64ROV-11) and consists of massive chalcopyrite with a thin outer rim where chalcopyrite is replaced by bornite. Talus material

from another small, active black smoker on the eastern crater rim of ANNA LOUISE was recovered with the slurp gun (64ROV-10). The sample consists of bright red, oxidized sulfides with remnants of secondary Cu-sulfides, as well as small chips of chalcopyrite and few pieces of sphalerite+anhydrite. Fluid samples were taken at this small black smoker during this dive.

At station 67GTV two different types of peridotites were recovered: the first group (67GTV-1A,B) consists of coarse-grained to pegmatoid orthopyroxenites with random orientation of the cm-sized orthopyroxene prisms. In part, olivine-rich sections were present. The second group (67GTV-2A to -2K; Fig. 3.18e) comprises distinctly serpentinized, medium- to coarse-grained peridotites, which are strongly fractured. In most cases, the 1-2 mm-wide fractures are filled with serpentine while one sample is cut by a 5 mm-wide talc- and quartz-bearing vein (67GTV-2B). Another suite of rocks (67GTV-3A1,-2,-3) sampled during this station consisted of greenish metabasalts, which in part displayed chilled margin textures. One sample (67GTV-3A3; Fig. 3.18h) displays distinct silicification and a magmatic contact to a coarse-grained ultramafic rock. The metabasites show mm-thick Mn-oxide crusts.

73ROV: Ultramafic rocks were recovered from a small outcrop near marker "C". The samples consist of strongly limonitized, reddish serpentinite (73ROV-1A1,2,-1B2) and one sample of coarse-grained, serpentinized harzburgite with a cm-thick, brownish alteration crust (73ROV-1B1). Piece 73ROV-1B2 is cut by several tiny quartz veins. Later in the dive, a dm high, pipe-like sulfide spire was sampled on the eastern side of the venting IRINA II complex (sample 73ROV-2). The spire was one of the few that were not covered by biota and consists of a porous mixture of pyrrhotite and sphalerite.

The aim of station 74GTV was to sample the sedimented area close to the Logatchev 1 mound. The host-rock found here consists of strongly fractured and distinctly weathered orthopyroxenite and websterite (group 74GTV-1; 15 samples) and peridotites with strong to complete serpentinization (group 74GTV-2; 10 samples). Weakly indurated, brownish-yellow sediment consists of carbonate with globigerina detritus, clay, Fe-oxides/hydroxides and stains of atacamite (groups 74GTV-3, -4, -5).

Station 77GTV sampled ultramafics to the west of IRINA II in the Logatchev 1 field. One mylonitic, partly serpentinized dunite shows mm-sized olivine porphyroclasts in a dense matrix of serpentine (77GTV-1A). The sample is characterized by a dark-grayish Mn-oxide crust. Furthermore, muddy, carbonate-rich, yellow-brownish sediment was recovered (77GTV-1,2).

During station 78GTV ultramafic rocks to the east of the Logatchev 1 field were sampled. The upper part of the grab sample consists of, up to 30 cm thick, Mn-crusts (group 78GTV-1; 30 samples, some with an Fe-oxide layer in the center). The Mn-layer shows several sublayers of shiny black, dense material with characteristic jointing (probably from rising diffuse hydrothermal fluids). The host rocks are serpentinized peridotites (in part with Mn-crusts; 78GTV-2,-5A,-5B), coarse grained websterites with cm-sized orthopyroxene and intergranular olivine (78GTV-3A,-3B), and distinctly weathered, coarse grained orthopyroxenites (78GTV-4A,-4B).

A full load of pelagic sediment overlying red to red-brown to orange Fe-oxyhydroxide-rich sediment was recovered during station 79GTV. Few semi-lithified pieces are encrusted in Mn-oxyhydroxides that show atacamite deposition in cavities or as crusts.

Station 82GTV aimed to sample in an area of a temperature anomaly, which was discovered during station 22-OFOS. Samples recovered include Fe-Mn-oxide crusts with irregular shape (82GTV1-1 to 8) and crusts of brownish material with intercalated Mn-Fe-layers and crusts (82GTV-2A1 to-4, -2B1 to -4). Ultramafics are greenish, dense pebbles mainly consisting of serpentine and talc (82GTV-3; 30 samples).

The objective of station 83GTV was to sample the clam field at ANYA'S GARDEN, that was found during a previous ROV dive. Upon reaching the target, shells were located and sampled. The grab recovered a full load of sulfide-rich material with few empty shells of Bathymodiolus. The surface of the grabbed material consists of Fe-oxyhydroxides with some atacamite (83GTV-1). Few pieces of a former sulfide chimney (83GTV-5) were also recovered from the surface. They show concentric growth with a Fe-oxyhydroxide rim and relict sulfides in the core. This oxidized material is overlying silicified pyrite-rich crusts that are either cementing fragments of clay altered wall rock including cm-sized orthopyroxene crystals (83GTV-2) or occur as porous massive pyrite crust (83GTV-3). The crusts are underlain by secondary Cu-sulfides that form largely unconsolidated mud with few rounded fragments and cobbles of massive secondary Cu-sulfides (83GTV-4). Only one small piece of primary chalcopyrite was recovered (83GTV-6). The lower part of the grab sample consists of mud of presumably altered rock material (83GTV-8) containing two cobbles (up to 10 cm in diameter) of talc-bearing serpentinite (83GTV-7).

Significance: Similar to previous grabs (35GTV, 62GTV) this grab shows that large parts in the vicinity of IRINA II are covered by silicified cap rocks allowing for conductive cooling of the hydrothermal fluids and enriching the sulfides in a thin veneer underneath this crust.

The aim of station 87GTV was sampling below a scarp south of the Logatchev 1 field. The most remarkable sample is a serpentinized peridotite/melanorite (87GTV-1) with a dense matrix and randomly oriented, cm-sized orthopyroxene crystals. The center of the sample contains a subrounded, 4 cm wide area, which could either be a xenolith or a somewhat less altered part of the rock. Strongly serpentinized dunite and websterite pebbles (group 87GTV-3) are regarded as part of the talus. One sample of fine- to medium grained gabbronorite contained dark labradorite and golden orthopyroxene crystals (87GTV-2).

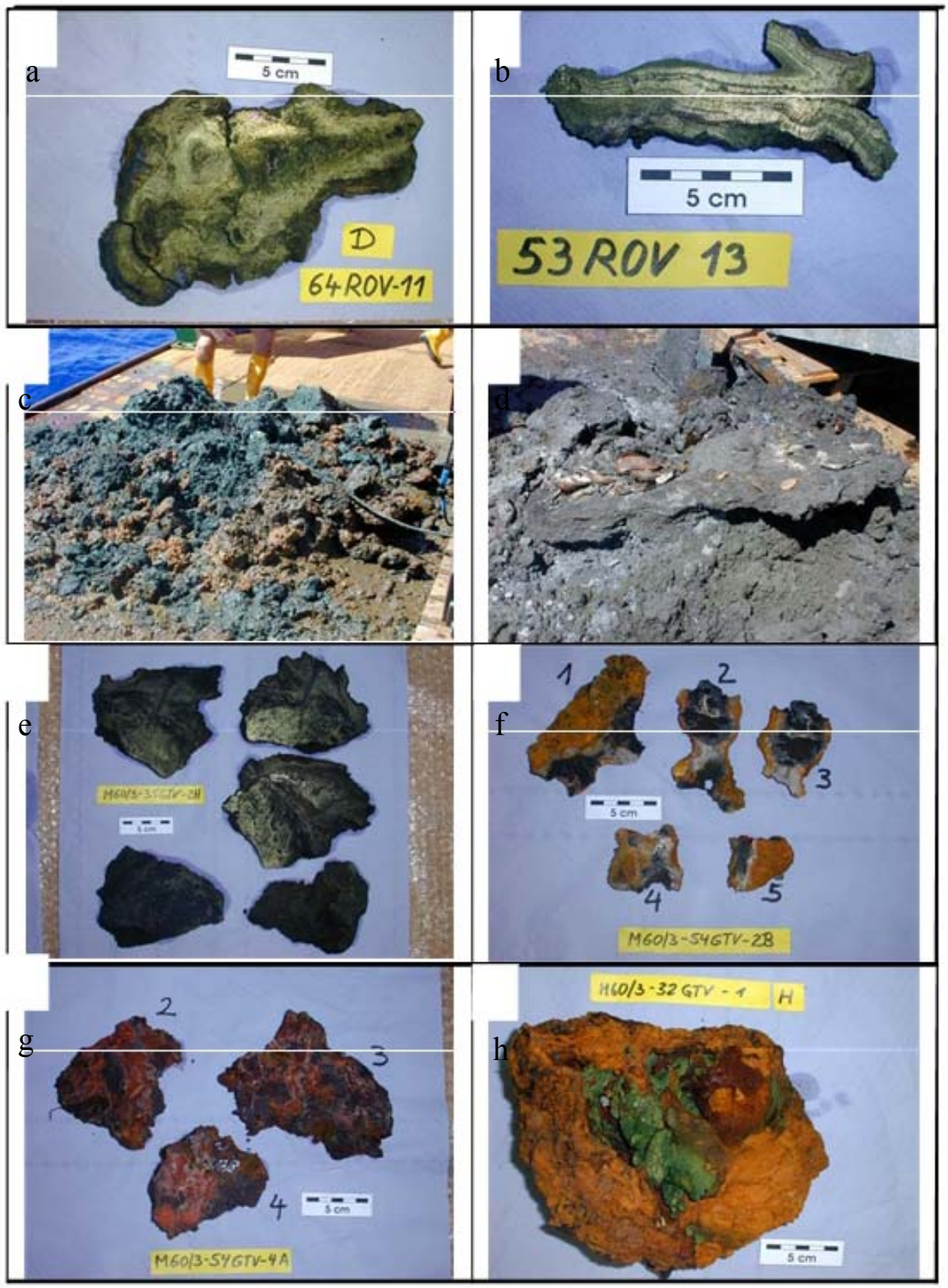

Fig. 3.17 Representative samples from the Logatchev 1 hydrothermal field. a,b) massive chalcopyrite chimney walls from black smokers. c) typical mud-rich sample from the periphery of the mound (32GTV). d) silicified crust acting as a cap rock (35GTV). e) massive chalcopyrite partly replaced by chalcocite and bornite. f) carbonate-quartz veins with native copper cutting secondary Cu-sulfides. g) hematite-rich breccias cementing chalcocite. h) Fe-oxyhydroxide crusts with abundant atacamite.

Fig. 3.18 Representative ultramafic samples from the Logatchev 1 hydrothermal field. a) websterite. b) fragment of an o rthopyroxenite. c) altered dunite with serpentine vein. d) pe ridotite mylonite. e) serpentinite with talc/quartz vein. f) peridotite with silicic melt layers. g) gabbronorite. h) basalt in contact with peridotite.

3.4.8 Gas chemistry

(R. Seifert, S. Ertl, J. Scholten)

3.4.8.1 Introduction

After the discovery of hydrothermal venting systems in 1977 continued research on vent sites made obvious that hydrothermal circulation plays an important role in the evolution of the earth. Much attention has been focused on serpentinization processes because of their potential importance to early earth hydrothermal systems and because they generate significant amounts of H_2, CH_4, and possibly other organic compounds during mineral-fluid reactions. The Logachev field at 14°45'N on the MAR is the first hydrothermal field which was found on the top of completely serpentinized ultramafic rocks outcropping at the seafloor.

This study aims to elucidate the transformation of carbon species and reduced gases brought along by hydrothermal fluids taking into account the extend and relevance of hydrothermal cyclicity. For this purpose, samples of hydrothermal fluids and plumes of two areas along the MAR (Logachev and 4°-11°S) will be sampled during several expeditions and analysed for the concentrations and isotope signatures (C, H) of the main reactive gases methane and hydrogen as well as of other components of the carbon cycle namely C_2-C_5 hydrocarbons, dissolved organic matter (DOC), CO_2, and biomass. Reported are first results from the first cruise to the Logachev field.

3.4.8.2 Samples and methods

For analyses of dissolved gases a total of 210 water samples were obtained from 17 CTD/Rosette and 7 ROV stations (Table 3.3).

CTD data were mostly recorded for the entire water column using a SEABIRD CTD Type 911 equipped with a rosette of 22 10L Niskin bottles. Water samples were taken during lifting keeping the sampler at a certain depth for a short time.

Light dissolved hydrocarbons were analysed on board applying a purge and trap technique (Seifert et al., 1991). The water sample is stripped by He and analyses in the outflowing gas stream are concentrated in cooled traps at -84°C. After degassing, the trapped gases are released to a gaschromatograph (CARLO ERBA GC 6000) equipped with a packed (activated Al_2O_3) stainless steel column and a flame ionisation detector (FID) to separate, detect and quantify individual components. Recording and calculation of results is performed using a PC operated integration system (BRUKER Chrom Star). Analytical procedures were calibrated daily with commercial gas standards (LINDE). Analyses were generally done within 12 hrs after sampling.

For on board measurements of dissolved hydrogen up to 615ml of sample is connected to a high grade vacuum in an ultrasonic bath and heated until boiling. Aliquots of the released gas are transferred via a septum from the degassing unit into the analytical system. A gaschromatograph (THERMO TRACE) equipped with a packed stainless steel column (Molecular sieve 5A, carrier gas: He) and a pulsed discharge detector (PDD) is used to separate, detect and quantify Hydrogen. Recording and calculation of results is performed using a PC operated integration system (THERMO CHROM CARD A/D). Analytical procedures were calibrated daily with commercial gas standard (LINDE).

Table 3.3: Sample list for CTD- and ROV stations.

Station	Long. N	Lat. W	No.	HC	H_2	$\delta^{13}CH_4$	δ^2H_2	He	δ^{13}C-DIC	δ^{13}C-DOC	^{222}Rn
17 CTD	14°39,9	44°60,0	18	18	12						2
25 CTD	14°45,1	44°58,7	11	11	11	11		11	11	11	11
31 CTD	14°48,5	44°58,2	12	12	11						5
37 CTD	14°45,2	44°58,8	18	18	12	12					8
44 CTD	14° 54.1	44° 54.6	17	16	13	13		7			3
51 CTD	14°44,8	44°58,8	6	6	6	6	1				5
52 CTD	14°43,4	44°57,6	6	6	6	6		6	6		3
58 CTD	14°44,1	44°58,4	6	6	6	6		6			4
59 CTD	14°44,4	44°58,9	8	7	8	7		7			4
68 CTD	14°44,0	44°57,5	8	8	8	8		8			6
69 CTD	14°45,5	44°58,0	8	8	8	8		8			5
71 CTD	14°45,0	44°56,4	9	9	9	9					
75 CTD	14°44,8	44°59,1	10	10	10	10		10			7
76 CTD	14°44,5	44°59,3	9	9	9	9		9			6
81 CTD	14°42,4	44°54,5	10	10	10						
85 CTD	14°45,1	44°58,9	13	13	13	13		13			12
86 CTD	14°44,0	44°59,6	11	11	11	11		11			
23 ROV			3	3	3	3					3
38 ROV			5	5	5	4		1			2
53 ROV			6	6	5	5	4		5	3	4
56 ROV			3	3	3	3			2		3
64 ROV			5	5	5	5	2		5		3
66 ROV			3	3	3	3			3		3
73 ROV			5	5	5	5	3	1	5		5

HC = CH_4 and C_2 -C_4 hydrocarbons

For onshore measurements of the He concentrations and isotopic signature, water samples were taken immediately after finishing the respective station. The samples were sealed head space free and gastight in copper tubes. Measurements will be performed at the Universität Bremen, Fachbereich 1 (Tracer Oceanography).

Samples for the determination of $\delta^{13}C$ of the dissolved light hydrocarbons were obtained by degassing the water samples with a vacuum - ultrasonic technique (see above). Aliquots of the released gas were transferred via a septum from the degassing unit into gastight glass ampoules filled with NaCl-saturated water for later on shore analysis by GC-Isotope-Ratio-Mass-Spectrometry.

For onshore analysis of stable carbon isotopes of dissolved inorganic carbon (DIC), aliquots of unfiltered sample was spiked with NaOH and $BaCl_2$ directly after recovery to precipitate carbonate species. The analyses of $\delta^{13}C$-DIC will be made by Dual-Inlet-Isotope-Ratio Mass-Spectrometry (THERMO MAT 252).

For onshore analysis of stable isotopes for dissolved hydrogen, up to 10mL of gas obtained by vacuum/ultrasonic degassing of sample was frozen on molecular sieve 4A under liquid nitrogen in a pre-vacuated glass vial. The samples will be analysed via a molecular sieve 5A PLOT column and a GC-Isotope-Ratio-Mass-Spectrometer for δ^2H-values.

Samples for radionuclide measurements were obtained by CTD and the ROV fluid sampling device. For ^{222}Rn analysis water samples were filled into an extraction apparatus and a water-immiscible scintillation cocktail (MaxiLight) was added. The sample was shaken for 1.5 hours and the organic phase was transferred into a low diffusive LS-vial which was stored for isotope equilibration for three hours. Two liquid scintillation counters (Gurdian and Triathler) were available for on-board ^{222}Rn measurements. Samples were counted for six hours. Final calibration of the procedure and calculations of specific activities will be performed in the home lab. A list of samples obtained during the cruise is given in Table 3.2. Additional water samples (up two litres) were taken for the determination of ^{228}Ra and ^{210}Pb from ROV stations 73 Rov, 66ROV, 53 ROV, 73ROV and 38 ROV.

3.4.8.3 Results

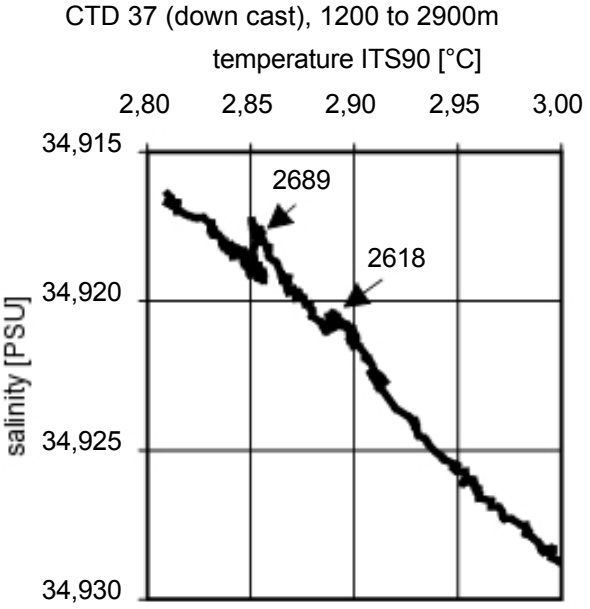

Fig 3.19 S/T diagram of deep waters, 37 CTD

dissolved gases and trace metals, this anomaly represents the hydrothermal plume of the Logatchev Field. However, such clear indications of hydrothermal influence did not appear in any of the other CTD profiles recorded. Therefore, on line information on the location of hydrothermal plumes within the water column for the selection of samples to be analysed for gases (hydrocarbons and hydrogen) and metal species was not available during most hydrocasts.

For most stations, no indication of hydrothermal plumes could be identified within the CTD-profiles. An exception is station 37-CTD for which the S/T plot evidences the intrusion of a component relatively depleted in salinity for the depth area from 2600m to 2700m water depth (Fig. 3.19). With regard to the data of

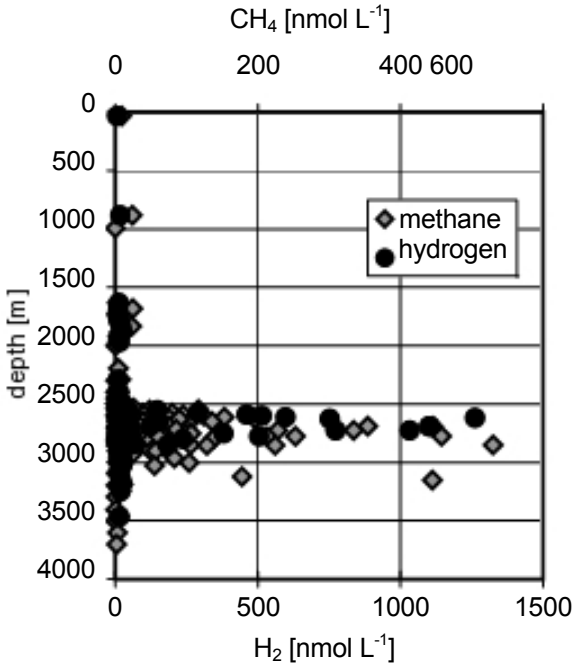

Fig. 3.20 Concentrations of CH_4 and H_2 in water samples of all CTD-stations

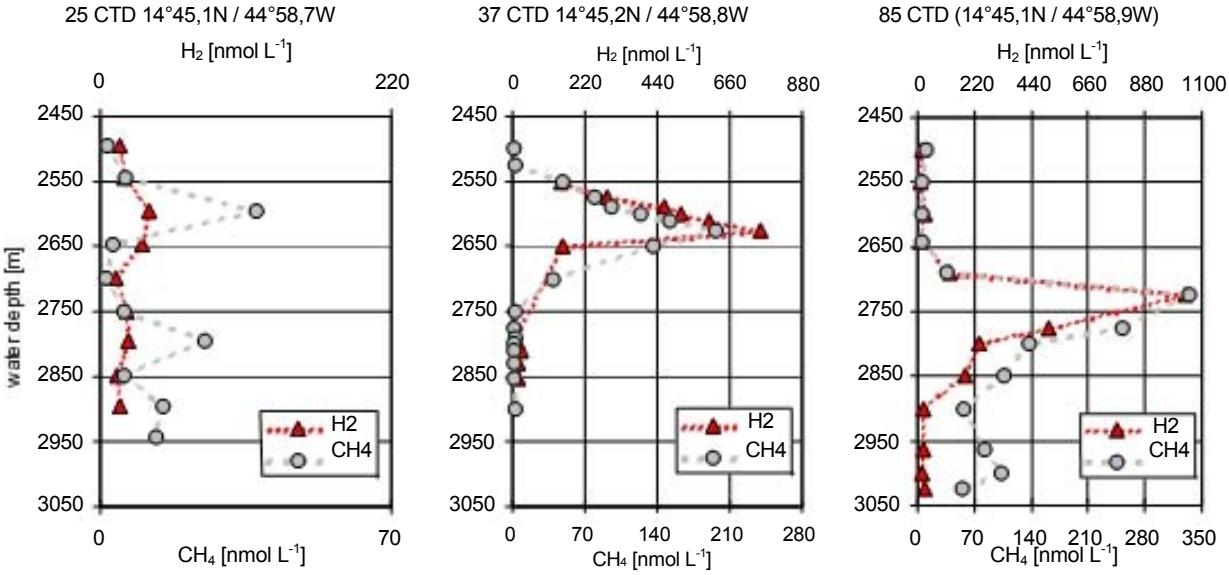

Fig. 3.21 Concentrations of CH_4 and H_2 in water samples of CTD-stations 25, 37, and 85.

Results for concentrations of dissolved methane and hydrogen obtained from CTD/rosette samples on board RV METEOR (Fig. 3.20) revealed a distribution of hydrothermal signatures over a wide zone of the water column covering the depth range from 2500m to 3000m water depth. Highest concentrations found are 0.53 and 1.26 µmol L^{-1} for methane and hydrogen, respectively.

High CH_4 concentrations correlate with high H_2 concentrations in most cases. A considerable variety of the depths of maximum concentrations and of maximum H_2/CH_4 ratios was observed. Figure 3.21 illustrates the results for 3 CTD stations carried out at the northern edge of Logatchev-1 field which are less than 0.2 nm apart.

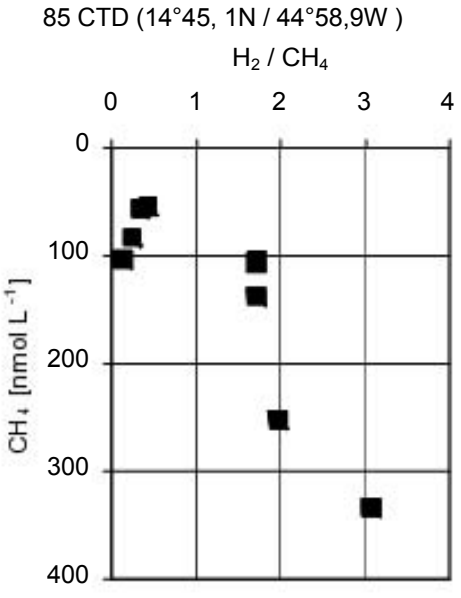

Fig. 3.22 H_2/CH_4 ratio vs. CH4 concentration for samples below 2700m water depth.

Two concentration maxima were present at station 25 at 2600m and 2800m water depth. (2600m: 37.5 nmol L^{-1} CH_4, 36.4 nmol L^{-1} H_2; 2800m: 25 nmol L^{-1} CH_4, 21.5 nmol L^{-1} H_2). Much higher concentrations were measured at stations 37 and 85. Station 37 revealed a distinct maximum at 2625m (196 nmol L^{-1} CH_4, 752 nmol L_{-1} H_2); at station 85 highest concentrations occurred at 2725m (335 nmol L^{-1} CH_4, 1033 nmol L_{-1} H_2) with strongly enhanced methane concentrations throughout the water column below. The H_2/CH_4 ratio for these samples (Fig. 3.22) appears to decrease with decreasing methane concentrations hinting to an enhanced consumption rate for H_2 compared to CH_4. This agrees with observations of Kadko et al. (1990) who found a very rapid removal of hydrogen from the plume compared to ^{222}Rn decay and

methane oxidation for the Endeavour Ridge hydrothermal plume, but at much lower H_2 concentrations of only up to 12 nmol L^{-1}.

Samples obtained by ROV directly at the hot fluid emanation sites revealed very high concentrations of dissolved hydrogen. Maximum concentrations found accounted for 0.28 mmol L^{-1} and 1.8 mmol L^{-1} of methane and hydrogen, respectively (Station 73 ROV). The resulting H_2/CH_4 ratio of about 6.4 for this sample is in accordance with data reported by Charlou et al. (2002) for hydrothermal fuids of the Rainbow field that is also hosted in ultramafic rocks at the MAR. These authors give Mg-based calculated endmember concentrations of 2.5 mmol L^{-1} (CH_4) and 18 mmol L^{-1} (H_2), slightly above endmember gas concentrations estimated for Logachev with 12 and 2.1 mmol L^{-1} for H_2 and CH_4 respectively. In view of the good match of the H_2/CH_4 ratios, one might assume our ROV sample to comprise about 10% of unaltered endmember fluid.

For hydrocarbons of carbon chain lengths from 2 to 4 only saturated homologues were observed (ethane, propane, butanes), but in low concentrations. Molar ratios between methane and higher homolgues (C_1/C_{2-4}) were generally above 2000.

3.4.9 Fluid chemistry

(A. Koschinsky, B. Alexander, L. de Carvalho, D. Garbe-Schönberg, U. Westernströer)

3.4.9.1 Fluid sampling system for the MARUM ROV QUEST

For the direct sampling of hydrothermal fluids from high temperature vents a pumped flow-through system (Kiel Pumping System, KIPS) was used. The system was newly constructed and is entirely made of inert materials (Teflon, titanium). Samples are collected via a titanium tube of 100 cm length which can be directly inserted into the hot vent orifice. PFA tubing connects this sampling probe to 7 parallel PFA Teflon sampling flasks (490 ml Volume each, “Bottle #1” to “Bottle #7”) and a standard deep sea impeller pump (SeaBird, U.S.A.) mounted downstream to the sampling flasks (Fig. 3.23). Each sampling flask has linked open-close valves (valve set #1 to #7) with handles which are operated by the ROV’s manipulator (Figs. 3.23, 3.24). The sampling flasks are mounted with a few degrees inclination and equipped with all-Teflon overpressure valves. Eventually released gases and fluids can be collected in gas-tight bags fitted to the valves. In-line PFA Teflon filter holders in front of each sampling flask allow in-situ filtration of sampled fluids. An additional open-close valve set (valve #8) bypasses the sampling flasks and was used as a sampling line for microbiology in-situ filtration. The whole system is contained within a plastic frame mounted on the ROV’s tools sled. For sub-sampling the whole system was removed from the ROV and transferred to the laboratory. Two sample flasks were filled at every sampling location (Bottles #2 and #7, #3 and #6, #4 and #5). This accomplishes the study of fluid chemistry and dissolved gases on sub-samples that are as identical as possible.

3.4.9.2 Fluid sampling and filtration

Three bottles from the KIPS fluid sampling system (bottle #2, #3, #4) and all three Niskin flasks (N1, N2, N3) mounted on the ROV were sub-sampled in the laboratory immediately after recovery of the ROV. The fluid samples were pressure-filtrated with Argon (99.999%) at 0.5 bar through pre-cleaned 0.2 µm Nuclepore PC membrane filters by means of polycarbonate filtration units (Sartorius, Germany). The filtrates were separated into aliquots for voltammetric and ICP analyses and acidified to pH 1 with 100 µl subboiled concentrated nitric acid per 50 ml (ICP) and with suprapure HCl to pH 2 (voltammetry), respectively. Procedural blanks were processed in regular intervals. All work was done in a class 100 clean bench (Slee, Germany) using only all-plastic labware (polypropylene, polycarbonate, PFA-teflon). Rinse water was ultrapure (>18.2 Mohm) dispensed from a Millipore Milli-Q system.

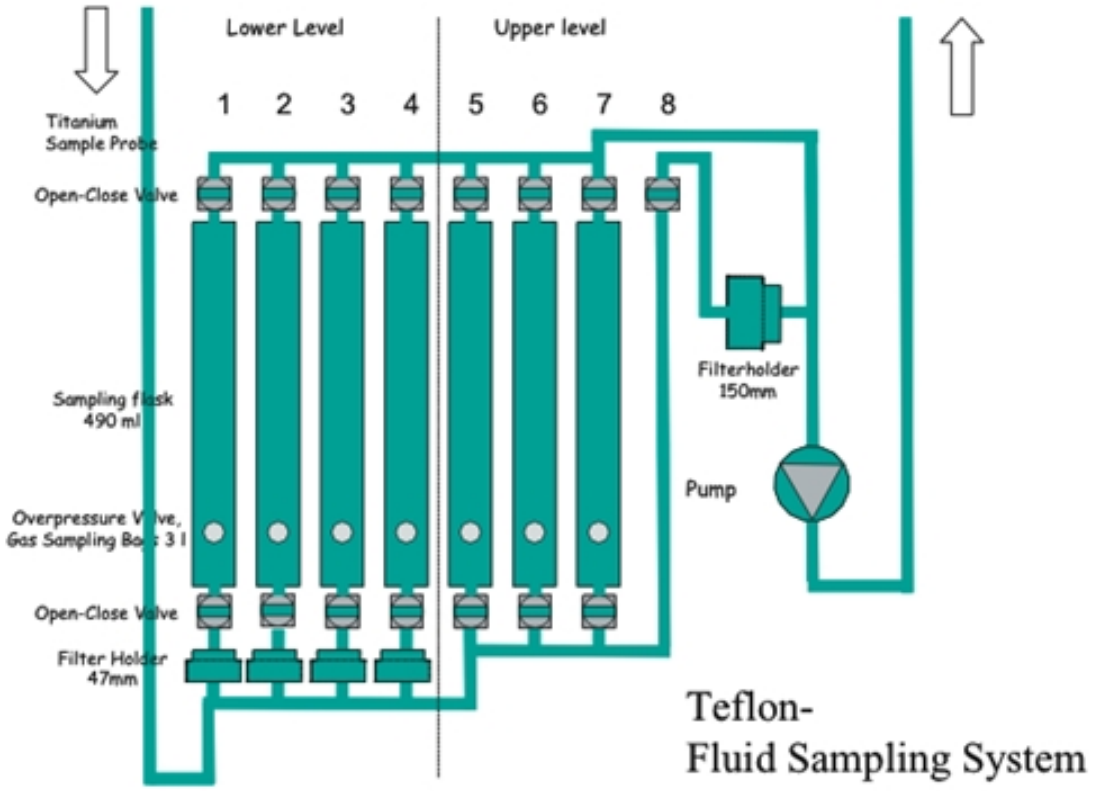

Fig. 3.23: Schematic drawing of the Kiel fluid sampling system for in-situ sampling of hydrothermal vent fluids.

A total of 34 bottle samples from the fluid sampling system, and 20 Niskin samples were taken (Table 3.4). After return to the home labs, in Kiel selected samples will be analysed for major (Mg, Ca, Ba, Sr, Na, K, Si, Fe, Mn, B, Cl) and trace element composition (e.g., I, Br, Li, Al, Cs, Ba, Sr, Y-REE, Fe, Mn, Cr, V, Cu, Co, Ni, Pb, U, Mo, As, Sb, W, PGE) by ICP-OES (Spectro Ciros SOP CCD) and ICP-MS using both collision-cell quadrupole (Agilent 7500cs) and high-resolution sector-field based instrumentation (Micromass PlasmaTrace2). At IUB in Bremen, voltammetry will be used for further trace metal analyses (Zn, Cd, Pb, Cu, Co, Ni, Ti, V, Mo, U, Tl, Pt). Li and Na will be analysed by flame photometry, and an autoanalyzer will be used to determine anionic compounds (silicate, phosphate, nitrate,

sulfate, chloride) and dissolved organic carbon DOC. The duplicate coverage of some elements with different methods will be used for the evaluation of the methods and the data.

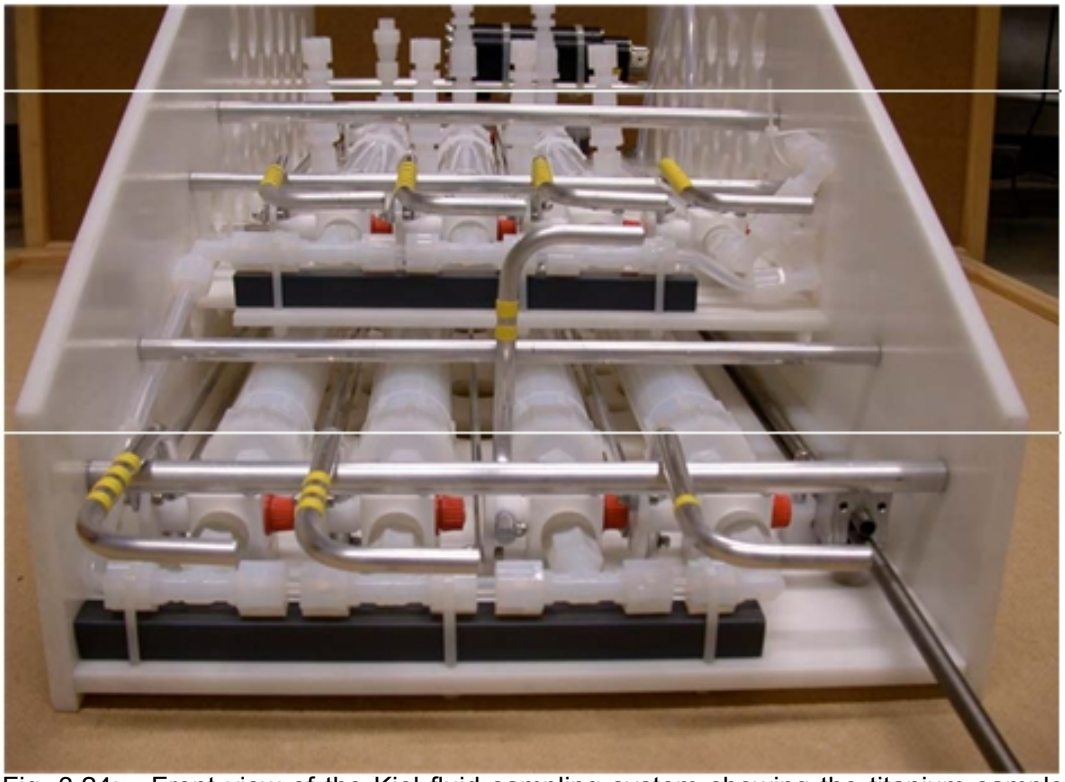

Fig. 3.24: Front view of the Kiel fluid sampling system showing the titanium sample probe (right), valve handles, PFA Teflon sampling flasks, and overpressure valves (top).

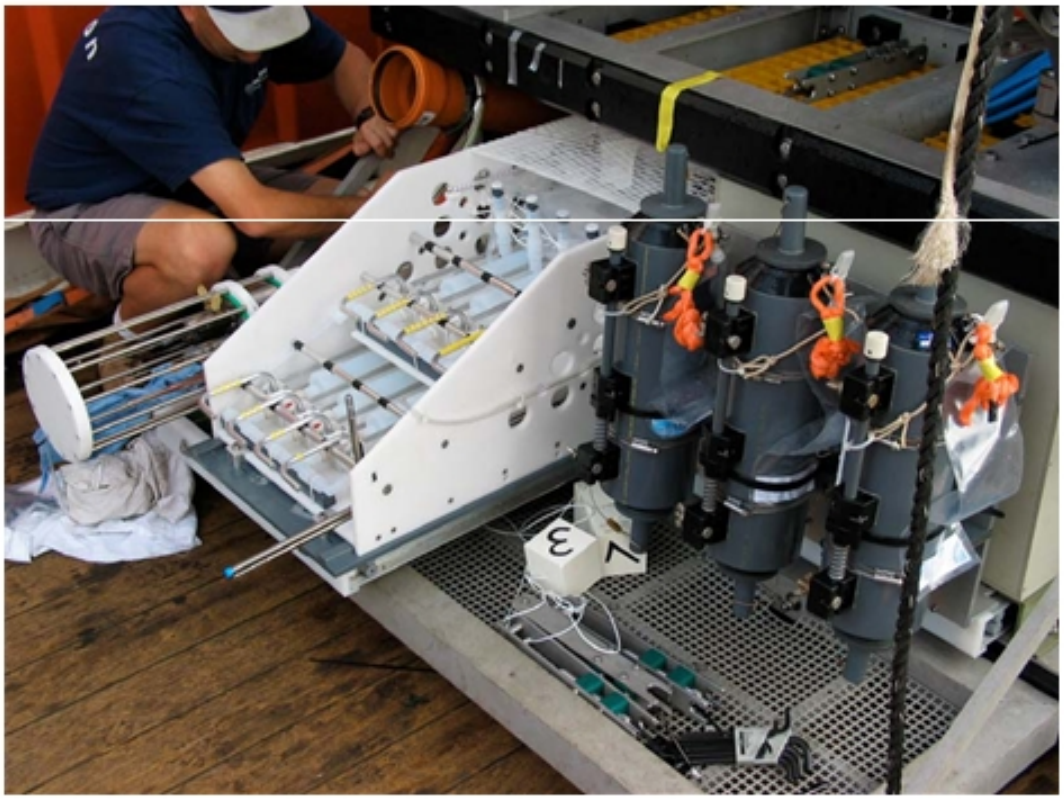

Fig. 3.25: The fluid sampling system mounted on the tools sled of the Bremen MARUM ROV QUEST besides Niskin bottles and the MPI Bremen sensor array.

Table 3.4: Samples for Trace Element Geochemistry

St. No M 60/3	Instrument	Dive type	Location	Lat (N)	Long (W)	Water depth (m)	B 1	B 2	B 3	B 4	B 5	B 6	B 7	B 8	N 1	N 2	N 3
23	ROV	Geo	IRINA II	14° 45,196	44° 58,787	3044			TM	TM	G		G	MB		G	
29	ROV	Geo	IRINA	14° 45,111	44° 58,710	2976		TM			G	G	TM G	MB	TM G	TM G	
38	ROV	Bio	IRINA II	14° 45,185	44° 58,750	3031	S	TM	TM	TM	G	G	G	MB	TM	TM	TM
53	ROV	Geo	IRINA	14° 45,084	44° 58,709	2959	S	TM	TM	TM	G	G	G		TM G	TM G	TM G
56	ROV	Bio	IRINA II	14° 45,217	44° 58,814	3041		TM				G	G	MB		TM G	TM
64	ROV	Geo	Anna-Louise	14° 45,070	44° 58,690	2948		TM	TM			G	G		G	TM G	TM G
66	ROV	Bio	IRINA & IRINA II	14° 45,083	44° 58,696	2959	TM	G	TM			G			TM	TM	TM G
73	ROV	Geo	IRINA II	14° 45,206	44° 58,741	3033	S	TM	TM	TM	G	G	G		TM G	TM G	TM

TM: Trace metals and speciation chemistry; G: Gas chemistry; MB: Microbiology; S: Sulfur isotopes and organic complexation; B: Sampling-Bottle from KIPS fluid sampling system; N: Niskin-Bottle. Bottle pairs (TM/S-Analytics and Gas chemistry): B2 - B7, B3 - B6, B4 - B5.

3.4.9.3 Onboard measurements : pH and Eh measur ements, sample preparation and chloride titration

The fluid samples were obtained from the fluid sampling system coupled to the ROV QUEST and from the CTD/Rosette water sampler. Especially the anoxic fluids from the hot vents were analyzed and stored immediately after system recovery. Filtered and non-filtered samples (partly acidified to pH 2 with suprapure HCl) were subjected to immediate voltammetric speciation analysis (see below). Parallel to that, pH and Eh measurements (Mettler electrodes with Ag/AgCl reference electrode) were carried out in unfiltered sample aliquots. All fluid samples were stored in a refrigerator at 4°C between the analyses. To identify a possible influence of phase separation, all vent fluid samples and some samples from the water column profiles were analysed for chloride by titration with $AgNO_3$ after the method of Fajans, using fluoresceine-sodium as indicator. From selected samples, about 150 ml of fluid were filled into specially precleaned bottles and immediately deep-frozen at -20°C. These samples were shipped in frozen state for the determination of organic metalcomplexation in the home laboratory of the project partner Dr. Sylvia Sander (University of Otago, New Zealand).

3.4.9.4 O nboard measurement s: Volt ammetric anal yses of trace metal speciations and concentrations

For onboard speciation and trace metal concentration analyses, the electrochemical method of voltammetry was used. Voltammetry is able to differentiate between different redox species and (in combination with UV digestion of the water samples) free and complexed forms of ions in solution and is highly sensitive. All voltammetric measurements were performed using two Metrohm equipments: a 693 VA Processor in combination with a 694 VA Stand (all from Metrohm, Herisau, Switzerland), and a 757 VA Computrace run with a standard PC. The three-electrode configuration consisted of the hanging mercury droplet electrode (HMDE) as the working electrode, an Ag/AgCl reference electrode (3 mol l^{-1} KCl), and a platinum wire as the auxiliary electrode.

Immediately after recovery, the fluid samples were prepared for speciation analyses onboard. The unfiltered samples were used for determination of the total content of the metals, while filtered (0.2 µm) samples were prepared for determination of the total dissolved content of the metals. Both the filtered and unfiltered samples were submitted to a digestion process in a UV Digestor (Model 705, Metrohm), which contains a high pressure mercury lamp (500 W). After 2 hours UV irradiation, the total content (filtered and non-filtered) of iron, chromium and arsenic in the samples were determined by the standard addition method (n = 3).

Before the voltammetric determination of the total content of the metals in the digested samples, the redox speciation of Fe, Cr and As was carried out. Firstly, the concentrations of active Fe (non-filtered), Fe(II) and Fe(III) were determined in the undigested samples using the cathodic stripping voltammetric method developed by van den Berg (Aldrich and van den Berg, 1998). In this method, Fe(III) is determined with 1-nitroso-2-naphtol as complexing reagent and catalytic reaction with bromate, masking of Fe(II) with Bipyridyl. Fe(II) is determined by subtraction of Fe(III) from total Fe. Total and total dissolved iron are

determined after UV digestion as iron(III) but without addition of Bipyridyl.After the determination of the iron redox species, the determination of the arsenic speciation was carried out in the undigested samples by cathodic stripping voltammetry (Barra and dos Santos, 2001). In this method, As(III) is determined in a 1 M HCl and 10 mg/L Cu(II) supporting electrolyte. As arsenate is electrochemically inactive at the mercury electrode, total As is determined after the UV digestion using the rotating gold electrode (Au-RDE; Application Bulletin Metrohm 226/2). As(V) is calculated by subtraction of As(III) from total arsenic. After evaluating of the iron and arsenic concentrations in the fluid samples, the chromium redox speciation was carried out in the undigested samples by the catalytic cathodic stripping voltammetric method developed by van den Berg (Boussemart et al., 1992) and adapted to hydrothermal fluid samples by Sander and Koschinsky (2000). This method uses diethylenetriaminepentaacetic acid (DTPA) as the complexing reagent for Cr(VI) and catalytic reaction with nitrate. Firstly, the concentration of reactive total Cr is determined by addition of DTPA to the sample just before the voltammetric measurement. For the determination of Cr(VI), DTPA is added to the samples and the voltammetric measurement is carried out after 30 min. The concentration of reactive Cr(III) is obtained by subtraction of reactive total Cr from Cr(VI). The total and total dissolved Cr concentrations are determined after the UV digestion. The concentration of dissolved total Cr(III) is obtained by subtraction of total dissolved Cr from Cr(VI).

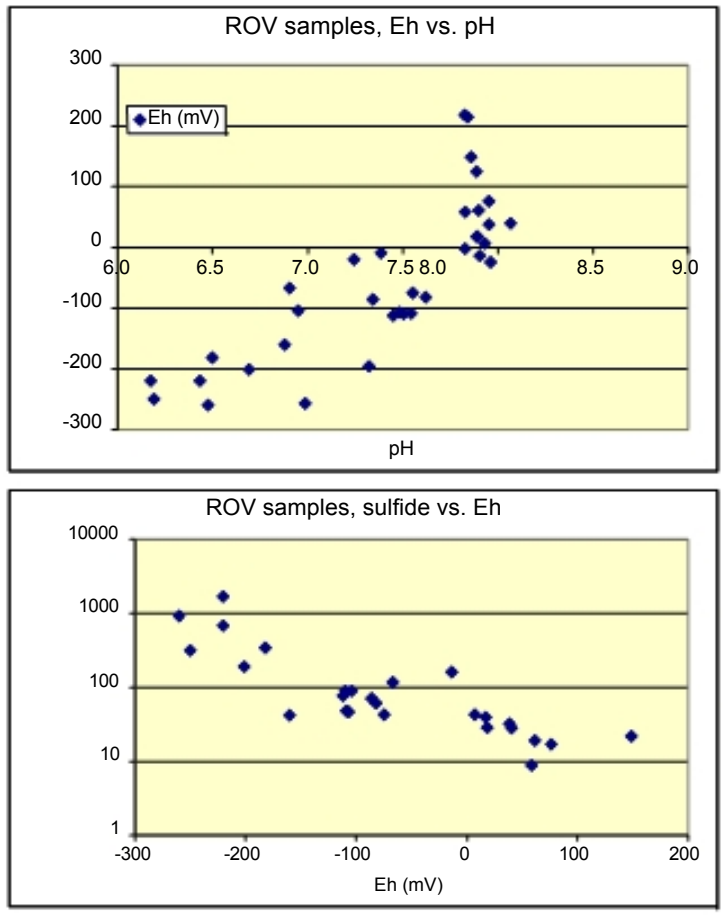

Fig. 3.26: Correlation of pH, Eh and sulfide concentrations in the ROV fluid samples

The analysis of S, Se, Mn, Cu, Pb, Cd, and Zn on ROV samples was sequential, and generally proceeded in the following order: 1) non-filtered, non-digested samples, 2) filtered, non-digested samples, 3) non-filtered and filtered digested samples. Following removal of samples from the ROV fluid sampling system, unfiltered samples were immediately analyzed for sulfide (S^{2-}) in a nitrogen purged 0.6 M NaCl solution using a polarographic method (Luther III et al., 1985). Following sulfide analysis, polarography (Madureira et al., 1997) was used to concurrently determine sulfate (SO_{32-}) and thiosulfate (S_2O_{32-}) concentrations in the non-filtered samples. Sulfur species concentrations were determined for only non-filtered, non-digested samples. Concentrations

of Se(IV) in non-digested samples was determined by anodic stripping voltammetry (ASV) with 10 mg/L Cu(II) and 0.025 M HCl as supporting electrolyte (van den Berg and Khan, 1990). Total Se was measured in digested samples, and Se(VI) calculated as the difference between total Se and Se(IV) measured in non-digested samples. Due to insufficient method detection limits, samples collected during ROV deployments subsequent to the 38ROV station were not analyzed for Se. Manganese concentrations were determined using ASV (Application Bulletin Metrohm 123/3) with 0.1 M sodium tetraborate as supporting electrolyte. For Cu, Pb, Cd, and Zn analyses samples were buffered at pH 4.6 with 1 M acetate before measurement by ASV (Application Bulletin Metrohm 231/2). The quantification of S, Se, Mn, Cu, Pb, Cd, and Zn in the samples was performed by the standard addition method (n = 3).

3.4.9.5 First results of the onboard analyses

ROV vent fluid samples

First of all it must be noted that all hydrothermal fluid samples were diluted by seawater and the results presented here are not yet recalculated to endmember compositions. The pH and Eh measurements in the samples taken directly from the vent sites with ROV clearly reflect the contribution of hot reducing hydrothermal endmember fluid and oxic seawater, respectively. The plot of Eh versus pH (Fig. 3.26) indicates only slightly depleted pH values (minimum 6.2) compared to the background value of 7.9. The most undiluted fluids show significantly reduced Eh potentials, which correlate with the contents of sulfide (Fig. 3.26). However, in contrast to fluids from many other hydrothermal fields, sulfide concentrations were found to be quite low (maximum 0.05 mM were measured) compared to the extremely high concentrations of methane and hydrogen (see chapter 3.4.7). This is interpreted as a typical feature of fluids influenced by serpentinization reactions.

The variability of Cl concentrations measured in the fluid samples is in the range of 4 % only, indicating that all samples have chlorinities very similar to ambient seawater. A slight tendency towards decreased salinities seems to be visible in Fig. 3.27 in which chloride was plotted against Fe as hydrothermal element. This would be consistent with a vapor-like fluid deriving from supercritical (>400°C, >300 bar) condensation, however, the range of the decrease is close to the range of the analytical precision (2 %).

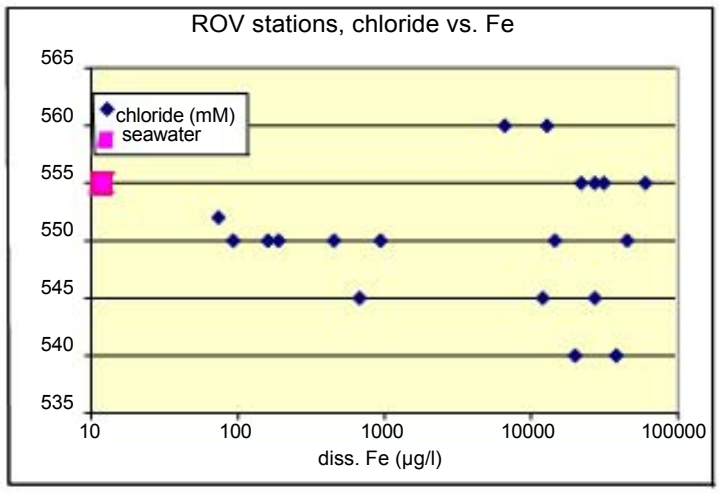

Fig. 3.27: Variability of chloride concentrations in relation to dissolved Fe concentrations

With respect to the speciation analyses, the Fe data provided the most interesting results while Se data were mostly below the detection limit of 2.5 nM. Also most data for

Cr and As species showed that these compounds were not enriched to a significant degree in the fluids, but were probably mostly bound in particulate phases, as some increased concentrations in non-filtered samples indicated. Also intermediate sulfur species (sulfite, thiosulfate) were found only at low concentrations in a few samples. Fe was the dominating heavy metal in all fluid samples, with a certain particulate contribution in the form of Fe sulfides. The speciation distribution graph (Fig. 3.28) demonstrates the dominance of Fe(II) over Fe(III) and shows that about 90 % of the total Fe are present in a free reactive form. Obviously, the Fe speciation can differ in different samples, for example 64ROV shows the highest Fe(II)/Fe(III) ratio of all samples, although the total Fe concentration (0.45 mM) is lower than that of 53ROV (3.8 mM).

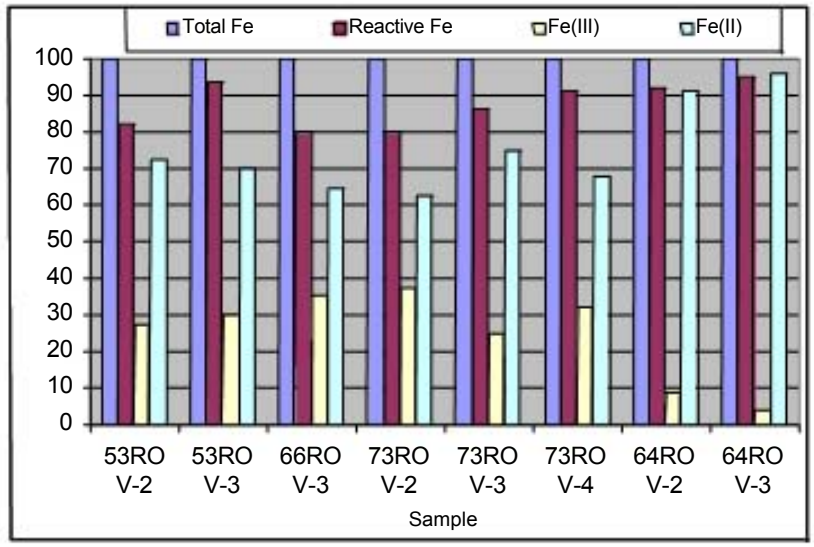

Fig. 3.28 Fe speciation in different ROV fluid samples

The second most enriched metal was Mn with maximum concentrations of 45 mM, followed by Cu (max. 27 mM total Cu) and Zn (max. 13 mM). Much of the Cu was found to be bound in particulate phases, while free dissolved Cu was found to be much lower with max. 1.5 mM. Pb (up to 0.09 mM) and Cd (mostly <0.005 mM) were comparatively low. The high Fe/Mn and Fe/Cu ratios in our M60/3 fluid samples compared to fluid data reported by Douville et al. (2001) for different MAR vent systems indicate a close similarity to the Rainbow hydrothermal field and a pronounced influence of serpentinization reactions compared to purely basaltic systems.

All data reported here are measured values and have to be extrapolated to endmember concentrations using Mg concentrations (hydrothermal endmember Mg = 0, seawater endmember Mg = 55 mM).

Water column profiles

In the samples taken by the CTD/rosette water sampler in vertical profiles in the water column, only pH and Eh measurements were carried out routinely, while for all other parameters, the hydrothermal signals were mostly too dilute to be detected. Eh measurements could be shown to be a good indicator for the hydrothermal plume because in profiles with pronounced methane and hydrogen maxima (see chapter 3.4.8), a good correlation of these maxima with decreased Eh values could be found (Fig. 3.29). This plume peak could also be identified by Fe measurements (Fig. 3.29).

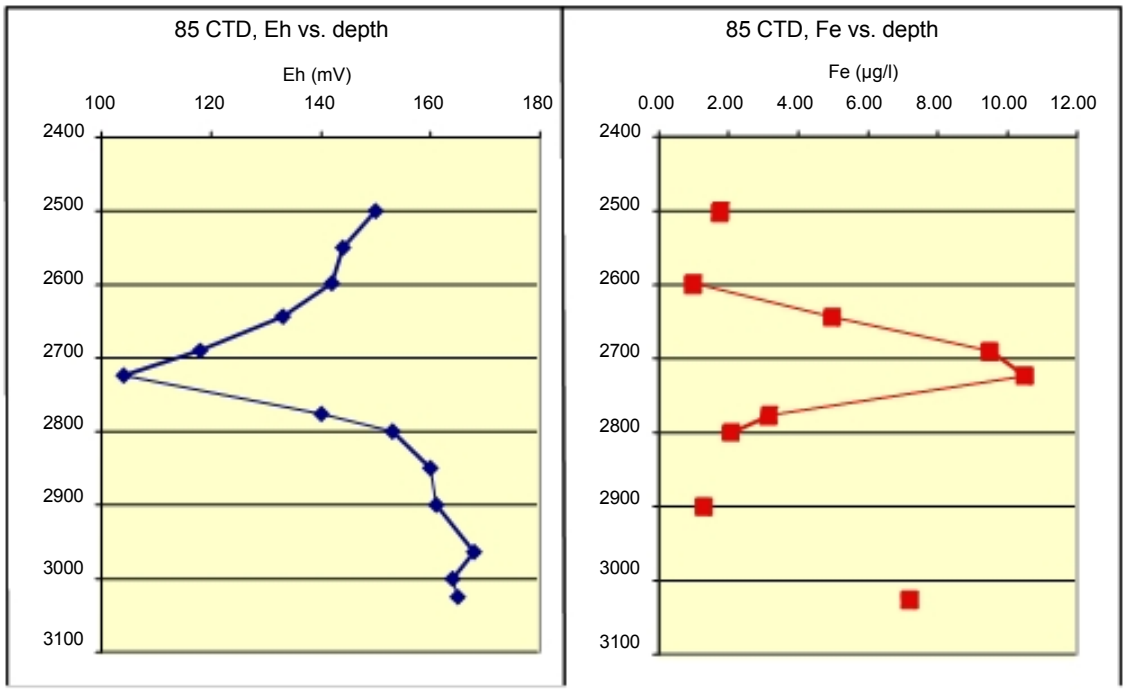

Fig. 3.29: Depth profiles for Eh and Fe at station 85 CTD, indicating a pronounced hydrothermal plume peak at about 2700 m depth

3.4.10 Hydrothermal symbioses

(C. Borowski, F. Zielinsky)

The biomass in the Logatchev vent field is primarily produced by the mussel Bathymodiolus aff. puteoserpentis (Gebruk et al. 2000) which lives in dual symbiosis with sulfide- and methane-oxidizing bacteria (Distel et al. 1995). This species was found during the M60/3 in dense aggregations around the IRINA II site. There was a large mussel bed with a diameter of more than 30 m along the southwestern slope of the chimney complex of the IRINA II mound and the vertical walls of the central sulfide complex were densely populated (mussel beds also occurred in the north and northwest of the chimney complex). Other symbiotic invertebrates encountered during M60/3 were shrimp of the genus Rimicaris which were densely aggregated on the IRINA II sulfide complex, and a population of thyasirid clams which we found buried in sediments near the marker "ANYA". We did not rediscover the population of vesicomyid clams reported from ANYA'S GARDEN by Gebruk et al. (2000), but instead observed an aggregation of empty vesicomyid clam shells in the vicinity of marker "Anya".

The major purpose of the symbiosis project was to sample, dissect, and preserve Bathymodiolus specimens from different microhabitats in order to investigate the relationship between the activity patterns of their thiotrophic and methanotrophic symbionts and the availability of their respective electron donors H_2S and methane. Further issues were to sample shrimp and clams for the phylogenetic and functional characterisation of their symbionts, mussels for analyses of trace metal accumulation in co-operation with the IUB fluid-geochemistry group. All analyses will be done at the MPI-Bremen and associated laboratories.

Different types of microhabitats of Bathymodiolus were identified during the ROV dives by video observation and in-situ temperature measurements with the "PROFILUR" sensor system (Chapter 3.4.4). Bathymodiolus specimens were scratched off specific microhabitat substrates with stalked scratch nets (20 cm diameter opening) operated by the seven-function manipulator arm of the ROV, and the filled nets were stored in the ROV sample storage box (Fig 3.30). At selected animal collection sites, additional water samples were collected for analysis of methane concentrations and $\delta^{13}C$ composition, as well as sulfide and trace metals concentrations to gain a more detailed characterization of the animals' geochemical environment. These samples were obtained with Niskin water samplers which were mounted to the front of the ROV tool sled, and individually tripped by the ROV manipulator arm. Analyses of the water samples were performed on board or will be done in the home-based laboratories of the IfBM biogeochemistry and the IUB fluid geochemistry groups. A considerable number of Bathymodiolus specimens was also recovered from the IRINA II mussel bed with 35 GTV. While these specimens were used for trace metal analyses, they were not useful for molecular and morphological analyses because the high temperatures of the substratum that they were attached to (>100°C measured in only 10 - 15 cm depth bsf) cooked the animals when the overlying water drained off as the grab was lifted from the water onto the ship. Thyasirid clams were collected by dredging with the scratch net in surface sediments. Shrimp were suctioned from their habitat with the slurp gun (Fig. 3.31) and transferred to a modified baited trap that was installed in the ROV sample storage box stored where they were kept during the rest of the dive.

Table 3.5: Specifics for ROV samples used for hydrothermal symbiosis research.

Sample no.	Location	Sample type	Time, UTC	ROV Position	PROFILUR temp. peak/aver., °C	Target organisms
38 ROV /4	Mussle bed near marker "IRINA II"	Scratch net	16:06	14°45.1842‘ N 44°58.7477‘ W	5.5 / 3.75	Mussels
38 ROV /6	Top of sulfide pillar next to IRINA II main structure	Scratch net	17:00	14°45.1878’ N 44°58.7469’ W	3.9 / 2.75	Mussels
56 ROV /6	Vertical wall of IRINA II main sulfide structure	Scratch net	22:07	14°45.1892’ N 44°58.7374’ W	2.76 / 2.7	Mussels
56 ROV /5	Vertical wall of IRINA II main sulfide structure	Slurp gun	21:47	14°45.1890’ N 44°58.7372’ W	3.6. / 2.7	Shrimp
66 ROV /13	Sediments near Marker "Anya"	Scratch net	19:19	14°45.2170’ N 44°58.8133’ W	2.7 / 2.7	Thyasirid clams
66 ROV /16	IRINA II mussel bed, downhill margin	Scratch net	20:20	14°45.1887’ N 44°58.7399’ W	3.0 / 2.8	Mussels

After recovery of the ROV, the animals were stored in chilled sea water and dissected as soon as possible for the various analytical purposes. The gills, foot tissues, and digestive glands of Bathymodiolus specimens were dissected and fixed for molecular biological analyses of 16S ribosomal RNA (rRNA) and messenger RNA (mRNA), fluorescence in situ hybridization (FISH), stable isotope analyses, trace metals and microbial biomarkers, and for

transmission electron microscopy (TEM). Tissues of the thyasirids were dissected as the mussels and preserved for analyses of 16S rRNA, FISH, and TEM. From the shrimp, the symbiont bearing maxillipeds were dissected and preserved for similar analyses.

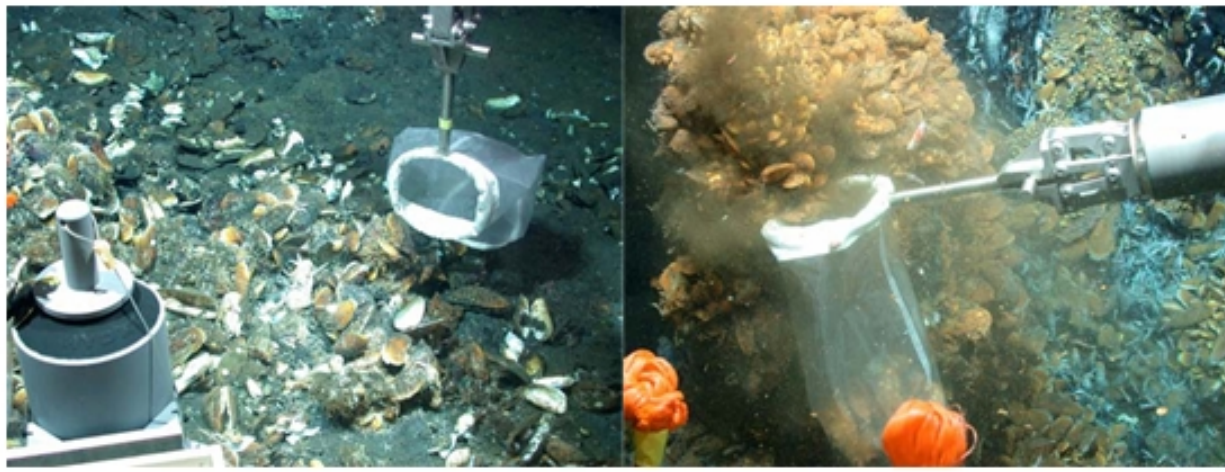

Fig. 3.30 Sampling of two different microhabitats of Bathymodiolus aff. puteoserpentis. Left: Sample 38 ROV /4 near marker IRINA II in the mussel bed; note the Niskin water sampler mounted to the ROV tool sled which is already closed. Right: sample location 38 ROV /6 on a sulfide pillar.

Fig. 3.31 Left: Dense aggregations of Rimicaris shrimp on the walls of the central sulfide structure of IRINA II. Right: Slurp gun sample of Rimicaris.

3.4.11 Marine microbiology

(J. Imhoff, J. Süling, J. Küver)

3.4.11.1 Introduction

Microbial life is abundant at hydrothermal vent ecosystems and is expected to span the whole temperature range that enables life and reproduction of microbial cells. Though quite a number of studies have been made at hydrothermal vent sites world wide, little information is available on the phylogenetic and metabolic diversity of microorganisms along physical and chemical gradients of hydrothermal vents. Parameter like temperature, availability of oxygen and electron donors and mineral salts composition of the hydrothermal fluids are considered

as major factors controlling microbial life in general and species distribution in particular. Due to the abundance of reduced sulfur compounds such as sulfide, sulfite, thiosulfate and tetrathionate, microorganisms depending on the turnover of sulfur compounds are abundant in hydrothermal vent habitats. Both autotrophic as well as heterotrophic sulfur oxidising bacteria apparently are abundant (Teske et al., 2000; Podgorsek et al., 2004). In recent years, Epsilonproteobacteria, many of which are known to reduce and oxidise elemental sulfur, were found to be abundant at hydrothermal vent sites. Their ecological function in hydrothermal vent ecosystems, however, is not well understood (Campbell et al., 2001; Reysenbach et al., 2000; Corre et al., 2001).

3.4.11.2 Main objectives

The main objectives during the METEOR M 60/3 cruise were:

- Identification of important functional microbial groups and their most prominent members.
- Determination of colonization structure, diversity and activity of bacteria and archaea and their change under the influence of the properties of hydrothermal fluids.
- Influence of physical and chemical factors on the succession of microbial communities in hydrothermal gradients.
- Determination of physiological groups of microorganisms in defined ecological niches.
- Enrichment and isolation of microorganisms adapted to hydrothermal vent ecosystems.

3.4.11.3 Sampling and experiments

In order to describe microbial communities of hydrothermal vent ecosystems and their mutual interdependencies on physical and chemical environmental conditions samples were taken by ROV QUEST 5 whenever possible, in order to enable precise location and characterisation of the sampling site and the sample properties. In addition water and sediment samples were taken by a CTD-rosette sampler and a TV-grab. Samples were processed immediately and in addition stored to be used in the home lab.

- The most important sampling devices during this cruise were those adapted to and managed by the ROV. These made it possible to take samples from exactly defined and recognised local sites.
  - ③ Water samples taken by 5l-Niskin bottles mounted to the drawer of the ROV were filtered (polycarbonate membrane filters, pore size 0.2 µm) and stored at 4°C for cultivation, frozen at -20°C or stored at -20°C in glycerol. Material from these samples also was used for enrichment cultures.
  - ③ At selected sites, microorganisms from hydrothermal fluids were collected by in-situ filtration (up to 60 liter) on membrane filters (polycarbonate membrane filters, pore size 0.2 µm) using a pump connected to the fluid sampling system or in bottles of the fluid sampling system used by the geochemical. Filter material was used for enrichment cultures or stored at 4°C, frozen at -20°C or stored at -20°C in glycerol.
  - ③ Rock samples taken by the manipulator arm were immediately used for enrichment cultures or stored at 4°C and frozen at -20°C.

- Sediment samples from 6 stations with the TV-grab, including hot sediments with large numbers of mussels, were used for enrichment cultures and also stored at -20°C for genetic analysis in the home lab.
- Water samples from 17 depth profiles at various sites within the Logatchev-field were taken with Niskin bottles (CTD-rosette sampler). Microorganisms were concentrated on filters and stored at -20°C.

With selected samples enrichment cultures and serial dilution series were inoculated immediately after sampling. A variety of media was used to cultivate bacteria involved in sulfur oxidation either aerobically or anaerobically. For isolation of aerobic bacteria suitable samples were diluted and plated on agar plates for separation and isolation. Temperature gradients were created in a heated and cooled metal block from 20 to 80°C and experiments set up to characterise the response of bacterial communities in regard to the selected temperature range.

3.4.11.4 Preliminary results

In contrast to our expectations the hydrothermal fluid samples obtained from locations inside the Logatchev field contained very low amounts of reduced sulfur compounds (see chemistry section). This result was confirmed by a low abundance of chemolithoautotrophic and mixotrophic sulfur-oxidizing bacteria as indicated by incubation experiments conducted in specific media during the cruise.

3.4.12 Weather conditions during M60/3

(Torsten Truscheit)

When R/V METEOR left the port of Fort-de-France/Martinique on the evening of the 16th January, northeastern winds of Bft 3 prevailed with the sky partly overcast and showers of rain. On the way to the working area 1, the "Logatchev Hydrothermal Field" on 14°45'N/44°59'W it was mainly cloudy with light to moderate showers of rain. The wind increased up to Bft 4 to 5, coming constantly from the east.

A low 948 hPa over Newfoundland on the 17th of January moved northeastwards, its swell reaching the working area with some temporal delay causing a delay of the dive of the ROV QUEST planned for the 21st of January. The swell reached a height of up to 4 meters coming from the north. An additional swell coming from easterly directions made the working with the ROV QUEST even more difficult.

Simultaneously a high southwest of the Canary Islands respectively north of the Cape Verde Islands remained stationary over a long period. Another high build up at the 30th of January east of Florida and moved further eastward connecting with the above mentioned high from which a wedge of 1018 hPa extended to the working area up to the 3rd February.

During the whole period repeatedly new lows built up over or closely east of New Foundland, initially moving eastward, veering northeastwards south of Cape Farvel. Therefore, a more or less significant swell with a relatively long period up to 14 seconds from northnorthwest

remained. Together with a second swell coming from easterly directions this made working conditions difficulty until the end of the cruise. During the whole period the trade wind blew with Bft 4 to 5 with rare and only insignificant exceptions. Beginning on the 6th of February the wind started to increase up to Bft 6 to 7 with gusts Bft 8 (40 kts) causing seas up to 4,5 meters, so that further dives of ROV QUEST had to be cancelled. There was no significant change of weather conditions during the transit back to Fort-de-France. METEOR arrived at Fort-de-France/Martinique on the 13th of February.

3.5 References

Aldrich,A.P. and van den Berg,C.M.G. (1998). Determination of iron and its redox speciation in seawater using catalytic stripping voltammetry. Electroanalysis 10: 369-373.

Application Bulletin Metrohm 123/3 - Voltammetric determination of iron and maganese

Application Bulletin Metrohm 226/2 - Determination of arsenic by anodic stripping voltammetry at the rotating gold electrode.

Application Bulletin Metrohm 231/2 - Voltammetric determination of zinc, cadmium, lead, copper, thallium, nickel, and cobalt in water samples according to DIN 38406

Barra, C.M. and dos Santos,M.M.C. (2001). Speciation of inorganic arsenic in natural waters by square wave cathodic stripping voltammetry. Electroanalysis 13: 1098-1104.

Batuyev, B.N., Kratov, A.G., V.F., M., G.A., C., S.G., K. and Y.D., L., 1994. Massive sulfide deposits discovered at 14º45'N Mid-Atlantic Ridge. Bridge Newsletter 6: 6-10.

Boussemart, M., van den Berg, C.M.G., and Ghaddaf, M. (1992). The determination of the chromium speciation in sea water using catalytic cathodic stripping voltammetry. Anal. Chim. Acta 262: 103-115.

Campbell, BJ, Jeanthon, C, Kostka, JE, Luther III, GW, and Cary, SC (2001) Growth and phylogenetic properties of novel bacteria belonging to the epsilon subdivision of the proteobacteria enriched from Alvinella pompejana and deep-sea hydrothermal vents. Appl. Environ. Microbiol.: 67, 4566-4572.

Charlou, J.-L. and Donval, J.-P., 1993. Hydrothermal Methane Venting Between 12°N and 26°N Along the Mid-Atlantic Ridge. J. Geophys. Res. 98(B6): 9625-9642.

Charlou, J. L., Donval, J. P., Fouquet, Y., Jean-Baptiste, P., and Holm, N. (2002). Geochemistry of high H_2 and CH_4 vent fluids issuing from ultramific rocks at the Rainbow hydrothermal field (36°14'N, MAR). Chem. Geol. 191: 345-359.

Cherkashev, G.A., Ashadze, A.M., and Gebruk, A.V., 2000. New fields with manifestations of hydrothermal activity in the Logatchev area (14°N, Mid-Atlantic Ridge). InterRidge News 9(2): 26-27.

Cline, J. D. (1969). Spectrophotometric determination of hydrogen sulfide in natural waters. Limnol Oceanogr 14: 454-458.

Corre, E, Reysenbach, AL, and Prieur, D (2001) ε-Proteobacterial diversity from a deep-sea hydrothermal vent on the Mid-Atlantic Ridge. FEMS Microbiol. Lett: 205, 329-335.

Douville, E., Charlou, J.L., Oelkers, E.H., Bienvenu, P., Jove Colon, C.F., Donval, J.P., Fouquet, Y., Prieour, D., and Appriou, P. (2002). The rainbow vent fluids (36°14'N, MAR): the influence of ultramafic rocks and phase separation on trace metal content in MidAtlantic Ridge hydrothermal fluids. Chem. Geol. 184: 37-48.

Eberhardt, G.L., Rona, P.A., and Honnorez, J., 1988. Geologic Controls of Hydrothermal Activity in the Mid-Atlantic Ridge Rift valley: Tectonics and Volcanism. Mar. Geophys. Res. 10: 233-259.

Gebruk, A.V., Chevaldonné, P., Shank, T., Lutz, R.A., and Vrijenhoek, R.C., 2000. Deep-sea hydrothermal vent communities of the Logatchev area (14°45'N, Mid-Atlantic Ridge): diverse biotopes and high biomass. J. Mar. Biol. Assoc. U. K., 80: 383-393.

German, C.R. and Parson, L.M., 1998. Distributions of hydrothermal activity along the Mid-Atlantic Ridge: interplay of magmatic and tectonic controls. Earth Planet. Sci. Lett. 160: 327-341.

Grasshoff, K. (1983). Determination of oxygen. In Methods of Seawater Analaysis (ed. K. Grasshoff, M. Ehrhardt, and K. Kremling), pp. 61-72. Verlag Chemie.

Jeroschewski, P., Steukart, C., and Kühl, M. (1996). An amperometric microsensor for the determination of H_2S in aquatic environments. Anal. Chem. 68: 4351-4357.

Kadko, D. C., Rosenberg, N. D., Lupton, J. E., Collier, R. W., and Lilley, M. D. (1990). Chemical reaction rates and entrainment within the Endeavour Ridge hydrothermal plume. Earth Planet. Sci. Lett. 99: 315-335.

Kühl, M., Steukart, C., Eickert, G., and Jeroschewski, P. (1998). A H_2S microsensor for profiling biofilms and sediments: application in an acidic lake sediment. Aq. Microb. Ecol. 15: 201-209.

Luther III, G.W., Giblin, A.E., and Varsolona R. (1985). Polarographic analysis of sulfur species in marine porewaters. Limnol. Oceanogr. 30: 727-736

Madureira, M.J., Vale, C., and Simões Gonçalves, M.L. (1997). Effect of plants on sulphur geochemistry in the Tagus salt-marshes sediments. Mar.Chem. 58: 27-37.

Mozgova, N.N., Efimov, A.V., Borodaev, Y.S., Krasnov, S., Cherkasov, G.A., Stepanova, T.V., and Ashadze, A.M., 1999. Mineralogy and Chemistry of Massive Sulfides from the Logatchev Hydrothermal Field (14°45'N Mid-Atlantic Ridge). Exploration Min. Geol. 8(3): 379-395.

Pfender, M. and Villinger, H. (2002). Miniaturized data loggers for deep sea sediment temperature gradient measurements. Mar. Geol. 186: 557-570.

Revsbech, N. P. & Jørgensen, B. B. (1986). Microelectrodes and their use in microbial ecology. In Advances in Microbial Ecology, Vol. 9 (ed. K. C. Marshall), pp. 293-352. Plenum Press.

Revsbech, N. P. (1989). An oxygen microelectrode with a guard cathode. Limnol. Oceanogr. 34: 474-478.

Reysenbach, AL, Longnecker, K., and Kirshtein, J. (2000) Novel bacterial and archaeal lineages from an in situ growth chamber deployed at a Mid-Atlantic ridge hydrothermal vent. Appl. Environ. Microbiol.: 66, 3798-3806.

Rona, P.A., Bougalt, H., Charlou, J.L., Appriou, P., Nelsen, T.A., Trefry, J.H., Eberhart, G.L., Barone, A., and Needham, H.D., 1992. Hydrothermal circulation, serpentinization, and degassing at a rift valley-fracture zone intersection: Mid-Atlantic Ridge near 15°N, 45°W. Geology 20: 783-786.

Sander, S. and Koschinsky, A. (2000). Onboard-ship redox speciation of chromium in diffuse hydrothermal fluids from the North Fiji Basin. Mar. Chem. 71: 83-102.

Seifert, R., Delling, N., Richnow, H.H., Kempe, S., Hefter, J., and Michaelis, W.(1999). Ethylene and methane in the upper water column of the subtropical Atlantic. Biogeochemistry 44: 73-91.

Sudidarikov, S. and Zhirnov, E. (2001). Hydrothermal plumes along the Mid-Atlantic-Ridge: preliminary results of CTD investigations during the DIVERS Expedition (July 2001). InterRidge News, 10(2): 33-36.

Teske, A., Brinkhoff, T., Muyzer, G., Moser, DP., Rethmeier, J., and Jannasch, HW. (2000) Diversity of thiosulfate-oxidizing bacteria from marine sediments and hydrothermal vents. Appl. Environ. Microbiol.: 66, 3125-3133.

van den Berg, C.M.G. and Khan, S.H. (1990). Determination of selenium in sea water by adsorptive cathodic stripping voltammetry. Anal. Chim. Acta 231: 221-229

METEOR-Berichte

MOVE (Meridional Overturning Variability Experiment)

Cruise No. 60, Leg 4

Feb 16 – March 4, 2004; Fort-de-France, Guadeloupe – Fort-de-France, Guadeloupe

Uwe Send, Christian Begler, Torsten Kanzow, Matthias, Lankhorst, Tom Avsic, Johannes Karstensen

Editorial Assistance:

Senatskommission für Ozeanographie der Deutschen Forschungsgemeinschaft
MARUM – Zentrum für Marine Umweltwissenschaften der Universität Bremen

Leitstelle Deutsche Forschungsschiffe
Institut für Meereskunde der Universität Hamburg

2012

Table of Contents

1 Participants

Name	Task	Institution
Send, Uwe	chief scientist	IFM-GEOMAR
Avsic, Tom	Tomography	IFM-GEOMAR
Bailey, John	Bottom pressure sensors	WHOI
Begler, Christian	Moorings	IFM-GEOMAR
Busack, Michael	Telemetry, microcats	IFM-GEOMAR
Kanzow, Torsten	Data processing	IFM-GEOMAR
Karstensen, Johannes	ADCP	IFM-GEOMAR
Koy, Uwe	Moorings, PIES	IFM-GEOMAR
Lankhorst, Matthias	CTD	IFM-GEOMAR
Link, Rudolf	Tomography, moorings	IFM-GEOMAR
Moeller, Helmut	Bottom pressure sensors	SIO / WHOI
Morozow, Andrey K.	Tomography	WRC
Neumann, Uta	CTD	IFM-GEOMAR
Niehus, Gerd	Moorings, current meters	IFM-GEOMAR
Ochsenhirt, Wolf-Thilo	Meteorology	DWD
Pinck, Andreas	Telemetry, CTD	IFM-GEOMAR
Scharffenberg, Martin	Moorings	IFM-GEOMAR

Participating institutions

IFM-GEOMAR	Leibniz-Institut für Meereswissenschaften, Düsternbrooker Weg 20, 24105 Kiel, Germany
WHOI	Woods Hole Oceanographic Institution, 266 Woods Hole Road, Woods Hole, MA 02543, USA
SIO	Scripps Institution of Oceanography, 8602 La Jolla Shores Drive La Jolla, CA 92037
WRC	Wave Research Center, 38, Vavilov street, Moscow 119991, Russia
DWD	Deutscher Wetterdienst, Postfach 301190, 20304 Hamburg, Germany

Summary

The fourth leg of METEOR cruise 60 served the MOVE (Meridional Overturning Variability Experiment) project which started in January 2000. The long-term observations of fluctuations in the thermohaline circulation of the western Atlantic Ocean were to be continued on a routine basis. The MOVE array is situated on a zonal section along 16◦N between the Antilles Arc in the west and the outskirts of the Middle Atlantic Ridge in the east. The array was exchanged last from FS SONNE in June 2003. The array comprises moored instruments for recording currents, density, bottom pressure and acoustic tomography signals. The successful redeployment of the instrumentation during M60/4 ensures that the long-term goal of the project can be achieved, namely to observe interannual and longer fluctuations of the thermohaline circulation with integral methods.

Zusammenfassung

Auf dem vierten Abschnitt der METEOR Reise 60 wurden hauptsächlich Arbeiten durchgeführt die im Zusammenhang mit dem MOVE (Meridional Overturning Variability Experiment) Projekt standen. Das MOVE Projekt startete im Januar 2000 und hat sich zur Aufgabe gesetzt ein Beobachtungssystem zu installieren und zu testen mit dem Schwankungen in der thermohalinen Zirkulation im Atlantik (AMOC) erfasst werden können. Das System ist etwa auf der Breite 16°N, zwischen den französischen Antillen (Guadeloupe) und dem Mittelatlantischen Rücken, installiert. Nach der letzten Auslegung im Juni 2003 wurde während METEOR 60/4 das System erneut gewartet. Die Instrumentierung besteht aus selbstregistrierenden Strömungsmessern, CTD Sonden, Bodendruck Sensoren und akustischer Tomographie. Die erfolgreiche Wiederauslegung der Messgeräte während M60/4 stellt sicher dass, durch Kombination mit Messdaten früherer Auslegungen, Zeitserien über mehrere Jahre gewonnen werden, die es erlauben zwischenjährliche Schwankungen der AMOC berechnen zu können.

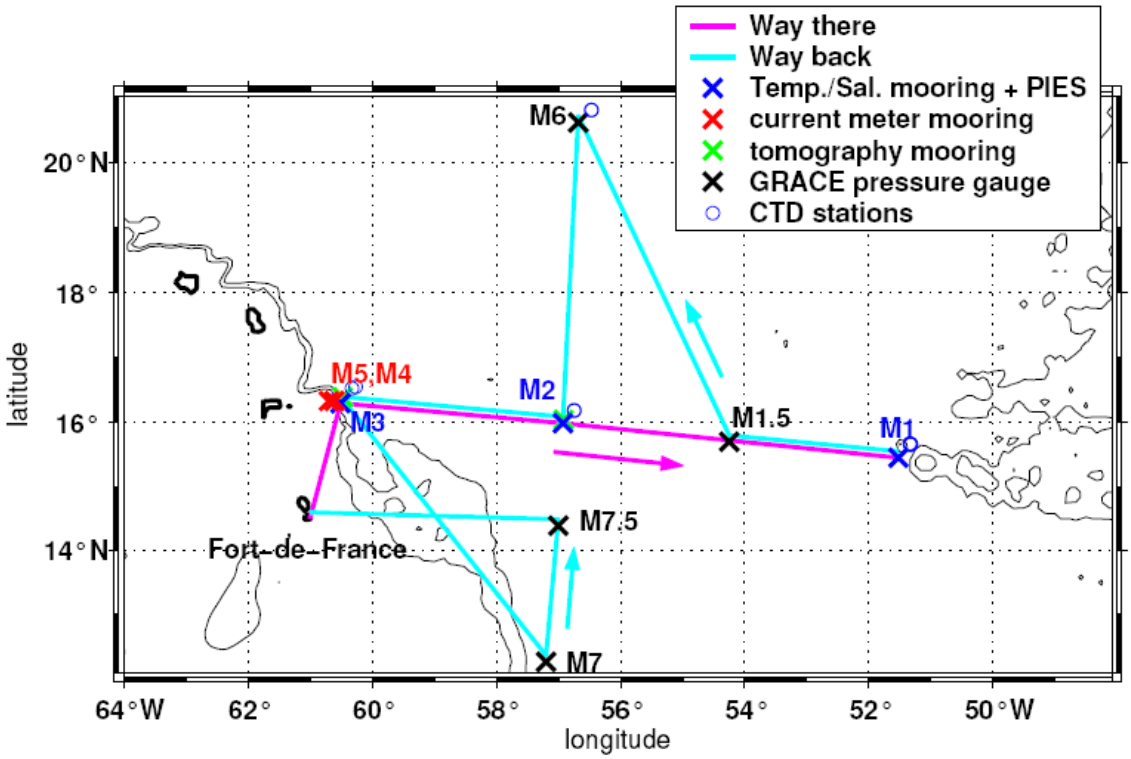

Fig. 3.1 Cruise track of 4th leg of cruise METEOR 60. Mooring and CTD stations are also indicated.

2 Research Program

Field observations in the tropical / subtropical North Atlantic Ocean in the frame of the German climate variability (CLIVAR) project B1-4 are accompanied by modelling studies of the structure and the variability of the current system and its relation to atmospheric forcing (http://www.awi-bremerhaven.de/Research/IntCoop/Oce/clivar/projects /projects-index.html). In co-operation with American agencies, calibration activities for GRACE (Gravity Recovery and Climate Experiment) were planned using high precision bottom pressure recorders. The latter will provide monthly estimates of the earth's gravity field with extraordinary precision.

The prime objectives of this cruise leg were to perform extended maintenance at the mooring sites along 16ºN and to extend the bottom pressure array perpendicular to the section. In addition a re-occupation of this section was conducted to measure the hydrographic stratification and the instantaneous structure of horizontal currents.

3 Narrative of the cruise

RV METEOR departed Fort-de-France (Martinique) on 16 February 2004 at 10:30 LT (local time) and sailed northwards towards the first working area off Guadeloupe, which was reached about 12 hours later. Over the following two days, four moorings (M3, M3.5, M4, M5), a moored echo sounder (PIES- near M3) and three transponders (near M3.5) were recovered successfully.

The SIO bottom pressure sensor near M3 could not be located however. It turned out that the tomography sound source (M3.5) had not worked at all due to a broken battery wire. A first CTD/lADCP cast was taken. After repairs M3.5 was redeployed together with a SIO bottom pressure sensor. After completion of the work on 19 February at 2:00 LT in this area, RV METEOR moved eastward most of that day towards position M2. Here a SIO bottom pressure sensor was deployed and the second CTD cast was conducted. No acoustic contact could be established with the PIES near M2. Nonetheless, the release command was sent but despite an intense search the instrument could not be located at any time. Three transponders were recovered. During the recovery of mooring M2 the ship drifted over the wire with glass spheres, which got stuck in the propeller. It could not be freed by pulling but a visual inspection (from a Zodiac) revealed that the wire was not wrapped around the propeller but was just loosely caught. It got free by itself and the Zodiac crew managed to get hold of the drifting spheres just before dark and re-attached the mooring to the ship. The mooring recovery was continued without loss of any instruments. Finally, a PIES was deployed near the nominal position of M2.

RV METEOR subsequently headed eastward and reached the position of the PIES near M1 on 22 February at 4:00 LT. Data from that PIES were dumped via acoustic telemetry. During the recovery of mooring M1 the telemetry wire was found cut 20 m below the fishing floats (nominally at 40 m) and most of those floats plus the 40 m MicroCAT (moored CTD recorder) were missing, but the loose telemetry wire above was braided to the remaining wire above the subsurface float and was thus held in place. The M1 SIO bottom pressure sensor was successfully recovered and, subsequently, the tomography receiver was lowered to 1000 m to try to receive acoustic signals from the sound source located 1000 km away at M3.5. Even though noise sources on ship were suppressed by shutting down / reducing generators, compressors, hydraulics, bowthruster and propeller, the acoustic signals could not be detected. CTD casts 3-7 were taken in this area with MicroCATs and MTD logger attached in order to carry out *in situ* calibration of these devices. A SIO bottom pressure sensor and a PIES were deployed. The PIES whose data had been transferred acoustically could be recovered which was necessary to install updated firmware. After a successful test of the telemetry for mooring M1, with the MicroCATs lying on deck, that mooring was deployed on 24 February. Soon afterwards the first ARGOS transmissions from all MicroCATs extending down to 4000 m were received. Thus all electric links, including the electrically-conducting swivels, were working.

RV METEOR then headed westwards again and a PIES (M1.5) was deployed half way between M1 and M2 on February 25. Subsequently METEOR sailed to the northwest to occupy the northern point of the bottom pressure sensor cross (M6). Here a PIES and a SIO bottom pressure sensor were deployed and CTD casts 8-9 with MicroCATs and MTD loggers attached were conducted on 26 February. The next day was spent sailing southward towards M2. Two days later the tomography source was lowered from the vessel near M2 to receive signals from the M3.5 sound source roughly 400 km away. All the vessel's

sources of noise were shut down completely. This time the signals from M3.5 were received. In the following, mooring M2 (including MicroCATs as well as the tomography receiver) and three tomography transponders were deployed. CTD cast 10 (without MicroCATs attached) was conducted.

Upon heading southward to cover the southern positions of the GRACE bottom pressure cross, it was discovered that the essential positions of M7 and M7.5 under the track of the GRACE satellites were located in the exclusive economic zone (EEZ) of Barbados and that the diplomatic clearance had not been requested in due time. So it was decided to carry out mooring works in the west (M3) first and at the same attempts were made to obtain diplomatic clearance for M7 and M7.5 from the Barbados authorities.

In the afternoon of 29 February at 30 km from sound source mooring M3.5, the work boat was deployed to lower a newly-built listening device to 1000 m, at sufficient distance from METEOR, which moved away 5 nm. Signals from the sound source were successfully received. Since the navigator device needed to be reprogrammed the sound source mooring M3.5 was recovered again. Subsequently, the final CTD cast 11 (with MicroCATs) was taken. The next day (March 1) the POL bottom pressure recorder (near nominal position of M3) was recovered successfully and the MicroCAT mooring M3 was redeployed. A short time afterwards, ARGOS signals from the five Micro-CATs in the inductive loop were also received. Data from the tomographic test receptions in 30 km were analyzed and the sound source was diagnosed. At night decision was taken to deploy the source and test/prepare two mooring navigators for this purpose. After successful tests with the fully assembled sound source, the current meter mooring M4 was deployed (including the sound source) plus three transponders. Afterwards the sound source transmissions could be received successfully at a distance of 0.5 nm from the mooring.

After a transponder survey, METEOR started to steam southeastwards towards the positions of M7 and M7.5 although no diplomatic clearance had yet been obtained. On 3 March at 360 km distance from M4, sound source transmissions were received clearly by a freely-floating receiver. On the afternoon of 4 March, the diplomatic clearance was issued by the foreign ministry of Barbados. M7 was reached several hours later where a PIES and a SIO bottom pressure sensor were deployed. After deploying the last SIO bottom pressure sensor at M7.5 (between M7 and M2) at noon, RV METEOR started to head westwards to Fort-de-France which was reached one day later.

Throughout the whole cruise, thermosalinograph data was acquired for transmission to the Coriolis data centre in Brest, France. In summary, the cruise can be regarded as very successful. The loss of one PIES and one SIO bottom pressure sensor are judged not to have affected the overall performance of the on-going MOVE experiment.

4.4 Preliminary Results

4.4.1 Moorings (T. KANZOW)

The main objective of the cruise was to service the MOVE moorings. The basic idea of MOVE is to determine the variability of the deep meridional mass transport across 16°N in the western basin of the North Atlantic as a part of the meridional overturning circulation. In the interior an array of three "geostrophic" moorings (M1-M3) is maintained which captures the meridional flow with a combination of dynamic height and bottom pressure measurements. West of this array, in a triangle over the continental slope, direct current measurements are applied (M3-M5) to capture that part of the deep flow, which passes inshore of M3 (see Fig. 4.1 for details). Furthermore, acoustic tomography is used to determine deep integrated temperature fluctuations between M2 and M3. The complete set of 6 moorings was recovered successfully. Ultimately, 4 moorings were redeployed on the cruise (see Table 4.1). It was decided not to redeploy the current meter mooring M5 since analyses had shown that its contribution to the transport estimates over the continental slope was negligible. The tomography mooring M3.5 that was redeployed on 17 February was again recovered on 29 February to make adjustments to the navigators. Due to lack of sufficient spare mooring wire, the tomography component was then integrated into the mooring M4, which does not influence its performance.

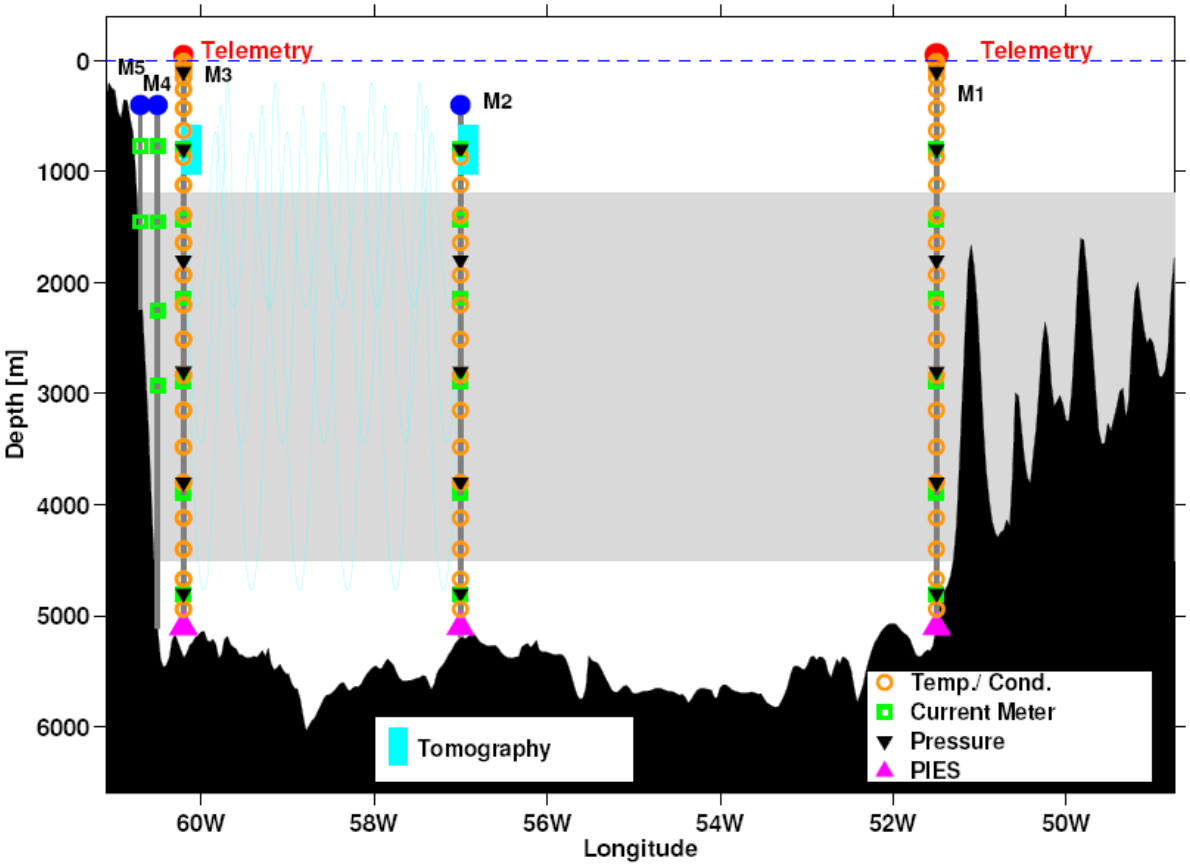

Fig. 4.1 MOVE mooring design at 16 N. To maintain lucidity, the tomography mooring M3.5 is not displayed, since it was deployed extremely close to M3. Its tomography sound source has been drawn in as a part of M3 instead.

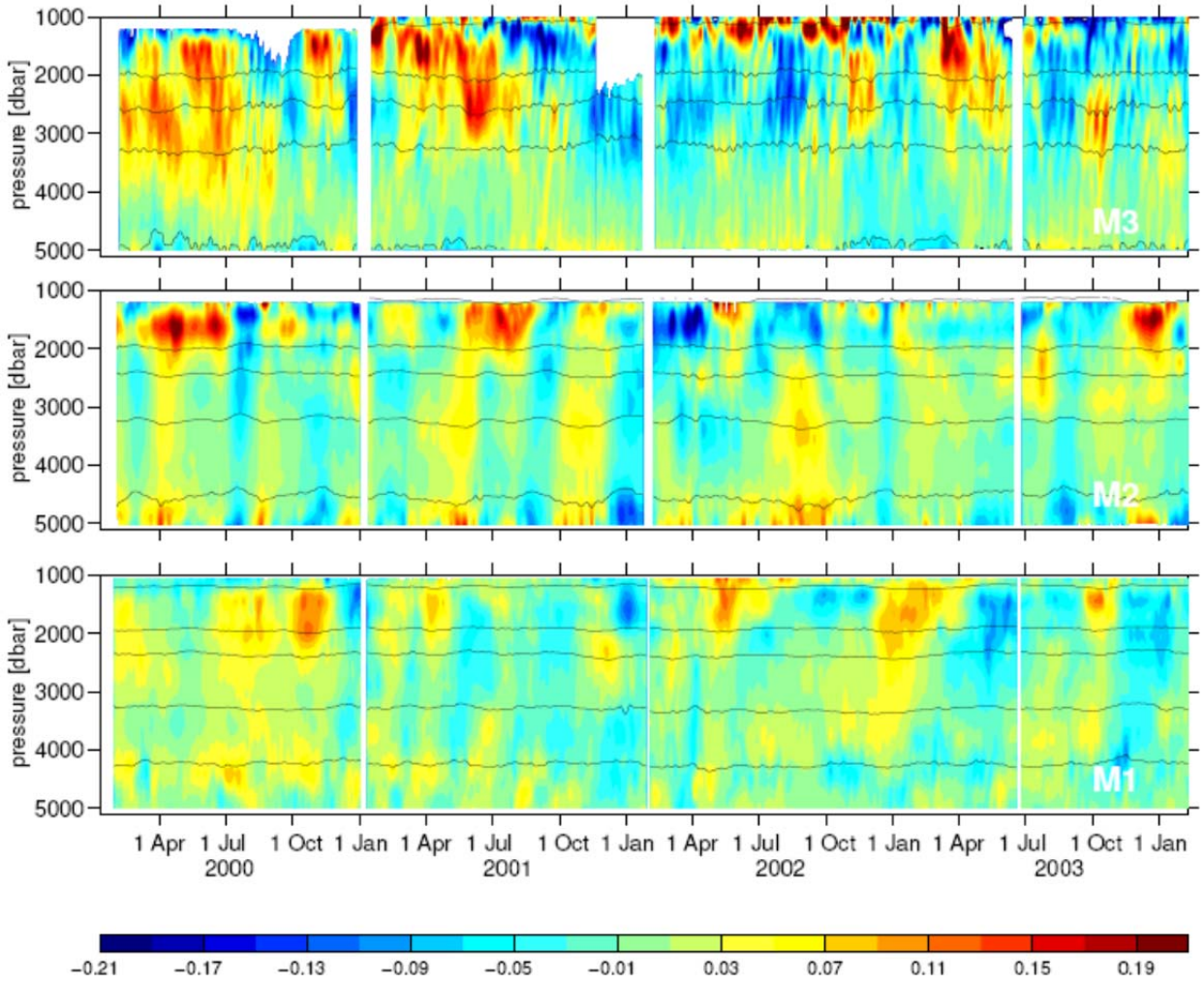

Fig. 4.2 Time series of temperature anomalies from MicroCATSs at moorings M3, M2 and M1 since February 2000 (Feb. 2000 - Feb. 2004 mean subtracted). The data recovered on the METEOR 60-4 leg spans the periods between June 2003 and February 2004. Data gaps result from period when moorings were being serviced.

Table 4.1: Overview over the mooring work carried out during the METEOR 60/4 cruise

Mooring ID	Period	Latitude	Longitude	Waterdepth [m]	Date deployed	Date recovered
M1	2003-2004	15N 27.00	51W 31.50	4984	23/06/03	22/02/04
M1	2004-2005	15N 27.00	51W 31.30	4970	24/02/04	–
M2	2002-2003	15N 59.20	56W 55.60	4985	25/06/03	20/02/04
M2	2002-2005	15N 59.05	56W 55.50	4985	28/02/04	–
M3	2003-2004	16N 20.30	60W 30.30	4960	27/06/03	18/02/04
M3	2004-2005	16N 20.34	60W 30.51	4929	01/03/04	–
M3.5	2003-2004	16N 20.20	60W 32.80	4100	30/06/03	17/02/04
M3.5	2004-2004	16N 20.15	60W 32.80	4080	19/02/04	29/02/04
M4	2003-2004	16N 20.00	60W 36.45	3010	27/06/03	17/02/04
M4	2004-2005	16N 20.01	60W 36.51	3010	02/03/04	–
M5	2003-2004	16N 20.01	60W 41.75	1600	28/06/03	17/02/04

4.4.2 Microcats (T. Kanzow)

Of the 59 MicroCATs that had been deployed on the FS SONNE cruise 172 in June 2003, 56 instruments were recovered. 55 of them acquired data of excellent quality throughout their operation in M1, M2 and M3. Only #952 showed minor problems in conductivity for the last 15 days of the time series. #936, #1716 and #1724 were missing upon recovery. All of the MicroCATs, including #952, did not show any large deviations relative to the CTD data during the calibration casts. For the new deployment period, 59 MicroCATs were deployed but their distribution in the moorings was changed slightly. While during the 4th deployment there had been 10 inductive MicroCATs in M1 and in M3, now there are 13 inductive instruments in M1 but only 5 in M3.

One reason for this change was to extend the telemetry of MicroCAT data to depths of up to 4000m at M1 (so far it had been to 1500m). As two of the missing instruments were inductive, and inductive instruments were needed in other projects (e.g. ANIMATE) it was decided to reduce the telemetry depth at M3 from 1500m to 150 m, where data from 5 inductive instruments are transmitted. Correspondingly, the number of serial MicroCATs was increased from 29 to 31. Figure 4.2 shows temperature anomalies derived from the MicroCAT measurements since the beginning of the MOVE project und February 2000.

The characteristics of the data from the latest deployment period (recovered on this cruise) correspond well to the preceding data segments at each of the moorings M1, M2 and M3.

4.4.3 MTD logger (T. Kanzow)

The Mini-Temperature-Depth Loggers (MTD) are used to determine the time variable vertical mooring motions in M1, M2, M3 and M4 and are required to allocate the MicroCAT temperature and conductivity measurements to the correct pressures. Thus the time series shown in Fig. 4.2 are based on the combination of MicroCAT and MTD measurements. All of the 16 MTD were successfully recovered and all of them had acquired data throughout the duration of the deployment. The MTD are used to determine the time-varying depth of the high precision MicroCATs (conductivity and temperature) in the moorings. The data in the MTD appear to be good except for one instrument: #46 showed an exponential drift of about18 dbar throughout the deployment period. During the following CTD calibration cast, #39 refused to work properly on two occasions, although it had acquired data of good quality while operating in the mooring. So it was decided to not deploy #39 and #46 again. 4 instruments were calibrated twice. MTD #39 and #29 showed a constant pressure during the calibration on CTD #5. It was found to be a connection-problem between the software and the MTD's when starting the instruments. The second calibration on CTD #9 brought out that the p-sensors were working correctly. MTD #20 and #19 went down on CTD #5 and on CTD #9. On CTD #9 plastic screws were mounted for the p-sensor to avoid rust falling in from Aanderaa current meters. The data showed no difference between the CTD casts #5 and #9. So one can expect that they should work, well with or without these protective screws. MTD #20 and #19 were deployed with these screws in mooring M2. The other MTD were redeployed in a slightly different distribution in the moorings M1, M2, M3 and M4. As in preceding years, especially strong vertical mooring motions of several hundred meters were detected in the DWBC area (Fig. 4.3).

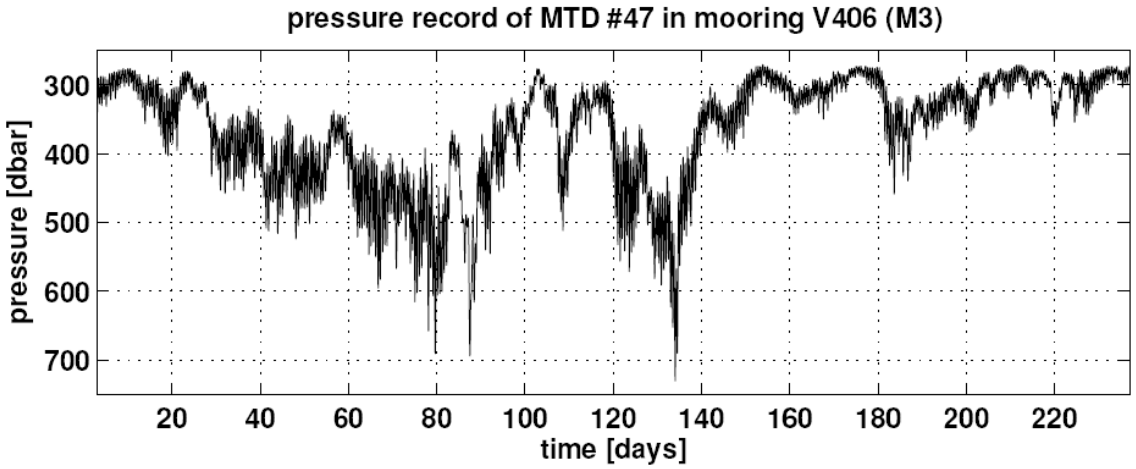

Fig. 4.3 Example of a MTD pressure time series: MTD #47 displays deep subduction of mooring M3 during events of strong flow in the Deep Western Boundary Current.

4.4.4 Bottom pressure measurements (T. Kanzow)

From the difference in bottom pressure fluctuations between the moorings M1, M2 and M3 the zonally integrated meridional near-bottom velocity fluctuations may be derived. An overview over the bottom pressure recoveries and deployments is given in Table 4.4.

From the three Pressure Inverted Echo Sounders (PIES) #012, #002 and #057 that had been deployed near M3, M2 and M1, respectively, #012 and #057 were recovered successfully and had acquired good data throughout the operation since their launch in June 2003. The acoustic communication to PIES #012 was unreliable, so it did not become clear when exactly it had been released and it was only heard properly with the survey programme when it was already close to the surface. Communication with #57 worked well.

PIES #002 could not be recovered. Communication could not be established with it, and the RELEASE command could not be confirmed. Furthermore, during deployment in June 2003 (aboard FS SONNE cruise 172) the slip-page had been folded around one of the tripod's legs by accident. So it was doubtful right from the start if the instrument could get clear of the tripod after release. However, hours after release three successive weak radio signals were received by the radio direction finder; whether those originated from the PIES never became clear. A search was started immediately, but without success. No further radio pulses were received. PIES #057 showed a surprisingly large exponential drift in the pressure record of about 50 cm whereas normally a drift in the order of 10 cm is seen. As #057 had been deployed for the first time it is expected that its drift rate will be much smaller in successive deployments.

From the two Filloux-type Bourdon tubes #003 and #012 provided by Alan Chave (WHOI), and deployed near M1 and M3, only #003 was recovered and showed reliable data. Communication to #012 failed completely.

The bottom pressure sensor provided by Peter Foden, Proudman Oceanographic Lab. (POL) was recovered. It is essentially a Paroscientific quartz pressure sensor similar to the one used in the PIES. Communication worked extremely well and the time series record looks promising. This instrument was needed in another experiment by POL and thus was not redeployed again.

This time, as a contribution to the GRACE satellite mission (gravity recovery and climate experiment), a much larger number of PIES and Chave's Bourdon tubes were deployed in a cross-pattern (see Fig. 3.1) with the one axis being the original MOVE line and the other axis (north-south) being almost orthogonal to it and intersecting it at site M2 (57.0W/16.0N). The east-west extent is about 1000 km while the north-south one spans almost 900 km. Altogether 6 PIES, 5 of them with the acoustic telemetry option (serial numbers #57 onwards), as well as 6 Bourdon tubes where launched.

PIES #57 had been deployed in June 2003 and were the first one with acoustic telemetry option. So prior to recovering it, its de-tided and daily averaged data were transferred acoustically. The data are encoded as time delays relative to a marker pulse (referred to as "PDT"). The main benefit is the low power consumption of this technique whereas a possible drawback arises as transmission becomes noisy when the vessel moves relative to the PIES. The data were received and stored without large problems using the Benthos7000 deck unit and the Matlab software FilePDT.m provided by the manufacturer (R. Watts). We then compared the telemetry data to the data stored inside the PIES after its recovery (Fig. 4.4). First of all, a reasonable overall agreement both in bottom pressure and travel time, was observed. Some data points were missing in the telemetry data, and sometimes the succession of days was not correct. This makes the data at times ambiguous. The rms difference between both data sets in terms of bottom pressure was about 0.006 dbar (or 6 mm). The difference could be explained by vessel movement relative to the PIES during transmission, given its data transmission window of 50 dbar and a window length of 8 seconds in the file telemetry mode. Then, vertical vessel movement of 1.5m is sufficient to account for this discrepancy. This 6 mm difference is more than we can accept as we are interested in the millimeter fluctuations. The newer generation firmware in the telemetry PIES uses a 2 dbar window for pressure data and has a length of 14 seconds. This should ensure that the noise induced by vessel movement should decrease by over one order of magnitude to an acceptable level. This new firmware is being used in all the PIES we deployed, including #057, which was updated during this cruise.

Table 4.2: Overview over the recoveries and deployments of bottom pressure recorders during cruise METEOR 60-4.

mooring	instrument	latitude	longitude	depth	launch	recovery
M1	PIES #057	15N 27.75	51W 31.90	4980m	19/06/03	23/02/04
M1	SIO-BPR #03	15N 28.00	51W 31.60		22/06/03	22/02/04
M1	PIES #127	15N 27.01	51W 31.60	4965m	23/02/04	
M1	SIO-BPR #03	15N 27.98	51W 31.57		22/02/04	
M1.5	PIES #012	15N 43.10	54W 13.50	5450m	25/02/04	
M2	PIES #002	15N 59.40	56W 55.31	4999m	26/06/03	failed
M2	PIES #123	15N 59.19	56W 56.59	5000m	21/02/04	
M2	SIO-BPR #01	16N 00.17	56W 56.53		20/02/04	
M3	PIES #012	16N 20.51	60W 29.30	5000m	26/06/03	18/02/04
M3	PIES #165	16N 21.30	60W 29.25	5000m	17/02/04	
M3	SIO-BPR #12	16N 21.32	60W 30.3		16/06/03	failed
M3	SIO-BPR #04	16N 21.43	60W 30.39		18/02/04	
M3	POL-BPR	16N 22.29	60W 30.32	4903m	28/06/03	01/03/04
M6	PIES #128	20N 36.51	56W 40.78	5093m	26/02/04	
M6	SIO-BPR #10	20N 36.00	56W 40.78		26/02/04	
M7	PIES #057	12N 15.03	57W 12.04	4451m	05/03/04	
M7	SIO-BPR #02	12N 15.58	57W 11.99		05/03/04	
M7.5	SIO-BPR #07	14N 23.41	56W 59.41		05/03/04	

Another concern, which became apparent during tests with the file telemetry mode has not been solved yet. Tests with PIES #123 and #165, which had both been deployed for more than 4 days such that they would switch from burst to file telemetry mode, showed that when downloading the data set acoustically for the first time, all worked without larger problems. When trying to transfer the data for a second time, the FilePDT.m programme could not receive any signal. All further attempts failed. Of course it would be desirable to download that same data set several times. This could help to overcome problems such as data gaps and ambiguities as seen in PIES #057 and further reduce the noise level. Theoretically (pers. communication R. Watts and G. Chaplin) the file telemetry should work as follows (see also manual "IES model 6.1E - Advanced Acoustic Telemetry Option", revised 04/02/2004): Data are transmitted in blocks of 34 data cycles (days). At the beginning of each block, one data cycle (consisting of pressure, travel time and year day) is transmitted in the MSB (most significant bit format), meaning that the absolute data values (of pressure and travel time) are transferred with limited resolution. MSB data are not exact enough for scientific use, but they might be useful to overcome ambiguities of the LSB data described below. The one MSB should be followed by 34 LSB (least significant bit) data cycles, beginning with the most recently acquired and proceeding backward in time. In the LSB format pressure is transferred modulo 2000 decaPascals and IES travel time modulo 0.5 seconds.

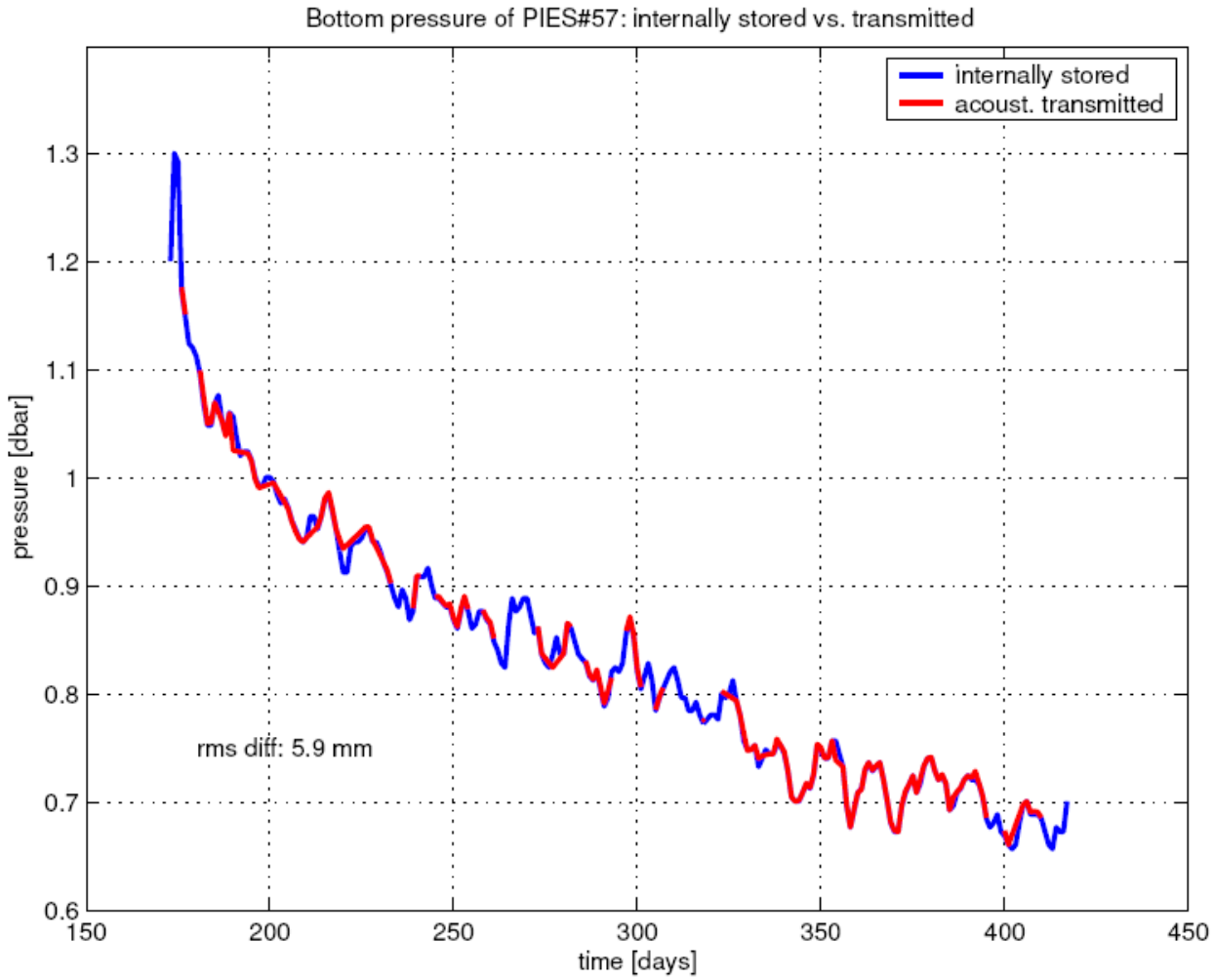

Fig. 4.4 Acoustic Telemetry of PIES #057: Bottom pressure time series as received via telemetry (red) and internally stored in the instrument (blue). An rms-difference of 5.9 mm (water column equivalent) is found between the two time series.

As said above, the data are encoded as delays relative to a marker pulse. The marker pulse for MSB has a frequency of 10.0 kHz, whereas for LSB it has 11.0 kHz. The pulses for pressure, travel time and year day have frequencies of 11.5, 12.0 and 12.5 kHz, respectively. This would require 5 frequencies to be received by the deck unit. In our case the DS 7000 has only four channels such that the recently provided PFilePDT.m software was modified only to listen for the LSB data and not to receive the MSB 10.0 kHz marker. This should not create any problems, but obviously the programme only received the LSB 11.0 kHz marker where used for the first time to transmit data from PIES #123 and #165. So PIES #057, which only was to be deployed at the very end of the cruise, was operated in the lab for several days, such that file telemetry could be used. When trying to transfer the data for the first time, everything worked reasonably well and the LSB data were received. When trying a second time (after sending the CLEAR command and then again the TELEM command) it could be heard by ear that the PIES was transmitting its data, but the PFilePDT.m programme did not receive the LSB 11.0 kHz marker. Then it was attempted to analyse the pulses that had actually been sent by the PIES: No LSB marker was sent at the beginning of each data cycle, but instead, every time, a 10.0 kHz MSB marker. What this means is not quite clear at this point and together with R. Watts and G. Chaplin we will try to analyse this problem further. If it should mean that after the first complete file telemetry data transmission (in LSB) during successive attempts only MSB data is sent, then this is a serious bug in the firmware which has to be modified. It is crucial to be able to transfer data in LSB more than once, especially when it is intended to keep an instrument deployed for many years but to dump the data several times within this period. This is exactly what the telemetry was intended for.

The fact that no LSB marker was sent explains why the PFilePDT.m software got stuck during recording. We therefore recommend modification of the software such that it does not wait for pulses of specific frequencies in a specified succession, but rather that each pulse is recorded in the succession they are received and that the decoding is then applied after the complete data set has been transmitted.

4.4.5 Current meters (C. Begler)

In the mooring deployment M1-M5 of 2003, 26 Aanderaa RCM current meters had been used. The RCMs in M3-M5 are used to determine that fraction of the DWBC transport over the western continental slope, that in M1-M3 give information about the interior dynamics complementary to the geostrophic measurements. All current meters could be recovered, however one instrument from mooring M1 had lost its bottom cap, and thus lost all its data. Some other instruments had not recorded currents near the end of deployment, probably caused by rotor problems (see Table 4.3). The new generation of Aanderaa RCM-9 instruments (based on Doppler-shift-measurements) worked well. In the redeployed mooring design two of the RCM-9 have been inserted in the telemetry-line of M1, since the absence of a vane (which is present in the RCM-8) makes it easier to bypass them with an electric connection. In summary, 22 RCM-instruments were redeployed in the moorings M1, M2, M3 and M4 (see Table 4.4). Fig. 4.5 exemplarily shows current time series recorded at M3. Strong southward flow related to the DWBC prevails over almost the entire length of the records. Only the two near-bottom instruments (moored below 4500m) do not seem to be influenced by its dynamics.

Table 4.3: Recovered Aanderaa current meters in moorings M1-M5

Mooring	Depth	Instrument	S/N	Variables	Comment
M1	771 m	Aanderaa RCM-9	051	U,V,T,C	
M1	1422 m	Aanderaa RCM-8	10662	U,V,T,C	
M1	2123 m	Aanderaa RCM-8	4570	U,V,T,C	bottom lost
M1	2873 m	Aanderaa RCM-8	11621	U,V,T,C	
M1	3872 m	Aanderaa RCM-8	9727	U,V,T,C	
M1	4884 m	Aanderaa RCM-8	9344	U,V,T,C	
M2	803 m	Aanderaa RCM-8	10075	U,V,P,T,C	
M2	1444 m	Aanderaa RCM-8	9345	U,V,T,C	
M2	2145 m	Aanderaa RCM-8	9728	U,V,T,C	
M2	2892 m	Aanderaa RCM-8	9732	U,V,T,C	
M2	3996 m	Aanderaa RCM-8	094	U,V,P,T,C	
M2	4553 m	Aanderaa RCM-8	9831	U,V,T,C	no SPD since 03-Oct-2003
M2	4934 m	Aanderaa RCM-8	11618	U,V,T,C	no SPD since 04-Feb-2004
M3	774 m	Aanderaa RCM-9	054	U,V,T,C	
M3	1423 m	Aanderaa RCM-8	8411	U,V,P,T,C	
M3	2124 m	Aanderaa RCM-8	10663	U,V,T,C	
M3	2877 m	Aanderaa RCM-8	4562	U,V,T,C	
M3	3877 m	Aanderaa RCM-8	8365	U,V,T,C	
M3	4655 m	Aanderaa RCM-8	11442	U,V,P,T,C	PRES defect
M3	4875 m	Aanderaa RCM-8	8349	U,V,T,C	
M4	772 m	Aanderaa RCM-8	10813	U,V,T,C	
M4	1450 m	Aanderaa RCM-8	10815	U,V,T,C	
M4	2255 m	Aanderaa RCM-8	9820	U,V,T,C	no SPD since 22-Jan-2004
M4	2931 m	Aanderaa RCM-8	11617	U,V,T,C	
M5	804 m	Aanderaa RCM-8	10077	U,V,T,C	
M5	1440 m	Aanderaa RCM-8	6160	U,V,T,C	

Table 4.4: Redeployed Aanderaa current meters in moorings M1-M4.

Mooring	Depth	Instrument	S/N	Variables	Comment
M1	1095 m	Aanderaa RCM-9	051	U,V,T,C	
M1	2129 m	Aanderaa RCM-11	293	U,V,T,C	
M1	3877 m	Aanderaa RCM-8	9727	U,V,T,C	
M1	4889 m	Aanderaa RCM-8	9344	U,V,T,C	
M2	805 m	Aanderaa RCM-8	10075	U,V,P,T,C	
M2	1447 m	Aanderaa RCM-8	9345	U,V,T,C	
M2	2147 m	Aanderaa RCM-8	9728	U,V,T,C	
M2	2897 m	Aanderaa RCM-8	9732	U,V,T,C	
M2	3997 m	Aanderaa RCM-8	094	U,V,T,C	
M2	4553 m	Aanderaa RCM-8	10662	U,V,T,C	
M2	4904 m	Aanderaa RCM-8	11618	U,V,T,C	
M3	788 m	Aanderaa RCM-9	054	U,V,T,C	
M3	1437 m	Aanderaa RCM-8	10077	U,V,P,T,C	
M3	2138 m	Aanderaa RCM-8	10663	U,V,T,C	
M3	2890 m	Aanderaa RCM-8	4562	U,V,T,C	
M3	3890 m	Aanderaa RCM-8	8365	U,V,T,C	
M3	4553 m	Aanderaa RCM-8	10502	U,V,T,C	
M3	4877 m	Aanderaa RCM-8	10664	U,V,T,C	
M4	824 m	Aanderaa RCM-8	6160	U,V,T,C	
M4	1436 m	Aanderaa RCM-8	10659	U,V,T,C	
M4	2242 m	Aanderaa RCM-8	11441	U,V,T,C	
M4	2919 m	Aanderaa RCM-8	11617	U,V,T,C	

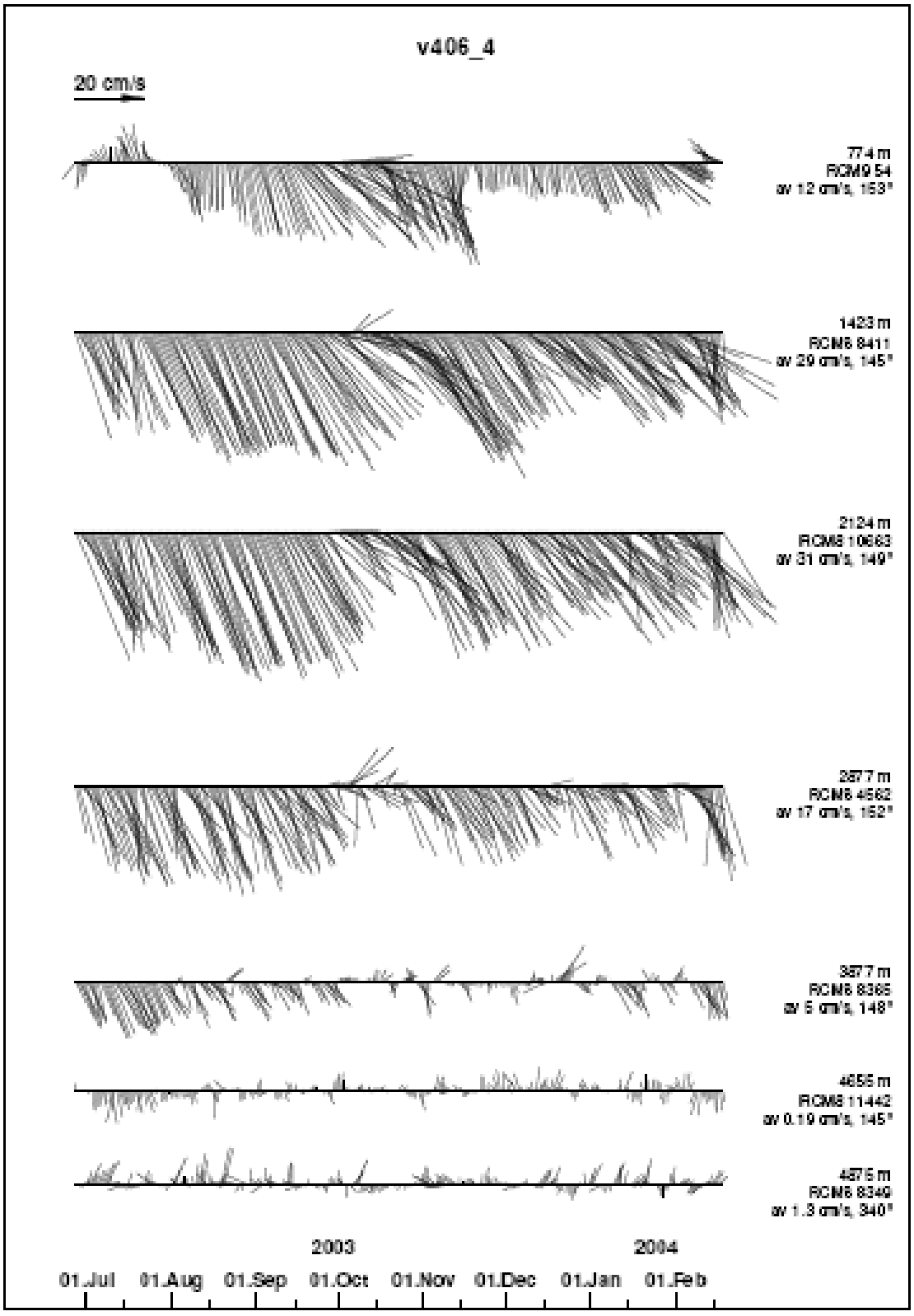

Figure 4.5: Stickplots of recovered current meter data from M3.

4.4.6 CTD programme (M. Lankhorst)

A total of eleven CTD casts were carried out during METEOR cruise 60/4. The purpose of these was to provide reference data at positions where moorings were to be recovered or deployed, as well as to calibrate MicroCATs and MTD loggers, which were attached to the CTD rosette. As some of the MicroCATs and MTPs were not designed for high pressure, not all CTD casts went to the bottom. Salinity reported by the CTD was calibrated using water sampled with the rosette and analysed with a laboratory salinometer. The CTD system was a SeaBird Electronics, model 911 plus type, referred to as IfM-Geomar serial number 1. A backup system was available but never used. The underwater unit was built into a rosette housing capable of holding 24 water sampler bottles. An lADCP system looking both up- and downward and a Benthos bottom pinger were also installed. Table 4.5 lists sensor model and serial numbers.

Table 4.5: Setup of the CTD system during METEOR cruise 60/4.

Instrument Type	Model No.	Serial No.
CTD deck unit	SBE 11 plus	
CTD underwater unit	SBE 9plus	09P22348-0572
Rosette water sampler	SBE 32	3222348-0291
Temperature sensor	SBE 3plus	03P2920
Conductivity sensor	SBE 4c	042443
Oxygen sensor	SBE 43	430215
Pump	SBE 5T	052603
Pinger	Benthos	
Bottom alarm	mechanic switch	

Calibration Applied to the Data

Pre-cruise laboratory calibrations of the temperature and pressure sensors were available (see below). Both of these yielded coefficients for a linear fit. Salinity was calibrated during the cruise with a Guildline Autosal 8 salinometer. For this purpose, the detected error in conductivity was linearly fitted to the conductivity data itself, and the residuals were linearly fitted to pressure. After this, mean residuals over intervals of 1000 dbar were less than 0.0005, with standard deviations of 0.003. With these corrections applied, a data set was created on board that can be considered final unless the next laboratory calibrations detect changes in the temperature and pressure coefficients. The oxygen sensor must be considered unreliable because no in-situ measurements were carried out during the cruise. The following pressure (in dbar) correction (laboratory calibration from February 2003) was applied:

Coefficients for static correction at temperatureT0
PRES(T0)=PCTD(T0)+Pol(PCTD(T0))
Polynomial degree is M=1
Number of data pairs is N=13
Coefficients,starting at lowest order:
co(0)= 1.483240e+000
co(1)=-7.943060e-004

The following temperature (in ◦C) correction (laboratory calibration from November 2003) was applied:

Coefficients for correction, TEMP=TCTD+Pol(TCTD)

Polynomial degree is M=1
Number of data pairs is N=16
Coefficients, starting at lowest order:
co(0)=-4.044333e-003
co(1)= 1.621552e-005

The following conductivity (in mS/cm) calibration was applied using MatLab:
cond = cond_raw + .polyval(coeff_c,cond_raw) + ... polyval(coeff_p,press);
with:
coeff_c = [3.8077e-04 -4.3522e-03]
coeff_p = [-3.6486e-07 9.1812e-04]
As a preliminary calibration, it would also have been appropriate to add 0.010 as a constant offset.

Table 4.6: Information on all CTD casts during METEOR 60/4, taken from the manually written log sheets.

Station	Cast	Start Time (UTC)	Start Position	Max. Pr.	Notes
99	1	18-Feb-2004 01:26	16°19.84'N 60°31.43'W	4879	clock offset of several minutes
107	2	20-Feb-2004 03:24	15°58.87'N 56°56.64'W	5050	
119	3	22-Feb-2004 19:45	15°28.48'N 51°32.46'W	5050	MicroCats attached
121	4	23-Feb-2004 12:03	15°27.54'N 51°31.87'W	5041	MicroCats attached
125	5	23-Feb-2004 21:15	15°27.88'N 51°31.85'W	3503	MicroCats and mini-loggers attached, only 3500 dbar
126	6	24-Feb-2004 02:20	15°27.60'N 51°31.44'W	990	MicroCats attached, only 1000 dbar
127	7	24-Feb-2004 04:20	15°27.45'N 51°31.49'W	5045	MicroCats and mini-loggers attached
132	8	26-Feb-2004 18:39	20°35.23'N 56°40.14'W	5460	MicroCats attached
132	9	27-Feb-2004 00:19	20°35.33'N 56°39.95'W	4005	Mini-loggers attached, only 4000 dbar
140	10	28-Feb-2004 19:05	15°59.38'N 56°56.89'W	5050	
143	11	01-Mar-2004 00:14	16°21.18'N 60°27.82'W	5171	no lADCP

PERFORMANCE AND STATION OVERVIEW

The overall impression of CTD performance is very positive. There were virtually no spikes in the data, nor did the recording computer have problems due to the large amounts of data. Further processing with a laptop (internal name "solo3") and software developed at IfM Kiel (CTDOK using MatLab) was troublesome, as there were different incompatible versions of the software, and as the software was clearly not designed for handling large data files. However, after spending some effort changing versions, the software could be run successfully, but required several hours to process a single profile. Apparently, there is need for improvement, and work on this has been started recently.

Table 4.6 summarizes the manually written log sheets for the individual CTD casts. During the casts with MicroCAT or logger instruments attached, the probe was halted for ten minutes at various depths during the upcast, which provides calibration points for these devices.

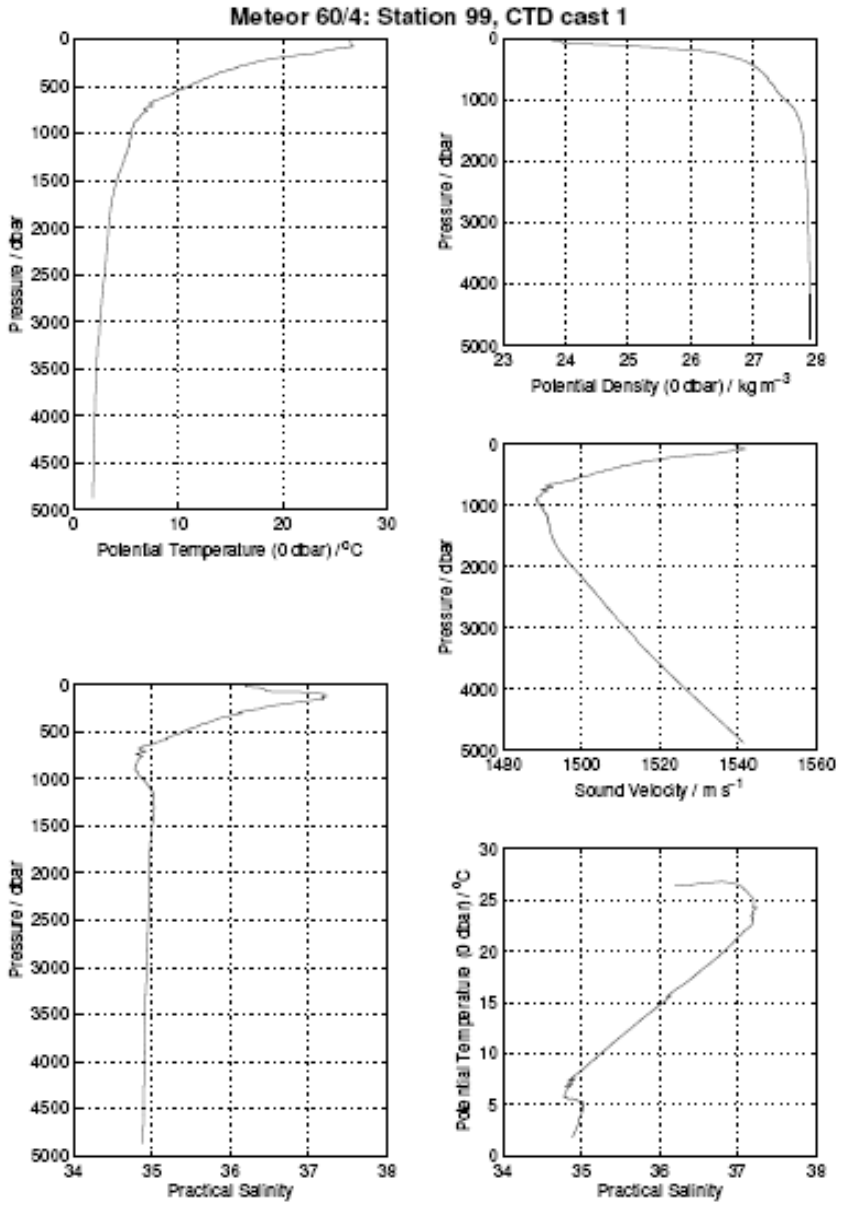

Figure 4.6: Data from CTD cast 1.

HYDROGRAPHY

The main features of the hydrography of the area are apparent in plots of salinity versus pressure (Fig. 4.6 highlights this exemplarily in the lower left panel). In most of the casts, the upper 50 m show a fresher layer influenced by tropical rainfall (not in the northernmost stations), followed by a salinity maximum at circa 100 m. From there downward, the profiles feature the linear T-S relationship characteristic of Central Water, until the salinity minimum of Antarctic Intermediate Water is reached at about 800 m. The largest part of the water column, approximately 1200-4500 m, is occupied by the various species of North Atlantic Deep Water, which is the main interest of study in the MOVE project. Below this near the bottom, remainders of Antarctic Bottom Water can be found.

4.4.7 Calibration of MicroCATs and MTDs (T. Kanzow)

As during the previous cruises related to the MOVE project, all of the recovered and redeployed MicroCATs and MTD were attached to the rosette during CTD casts to carry out in situ calibrations (see Table 4.7 for an overview). This routine is crucial for the high accuracies required in this project. As in the previous years the rms difference between the calibrated CTD and MicroCAT temperatures and conductivities is around 0.005 K and 0.01 mS/cm, respectively, with the individual MicroCATs showing a relatively stable offset relative to the CTD from year to year (i.e., the year-to-year drift of the individual MicroCATs typically displays much lower values than those given above). Thus, by carrying out calibrations prior and after the deployment, the errors of the MicroCATs relative to the CTD can be reduced to less than 0.002 K and 0.002 mS/cm, respectively. As said above, similar calibrations are carried out with the MTD. Here the pressure measurements are of particular importance (see MTD section). The usual differences between the CTD and MTD pressures are below 8 dbar even in the deep ocean (Fig. 4.7). Here again the year-to-year differences of individual MTD relative to the CTD are much smaller than that, such that MTD pressure accuracies of < 2 dbar relative to the CTD should be achievable.

Table 4.7: MicroCATs and MTD logger lowered with the CTD during calibration casts.

CAST	MicroCAT / MTD logger
1	–
2	–
3	**MicoCAT**: 945 953 949 1550 1276 941 910 1280 1268 1269 1279 1277
4	**MicoCAT**: 962 948 960 1718 1721 944 1722 1720 1723 1278 1288
5	**MicroCAT**: 3411 3412 3413 3414 **MTD**: 19 20 22 23 30 46 47 48 52 55
6	**MicroCAT**: 1717
7	**MicoCAT**: 934 939 950 954 959 961 1321 1719 **MTD**: 39 56 57 58 59
8	**MicoCAT**: 0933 0935 0937 0942 0952 0957 0958 1162 1271 1273 1275 1319
9	**MTD**: 19 20 29 33
10	–
11	**MicroCAT**: 0929 0938 0940 0946 1270 1272 1274 1316 1317 1318 1320 1322 1323 2048 2279

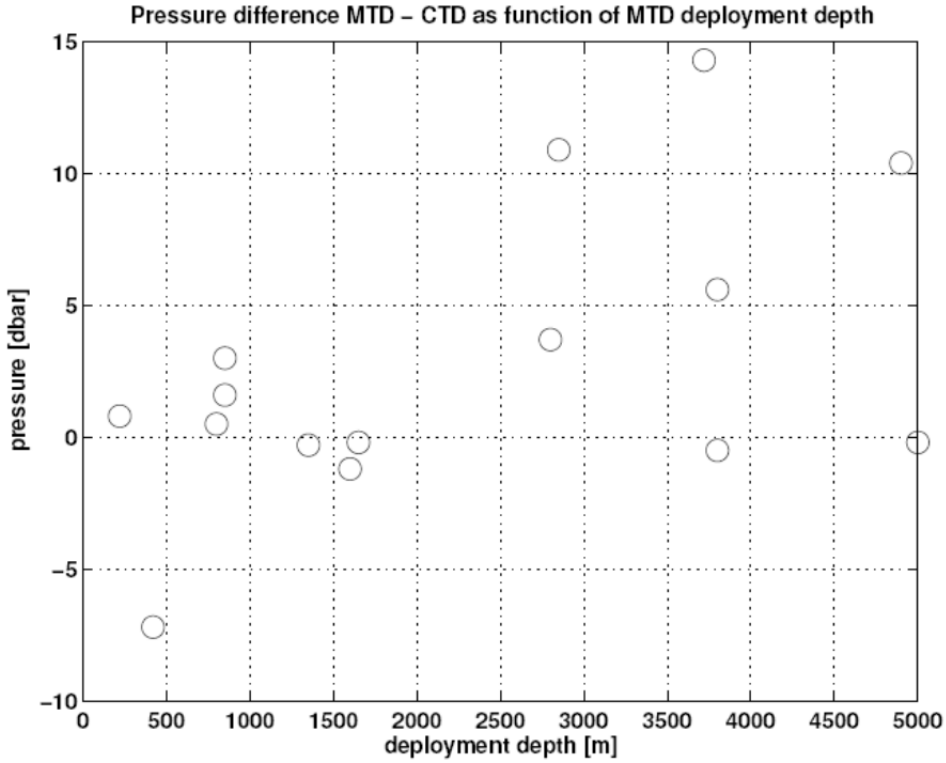

Figure 4.7: MTD calibration: Pressure differences MTD - CTD as a function of MTD deployment depth

4.4.8 ADCP (J. Karstensen)

ADCP DATA

Two types of ADCP were used during the M60/4 cruise: a vessel mounted ADCP (38kHz) mounted in the ships hull acquiring data to about 1000m depth and a lowered ADCP (2 workhorse 300 kHz) mounted on the CTD rosette and acquiring full depth current profiles.

LOWERED ADCP (LADCP)

During the cruise 8 single lADCP profiles where acquired (see Table 4.8 and Figure 4.8) while no section sampling was planned. The devices were configured as on SO172 MOVE cruise in 2003 (see end of this section for the master command file). For starting the master/slave devices it is critical to first start the slave as the devices have been correctly synchronized. This was done for all casts properly. Bin size length was 10 m.

Data processing was carried out with the lADCP package provided by M. Visbeck (Lamont-Doherty, Palisades, NY, USA) (1). The velocities are determined from integrating the shear between up and down cast which, assuming a constant velocity profile during the cast, should cancel out assuming a certain velocity profile. The advantage of using an upward and downward looking instrument is the knowledge of exact velocities at the bottom using the bottom track feature of the downward looking instrument (slave) which further constrains the shear derived velocity profiles.

However, for most casts (except 1, 2, and 4) the bottom was not found. As an additional constraint the vmADCP velocities were used for the upper 1000 m as second boundary condition (except station 1). Navigational information was extracted from the GPS positions during the casts and considered during the processing procedure. No tidal current corrections were applied. The profiles are shown in Figs. 4.9 and 4.10.

The profiles shown are derived by the shear based estimate without considering the reference velocity measurements from the vmADCP and the bottom velocity (magenta line) as well as derived from the inverse solution considering the velocity constraints (thick black line). Overall there is not a good agreement between the two solutions (shear vs. inverse). Typically the error in velocities obtained (stippled line) exceeds the velocity. Profiles which were recorded at the same location but just a few hours apart (profile 3, 4, 7 and profiles 8, 9) are not very similar in structure. The profile from station 3 shows large velocities of O(0.5m/s) at the bottom which is unrealistic considering the small velocities obtained from the direct bottom track profiles (1,2,4). Station 1, near the western boundary, is the only one which shows a reasonable agreement between the shear and the inverse solution. Here velocities are larger than the errors.

Table 4.8: lADCP casts during M60/4. BT: bottom track

St.	Cast	Start Time (UTC)	Start Position	depth	Notes
99	1	18-Feb-2004 01:26	16°19.84'N 60°31.43'W	4879	BT
107	2	20-Feb-2004 03:24	15°58.87'N 56°56.64'W	5050	BT
119	3	22-Feb-2004 19:45	15°28.48'N 51°32.46'W	5050	no BT
121	4	23-Feb-2004 12:03	15°27.54'N 51°31.87'W	5041	BT
127	7	24-Feb-2004 04:20	15°27.45'N 51°31.49'W	5045	no BT
132	8	26-Feb-2004 18:39	20°35.23'N 56°40.14'W	5460	no BT
132	9	27-Feb-2004 00:19	20°35.33'N 56°39.95'W	4005	no BT
140	10	28-Feb-2004 19:05	15°59.38'N 56°56.89'W	5050	no BT

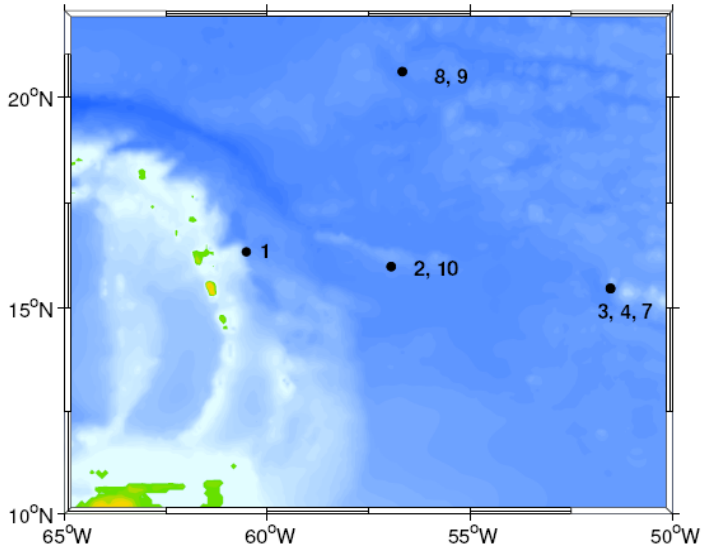

Figure 4.8: Station map of lADCP casts during M60/4.

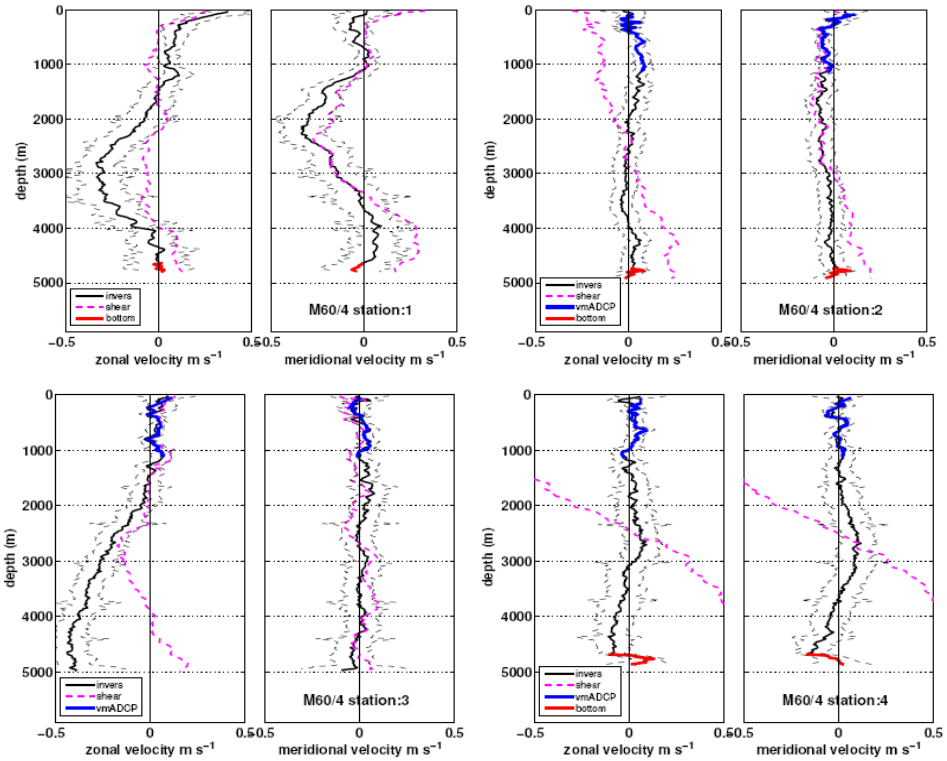

Fig. 4.9 Station 1 to 4 lADCP profiles. The vmADCP as well as the bottom velocities are displayed when available. The broken line indicates the uncertainty of the measurement. Processing is based on (1).

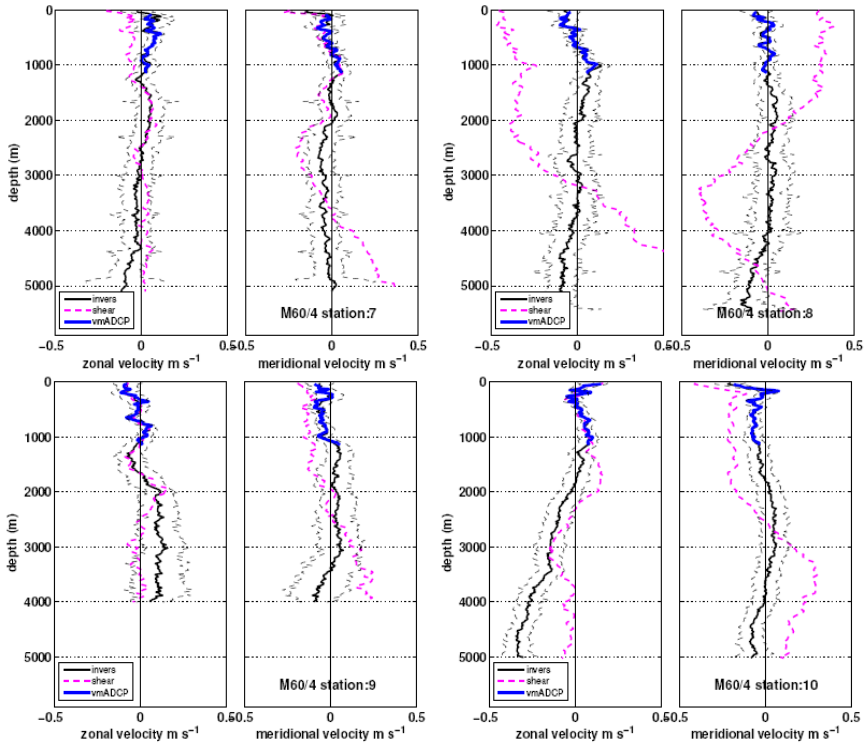

Fig. 4.10 Station 7 to 10 lADCP profiles. The vmADCP as well as the bottom velocities are displayed when available. The broken line indicates the uncertainty of the measurement. Processing is based on (1).

Vessel mounted ADCP (vmADCP)

The vmADCP used on M60/4 was the 38 kHz Ocean Surveyor mounted in the ship's hull. The 75 kHz instrument which is permanently installed and normally used on RV METEOR was not ready for operation. The instrument was used with 16m bin length, 70 bins and 2 second ensemble interval. Navigation was fed in from the ASHTECH 3d GPS and the fiber optical gyro (FOG). In particular the quality of the ship heading information can be different between the two instruments while we gave the ASHTECH headings a preference. In case no ASHTECH data was available the FOG heading was used considering the average heading difference between FOG and ASHTECH. A converter was needed to transform some navigational data to be usable for the ADCP. The converter was not working properly during the beginning of the cruise and the data could not be processed. There were certain gaps in the vmADCP data collection during the cruise (Figure 4.11). Beside the aforementioned problem with the navigational data converter at the beginning of the cruise the device was stopped in the EEC of Barbados and Martinique. Removing the mean profile from the data during station work gives a measure of flow variability as well as a lower limit of the accuracy of the data (Figure 4.12). A normal distribution with an average standard deviation of 0.03 m/s in both (u,v) components was found.

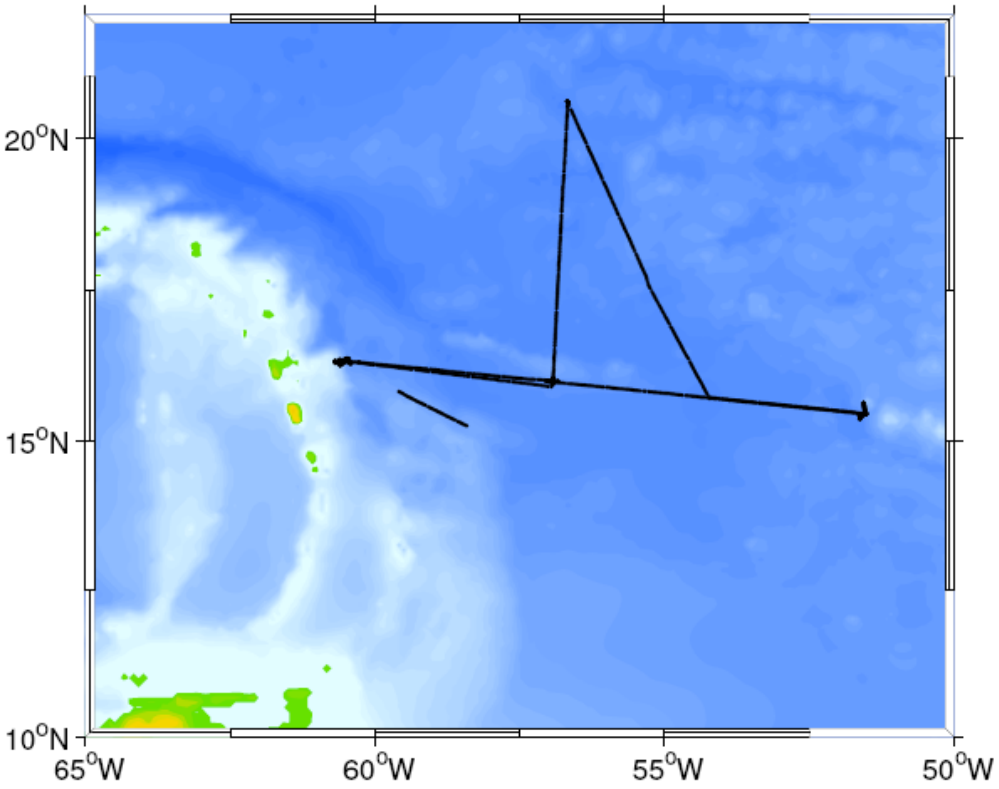

Figure 4.11: Positions of vmADCP data collected during M60/4.

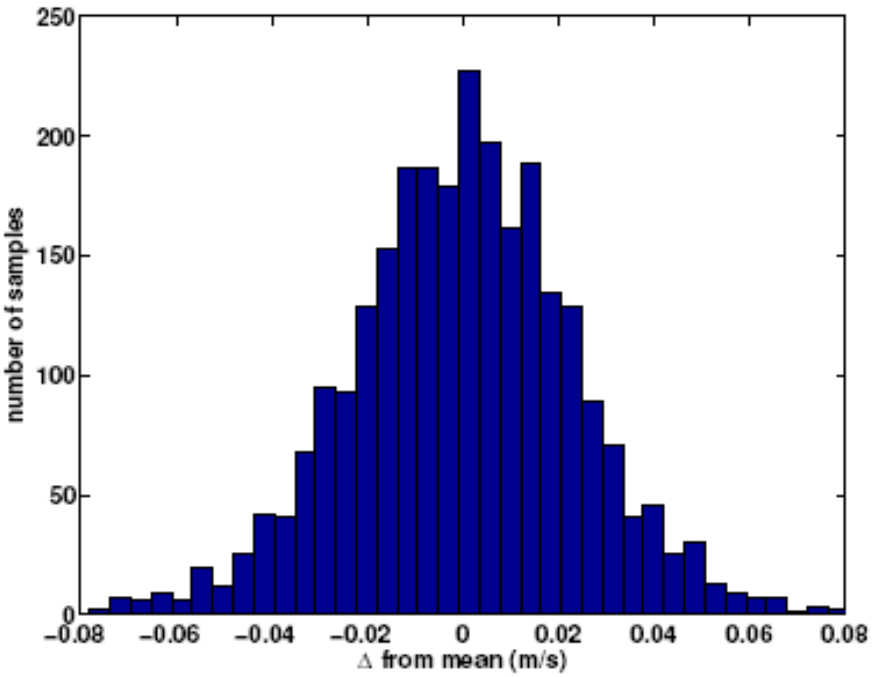

Fig. 4.12 Distribution of velocity deviations from their mean for on station data during M60/4.

The data are shown here as a zonal section acquired on the way to the easternmost mooring (Figure 4.13) and two meridional sections acquired on the way to and back from the northernmost PIES position (Figures 4.14 and 4.15). Readily visible are quasi barotropic structures indicating the existence of eddies. In the southward meridional section (Figure 4.15) an eddy diameter of about 3.5◦ (400km) can be estimated from the data. Along the northward section (Figure 4.14) indications of the same feature are observed. Its wavelength may correspond to that of baroclinic Rossby waves observed in the region (2)

The master control files used during all casts was:

```
; LADCP *.CMD file made for
PALMER-1999/2000 cruise ;by
Martin Visbeck modified for Oden
cruise 3/1/02 ; fuer m60 4
modifiziert 17.02.2004 jk
;  master.cmd
;CR1 retrieving parameter
CR1
;$LMR.TXT will capture all
communications to M60_mlog.TXT
$LM60_mlog.TXT
;ED0000 Depth of transducer
ED0000
;ES35 salinity
ES35
;EX11111 coordinate transformation
;earth coordinates
EX11111
;TE00:00:03.50 time per ensemble, 3.5 second
ensemble interval TE00:00:03.50
;TP00:00.70 time between pings s
TP00:00.70
;EZ0011111 sensor source
; defaults to manual depth setting, uses internal
heading,pitch,roll ;uses EC command to set speed
of sound
EZ0011111
;EC1500 set speed of sound to 1500m/s
EC1500
```

```
;EA00000     heading alignment correction = 0
EA00000
;EB00000     heading bias correction = 0
EB00000
; RNdm604_ sets deployment name to dm604_
RNdm604_
;CF11101     flow control, serial output disabled
CF11101
;---------- SPECIAL LADCP commands
;LD111100000     data out (vel,corr,intensity, good,status...)
LD111100000
;LF0500 blank after transmit (0-9999cm),Note:  half of bin length
LF0500
;LP00003    3 pings per ensemble 1 ping per ensemble for anslope
LP00003
;LJ1 receiver gain
LJ1
;LN025 number of depth cells 250 m range covered by
25              bins            *               10              m
LN025
; LS1000 bin length (cm)        = 10m
LS1000
; LV250 correlation velocity (cm/s radial)
LV250
; LW1  band width
LW1
;LZ30,220 Amplitude, Correlation Thresholds
LZ30,220
; SI0    master waits 1 ensemble before sending sync pulse
SI0
; SM1 set this instrument to master
SM1
; SA011 master sends pulse before ensemble
SA011
; SW4500 synchronization delay
;            the master waits .5500 s after sending sync pulse
SW5500
;   -----------   END   of   LADCP
commands                ----------
; CK keep parameters as user
defaults
CK
CS start pinging
CS
;$ L close log file
$L
```

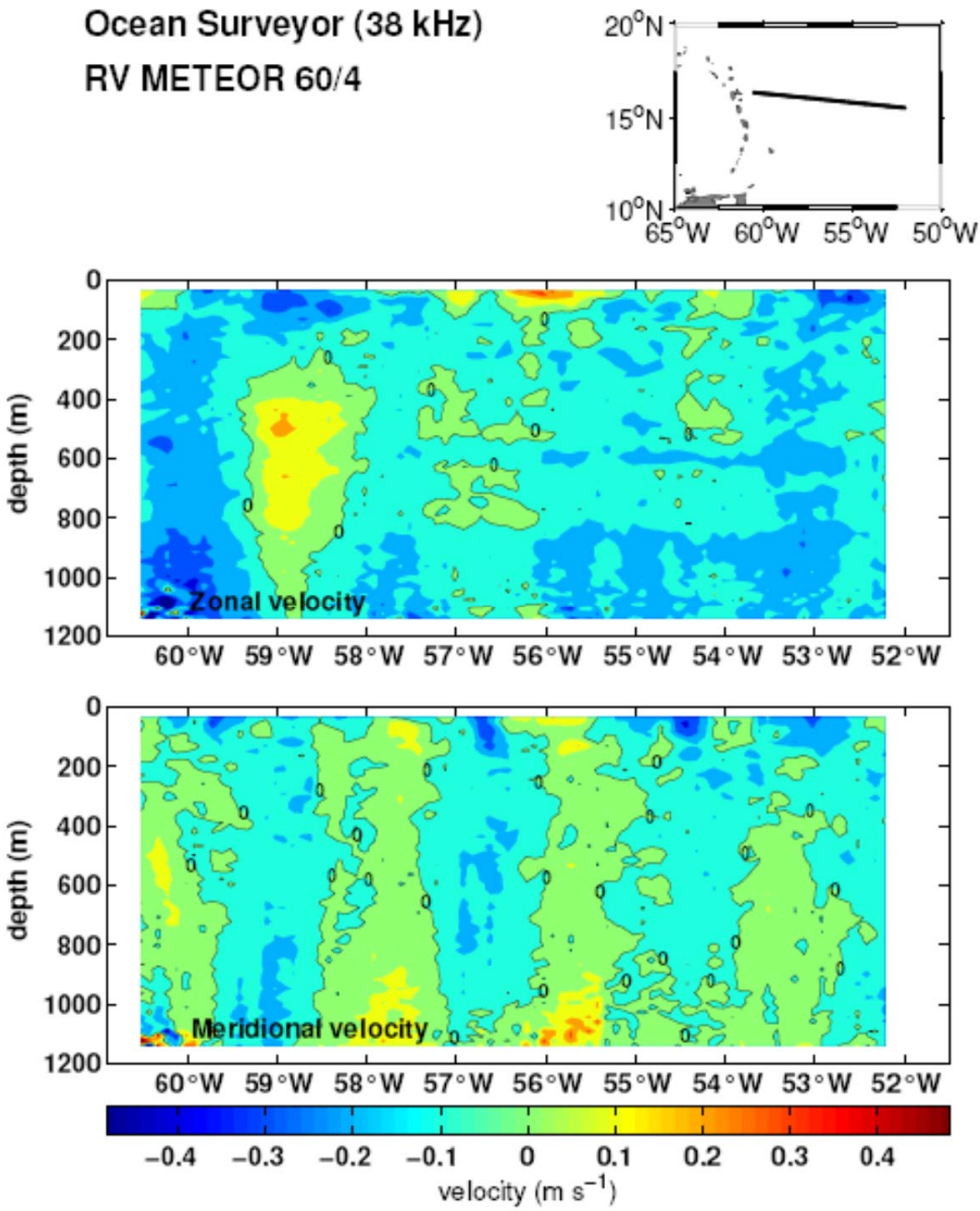

Fig. 4.13 Meridional section acquired on the way to the easternmost mooring position (see map for track).

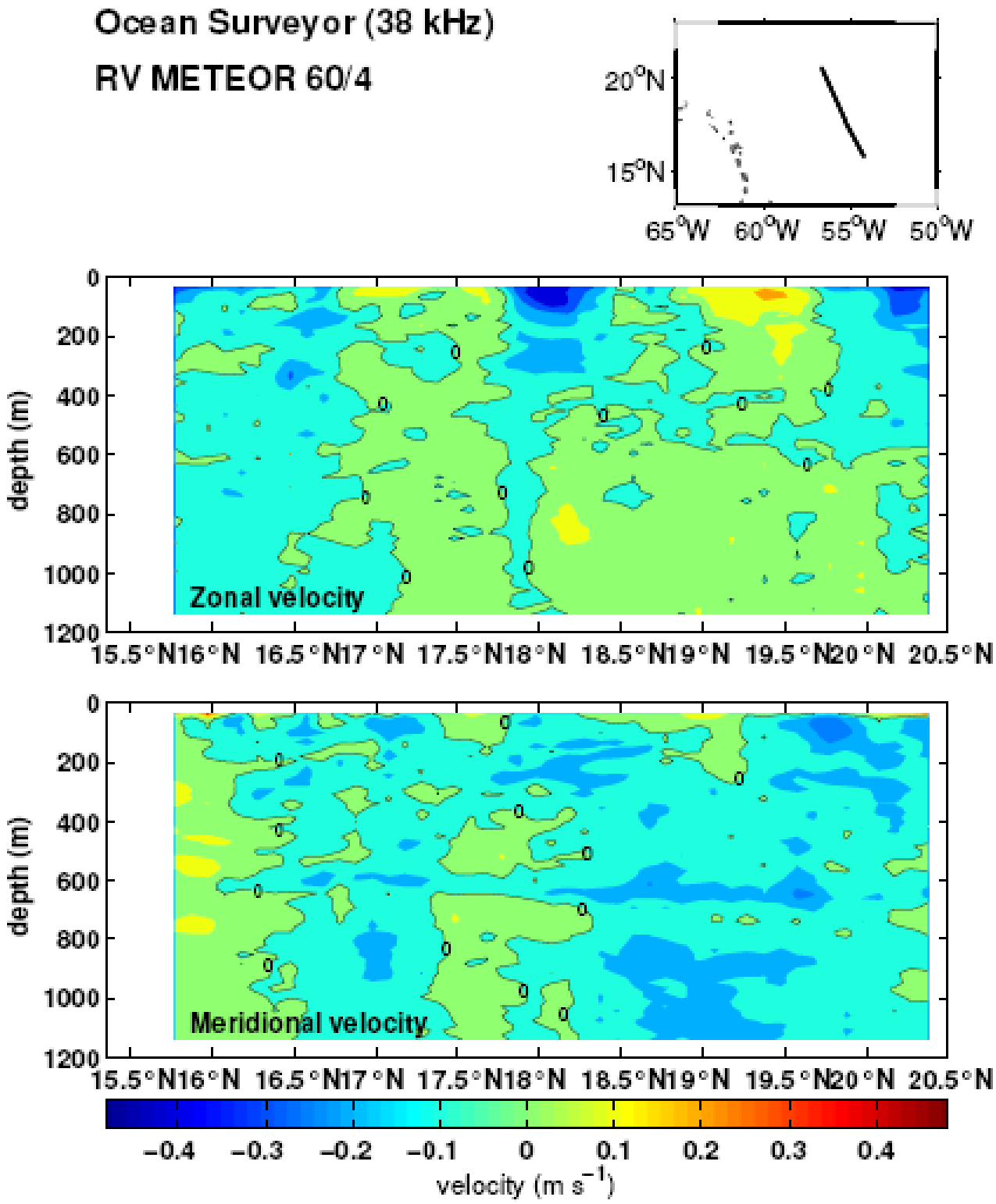

Fig. 4.14 First zonal section, acquired on the way to the northernmost PIES deployment position (see map for track).

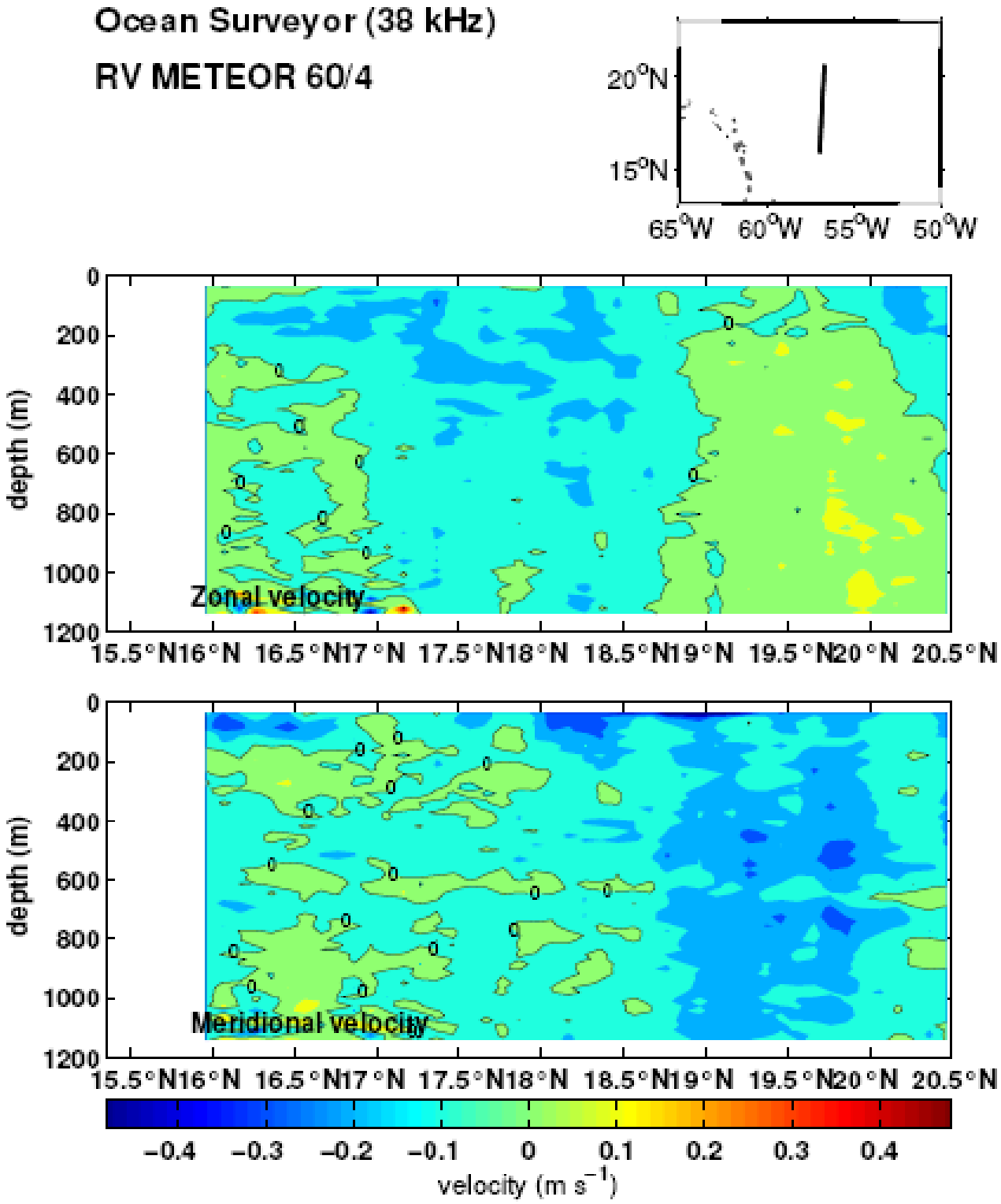

Fig. 4.15 Second zonal section, acquired on the way south from the northernmost PIES deployment position (see map for track)

.

4.4.9 Tomography (T. Avsic)

The tomographic instruments measure the travel time of different acoustic rays (eigenrays) between a sound source and a receiver (see Figure 4.16). In the MOVE mooring array a sound source was moored in M3.5 and a receiver in M2. They were deployed during the FS SONNE cruise 172 in 06/2003. On this cruise first the sound source was recovered on the 17.02.2004. Unfortunately the instrument did not wake up through the SAIL interface and it turned out, that it had no battery power. Powering the system up with external power supply allowed us to communicate with the system. The read out of the internal data showed that there was not one single transmission done by the source. Further investigations showed that the battery cable was clamped between shell and battery. This could only have happened during the assembly of the instrument at Webb Research and most probably, during the deployment of the source it was cut due to shocks of movement on deck.

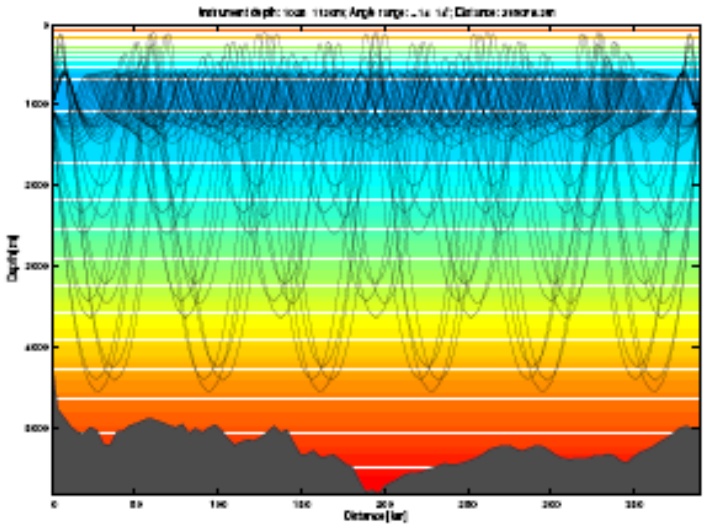

Fig. 4.16 Eigenrays between M3.5 and M2 with instruments at 1025 and 1130m.

The following measurements done by Andrey K. Morozov and Rudolf Link showed that the electronics and also the battery power were okay. The battery cable was changed and the source was lowered at 20m depth to test its full power capability. As many of the ship's aggregates as possible were switched off, so the source could be heard in the bilge of the ship. Sometimes the system reset itself, however this was attributed to high frequency noise penetrating through the SAIL loop.

The source was deployed on the 18 February in order to get some first test receptions at the receiver. The receiver was recovered on the 20 February. Analyzes of the data showed that in fact the source did not work during the last deployment, however very good receptions had been recorded for the last two days (Figure 4.17). The spectrum shows a clear sweeping signal from 200Hz to 300Hz and the correlation shows arriving times of the different rays similar to the predicted times. Converting the data to an audio file let us also hear the signal. This gave us the idea to build a simple and small receiver which can easily be lowered from the ship. John Bailey, Andrey K. Morozov, Rudolf Link and Tom Avsic constructed from some electronic components, one RAFOS hydrophone and a mini-disc recorder an easy-to-use receiver which fits into an Aanderaa shell, which was originally used for carrying batteries of the lowered ADCP. Another receiver with similar electronic components was built in the glass ball of a spare transponder and connected to its transducer. Both systems were lowered together with the much bigger and heavier SeaScan receiver to

1000m depth on the 28 February in order to listen to the 5:54 UTC transmission of the source. None of the systems received the signal.

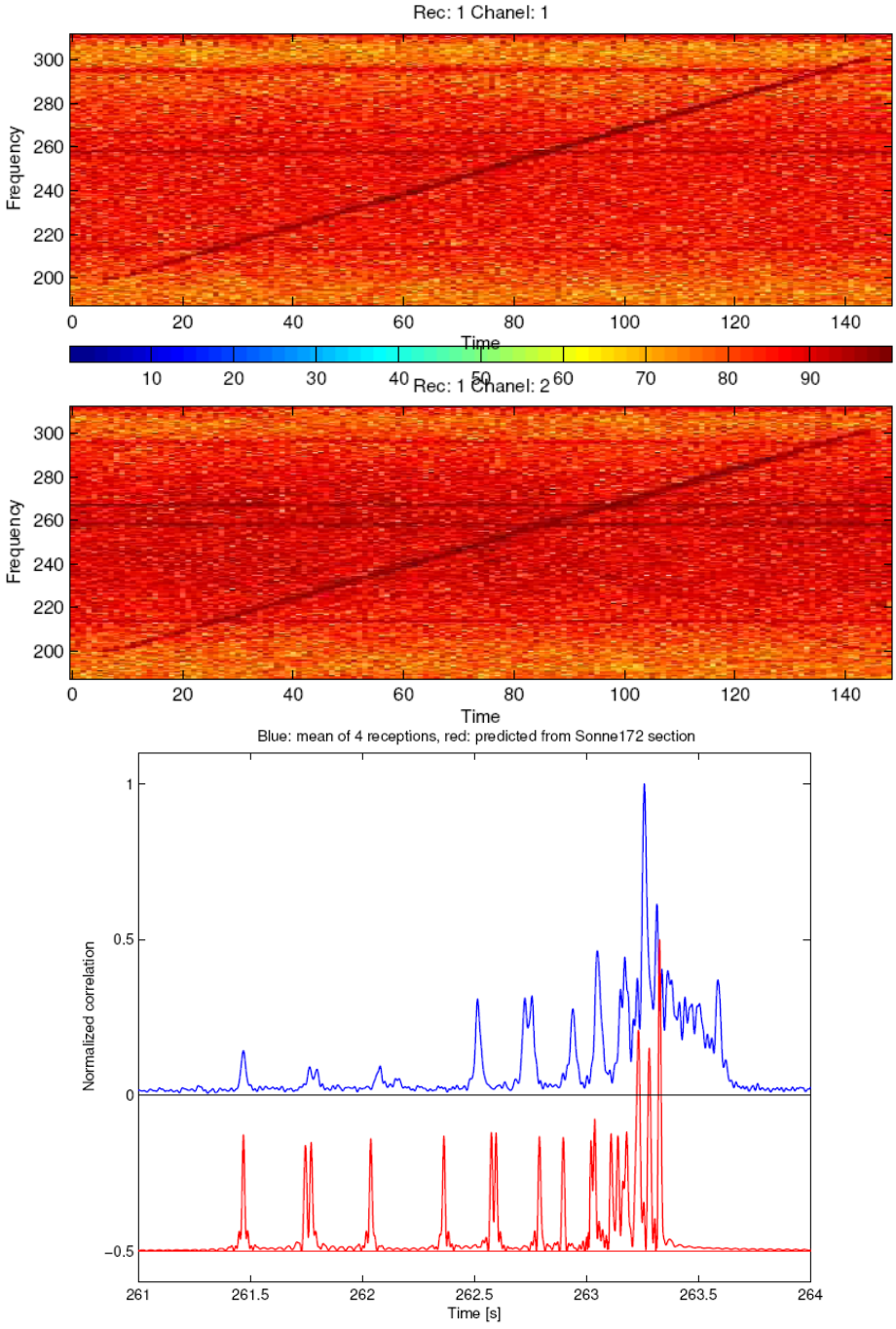

Fig. 4.17 Upper panel: Spectrogram of the first record of the sound source reception at M2. The sweep signal from 200Hz to 300Hz in 135s is clearly visible. Lower panel: Normalized mean correlation of all four receptions (blue) together with the theoretically predicted correlation derived from the SONNE 172 CTD section (red, shifted by -0.5).

Noise estimations showed that the noise under the ship was about 20dB higher than in the moored measurement, therefore we expected to be able to record the signal and the suspicion grew that the source had stopped working again. Anyway all of the receiver systems seemed to work correctly. On the same day the receiver was deployed in the mooring M2 and we left for the recovery of the sound source

mooring M3.5. This had to be done anyway because the navigator was programmed to make two measurements per hour which would have resulted in a full memory after 6 months. About 30 kilometers before the M3.5 mooring the working boat METEORIT was deployed to listen again to the sound signal with the two small receivers. While the instruments were lowered to approximately 800m depth the ship steamed away to recover the mooring just after the transmission. The instrument on deck again could not be woken up. Measuring the battery power gave a value of 0.3V. This time a faulty connector was the cause for this. However reading out the internal data showed that the source worked fine including the transmission before recovery. Again this happened due to movement shocks, necessitating easy-to-use receivers for testing whether the moored source was still working or not.

Analysing the recorded data on the two mini-disc recorders showed also that the source was working, however estimates of the source level lead to uncertain results. The results showed however, that the receiver with the RAFOS hydrophone (named Altoids) was more appropriate for listening the source. The transponder also received the signal, but it was pervaded with loud hitting noise. After testing the whole electronics of the sound source and another in-water-test at 20m depth, the source was deployed in the M4 mooring. Another listening with the Altoids receiver was carried out at 800m depth and at about 1km distance to the mooring. The Altoids was attached to the winch by a rubber rope of about 3m length. The signal was clearly recorded on the mini-disc and also the noise seemed to be strongly reduced compared to the previous records.

While the ship steamed to the bottom pressure site M7, it stopped again at about 360km distance to the sound source. This time the Altoids was attached to 800m rope which had two Benthos balls, a watch-dog and a radio signal at the top. Directly above the Altoids were two rubber ropes of 1.5m length. The Altoids was deployed from the ship and the ship steamed away about 4nm. After recovery the signal was clearly seen in the spectrum. Also the correlation showed clear arrivals of different rays (Figure 4.18). This time the record level was chosen to be very good, however sometimes it sounded like the two rubber ropes hit each other. The setting on the mini-disc recorder were: hydrophone connected to Mic In, record level 14, record mode mono.

ATOMIC CLOCKS

The receiver and the sound source were equipped with ORCA atomic clocks. The manufacturer specifies the drift to be less than 10^{-9} . The drift of the source clock could not be measured, because it did not work without power supply, however the drift of the receiver's clock was 35ms in 241days. This corresponds to 1.68×10^{-9} .

TRANSPONDER

Six TR6000 transponders for mooring navigation (three at both moorings) were recovered and redeployed. All six instruments were released after their one and a half year deployment. The burning time of the release wire was about 10 min, which is the same as was found one year before after the 6 month deployment. The ascending time was between 60min and 75min. The transponder locations were determined by a survey. See the Table 4.10.2 for transponder positions.

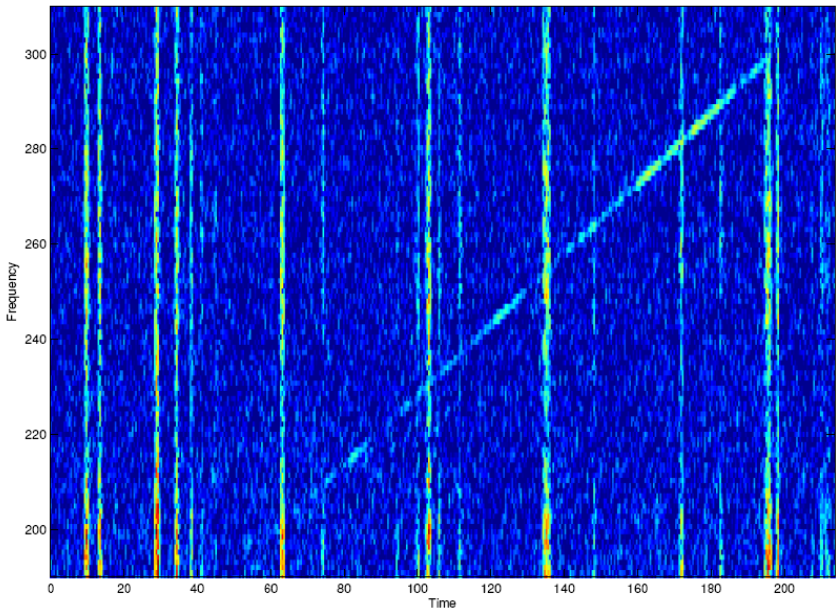

Fig. 4.18 Upper panel: Spectrogram of Altoids record 360km away from the sound source. Lower panel: Associated Correlation.

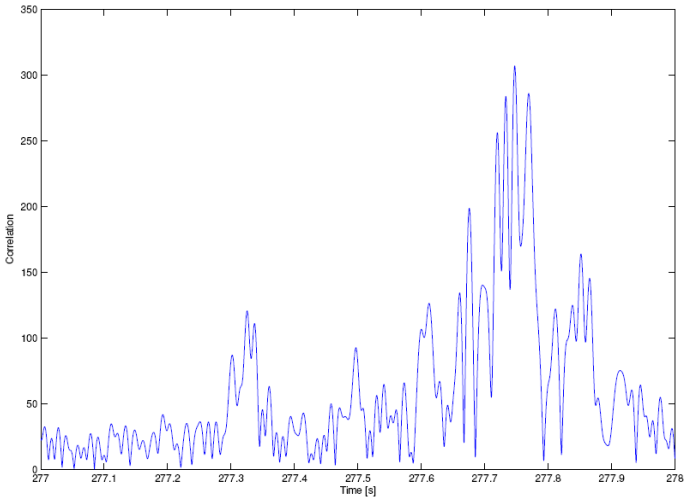

Table 4.9: Location of transponder positions (including error estimates) based on an acoustic survey

		rx [kHz]	tx [kHz]	rel.code	latitude	longitude	depth	error
M2	XP-1	10.0	11.5	A	15°N 58.386	056°W 56.975	4991m	± 6.5m
M2	XP-2	10.0	12.0	D	15°N 58.387	056°W 54.164	4970m	± 7.5m
M2	XP-3	10.0	12.5	F	16°N 00.653	056°W 55.606	4930m	± 6.6m
M4	XP-1	10.0	11.5	A	16°N 19.013	060°W 38.330	2367m	± 6.5m
M4	XP-2	10.0	12.0	B	16°N 19.045	060°W 35.224	3327m	± 3.5m
M4	XP-3	10.0	12.5	F	16°N 21.814	060°W 36.011	3141m	± 5.8m

ALTOIDS TOMOGRAPHY RECEIVER

The Altoids tomography receiver is a simple receiver used for recording hydrophone data from a Benthos hydrophone to a minidisk recorder. The receiver was built primarily to test the operation of the Webb Research sound source. The Benthos hydrophone (as used on RAFOS floats) is coupled to the Altoids amplifier through a shielded cable. The amplifier provides 80dB of gain with a band pass between 100 - 500 Hz. A pair of 9-volt batteries serves as continuous power supply for up to 2000 hours. The amplified output terminates with a 3.5mm phone connector. The phone connector plugs into the standard input jack of a minidisk recorder. With the recorder set to mono mode, 138 minutes of recording time is available. After a recording is made, playback into a computer's microphone input to capture the recording to a .WAV file. The .WAV file can then be read into Matlab for analysis.

Testing of Altoids has shown that ship generated noise in the water is the most serious problem encountered. Deployment from a small boat or float mooring and moving the ship away from the receiver solves the noise problem. The second source of noise is surface noise. Lowering Altoids to a depth of about 1000 meters provides a quiet environment for the receiver. Empirical testing with the minidisk recorder has shown that using the microphone input with the input level set to a value of 14 works best.

SELF NOISE ESTIMATION ON THE SEASCAN-ERATO R10 AND THE ALTOIDS RECEIVER

The self noise of both receivers were measured by Andreas Pinck and Rudolf Link by a shortcut through the input pins of the amplifier. The measured voltage at the amplifier's output was assumed to be the noise produced by the amplifier itself. Both amplifiers were stored in their metal HF-shieldings to prevent noise due to electro-magnetic-smog on the ship. The Altoids amplifier still showed some 50Hz output which must have originated from radiation outside the amplifier. This 50Hz signal was subtracted from themeasurement. The voltage read at the oscilloscope was about 5mV peak to peak at the Altoids and 30mV at the ERATO system. The gain of the Altoids is fixed to 80dB where the measurement on the ERATO was made at 104dB (18dB+56dB+80*.375dB). Converting the 30mV reading to a gain of 80dB gives:

$$30mV/10^{\frac{104-80}{20}} = 1.9mV \qquad (4.1)$$

20

Furthermore the peak to peak voltage needs to be converted to an effective voltage to make it comparable with other noise measurements on this cruise:

$$Altoids@80dB : 5mV/2 * \frac{1}{\sqrt{2}} = 1.75mV \quad (4.2)$$

$$ERATO@80dB : 1.9mV/2 * \frac{1}{\sqrt{2}} = 0.65mV \quad (4.3)$$

Noise estimation on the SeaScan-ERATO R06 receiver

The 250Hz noise level in the ocean can be estimated on a SeaScan-ERATO receiver by the following formula:

$$NL1 = -SH - DI + Vrms \quad (4.4)$$

where SH is the sensitivity of a single hydrophone (SH = -202dB) and DI the directivity of hydrophone (DI = 6dB). Vrms is the root-mean-square voltage output of the hydrophone during the noise measurement of the receiver converted to dB. It can be calculated from receiver's data by:

$$V\ rms = 20 * log10(RMS * Q) - Gp - Gf - GAIN * .375 \quad (4.5)$$

where RMS is the rms noise value saved by the receiver. Q is 1.22/1000 according to AD Conversion 13bits ref 5V ($2 * 5/2^{13} = 1.22mV$), Gp = 56 due to fixed gain preamplifier, Gf = 18 due to band-pass filter and GAIN the value of the auto adjusting amplifier which is also saved by the receiver.

Using the last few receptions from the moored receiver R06 (M2), when the signal of the sweep sound source in M3.5 had been successfully received, lead to noise estimates between 82 to 83dB on channel 1 and 75 to 79dB on channel 2. When the same receiver was lowered directly from the ship to 1000m depth the noise level was 100dB on channel 1 and 85dB on channel 2. Systematically higher noise levels on channel 1 seemed to be a problem caused by the receiver, however the noise on both channels was much higher during the lowered measurements. Reasons for that could be the noise of the ship (even though we tried to power down many noise sources in the ship) and the up and down movement of the receiver in the water due to high waves at the surface.

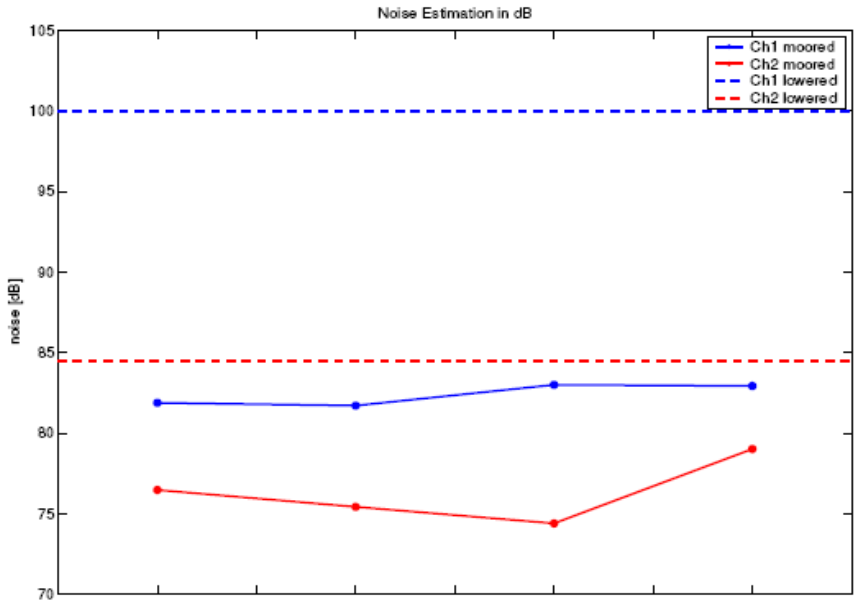

Fig. 4.19 Noise Level during moored and lowered receptions.

Source level estimation from the moored SeaScan-ERATO R06 system

The Source Level SL of the sound source can be estimated from the record of the receiver moored 400km away from the source. Basically the following formula was used:

$$SL = SNR + NL + 20 \times \log10(r) + a \times r/1000 - Gc \qquad (4.6)$$

where SNR is the Signal to Noise Ratio, NL the Noise Level, $20 \times \log10(r)$ loss due to distance, $a \times r/1000$ attenuation and Gc gain due to correlation. The SNR was calculated through the correlated data, therefore the Gc has to be subtracted. NL was already calculated in the previous section. The distance r was 383897 m. Additional formulae are:

$$SNR = 20 \times log10(\frac{corr_{ray}}{corr_{noise}}) \qquad (4.7)$$

$$Gc = 10 \times log10(B \times T) \qquad (4.8)$$

$$a = 0.115 \times 10^{-3} \times (\frac{0.435 \times f^2}{0.64 + f^2} + \frac{36 \times f^2}{5000 + f^2}) \qquad (4.9)$$

where corrray is the value of the correlation of a single ray and cornoise the rms value of noise in the correlation. B is the bandwidth (100Hz) and T the duration (135s) of the signal. So the attenuation coefficient a for 250Hz is 0.036, NL was found to be 82 − 83dB on channel 1 and 75 − 79dB on channel 2. The SNR was calculated with the −13 ray. It seemed that the earlier ray had more attenuation due to small structures in the surface layer or possible reflections at the sea surface. Unfortunately the −13 ray was rather weak in the last record, therefore it was not used in this calculation. The SNR varied from 23 − 28 dB on both channels which gave a Source Level of 183 − 189 dB on channel 1 and 189 − 194 dB on channel 2 (Figure 4.20).

Modified tomography receiver R10 test on 20/21.02.2004

The SeaScan receiver R10 was modified to be able to receive the 200-300Hz sweep signal. The filters were changed and the buffer size increased to 1MB by its manufacturer. Set up this way a task was run in the laboratory on the SYS01 system. The other components were: SS16, CK30, INT16, HYD03, Sharp MiniDisc SN:90212663 and Hi-Tex LX-38 stereo speakers. The signal was simulated by the MD Player with its speakers lying on the hydrophone. The volume was turned to maximum on the recorder and to 1/4 at the speaker's amplifier. The task was:

120 Par
240 Nav 2
295 Rx 0 0 18750

Start time : 19.02.2004 20:20:00 UTC
End time : 20.02.2004 18:00:00 UTC
Periodicity : 10min

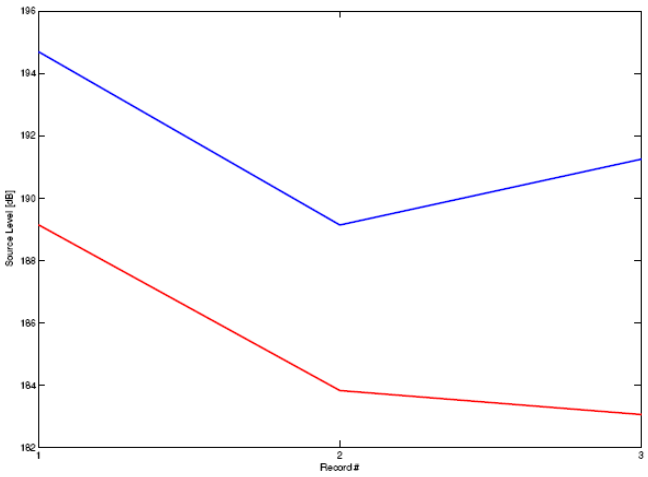

Fig. 4.20 Source Level during moored receptions, red channel 1,blue channel 2.

Over all, the system received 129 times the signal from the MD-Player and made 258 navigations as expected. During the first record, the MD-Player was not switched on yet, however all other records showed a proper signal in spectrum and correlation and were properly saved on the instrument's hard disk.

Power consumption of Sweep Sound Source

Basic values

Standby current:	1.5mA	1.5mAh
Clock recalibration :	ca. 1.2A for 12min	0.24Ah
Transmission:	3.0A for 140sec	0.1167Ah

For one year:

Standby	13.14Ah
Clock recalibration interval 24h	87.6Ah
Overall consumption without transmission	100.74Ah
Battery pack 45V - 22 slices (11Ah each)	232Ah
Capacity for transmission:	131.26Ah
Maximum of transmissions:	1125 = 3 per day

12.0kHz PIES#002 received @ navigation of tomography receiver in mooring M2

Mooring navigations of four measurements in group have been repeated every 6 hours on following times: 0:15:00, 0:25:00, 0:35:00, 0:45:00, 0:55:00, 1:55:00, 2:55:00, 3:55:00, 4:55:00, 5:15:00. The 4 navigations were carried out in a 13s interval.
The PIES deployed near M2 was supposed to do its acoustical travel time measurement every 10 minutes starting at 00:00:00. However on the 14 November 2003 at 12:25:52 it was first seen in the navigation data. It was continuously detected earlier in the navigation data, suggesting a constant clock drift of the PIES. The clock drift was estimated to be 3.078s per day (running too fast). The clock was already drifted 253 seconds (12:30:00-12:30:52 and assuming 5s of travel time between PIES and navigator) when it was first seen in the data. 253/3.086 = 81.9 suggest that the clock started to drift 82 days before the 13 November 2003, which is the 24 June 2003 and one day before its deployment. On the 17 October 2003 the PIES was last seen in the navigation data, suggesting that the time between his first and last ping of a single measurement was 50s. It can be ruled out that the received signal was the RELEASE signal of the PIES. Most likely it was its usual travel time measurement with 4 ping 16.5s apart. This is also supported by the interval structure of the receptions in the navigation data (Fig. 4.21).

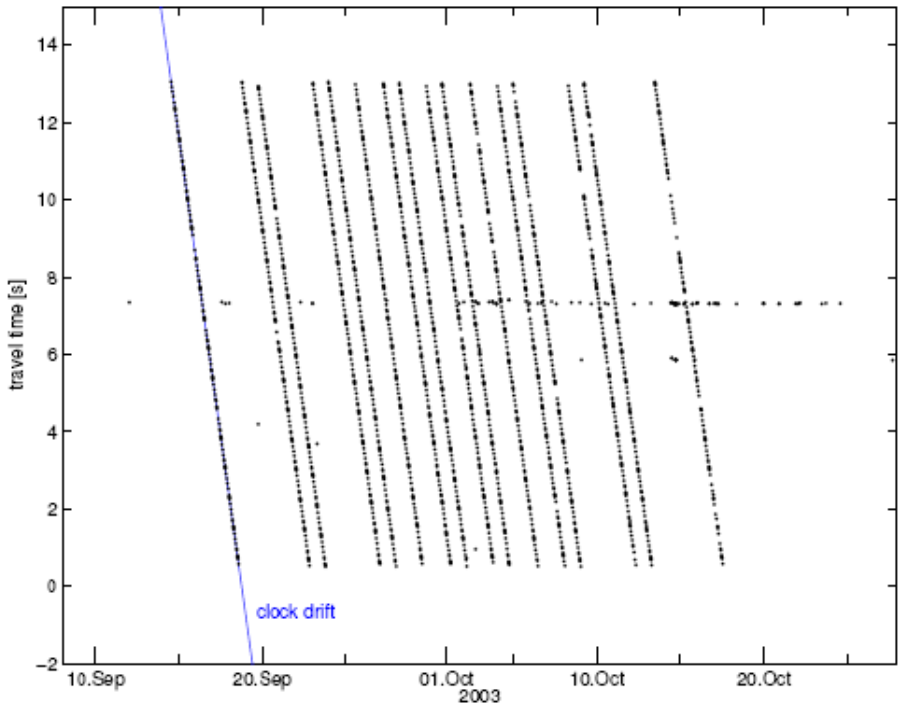

Fig. 4.21 Navigation data for the 12.0kHz signal.

TASKS

The sound source was programmed to transmit two times a day the 200-300Hz and 135s long sweep signal. The transmission times are 05:54:52 and 17:54:52 UTC. Clock recalibrations were set to 24:00:00 UTC with one day period. Also the receiver was programmed to listen two times a day for 150s. The

schedule is 05:59:10 and 17:59:10 UTC. The clock in the receiver is recalibrating at 17:00:00 UTC with a one day period.
Navigations of the sound source mooring were started to navigate at 01:40:00 and 02:10:00 UTC with a period of 2 hours. The navigations of the receiver were set to 05:45:00, 05:55:00, 06:05:00 and 06:15:00 UTC. The period here is 6 hours.

Sound source task

Start day = 426, Period0 = 1 days, Period1 = 1 days Number of tasks = 2
Task Hour Minutes Seconds
0 5 54 52
0 17 54 52

Receiver task

Navigation Task after 17:00 Calibr.

0424:12:20:00 StartTime
0424:16:00:00 StopTime
0000:00:10:00 Periodicity

600 Nav 40:10:00

Receiver Task, M2 Move Experiment

0424:17:30:00 StartTime
1154:17:30:00 StopTime
0000:12:00:00 Periodicity

900 Nav 4 0:15:00
1200 Par 0:20:00
1500 Nav 4 0:25:00
1750 Rx 0 0 18750 0:29:10 SS@ 0:24:56 (54:56)
2100 Nav 4 0:35:00
2400 Par 0:40:00
2700 Nav 4 0:45:00

M4 mooring navigator #I4 task
Start on day = 426 hour = 23 minute = 40
Measurement interval, minutes = 120 Scheduler is ARMED BUT NOT ACTIVE

M4 mooring navigator #I6 task
Start on day = 427 hour = 02 minute = 10
Measurement interval, minutes = 120 Scheduler is ARMED BUT NOT ACTIVE

DVS data (J. Karstensen)

Underway data was collected by a number of sensors and distributed via the DVS (Datenverteilungssystem). Data was recorded every ten seconds stored on hard disc and later a DVD was created from the data. A subset of all parameters - those often required for supporting analysis - was extracted from the original files and written into a MatLab *.mat structure 'dvs'. No interpolation in time was performed. The following variables are available:

% dvs.jul Julian Days [days]
% dvs.lat Latitude [decimal degrees]
% dvs.lon Longitude [decimal degrees]
% dvs.cog Course over Ground [degrees]
% dvs.sog Speed over Ground [m/s]
% dvs.dep Hydrosweep Depth [m]
% dvs.tws True Wind Speed [m/s]
% dvs.twd True Wind Direction [degrees]
% dvs.rws Relative Wind Speed [m/s]
% dvs.rwdRelative Wind Direction [degrees]
% dvs.ate Air Temperature [degrees C]
% dvs.humHumidity [%]
% dvs.apr Air Pressure [hPa]
% dvs.temTemperature [degrees C]
% dvs.sal Salinity

MEASURED VARIABLES

Overall there was no suspicious data. The Thermosalinograph (TSG) did not record data during some hours on the 22. February due to problems in restarting the device after a total power outage. The meteorological system was serviced from a representative of the DWD (Deutscher Wetterdienst) during the cruise and can be considered as high quality. TSG sample 1.5 m below surface and is a SBE21 device. The meteorological sensors are installed at the following height (all above NN): wind at 40.1 m, air pressure at 10.6 m, humidity 28.3 m, air temperature at 28.3 m, water temperature (PT100, other than TSG) at 2.1 m depth, radiation at 40.5 m. By analyzing TSG samples with the salinometer, M. Lankhorst determined a too high salinity of the TSG and proposed a correction:

$$\text{salinitytrue} = \text{salinityT SG,measured} - 0.08$$

The overall meteorological conditions during the cruise where not exceptional (Figure 4.23 to 4.22) and typical for the region with westward trade wind. Air and surface water temperature decreased towards the open Atlantic, while salinity increased. In particular at the eastern most position there was a drop in temperature and an increase in salinity with accompanying high surface water density. There was always a high pressure system with daily modulation. The radiation variables show the typical daily variations. Only a few daytime drops in short-wave radiation can be seen as a result of a few clouds.

DERIVED VARIABLES

Another set of variables was derived from the aforementioned: surface density, sensible and latent heat flux, wind stress. The heat fluxes are derived using the Fairall et al. (1996) parameterizations, the wind stress is based on the Smith (1988) algorithm. Surface density was high at the easternmost part of the section as very saline (and colder) water was found here. The sensible heat flux was always negative (ocean loses heat) as surface water was warmer than air temperature. Latent heat was high and typical for the evaporative trade wind region.

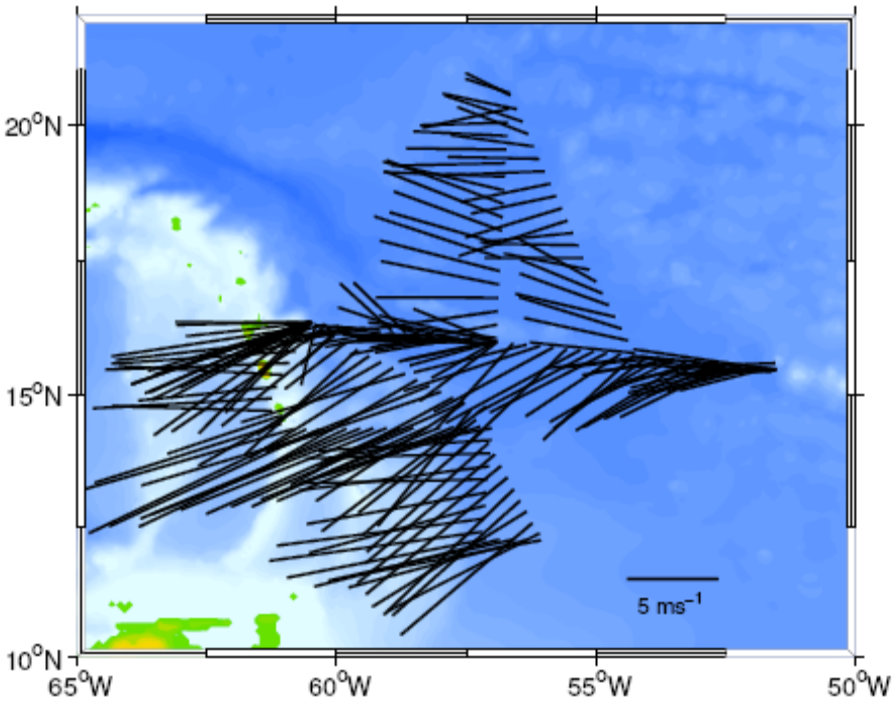

Fig. 4.22 Wind vectors during the M60/4 cruise.

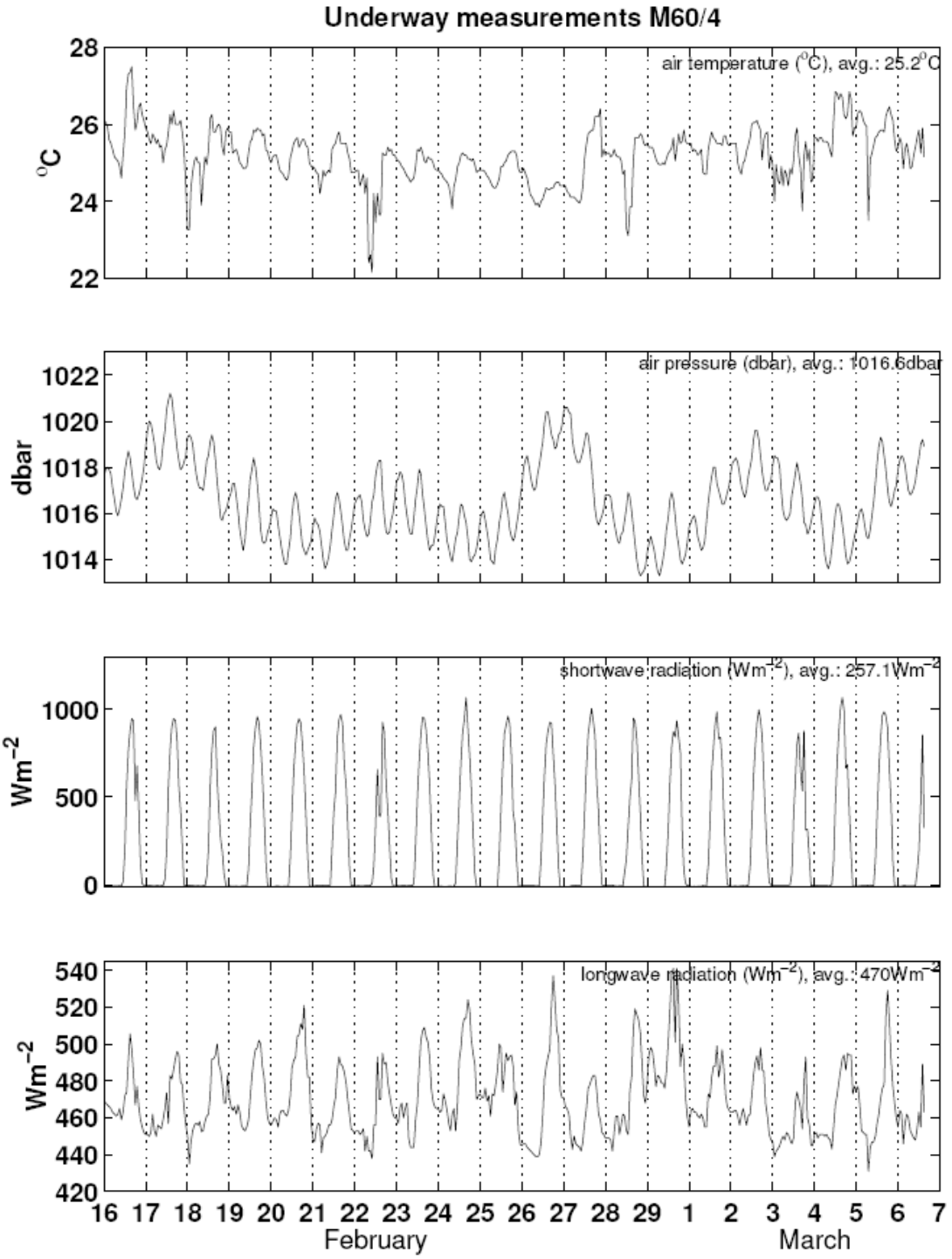

Fig. 4.23 Underway measurements collected via the DVS system and interpolated through full hour values. From top to bottom: Air temperature, air pressure, short-wave radiation, long-e radiation.

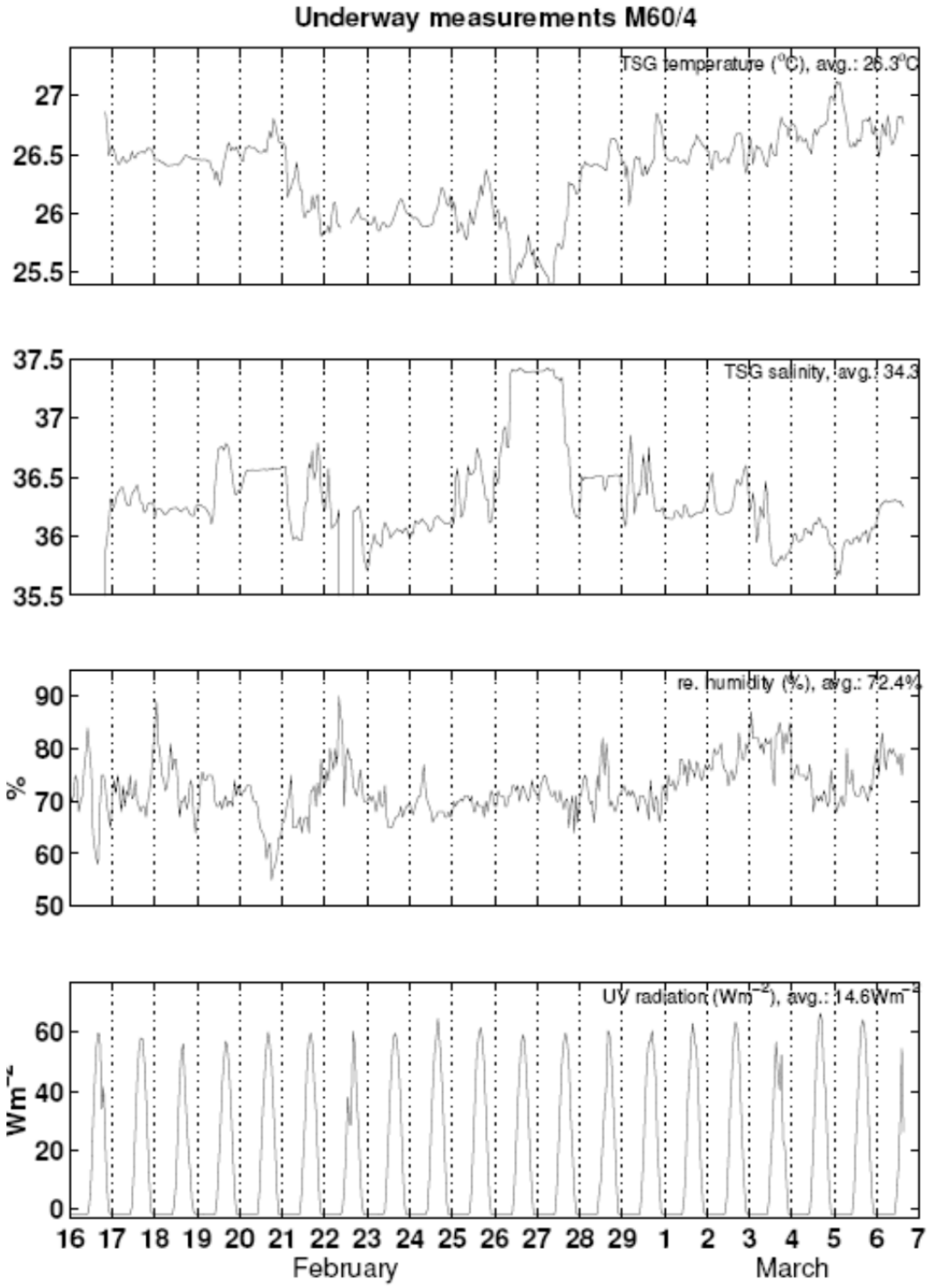

Fig. 4.24 Underway measurements collected via the DVS system and interpolated through full hour values. From top to bottom: TSG temperature, TSG salinity uncorrected), relative humidity, ultraviolet radiation.

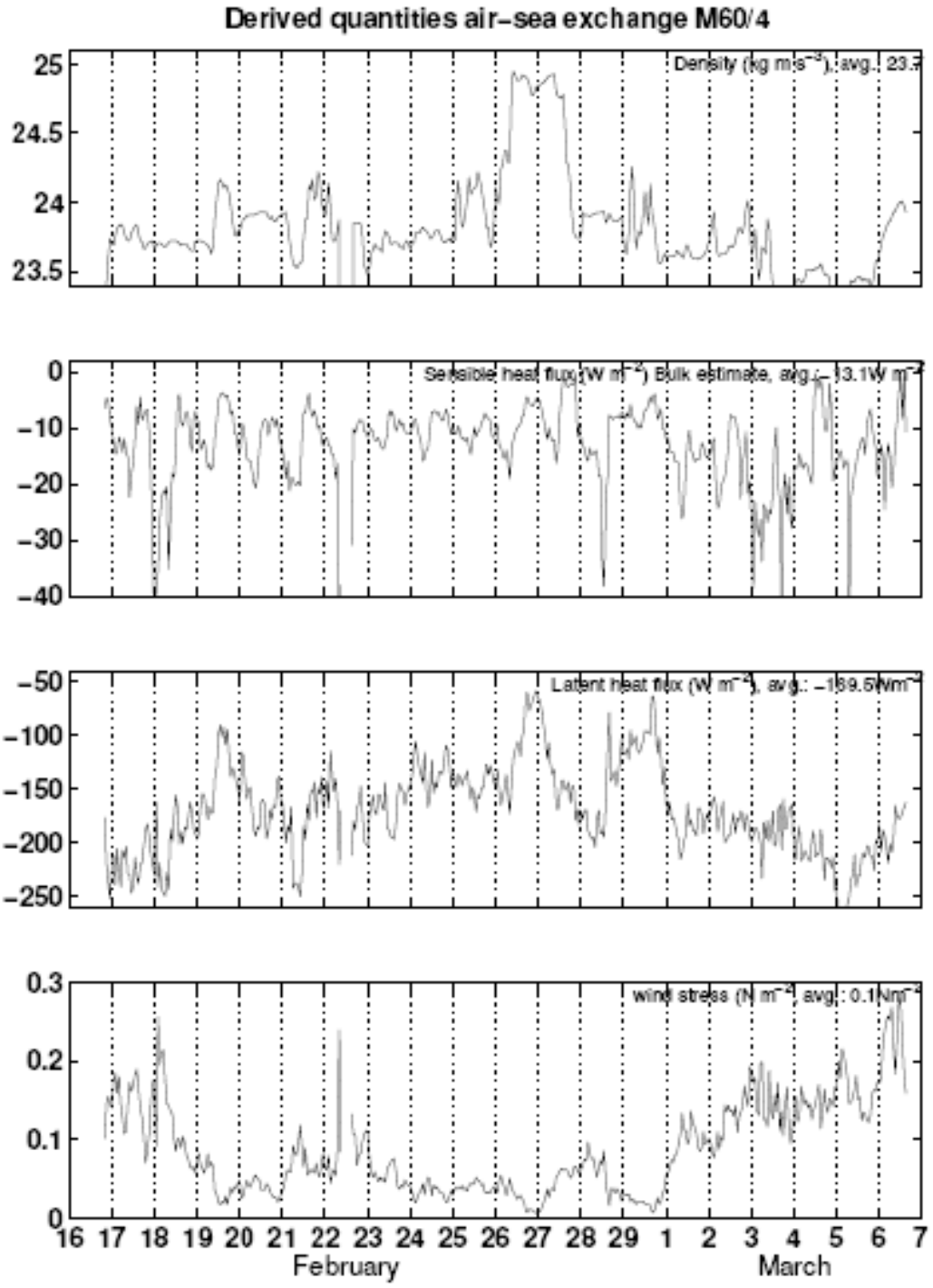

Fig. 4.25 Derived quantities from the DVS data - value for every full hour is shown. From top to bottom: water density (derived from TSG temperature and salinity), sensible heat flux, latent heat flux, wind stress

5. TABLE OF STATIONS

RV Meteor Station	Activity short	Date	Time (UTC)	Activity summary	Grad	Min	N/S	Grad	Min	E/W
M90	Deployment PIES	2/17/04	4:05	PIES # 165 deployed	16	21.38	N	60	29.25	W
M91	Recovery SIO 3	2/17/04	4:38	Recovery SIO #3 – failed	16	21.64	N	60	30.38	W
M92	Recovery M5	2/17/04	13:00	Mooring M 5 on deck	16	20.38	N	60	41.90	W
M93	Recovery M4	2/17/04	15:20	Mooring M 4 on deck	16	20.44	N	60	36.43	W
M94	Recovery TP 1	2/17/04	17:09	TP 1 on deck	16	19.16	N	60	34.14	W
M95	Recovery TP 2	2/17/04	18:29	TP 2 on deck	16	18.97	N	60	31.41	W
M96	Recovery TP 3	2/17/04	19:37	TP 3 on deck	16	21.58	N	60	32.76	W
M97	Recovery M 3.5	2/17/04	22:42	Releaser on deck, M3.5 recovered	16	21.66	N	60	33.07	W
M98	SIO 12	2/18/04	0:27	Recovery SIO #12 - failed	16	21.32	N	60	30.25	W
M99	CTD/lADCP	2/18/04	5:03	CTD/lADCP on deck	16	20.49	N	60	31.02	W
M100	SIO deployment	2/18/04	5:36	SIO in water	16	21.30	N	60	30.33	W
M101	Acoustic Test	2/18/04	6:03	acoustic communication with PIES 165	16	21.33	N	60	29.28	W
M102	Recovery PIES	2/18/04	13:00	Recovery PIES # 12	16	21.70	N	60	29.30	W
M103	Recovery M3	2/18/04	17:55	Mooring M 3 on deck	16	22.14	N	60	30.13	W
M104	Test releaser	2/18/04	20:00	Releaser in water	16	21.83	N	60	28.46	W
M105	Deployment M 3	2/19/04	3:04	anchor in water	16	20.19	N	60	32.31	W
M106	Deployment SIO	2/20/04	2:45	SIO in water	16	0.16	N	56	56.54	W
M107	CTD/lADCP	2/20/04	5:05	CTD/lADCP on deck	15	59.25	N	56	56.59	W
M108	Recovery PIES	2/20/04	8:42	Recovery PIES #2 - failed	16	0.13	N	56	56.18	W
M109	Recovery TP 1	2/20/04	14:25	TP 1 on deck	15	58.41	N	56	56.91	W
M110	Recovery TP 2	2/20/04	15:32	TP 2 on deck	15	58.30	N	56	54.15	W
M111	Recovery TP 3	2/20/04	16:57	TP 3 on deck	16	0.66	N	56	55.49	W
M112	Recovery M2	2/21/04	1:16	M2 recovered	15	58.62	N	56	55.42	W
M113	Deployment PIES	2/21/04	1:37	PIES # 123 deployed	15	59.18	N	56	56.58	W
M114	Acoustic PIES 1	2/22/04	8:00	Acoustic data retrieval PIES ser.#57	15	27.46	N	51	32.01	W
M115	CTD/lADCP	2/22/04	9:49	CTD/lADCP on deck	15	28.35	N	51	32.44	W
M116	Recovery M1	2/22/04	14:14	M 1 on deck	15	28.94	N	51	32.81	W

RV Meteor Station	Activity short	Date	Time (UTC)	Activity summary	Grad	Min	N/S	Grad	Min	E/W
M117	SIO 1 recovery	2/22/04	16:33	SIO 1 (ser.#3) on deck	15	28.11	N	51	31.22	W
M118	TOMO-Test	2/22/04	19:05	TOMO on deck	15	28.27	N	51	32.08	W
M119	CTD/lADCP	2/23/04	0:40	CTD/lADCP on deck	15	28.65	N	51	31.70	W
M120	Deployment SIO	2/23/04	1:48	SIO1(#3) in water	15	28.00	N	51	31.60	W
M121	CTD/lADCP	2/23/04	16:48	CTD/lADCP on deck	15	27.59	N	51	31.94	W
M122	Recovery PIES	2/23/04	19:00	PIES # 57 on deck	15	27.56	N	51	31.89	W
M123	Deployment PIES	2/23/04	19:35	PIES # 127 in water	15	26.99	N	51	31.59	W
M124	Test releaser	2/23/04	20:50	Releaser on deck	15	27.81	N	51	31.87	W
M125	CTD/lADCP	2/24/04	1:03	CTD/lADCP on deck	15	27.87	N	51	31.75	W
M126	CTD/lADCP	2/24/04	3:36	CTD/lADCP on deck	15	27.57	N	51	32.28	W
M127	CTD/lADCP	2/24/04	9:06	CTD/lADCP on deck	15	27.65	N	51	31.35	W
M128	Deployment M 1	2/24/04	20:06	anchor in water	15	27.00	N	51	30.97	W
M129	Deployment PIES	2/25/04	11:51	PIES 12 in water	15	43.10	N	54	13.50	W
M130	Deployment SIO	2/26/04	17:17	SIO serial # 10 in water	20	36.00	N	56	40.78	W
M131	Deployment PIES	2/26/04	17:36	PIES serial # 128 in water	20	35.50	N	56	40.79	W
M132	CTD/lADCP	2/26/04	23:53	CTD/lADCP on deck	20	35.35	N	56	40.00	W
M133	CTD/lADCP	2/27/04	3:45	CTD/lADCP on deck	20	35.24	N	56	40.15	W
M134	Tomo receiver	2/28/04	6:17	Test Tomo receiver	16	3.33	N	56	55.36	W
M135	Deployment TP	2/28/04	7:51	Transponder Xp3 in water	16	0.74	N	56	55.59	W
M136	Deployment TP	2/28/04	8:35	Transponder Xp2 in water	15	58.43	N	56	54.19	W
M137	Deployment TP	2/28/04	9:14	Transponder Xp3 in water	15	58.42	N	56	57.00	W
M138	PIES-Telemetry	2/28/04	9:35	Data retrieval from PIES via Telemetry	15	59.19	N	56	56.59	W
M139	range TP	2/28/04	10:55	Begin range 3 transponder	16	0.40	N	56	57.30	W
M140	Deployment M2 (405/5)	2/28/04	17:55	Anchor in water	15	59.05	N	56	54.93	W
M141	CTD/lADCP	2/28/04	22:48	CTD/lADCP on deck	15	59.25	N	56	56.42	W
M142	Recovery M 3.5	2/29/04	21:36	M 3.5 on deck	16	19.67	N	60	34.21	W
M143	CTD/lADCP	3/1/04	4:57	CTD/lADCP on deck	16	21.26	N	60	28.09	W

RV Meteor Station	Activity short	Date	Time (UTC)	Activity summary	Grad	Min	N/S	Grad	Min	E/W
M144	Deployment M 3	3/1/04	16:39	M3 anchor in water	16	20.62	N	60	29.91	W
M145	Recovery POL	3/1/04	20:30	POL on deck	16	21.20	N	60	30.57	W
M146	TOMO-Test	3/2/04	10:22	TOMO on deck , Hydrophone on deck	16	19.97	N	60	41.74	W
M147	Deployment M 4	3/2/04	15:00	M4 anchor in water	16	20.14	N	60	36.16	W
M148	Deployment Tr 3	3/2/04	15:59	Transponder Tr 3 in water	16	22.02	N	60	36.00	W
M149	Deployment Tr 2	3/2/04	16:34	Transponder Tr 2 in water	16	19.24	N	60	35.21	W
M150	Test Tomo M4	3/2/04	17:40	Test Tomo	16	19.68	N	60	35.97	W
M151	Test Tomo-Receiver	3/3/04	17:42	Tomo receiver test	14	50.61	N	57	33.63	W
M152	Deployment SIO	3/5/04	1:49	Deployment SIO # 2	12	15.56	N	57	11.96	W
M153	Deployment PIES	3/5/04	2:09	Deployment PIES # 54	12	15.03	N	57	12.04	W
M154	Deployment SIO	3/5/04	16:24	Deployment SIO # 7	14	23.39	N	56	59.40	W

6. REFERENCES

Visbeck, M., Deep velocity profiling using lowered acoustic Doppler current profilers: Bottom track and inverse solutions. Journal of Atmospheric and Oceanic Technology, 19(5): 794-807, 2002.

Kanzow, T., Monitoring the Integrated Deep Meridional Flow in the Tropical North Atlantic. Dissertation at the Christian-Albrechts-Universät Kiel, 2004.

Fairall, C. W., E. F. Bradley, D. P. Rogers, J. B. Edson, and G. S. Young, Bulk parameterization of air/sea fluxes for tropical ocean-global atmosphere coupled-ocean atmosphere response experiment, J. Geophys. Res., 101C, 3747-3764, 1996.

Smith S.D., Coefficients for sea surface wind stress, heat flux, and wind profiles as a function of wind speed and temperature, J. Geophys. Res., 93 (C12), 15467-15472, 1988.

METEOR-Berichte

Cruise No. 60, Leg 5

9 March - 15 April, 2004
Fort-de-France (Martinique) – Lisbon (Portugal)

D. Wallace, E. Achterberg, M. Moore, M. Mills, R. Langlois, T. Tanhua, B. Quack, G. Petrick, S. Walter, H. Lüger, J. Schafstall, C. Joppich, S. Grobe, C. Joppich

Chief Scientist:Douglas Wallace

Editorial Assistance:

Senatskommission für Ozeanographie der Deutschen Forschungsgemeinschaft
MARUM – Zentrum für Marine Umweltwissenschaften der Universität Bremen

Leitstelle Deutsche Forschungsschiffe
Institut für Meereskunde der Universität Hamburg

2011

Table of Contents; Leg 5

5.1 Participants M 60/5

Name	Task	Institution
Wallace, Douglas William Roy	chief scientist	IFM-GEOMAR
Achterberg, Eric	Trace metals, bioassays	SOC
Breitenbach, Uli	N2O	IFM-GEOMAR
Fischer, Tim	CFCs	IFM-GEOMAR
Freese, Elke	CFCs	ICBM
Grobe, Susann	CO2	IFM-GEOMAR
Fritsche, Peter	Biolofy, nutrients	IFM-GEOMAR
Lüger, Heike	CO2	IFM-GEOMAR
Nachtigall, Kerstin	Bioassays	IFM-GEOMAR
Ophey, Jannes	CO2	IFM-GEOMAR
Schimanski, Jens	CO2	IFM-GEOMAR
Schmidt, Kerstin	Biology, marine snow	IFM-GEOMAR
Schütt, Martina	CFCs	IFM-GEOMAR
Langlois, Rebecca	Bioassaya	IFM-GEOMAR
Schweiger, Bianca	N2O	IFM-GEOMAR
Malien, Frank	Nutrients	IFM-GEOMAR
Mills, Mat	bioassays	IFM-GEOMAR
Smarz, Christopher	CTD	IFM-GEOMAR
Tanhua, Toste	CFCs	IFM-GEOMAR
Petrick, Gert	Halocarbons	IFM-GEOMAR
Quack; Birgit	Halocarbons	IFM-GEOMAR
Tank, Marcus	Marine snow	IFM-GEOMAR
Milne, Angela	Trace metals, bioassays	SOC
Schafstall, Jens	CTD	IFM-GEOMAR
Moore, Mark	Bioassays	SOC
Walter, Sylvia	N2O	IFM-GEOMAR
Joppich, Christoph	Meteorology	DWD

Participating institutions

IFM-GEOMAR	Leibniz-Institut für Meereswissenschaften, IFM-GEOMAR, Düsternbrooker Weg 20, 24105 Kiel, Germany
SOC	Southampton Oceanography Centre, George Deacon Division for Ocean Processes, Waterfront Campus, European Way, Southampton SO14 3ZH, UK
ICBM	Institut für Chemie und Biologie des Meeres (ICBM), Carl von Ossietzky Universität Oldenburg Carl-von-Ossietzky.Str. 9-11, Postfach 2503, 26111 Oldenburg
DWD	Deutscher Wetterdienst, Postfach 301190, 20304 Hamburg, Germany

5.2 Research Programme

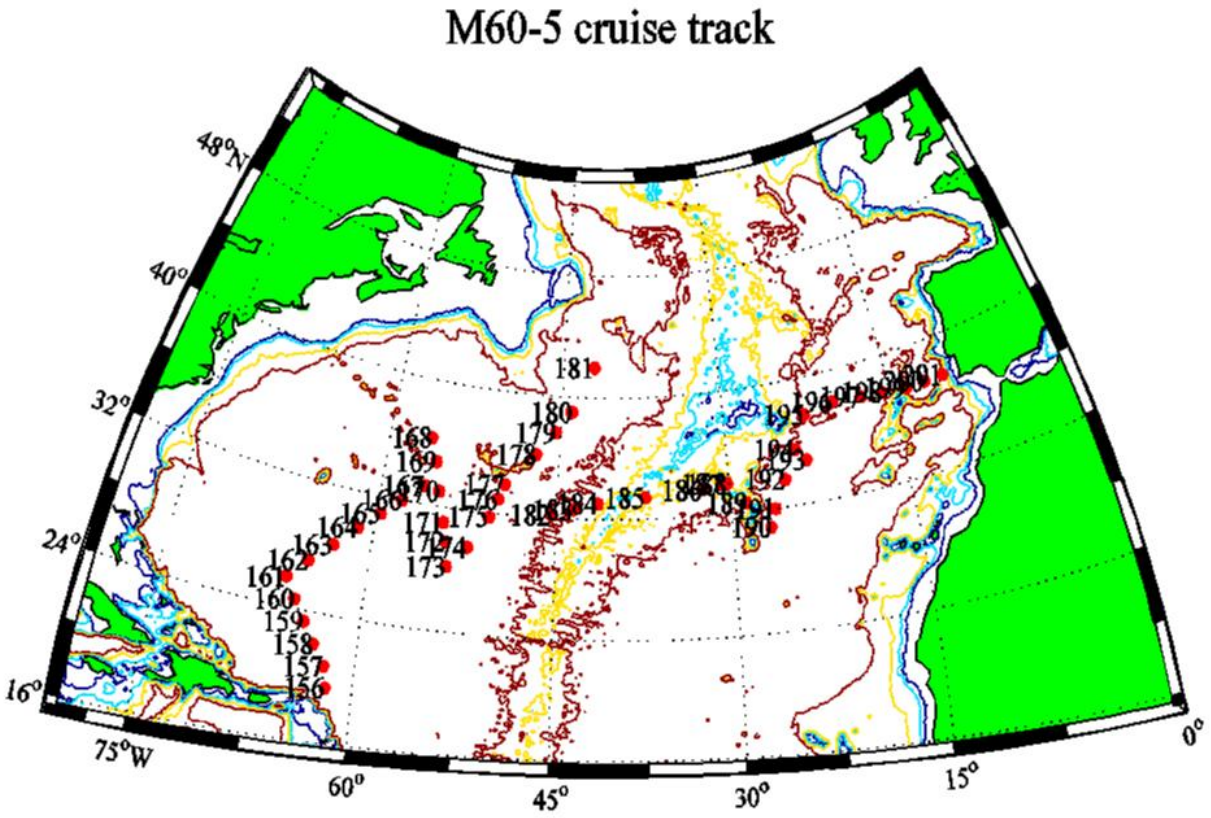

Figure 5.1: The cruise track of Meteor 60 Leg 5.

5.2.1 TTO Revisited and Water-Column Chemistry

The main theme of Meteor 60-5 was to resample a set of hydrographic stations that had been occupied in 1981 during the US-led Transient Tracers in the Ocean program (TTO). We therefore gave Meteor 60-5 the nickname: 'TTO Revisited'. The TTO expedition was itself, partly a reoccupation of the famous GEOSECS expedition of the early 1970's. Both GEOSECS and TTO were concerned with the penetration into the ocean of tracers derived from nuclear fallout: particularly tritium (^{3}H) and radiocarbon (^{14}C). The atmospheric weapons testing of the early 1960's had initiated a global-scale tracer-labeling experiment that was monitored by worldwide expeditions such as GEOSECS and TTO. These expeditions and the tracers measured, returned major new insights, as well as some new questions, concerning the circulation of the deep ocean.

By the time of TTO however, concern was already shifting away from the decaying problem of man-made radioactivity towards the growing problem of man-made CO_2. Hence the

TTO cruises included extensive measurements not only of fallout tracers but also of oceanic CO_2.

More than two decades on from TTO, there is still no generally accepted carbon equivalent of the Nuclear Test Ban Treaty, and the result is that the CO_2 problem continues to grow. Human beings continue to release more and more CO_2 into the atmosphere, with 30-50% of the amount released 'disappearing' into the ocean. The consequence of the ocean uptake is that ocean CO_2 levels are rising. The major goal of the Meteor 60-5 cruise was to collect data to document and quantify this increase of oceanic CO_2 over time. Comparison of our data with the high-quality data collected 23 years previously during TTO, gives us an unprecedented view into the magnitude of this change and its geographical distribution. This information in turn can be used to check and improve the models that try to predict how much CO_2 the ocean will take up in the future.

During Meteor 60-5, we travelled along the long path trod by the RV Knorr, 23 years previously. The result is a strange looking cruise track (Figure 1) that zigs and zags across the mid-latitude Atlantic in order to reoccupy as many TTO stations as possible. The Meteor 60-5 cruise, combined with a northern North Atlantic cruise of Meteor and two related US-led cruises conducted in 2003, provide an almost complete 'snapshot' of the North Atlantic for the period 2003-2004. This can be compared directly with how the Atlantic looked in 1981. In addition to the expected CO_2 increase, we were looking for changes in temperature, salinity, oxygen, nutrients and tracers such as the CFCs (Freons) using the high-quality TTO data as a baseline. Our comparison with data collected in 1981 required chemical measurements of extremely high accuracy. The atmospheric pCO_2 had increased by about 35-36 μatm since 1981: the time of the TTO expedition. This is an ~10% increase in the carbon content of the atmosphere but the equivalent increase in the surface ocean is 25 μmol/kg: just over 1% of the background seawater carbon content. Obviously detecting anthropogenic changes of 1% or less over 23 years requires extremely accurate measurements. And the problem doesn't stop with carbon: ocean carbon is subject to natural variability associated with photosynthesis and respiration. To correct for variable amounts of carbon respired in subsurface waters we use dissolved oxygen: these data have to be accurate to about 1-2 parts in 300. To interpret any changes in oxygen we needed the most accurate measurements of temperature and salinity, and so it goes on with the accuracy needs cascading down from one measurement to another.

The CO_2 measurements were made on board by a team of 5 IfM-GEOMAR analysts who worked shifts around the clock to keep up with the samples being collected (see Figure 2). Samples were also collected for shore-based analyses of ^{13}C at Kiel University's Leibniz Labor

für Altersbestimmung. These analyses can provide an independent estimate of anthropogenic CO_2, by detecting the progressive dilution of the heavier isotope of carbon by 'lighter' carbon released into the environment with the burning of fossil fuel.

To complement the CO_2 measurements, we had a significant transient tracer measurement program on board, including measurements of CFCs 11 and 12, CH_3CCl_3, CCl_4, and for the first time in this region, SF_6. All of these compounds are man-made and have, like CO_2, increased in the atmosphere and hence in the ocean over the past 40 (SF_6), 60 (CFC11 and 12), to 80 (CCl_4) years as a result of human emissions. Unlike CO_2, these compounds have no natural background. In addition to these 'tracer' gases, we measured a range of naturally-produced gases. These include the important greenhouse gas, N_2O, and a wide range of halocarbons including some 'exotic' brominated and iodinated compounds that play key roles for atmospheric chemistry.

5.2.2 Biological Program and Bioassay Experiments

Meteor 60-5 also had a biology program with two components: one small group from IFM-GEOMAR (Kiel) was catching particles and 'marine snow' with a custom large-volume water sampler ('Snow Catcher') deployed on a hydro-wire. There was also a larger 'Bioassay Group' comprised of scientists from IfM-GEOMAR, the University of Essex, the University of Plymouth and the Southampton Oceanography Centre. This group conducted on-board experiments to study nutrient limitation.

In some ways, Meteor 60-5 was two separate expeditions sharing the same vessel and cruise track. The program of physical and chemical measurements of the deep water column occupied the majority of the scientific staff on board. However the Bioassay group rarely went near the CTD/rosette system and their activity was almost completely out-of-phase with that of the rest of the scientific staff.

The Bioassay Group was seeking to determine the nutrient(s) (nitrogen, phosphorus, or iron) that limit the productivity and biomass of the phytoplankton, the fixation of nitrogen (N_2) by the microbial community, as well as the bacterial productivity. They conducted a series of on-board experiments involving manipulations of surface seawater pumped from a towed 'fish'. Each experiment consisted of filling approximately 150 1-liter bottles under trace-metal clean conditions in an on-board clean laboratory container. Nutrient forms of nitrogen, phosphorus, iron are then added to these bottles in all possible combinations. The bottles were incubated on-deck for 48 hours. Parameters such as phytoplankton productivity and chlorophyll, as well as nitrogen fixation, and bacterial productivity were measured both at the beginning and end of the

incubations in order to determine the effects of the different nutrient additions. Samples were also collected for molecular analysis of DNA and RNA in order to identify and quantify organisms responsible for nitrogen fiaxation.

The Bioassay Group also examined how dust derived from the African continent might affect these biological processes. Atmospheric transport of dust from the Saharan desert is well known to be an important source of iron. During Meteor 55 to the tropical Atlantic, similar bioassay experiments had suggested that additions of Saharan Dust might stimulate nitrogen fixation by relieving both phosphorus and iron limitation. Similar experiments were conducted during M60-5 to determine the amount of N, P and Fe released when dust is added to seawater.

5.3 Cruise Narrative

Week 1 (9.3.2004 - 14.3.2004)

Meteor 60 Leg 5 departed Fort-de-France (Martinique) at 1330 (local) on March 9. Unpacking and laboratory set up had continued right up until the time of departure, but we were at that point able to relax a little and enjoy the view as we sailed along the western coast of Martinique.

During the first week, we sampled 6 of the old TTO stations. Overall the data quality looks very good, with our nutrient and oxygen data falling exactly on top of the older data. We could already see evidence for a significant increase of CO_2 in the top 700-800m of the water column. After sampling at TTO station 22 (25° 47'N; 66°W) we made a right turn, and headed northeast towards a cluster of TTO stations located 750 nautical miles south of Newfoundland. As we travelled slowly north, we had warm and calm conditions.

Week 2 (15.3.2004 – 21.3.2004)

By the end of the second week we had made good progress and had occupied 17 stations. Eleven of these were re-occupations of stations occupied by the Transient Tracers in the Ocean expedition of 1981. Data collection had settled down to a more-or-less routine operation. The CTD/rosette operations were going well and Christopher Smarz managed to repair our fluorometer with some ingenious 'Bastelei'.

From a first look at our data from southern stations we saw a very clear signal of the post-1981 anthropogenic CO_2 increase down to depths of about 700m, or to seawater potential densities of about 1027. Further north there were indications of the signal being found in deeper and denser waters.

During the 2nd week, we benefitted from the route-planning assistance provided by the Bordwetterwarte of the Deutscher Wetterdienst. In particular, we were able to 'snatch' an extra, northern TTO station out of the jaws of two storm depressions thanks to insight into model predictions from our meteorologist.

Week 3 (22.3.2004 – 28.3.2004)

During the third week, we retraced an old TTO cruise track and the even older GEOSECS-Atlantic track as far as 42°N 42°W, 350 miles east of the Tail of the Grand Banks. Along the way we sampled at a US CLIVAR-Carbon station of WOCE line A20 (29°34'N

52°20'W) that was occupied by our US colleagues during 2003. The intention had been to resample this station as a cross-check on data intercomparability. Unfortunately at this station we encountered a major technical difficulty when signal transmission to/from the CTD was interrupted during two separate attempts at a deep cast. Both times the connection was lost at depths of about 5000m. Eventually we left the station with complete CTD downcast profiles available for comparison, but only 7 water samples. While limited in scope, comparison of these 7 deep water samples with their CLIVAR equivalents was encouraging, with the chemical properties such as nutrients, oxygen and carbon agreeing to within the desired tolerances.

In general, weather conditions were remarkably favourable, including sunny and warm conditions at our northernmost station. The region of the Atlantic covered by the cruise to this point had been filled with high pressure systems, both north of the Azores and SW of Newfoundland. Nevertheless, in the middle of the 3rd week we were located directly at the air mass boundary between the two Highs which gave us strong winds and swell and forced us to miss one planned station. The missed station was a shallow TTO station that had been occupied on top of a seamount with relatively few chemical measurements: our failure to 'collect' it, was therefore not too damaging to our program.

Photo: Part of the Bioassay Group ready for a long night in the Clean Lab. Container. From left to right: Mark Mills, Rebecca Langlois (IfM-GEOMAR), Angie Milne and Eric Achterberg (Plymouth Univ., UK).

By the end of the 3rd week, the Bioassay Group had already successfully completed four

experiments. The experiments benefitted from the wide range of conditions that we encountered on the cruise, ranging from oligotrophic surface waters of the tropics to pre-bloom, 400-m deep mixed layers of the northern Atlantic. Initial results showed that nitrogen additions stimulated phytoplankton productivity and chlorophyll concentrations, whereas a combination of nitrogen and phosphorus was required to stimulate bacterial productivity. This result runs counter to some earlier work suggesting a primary role for phosphorus in limiting productivity. Further conclusions have to await more detailed analysis of the results including analysis of stored samples in Kiel.

Week 4 (29.3.2004 – 4.4.2004)

The fourth week of Meteor 60-5 saw fewer stations being occupied in part due to a long transit southwards in order to resume our eastward transect along about 33°N. This planned gap was followed later by an enforced ~24-hour halt to stations due to strong winds and high seas. The transit time was used by the various chemical measurement groups on board to make adjustments to their systems, perform more extensive calibrations, and work up data. It also allowed our two CTD operators to take a much-needed break. Despite the bad weather, we managed to sample at, or close to, all planned TTO stations and so remained on schedule. By the end of the week, we had just completed a re-occupation of TTO station 49 at 33° 46'N 25° 8'W. Immediately after this we attempted a biological CTD and particle-catching station in about 280m of water on top of the nearby Atlantis Seamount (33 deg 59'N 30 deg 5 W). We found a good shallow location for the station and collected an interesting-looking fluorescence and oxygen profile with the CTD. Unfortunately difficult wind, current and wave conditions then forced us to cancel the particle catcher deployment.

We also took the opportunity of the long transit at the beginning of the week to hold our 'Bergfest'. This included the cultural highlight of the cruise with the awarding of prizes for the Meteor 60-5 photo contest. Twenty excellent entries had been submitted in the categories: 'Science', 'Life on Board', and 'Art: Hands or Feet'. Upon examination of the entries, the judges were forced to add an additional category: 'uncategorisable'. Later in the week, on April 1, the Chief Scientist was the victim of an extraordinarily elaborate hoax involving a lost CTD/rosette..

Week 5 (5.4.2004 – 11.4.2004)

The 5th week saw us following the footsteps of Larry Armi's TTO Leg 3 into the Canary Basin. The 'bioassay group' started another of their experiments at our southernmost point. Then we

made a northwards transect, to the east of the Azores, and started the final transect eastwards towards Lisbon along 37°N, following the path of TTO Leg 4 (Chief Scientists: Wally Broecker and Claes Rooth).

As we headed southeast into the Canary Basin, we gradually encountered progressively stronger influence of Salinity Maximum Water (SMW, sometimes known as the Subtropical Underwater). This water mass is formed convectively in the eastern Atlantic as a result of strong evaporation driven by dry winds leaving NW Africa. The salinity of this water mass has increased over the past several decades, perhaps reflecting large-scale changes in the hydrological cycle. However this water mass appears to be of significance not only for climate but also for biogeochemistry.

The same hot, dry winds that drive evaporation also deposit dust carried from the Sahara/Sahel onto the ocean surface. And our experimental and field results from Meteor 55 had strongly supported the hypothesis that dust addition can stimulate nitrogen fixation. During the first week of our cruise we had already sampled SMW as a subsurface layer off the Caribbean Islands, where it was marked by high levels of nitrate relative to phosphate. This 'excess nitrate' signal has been attributed to high rates of oceanic nitrogen fixation in the source regions of this water mass. Our transit towards the SMW formation region provided a perfect opportunity for our biologists to start their 7th nutrient limitation bioassay experiment. Interestingly, along the transit, the on-board iron measurements revealed increased levels of Fe (II), perhaps a signal of increased dust deposition. We collected DNA samples in the region for characterization of nifH genes coding for the nitrogenase enzyme. This will help us to determine the type of organisms responsible for any enhanced nitrogen fixation measured there.

This part of the cruise was marked by flat calm conditions, sun and warm temperatures and was very, very pleasant.

The southernmost point on this part of the cruise was reached on the 6th of April at 30° 49'N 26° 44'W. We then returned along a line of TTO stations, in a northeasterly direction, towards the Azores. Upon approaching the Azores it was decided to make a detour to Ponta Delgada to offload a sick crewmember. Thanks to thorough preparations by Captain Jakobi and the other Officers, the entire operation consumed the absolute minimum of time. Only one station was cancelled and this, fortunately, was not a TTO station.

During this week, we were able to celebrate Easter Sunday in a relaxed manner, with an excellent lunch. Life on board Meteor had settled into a routine and we had been well cared for

Photo: Warm. sunny skies and calm seas in the Canary Basin.

by the crew. But as the cruise drew to an end, we were increasingly thinking about the end of the voyage and looking forward to returning home.

Week 6 (12.4.2004 – 17.4.2004)

The final days of the cruise saw us occupy 4 more TTO stations. After that, the last analyses were completed and then we moved closer to the coast in order dismantle equipment

Photo: Gas-chromatograph/Mass spectrometer system in the GeoLabor.

and pack before arriving in Lisbon on Thursday morning (15.4.2004). In Lisbon, the ship was unloaded on the Friday and most cruise participants departed for home. The Chief Scientist and crew remained aboard, and hosted a reception, lunch and information exchange for the German Ambassador, embassy staff, Portuguese foreign affairs specialists and scientists on the Saturday (17.4.2004).

5.4 Preliminary Results.

5.4.1 Overview of water-column programme

The circulation tracers that we were measuring include the chlorofluorocarbons 11 and 12 (CCl_3F and CCl_2F_2), together with CCl_4 and SF_6. CFC-11 and CFC-12 have been measured worldwide since the 1980's. We re-sampled some stations where the very first North Atlantic measurements of these compounds were made, during TTO, in 1981. Not surprisingly, our data revealed a large increase in the concentrations of these compounds, at all depths, since that time. Much less commonly measured are CCl_4 and SF_6. Both compounds are also exclusively man-made, but have very different time-histories of input to the oceans compared to the CFCs. CCl_4 has been used widely as a solvent since the early 1900's, and has had significant environmental concentrations since the late 1920's. SF_6 in contrast has increased rapidly in the environment since the 1960's. Taken together, the suite of compounds covers input timescales of <80 years (CCl_4), <60 years (CFCs 11 and 12) and <40 years (SF_6). The distributions of the tracers that we measured in the western basin reveal the impact of ventilation of the interior ocean over these three distinct timescales.

In the deep waters of the western basin we saw some striking variations in the relative distributions of CFC11 and CCl_4. On some density horizons we have found relatively high levels of CCl_4 in the near-absence of CFC11. This signaled tracer associated with a water mass component that was ventilated at a time when CCl_4 was already present in surface waters but CFC levels were still low. At other density surfaces and locations we have found similar levels of CCl_4 associated with much higher CFC11 levels. This water therefore represents a component that was ventilated when both CCl_4 and F11 were present in surface waters. Only in the upper 1000-2000m and in North Atlantic-derived deep water masses along the boundaries did we find evidence of a 'young' component containing detectable SF_6. The 'senior' water contains no detectable SF_6. The deep water distribution of SF_6 shows some strong similarities with the distribution of CFC11 as it was at the time of TTO. One of our goals was to employ this diverse tracer information to help us interpret the patterns of increase of CO_2 that we measured through our comparison with TTO data.

We also measured a variety of biogenic gases ranging from the important greenhouse gas, N_2O, through to a variety of naturally produced halocarbons. The relation to dissolved oxygen dominated the sub-surface N_2O distribution. The Meteor 60-5 data can be compared to data from earlier zonal sections collected by the IFM-GEOMAR group at 42°N and along 10°N over the

past 3 years. A strong correlation with O_2 is present in all the data sets, but the regression slope and intercept varies with latitude and between the western and eastern basins for reasons that are not yet clear.

On a separate gas chromatograph, we measured the concentrations of a range of compounds including bromoform ($CHBr_3$), chloroform ($CHCl_3$), dichloromethane, dibromomethane, and methyl iodide. These compounds play potentially significant roles in atmospheric chemistry. We measured their distributions in vertical profiles, surface water and air. The vertical profiles, in particular, were quite different between western and eastern Atlantic basins and these differences likely contain clues to the underlying oceanic production and consumption processes. Of particular interest was the behavior and sea-to-air flux of $CHCl_3$: an important trace gas that definitely has oceanic sources but about which very little is known.

5.4.2 Papers that have resulted directly from water-column programme:

Tanhua, T, Wallace, DWR, Consistency of TTO-NAS inorganic carbon data with modern measurements, GEOPHYSICAL RESEARCH LETTERS, 2005, 32, L14618.

Tanhua, T, Biastoch, A, Kortzinger, A, Luger, H, Boning, C, Wallace, DWR, Changes of anthropogenic CO2 and CFCs in the North Atlantic between 1981 and 2004, GLOBAL BIOGEOCHEMICAL CYCLES, 2006, 20, GB4017.

Tanhua, T, Kortzinger, A, Friis, K, Waugh, DW, Wallace, DWR, An estimate of anthropogenic CO2 inventory from decadal changes in oceanic carbon content, PROCEEDINGS OF THE NATIONAL ACADEMY OF SCIENCES OF THE UNITED STATES OF AMERICA, 2007, 104, 3037-3042.

Tanhua, T, Waugh, DW, Wallace, DWR, Use of SF6 to estimate anthropogenic CO2 in the upper ocean, JGR-Oceans, In Press, 2008.

Walter, S, Bange, HW, Breitenbach, U, Wallace, DWR, Nitrous oxide in the North Atlantic Ocean, BIOGEOSCIENCES, 2006, 607-619

5.4.3 Overview of Bioassay Experiments

Initial results from the Bioassay group showed that at the five oligotrophic sites primary production and chlorophyll a production was nitrogen limited (Figure 2). Once nitrogen limitation was relieved CO_2 fixation rates and chlorophyll a concentrations increased further with the addition of phosphate. Likewise the bacterial productivity was stimulated by the combined addition of nitrogen and phosphorus. Further additons of Fe did not generally enhance primary production, chlorophyll a concentrations, or bacterial production. The addition of glucose did not stimulate bacterial production on its own, but increased productivity approximately 100x when added to the combined N and P treatments.

In all experiments where surface nutrient concentrations were undetectable the addition of Saharan dust stimulated primary production, chlorophyll a biomass, and bacterial productivity.

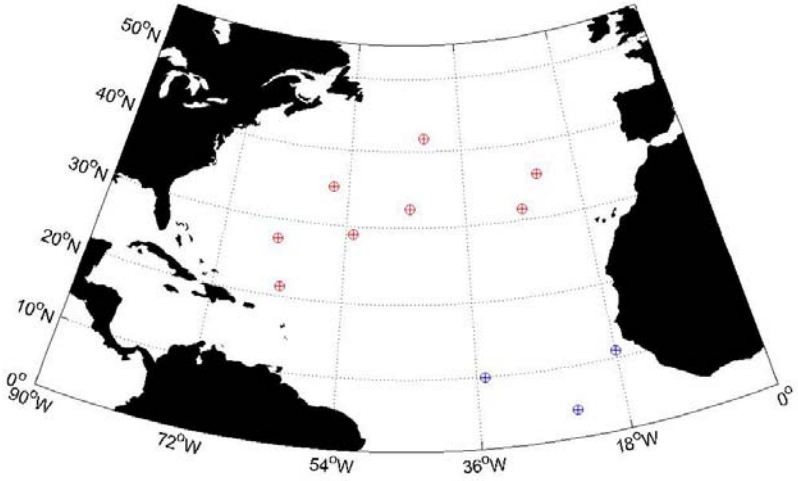

Figure 5.2. Map showing sites of M60/5 (red) and M55 (blue) bioassay experiments.

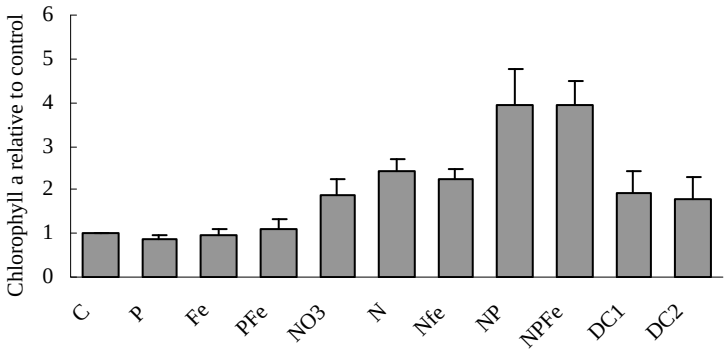

Figure 5.3. Mean chlorophyll a response in at the five sites with undetectable levels of nutrients in the surface waters (oligotrophic). Responses are relative to control.

Considerable work had to be carried out after the cruise. Samples for the nitrogen fixation rates were analyzed in Kiel, together with the DNA/RNA samples. Additionally, flow cytometry samples collected for cell abundance and diversity, and low level phosphate measurements, were measured after the cruise,

5.4.4 Papers that have resulted directly from bioassay programme:

Moore, CM, Mills, MM, Milne, A, Langlois, R, Achterberg, EP, Lochte, K, Geider, RJ, LaRoche, J, Iron limits primary productivity during spring bloom development in the central North Atlantic, GLOBAL CHANGE BIOLOGY, 2006, 12, 626-634.

Moore, C. Mark, Matthew M. Mills, Rebecca Langlois, Angela Milne, Eric P. Achterberg, Julie La Roche, and Richard J. Geider, Relative influence of nitrogen and phosphorous availability on phytoplankton physiology and productivity in the oligotrophic sub-tropical North Atlantic Ocean Limnology and Oceanography 53(1) In press

Mills, M. M., C. M. Moore, R. Langlois, A. Milne, E. Achterberg, K. Nachtigall, K. Lochte, R. J. Geider, and J. La Roche, Nitrogen and phosphorus co-limitation of bacterial productivity and growth in the oligotrophic subtropical North Atlantic In Press 2008 Limnology and Oceanography vol 53(2)

Rebecca J. Langlois, Diana Hümmer, and Julie LaRoche, Abundances and Distributions of the Dominant /nifH/ Phylotypes in the Northern Atlantic Ocean, Appl. Envir. Microbiol. 2008 : AEM.01720-07v1 In press

5.4.5 CTD Measurements during Meteor Cruise 60/5

(Jens Schafstall)

Introduction

During the 47 stations of Meteor cruise 60/5 a total of 75 CTD casts were carried out. On every station one CTD cast went to the bottom, additionally on most of the stations another cast went to approximately 400 m because in order to collect additional water samples. Salinity reported by the CTD was calibrated using water sampled with the rosette and analysed with a laboratory salinometer.

Description of the System

The CTD system used was a SeaBird Electronics, model 911 plus type, referred to as "IfM-Geomar serial number 1". A backup system was available but not used except at the last station, when this system was tested by a cast down to 1000 m in preparation for the following cruise. The underwater unit was built into a rosette housing capable of holding 24 water sampler bottles (carousel). Table 5.1 lists sensor models and serial numbers. Additionally a Dr Haardt fluorometer was installed on the rosette.

Instrument Type	SBE 11 plus	Serial No.
CTD deck unit	SBE 9plus	
CTD underwater unit	SBE 32	09P22348-0572
Rosette water sampler	SBE 3plus	3222348-0291
Temperature sensor	4c	03P2920
Conductivity sensor	SBE	042443
Oxygen sensor	SBE 43	430214
Pump	SBE 5T	052603
Pinger	Benthos	
Bottom alarm	mechanic switch	

Table 5.1: Setup of the CTD system during Meteor cruise 60/5

Calibration applied to the Data

Pre-cruise laboratory calibrations of the temperature and pressure sensors were available (see below). Both of these yielded coefficients for a linear fit. Salinity was calibrated with a Guildline Autosal 8 salinometer. For this purpose the detected error in conductivity was fitted in a least square sense to the conductivity data itself, pressure and time.

The following pressure correction (in dbar, laboratory calibration from February 2003) was applied:

Coefficients for static correction at temperature T0
PRES(T0) = PCTD(T0) + Pol(PCTD(T0))

Polynomial degree is M=1
Number of data pairs is N=13
Coefficients, starting at lowest order:
co(0)=-1.483240
co(1)=-7.943060*10^{-4}

The following temperature correction (in °C, laboratory calibration from November 2003) was applied:

Coefficients for correction, TEMP=TCTD+Pol(TCTD)

Polynomial degree is M=1
Number of data pairs is N=16
Coefficients, starting at lowest order:
co(0)=-4.044333*10^{-3}
co(1)= 1.621552*10^{-5}

Reversing thermometers were mounted on some water samplers. Only at the beginning of the cruise four thermometers –two attached to the same sampler, the other two attached to one sampler each- were in use, most of the time only three thermometers were working.
The recorded temperatures of these relatively inaccurate thermometers have not been used for calibrating the temperature sensor. Their purpose was to obtain an easy way of checking reliability of the trip unit by comparing the CTD data from the bottle files with the recorded temperature from the reverse thermometers. The reverse thermometers were found to be inaccurate but with a more or less constant offset so that the data could be used as control for the stability of the CTD temperature measurements.

The following conductivity calibration (in mS/cm) was applied using Matlab:

Cond = cond_raw + offset + coeff_c * c + …
coeff_p * p + coeff_t * time
with c in mS/cm, p in dbar and time in days since 1.1.2004.

Because of an abnormal behaviour of the system (see Figure 5.4a) it was necessary to use different sets of coefficients during the cruise. For the first part of the cruise the system was quite stable and almost no time-dependent correction was necessary.

The coefficients used for stations 155 to 169 were:

coeff_c = $6.1022720*10^{-4}$;
coeff_p = $-3.4853108*10^{-7}$;
coeff_t = $-3.1840056*10^{-5}$;
with offset = $-6.78145512*10^{-5}$;

This is almost the same calibration, which had been used on the previous leg Meteor 60/4 for the same system. After station 169 the differences showed a small jump to slightly larger deviations, calculated coefficients were:

coeff_c = $6.9158705*10^{-4}$;
coeff_p = $-2.1797090*10^{-7}$;
coeff_t = $4.9920107*10^{-5}$;
with offset = $-1.12269353*10^{-2}$.

After station 174 the behaviour of the conductivity sensor changed dramatically. Hence some more sets of calibration coefficients with a stronger time dependency were required.

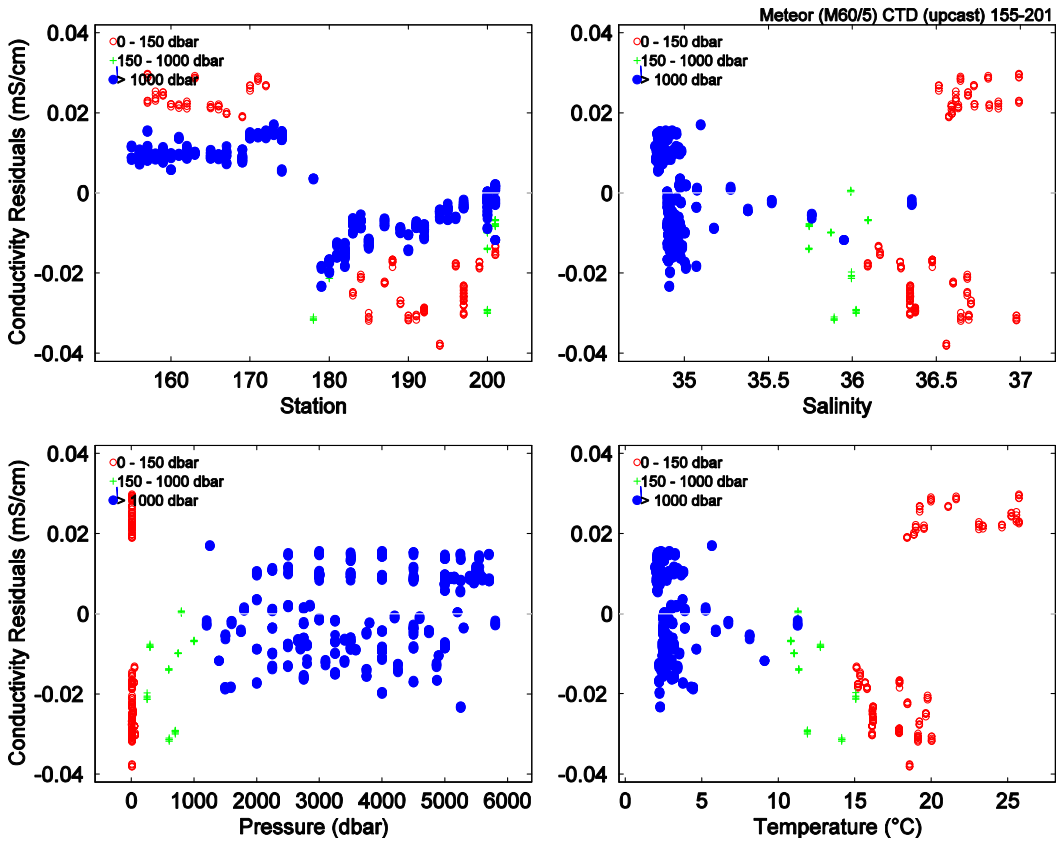

Figure 5.4: Differences between salinometer and uncalibrated CTD conductivities against station number, salinity, pressure and temperature.

Set of coefficients for station 175 to 181:

coeff_c = $-3.0616773*10^{-4}$;
coeff_p = $-5.0747001*10^{-7}$;
coeff_t = $7.3652944*10^{-3}$;
with offset = $-6.4198981*10^{-1}$.

Set of coefficients for station 182 to 184:

coeff_c = $-5.6146121*10^{-4}$;
coeff_p = $1.97613661*10^{-6}$;
coeff_t = $7.84050869*10^{-3}$;
with offset = $-7.086107562*10^{-1}$.

Set of coefficients for station 185 to 188:

coeff_c = $-7.6423786*10^{-4}$;
coeff_p = $1.57034394*10^{-6}$;
coeff_t = $3.52198331*10^{-3}$;
with offset = $-3.1628436*10^{-1}$.

Set of coefficients for station 189 to 201:

coeff_c = $-1.41473306*10^{-3}$;
coeff_p = $8.586466*10^{-8}$;
coeff_t = $1.22237985*10^{-3}$;
with offset = $-8.04018488*10^{-2}$.

Figure 5.5a is a Theta-S diagram for the deep CTD bottle data form Stations 189 to 201. Further the Saunders Theta-S relation is drawn. This curve characterises the Theta-S relation in the east Atlantic north of 25°N. The red circles assign the data without conductivity calibration and the blue ones the recalibrated values. It is easy to see, that despite the problems with the conductivity sensor the recalibrations worked reasonably well. Figure 5.5b shows the analog plot for the salinity values measured by a salinometer.

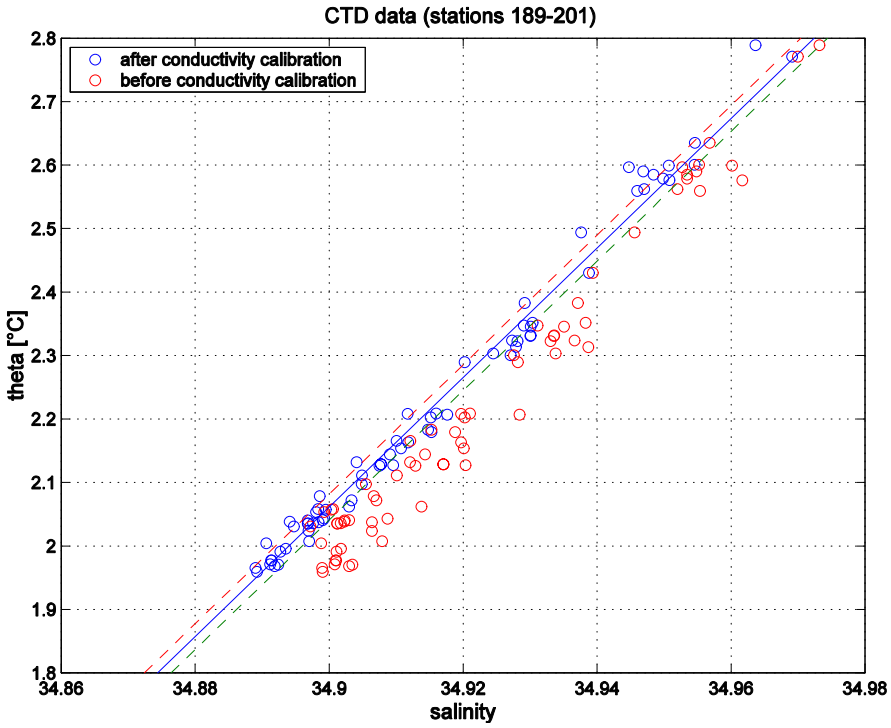

Figure 5.5a: Theta-S diagram for the last part of the cruise (station 189 to 201). Red circles mark uncalibrated salinity values and the blue ones the salinity after conductivity recalibration. The blue line describes the Saunders Theta-S relation with error margins of ± 0.002 psu (red and green)

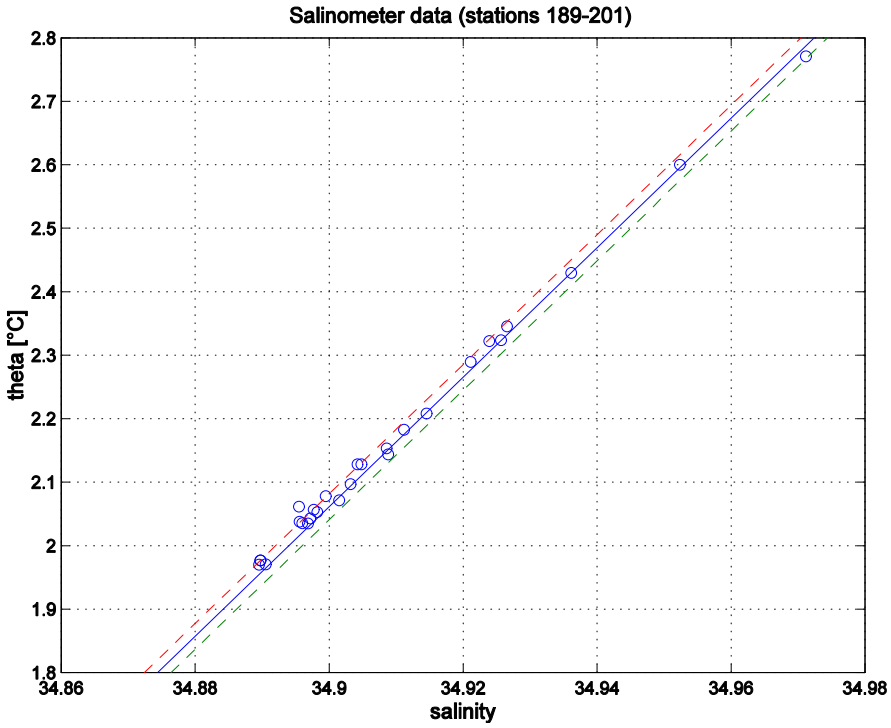

Figure 5.5b: Same as figure 5.5a, but for salinity measured by a salinometer.

Performance and Station Overview

Apart from these conductivity sensor problems, the overall impression of the CTD performance was positive. There were no spikes in the data, but twice the recording computer had problems with data acquisition, likely due to unauthorized network access. Besides this, the connection with the underwater unit was cut off for a total of three times. Once due to a short cut in the sea cable and two times because of some problems with the drag along rings.
The trip unit worked well: during the whole cruise only four times a misfire had been noticed.
Table 2 summarizes the manually written log sheet for the individual CTD cast and figure 3 shows the cruise track with markers at the locations of all stations.

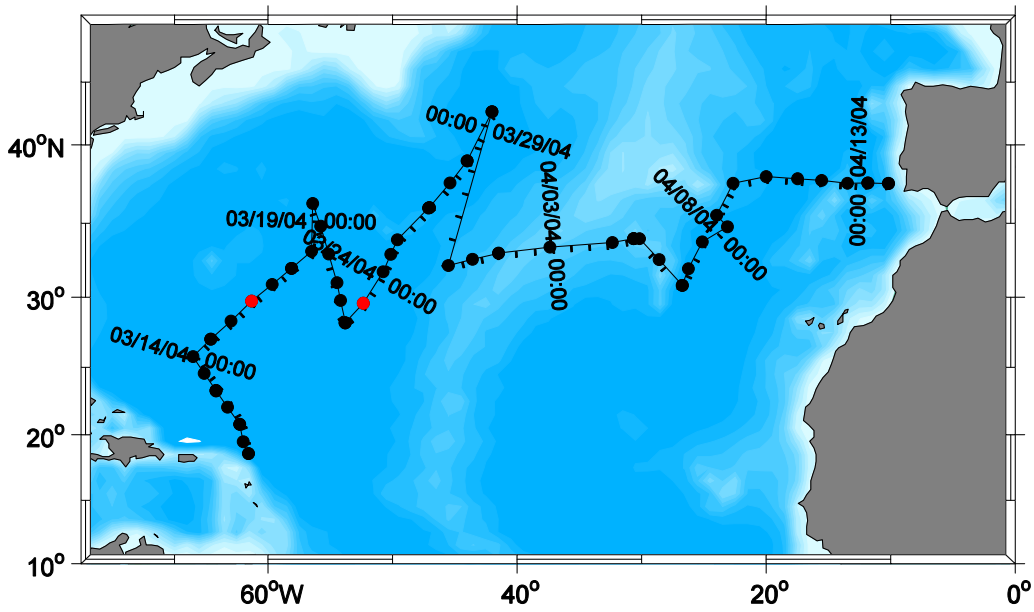

Figure 5.6: Cruise track and position of stations, points marked red are stations where problems with the CTD appeared

Table 5.2: CTD casts during Meteor 60/5

Station No.	CTD Profile No.	Date Start UTC	Time Start UTC	Latitude Degrees Start	Latitude Minutes Start	Longitude Degrees Start	Longitude Minutes Start
155	1	3/10/2004	18:15	18° N	34.1'	61° W	33.6'
155	2	3/10/2004	19:15	18 °N	34.1'	61 °W	33.1'
156	3	3/11/2004	2:39	19 °N	29.1'	61 °W	58.1'
157	4	3/11/2004	14:26	20 °N	47.4'	62 °W	16.0'
157	5	3/11/2004	16:10	20 °N	47.9'	62 °W	15.6'
158	6	3/12/2004	5:07	22 °N	3.8'	63 °W	13.9'
158	7	3/12/2004	5:55	22 °N	3.8'	63 °W	13.8'
159	8	3/12/2004	17:55	23 °N	17.7'	64 °W	9.6'
159	9	3/12/2004	19:20	23 °N	18.1'	64 °W	10.3'
160	10	3/13/2004	8:41	24 °N	33.7'	65 °W	6.2'
161	11	3/13/2004	21:40	25 °N	47.0'	66 °W	0.0'
161	12	3/13/2004	23:14	25 °N	47.3'	65 °W	59.9'

162	13	3/14/2004	14:29	27 °N	2.0'	64 °W	34.2'
162	14	3/14/2004	15:50	27 °N	2.4'	64 °W	34.7'
163	15	3/15/2004	8:05	28 °N	20.0'	62 °W	58.0'
164	16	3/16/2004	0:38	29 °N	43.0'	61 °W	18.0'
164	17	3/16/2004	1:58	29 °N	43.1'	61 °W	18.0'
164	18	3/16/2004	6:56	29 °N	43.1'	61 °W	18.2'
165	19	3/16/2004	21:39	30 °N	52.5'	59 °W	40.0'
165	20	3/17/2004	0:03	30 °N	52.3'	59 °W	39.9'
166	21	3/17/2004	14:10	31 °N	59.4'	58 °W	5.2'
166	22	3/17/2004	15:18	31 °N	59.2'	58 °W	6.1'
167	23	3/18/2004	5:43	33 °N	8.2'	56 °W	29.6'
167	24	3/18/2004	7:57	33 °N	8.1'	56 °W	29.4'
168	25	3/19/2004	8:35	36 °N	17.2'	56 °W	24.1'
168	26	3/19/2004	10:05	36 °N	17.2'	56 °W	24.1'
169	27	3/20/2004	1:10	34 °N	48.2'	55 °W	45.4'
170	28	3/20/2004	17:06	32 °N	56.9'	55 °W	6.3'
171	29	3/21/2004	8:50	31 °N	0.0'	54 °W	27.0'
172	30	3/21/2004	20:40	29 °N	46.0'	54 °W	9.0'
173	31	3/22/2004	10:50	28 °N	12.6'	53 °W	46.7'
173	32	3/22/2004	12:48	28 °N	12.2'	53 °W	48.6'
174	34	3/23/2004	5:12	29° N	34.0'	52° W	20.1'
175	35	3/24/2004	4:06	31° N	44.8'	50° W	45.1'
175	36	3/24/2004	5:45	31 °N	44.7'	50 °W	45.1'
176	37	3/24/2004	16:24	32 °N	56.0'	50 °W	7.9'
177	38	3/25/2004	2:09	33 °N	55.1'	49 °W	35.3'
178	39	3/26/2004	8:39	35 °N	59.5'	47 °W	6.0'
178	40	3/26/2004	10:31	36 °N	1.8'	47 °W	2.3'
179	41	3/27/2004	2:22	37° N	37.2'	45° W	22.6'
180	42	3/27/2004	16:34	38° N	59.7'	44° W	0.0'
180	43	3/27/2004	18:13	39 °N	0.0'	44 °W	0.0'
181	44	3/28/2004	14:58	42 °N	0.0'	41 °W	59.9'
181	45	3/28/2004	16:38	41 °N	59.7'	41 °W	59.7'
182	46	3/31/2004	12:08	32 °N	10.3'	45 °W	29.9'
182	47	3/31/2004	13:28	32 °N	10.7'	45 °W	30.4'
183	48	4/1/2004	2:31	32 °N	36.2'	43 °W	34.4'
184	49	4/1/2004	15:55	33° N	0.4'	41° W	29.3'
184	50	4/1/2004	17:42	33 °N	0.9'	41 °W	29.1'
185	51	4/2/2004	21:04	33 °N	24.9'	37 °W	21.3'
186	52	4/4/2004	7:47	33 °N	42.7'	32 °W	20.2'
187	53	4/4/2004	18:51	33° N	59.0'	30° W	37.5'
187	54	4/4/2004	18:51	33° N	59.0'	30° W	37.5'
188	55	4/5/2004	2:26	33 °N	58.6'	30 °W	10.4'
189	56	4/5/2004	14:35	32° N	35.1'	28° W	35.0'
189	57	4/5/2004	16:13	32 °N	34.8'	28 °W	35.1'
190	58	4/6/2004	9:00	30 °N	48.7'	26 °W	43.8'
190	59	4/6/2004	10:26	30 °N	48.9'	26 °W	44.5'
191	60	4/6/2004	21:19	31 °N	57.4'	26 °W	14.0'
192	61	4/7/2004	12:58	33° N	46.1'	25° W	7.9'
192	62	4/7/2004	14:27	33 °N	46.0'	25 °W	7.7'
193	63	4/8/2004	5:16	34 °N	46.0'	23 °W	6.0'
194	64	4/8/2004	15:10	35 °N	31.5'	23 °W	58.9'
194	65	4/8/2004	16:47	35 °N	31.7'	23 °W	58.9'
195	66	4/10/2004	2:14	37 °N	35.1'	22 °W	39.4'
196	67	4/10/2004	20:15	38 °N	0.0'	20 °W	0.1'
197	68	4/11/2004	12:45	37 °N	52.2'	17 °W	28.2'
197	69	4/11/2004	14:22	37 °N	52.3'	17 °W	28.2'
198	70	4/12/2004	3:12	37 °N	45.6'	15 °W	33.4'
199	71	4/12/2004	16:34	37 °N	35.3'	13 °W	28.6'
199	72	4/12/2004	18:09	37 °N	35.3'	13 °W	28.7'
200	73	4/13/2004	5:49	37 °N	36.5'	11 °W	49.6'
200	74	4/13/2004	7:10	37 °N	36.5'	11 °W	49.6'
201	75	4/13/2004	19:32	37 °N	34.6'	10 °W	10.3'

5.4.6 CO_2-Measurements

(Heike Lüger, Susann Grobe, Jens Schimanski, Bianca Schweiger, Jannes Ophey)

Measurements and sampling

Two analytical strategies were applied on this cruise for the determination of CO2 in seawater: discrete and continuous measurements. The discrete samples were taken from the CTD and focussed on the water column whereas the continuous measurements surveyed the surface ocean only. *Results are reported in a series of papers including: Tanhua, T. and Wallace, D.W.R., 2005. Consistency of TTO-NAS Inorganic Carbon Data with modern measurements. Geophysical Research Letters, 32, L14618, doi:10.1029/2005GL032348 and T. Tanhua, A. Körtzinger,, K. Friis, D. W. Waugh, and D.W.R. Wallace, 2007, Direct observation of anthropogenic carbon content in the North Atlantic Ocean., Proc. Natl. Acad. Sci.. 104: 3037-3042.*

Discrete measurements of Total Dissolved Inorganic Carbon (C_T) and Alkalinity (A_T)

The C_T analyses were made by a coulometric titration method using the SOMMA (single operator multi-parameter metabolic analyzer) system (Johnson et al., 1993). The SOMMA collects and dispenses an accurately known volume of seawater to a stripping chamber, acidifies it, sparges the CO_2 from the solution, dries the gas, and delivers it to a coulometer cell where a coulometric titration proceeds. Total Alkalinity (A_T) was determined by titration of seawater with a strong acid, following the emf with a proton-sensitive electrode. The titration curve shows two inflection points, characterizing the protonation of carbonate and bicarbonate, respectively. The acid consumption up to the second point is equal to the titration alkalinity.Total Alkalinity was determined by a semi-automatic analyzer, the VINDTA instrument (Versatile Instrument for the Determination of Titration Alkalinity (Mintrop et al., 2000).

Quality Control of the Discrete C_T and A_T measurements

An integral part of the SOMMA is a gas calibration system that is used to calibrate the coulometer performance for each new coulometer cell using injections of known masses of pure CO_2 gas. After the instrument was calibrated, as an additional reference, a bottle of certified reference material (CRM) and two duplicate samples per station were analyzed. The CRM were prepared by Dr. Andrew Dickson's laboratory at the Scripps Institution of Oceanography. Normally the CO_2 content measured by the SOMMA should be within two micro moles/kg (about 0.1%) of the Certified Value. For the A_T determination the standardization is done the same way, running a CRM in the beginning and two duplicates per station and finishing with a CRM. The alkalinity results should be within 2-3 µmoles/kg of the CRM values. Preliminary results of accuracy and precision of the analyses are shown in Table 1 which show that the measurements passed the quality control checks.

CRMs	**CT**	**AT**
Analyzed bottles	86	71
Batches used	58/60/63/64	58/60/63/64
Mean deviation from CRM value [µmol/kg]	2,21	-1,23
Standard deviation of the mean (+/-)	2,20	2,79
Duplicates		
Analyzed bottles	88	83
Mean deviation from CRM value [µmol/kg]	1,07	2,86
Standard deviation of the mean (+/-)	1,48	3,71

Table 5.3: Initial at-sea quality control of C_T and A_T measurements. CRM – certified reference material, C_T – total dissolved carbon, A_T –titration alkalinity. The CRM deviation denotes the accuracy and the duplicate deviation the precision of the analysis.

Underway measurements of pCO_2 and C_T

The second analytical strategy involved semi-continuous determination of the partial pressure of CO_2 (pCO_2) and total dissolved carbon dioxide (C_T) in surface waters. A continous flow of seawater was drawn at 5 m depth from the ship's "moon pool"which was equipped with a CTD. The automated pCO_2 system and semi-automated C_T-system were both supplied with water in this way. The underway pCO_2 system (Körtzinger et al., 1996) used a non-dispersive infrared gas detector for CO_2 and a pCO_2 data point together with temperature and salinity from the CTD were logged every minute together with the position data from an independent GPS system. The instrument was calibrated using three standard gases with a known CO_2 concentration. These gases were measured every 6 to 12 hours.

The underway determination of C_T was based on the method for the discrete C_T analysis described above. A sample bottle was continuously filled with surface seawater and every 15 to 20 minutes a subsample was taken from this bottle and C_T was determined via the titration method. The cell was replaced roughly every 12 hours and subsequently a gas calibration was conducted followed by a CRM determination.

Acknowledgements

The CO_2 group would like to thank Heinz Wentzel and Rudolf Angermann from the Meteor's WTD department for their patient help with our instruments during the cruise. We are also very grateful for the continuous support from the Bosun and the deck crew who helped to set up the water line and secure our lab.

5.4.7 Nutrients and Oxygen

(F. Malien, P. Fritsche)

Nutrients (ammonia, nitrate, nitrite, phosphate, silicate) were determined from 1310 Niskin bottles. The analysis of ammonia was made with the manual method (Koroleff, 1969, 1970) as described in Methods of Seawater Analysis by Grashoff et al. (1999). The analysis of nitrate, nitrite, phosphate and silicate was made with an autoanalyzing system according to Grashoff et al. (1999). The accuracy for nutrient analysis was approximately 1 % of the nutrient standards. The corresponding accuracy and precision estimates were 0.31 µmol/kg for nitrate, 0.01 µmol/kg for nitrite, 0.025 µmol/kg for phosphate, 0.5 µmol/kg for silicate and 0.01 µmol/kg for ammonia. However there were larger within-run variations in phosphate accuracy due to laboratory temperature variations, and these data require closer assessment..
In addition, 461 nutrient samples from the Bioassay Group were analysed for several experiments. For quality control the Marine Nutrient Standards Kit from Ocean Scientific International were used to make calibration curves for the autoanalyzer (12 times during the cruise) and the manual method of ammonia (every day). Oxygen was analysed on 1310 Niskin bottles according to a standard titration after Winkler (Grashoff et al., 1999). For precision estimate five samples were taken and analyzed from one Niskin bottle at 21 stations. The measurements had a standard deviation of 0.35 µmol/kg. Results from these measurements are available from http://cdiac.ornl.gov/ftp/oceans/CARINA/Meteor/06MT605/

1.4.8 Transient Tracers (Toste Tanhua, Martina Schütt, Tim Fischer, Elke Freese)

Objectives:
The CFCs (i.e CFC-11 and CFC-12) are anthropogenic gases that are released to the atmosphere and subsequently equilibrated with surface water of the ocean. The transient signal of the CFCs in the atmosphere provides a convenient method for determining ages of seawater, i.e. the time that has elapsed since the water-parcel last was in contact with the atmosphere.
Historically, some of the very first measurements of CFC were made in the Atlantic during the TTO cruise in 1981. This was during a time when the CFCs were rapidly increasing in the atmosphere, while today they are slowly decreasing. Therefore has two additional tracers been included in the measurements during M60-5; SF_6 and CCl_4. These are gases with similar properties to the CFCs and that enters the ocean in the same way, but they have different atmospheric histories. SF_6 has the shortest history, and started to rise rapidly in the atmosphere during the early 1970's, whereas CCl_4 has the longest history, stretching back to the 1920's. This suite of tracer thus enables us to date water masses in different 'age-ranges'. By comparing the tracer signature from the TTO expedition with today's, valuable information on any changes in ocean circulation can be gained. The inventory of transient tracers are furthermore important for evaluating the uptake of anthropogenic carbon in the ocean, one of the main objectives of this cruise. Another aspect of this cruise was to conduct experiments with a new analytical system with the objective of measuring new transient tracers, mainly CF_4 which is a very stable gas with both a natural and anthropogenic sources.

Technical Aspects:

Samples for SF_6 measurements were taken, and analysed, from 45 CTD stations during the cruise, and 995 samples were successfully analysed. The samples were collected in 500 ml glass-bottles with a removable inner lid that ensures that the sample does not get in contact with ambient air during storage. The samples were stored cold before analysis, which normally took place within 12 hours from sampling. The analytical system consisted of a vacuum-sparge sample pre-treatment unit in which 356 ml of the sample is introduced into an evacuated purge-chamber. The sample was then stripped of its content of SF_6 during 5 minutes of purging with clean nitrogen gas. The analyte was trapped in a 1/16", large ID, stainless steel tube packed with carboxen-1000 which was kept cold in the vapours above liquid nitrogen. After the sampling phase, the analyte is thermally desorbed from the trap and passed through a 1/8" pre-column packed with mol-sieve 5A, cutting out the SF_6 interfering compounds. The analyte was then refocused on a 1/32" packed micro-trap kept cold at controlled temperature over LN2. The sample was injected to a capillary column kept isothermally at 100°C and detected with an ECD. The analytical precision of the instrument was determined to 1.7% from 11 samples collected at 100 meters depth from two different Niskin bottles.

Samples for CFC measurements were drawn in syringes and transferred in amounts of 20 ml to a purge and trap gas-chromatographic unit. Separation of the dissolved gases was performed using a packed column and detection was with a Electron Capture Detector (ECD). The CFCs are calibrated against a standard gas, which was re-calibrated against a new gas standard provided by CMDL/NOAA in Boulder, CO. Any temporal drift of the ECD is corrected for by applying calibration curves made before and after each station. In total, 1136 samples from 46 stations were successfully analysed. The measurement of CCl_4 was performed on a similar system, although equipped with a capillary column instead of a packed column. In total 1112 number of samples from 45 stations were successfully analysed for CCl_4.

A total of 35 water samples from 9 stations were successfully sampled for CF_4 measurements. The samples were vacuum-sparged into 9.5 L evacuated glass chambers. The samples were then purged with helium in the lab, and the trace gases were collected on cold-traps that were flame-sealed for further analysis on a shore-based laboratory.

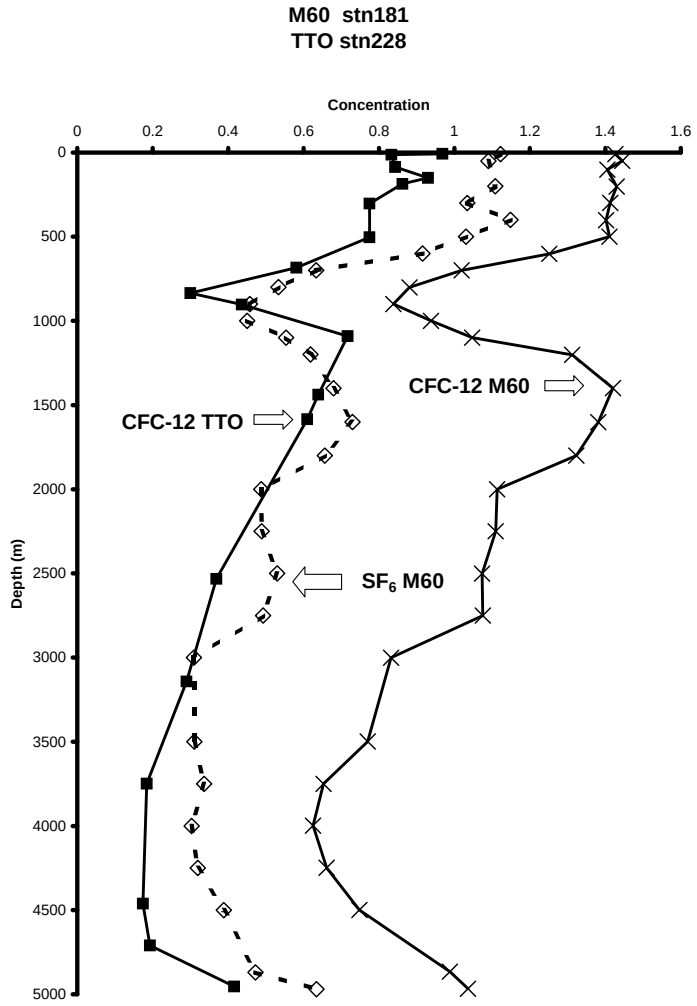

Figure 5.7**.** Tracer data from M60-5 station 181, which is at the same position as TTO station 181, at 42°N and 42°E. Note how the increase in CFC-12 is parallel through the whole water column. The tracer SF6, which was not measured during TTO, has a profile that resembles, but is not identical to, the CFC-12 profile form 1981, although the concentrations are 3 orders of magnitude lower.

.

5.4.9 Trace gas measurements: Biogenic halocarbons

(B. Quack, G. Petrick, and D. Wallace)

Sampling and Measurement Systems Used.

Sampling from: CTD rosette, underway pumping system, underway air sampling system.
On-board analyses: Purge-and-trap Gas Chromatograph with Mass Spectrometry for halocarbons

Sea to air-flux of natural halocarbons

The ocean plays a significant role in the trace gas composition of the atmosphere, via sea-to-air emissions, which are controlled by biotic and abiotic production and consumption processes occurring within the water column. Halocarbons affect the 'oxidising capacity' of the atmosphere, primarily as a result of their influence on ozone. Bromine (Br) and chlorine (Cl) both contribute to ozone depletion. Whereas Cl supply is dominated by long-lived, man-made compounds, Br is supplied mainly by natural, short-lived species. A Br-Cl synergy, coupled with increased levels of Cl, implies that these natural Br sources exert a stronger influence on ozone now than in the past. Oceanic bromoform ($CHBr_3$) is the major source of organic Br to the atmosphere. To elucidate source and sink terms, which are important for the global bromine budget and for atmospheric chemistry, measurements of bromoform as well as other brominated and chlorinated trace gases were performed in both the lower atmosphere and surface ocean during the cruise.

In addition to using data to infer production mechanisms, chlorinated and brominated volatile hydrocarbons were analysed in the water column of the subtropical Atlantic, in order to investigate if these compounds can be used as chemical tracers in oceanic studies. The hypothesis is, that e.g. bromoform is biologically produced in the oceanic surface layer and degraded mainly via Cl-substitution during transport of water masses originating from high latitudes towards lower latitudes. Dilution, transformation and degradation of the subsequent compounds occur during transport. This will potentially be reflected in concentration differences and ratios of various brominated compounds among the water masses. The ratio between bromoform and its likely degradation products $CHBr_2Cl$ and $CHBrCl_2$ could potentially be used as an “age-like “quantity for water mass transport in addition to other chemical tracers. Chloroform ($CHCl_3$), which is released from the ocean to the atmosphere, may be formed as endproduct of this reaction-chain.

Measurements and sampling performed during M60-5:

1) Samples from 20 water-column profiles (240 samples) where analysed for halocarbons (bromoform, dibromochloromethane, dichlorobromomethane, dibromomethane trichloro-methane, tetrachloromethane, methylchloroform, dichloromethane and iodomethane) using purge-and-trap gas chromatography with mass spectrometry, performed on board the ship.

2) Halocarbon measurements of underway surface water using purge-and-trap gas chromatography with mass spectrometry (40 samples) were also performed on board.

3) Atmospheric measurements of halocarbons (90 samples), using gas chromatography and mass spectrometry were performed on board. Air samples were pumped through a „Teflon“ tube from the bow of the ship.

In total, about 900 GC-MS-Analyses for sample measurements, standardizations and system test were performed. The GC-MS system, with the speciality of all glass-transfer lines performed well for aquatic and atmospheric samples after fixing of some initial problems. The mass spectrometer's filament broke in the last days of the cruise. After quick replacement, initially varying responses factors settled to generally 100% higher response factors, relative to the period with the old filament. After filament change there was also a discrepany between liquid and gaseous standards for bromoform, which is not understood.

Preliminary results

Table 5.4

	CH3I	*CH2Cl2*	*CHCl3*	*CCl4*	*CH3CCl3*	*CH2Br2*	*CHBrCl2*	*CHBr2Cl*	*CHBr3*
Mean	0.93	10.53	3.38	0.98	1.80	1.10	1.02	0.79	1.89
Median	0.19	10.56	2.28	0.72	1.16	0.95	0.41	0.63	1.86
Min	0.02	0.63	0.12	0.01	0.01	0.04	0.08	0.01	0.11
Max	7.67	43.17	52.85	11.64	14.36	8.23	80.40	21.20	6.66
STDV(% of mean)	156	55	166	101	103	78	518	181	43
Samples	198	190	236	229	233	243	249	253	254

Methyl iodide concentrations were c. 10x times higher in the upper 100 m than in deep water, revealing a surface source. Frequently it showed slightly elevated concentrations at 50 to 100 m depth. Dichloromethane showed the highest overall concentrations and the highest concentrations in surface waters of all compounds measured. Its concentrations decreased steadily with depth.

Chloroform concentrations were low in the surface waters, increasing with depth and revealing maxima in North Atlantic Deep Water. Two to three fold higher concentrations of chloroform were found in deep waters of the eastern, compared to the western Atlantic basin. Very high concentrations of chloroform were detected in the salinity maximum water of the Mediterranean Water.

Dibromomethane revealed concentration maxima at 50 to 200 m depth, showing a steep decrease with depth. Bromodichloromethane and dibromochloromethane increased steadily from the surface ocean to 1000 to 1500m depth. The former compound increased steadily further down to the bottom, whereas the latter had a mid-depth maximum at around 2000m.

Bromoform concentrations were rather low throughout the cruise. Highest concentrations were

found in the surface ocean where frequently two maxima were observed, one shallow maximum at around 50 m and another maximum at around 200 m. Below this, concentrations decrease down to 1000m depth, elevated concentrations of bromoform were observed between 1000 and 2000m depth.

Atmospheric data

Table 5.5

	CH3I	*CH2Cl2*	*CHCl3*	*CCl4*	*CH3CCl3*	*CH2Br2*	*CHBrCl2*	*CHBr2Cl*	*CHBr3*
Mean	0.34	28.22	6.88	91.70	21.99	1.06	3.21	2.19	1.42
Median	0.14	29.95	3.95	97.62	24.38	1.16	1.24	1.24	1.28
Min	0.06	9.63				0.03	0.24	0.05	0.06
Max	1.07	41.75	51.58	147.82	34.10	2.10	22.91	15.72	4.77
STDV(% of mean)	98	30	117	31	35	42	136	136	65
Samples	37	38	55	51	55	57	53	60	62

Three regimes were distinguishable during the cruise. The first part of the cruise was dominated by varying winds and directions of the west wind belt, bringing air with varying mixing ratios of brominated compounds to the ship, whereas in the middle part a constant, however atypical depres7sion in the area of the usual subtropical high west of the Azores brought wind with local North Atlantic trajectories to the ship, revealing stable and low mixing ratios of most compounds. The last part of the cruise entered the area of the North East Trades, where varying mixing ratios of the compounds were encounterd.

5.4.10 Trace gas measurements: N_2O

(Sylvia Walter, Uli Breitenbach)

Introduction

Nitrous oxide (N_2O) is an important atmospheric trace gas due to its influence on the Earth's climate. Like CO_2, N_2O is a radiatively active atmospheric trace gas in the troposphere, however, its global warming potential is, on a 100 years time horizon, about 300 times higher than that of CO_2. Due to its relatively long atmospheric lifetime of 120 years, N_2O is mixed into the stratosphere where it is photochemically decomposed forming nitric oxide radicals which are involved in one of the major catalytic ozone reaction cycles. Since the beginning of the industrial revolution the global mean tropospheric N_2O mole fraction has risen rapidly to values of 318 ppb in 2003. N_2O in the ocean is mainly formed during microbial processes such as nitrification and denitrification, but up to now the dominant production pathway for N_2O remains unclear. About 24% of the natural sources of atmospheric N_2O are contributed by the oceans, and the ocean-atmosphere system plays an important role in the past and present Earth's climate. Information on the N_2O distribution in this region of the Atlantic is sparse. However, dual-isotope data from the Atlantic Ocean are not available yet. Moreover, the responsible organisms involved in formation of oceanic N_2O are largely unknown.

Measurements and sampling

Triplicate water samples from various depths were taken from the rosette. Samples were poisoned with mercuric chloride solution. Afterwards each vial was provided with 10ml of a helium headspace and after equilibration the N_2O-concentration was measured with a gaschromatograph, equipped with an electron-capture-detector. Atmospheric samples were taken with gas tight syringes directly from the bow of the ship.

Additionally samples for the dual-isotope signature of N_2O (^{15}N and ^{18}O) and molecular investigation of organisms involved into the nitrogen cycle were collected for later analysis. On this cruise we measured the N_2O-concentration at 37 stations, samples for isotopic and molecular investigations were taken at 9, respectively 8 stations. Moreover the atmospheric concentration of N_2O was measured at 50 waypoints. Table 5.6 gives an overview of samples collected.

The atmospheric concentration was 319ppb ± 3 ppb, with a precision of about 1.0%. For the deep profiles the mean relative error was about 1.4% for all profiles.

3. Preliminary findings

The vertical distribution of N_2O showed one-peak profiles with maxima at 800 to 1000m, corresponding to the oxygen minimum (for example see #156, Fig. 5.9(left)).

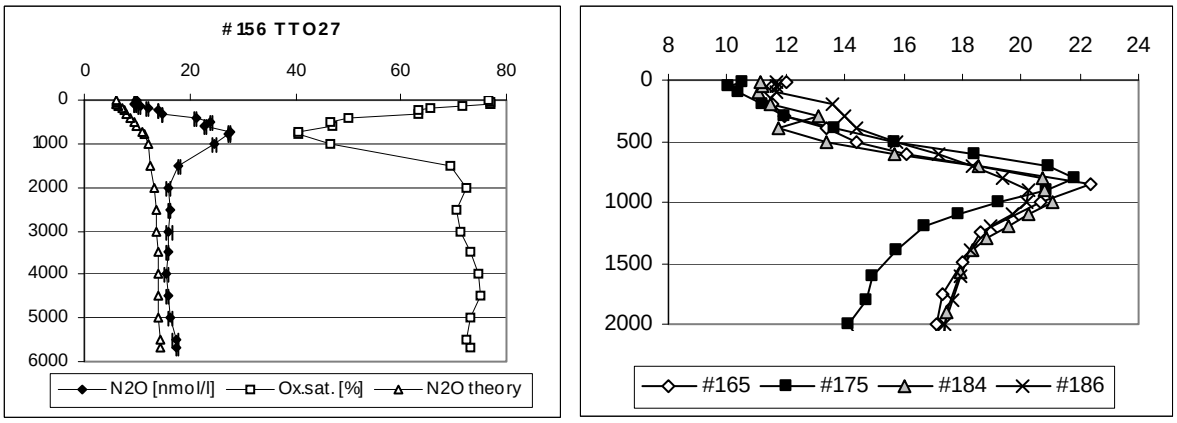

Figure 5.8. Vertical profiles of N_2O concentrations during Meteor 60 Leg 5.

N_2O was supersaturated throughout the water column, with a considerable accumulation of N_2O found below the euphotic zone with maximum values up to 27.5 nmol/l. On this cruise we found decreasing maximum concentrations from the southern to the northern and from the western to the eastern North Atlantic (see selected stations in Fig. 5.9(right)), this in contrast to a previous cruise into the tropical North Atlantic (Meteor 55 from Curacaou to Douala).

Table 5.6 N2O Sampling during Meteor 60 Leg 5.

Station No.	Date (UTC)	Latitude	Latitude	Longitude	Longitude	Konzentrationsproben (Tiefe) a)	Isotopenproben (Tiefen) a), b)	Filtrationsproben (Tiefen) a), b)
156	3/11/2004	19° N	29.6'	61° W	58.1'	24	-	-
157	3/11/2004	20° N	47.4'	62° W	16.0'	24	-	-
158	3/12/2004	22° N	3.7'	63° W	13.9'	24	-	-
159	3/12/2004	23° N	17.7'	64° W	9.6'	24	12	11
160	3/13/2004	24° N	33.7'	65° W	6.2'	24 b)	-	-
161	3/13/2004	25° N	47.0'	66° W	0.0'	24	-	-
163	3/15/2004	28° N	20.1'	62° W	58.1'	18 b)	-	-
164	3/16/2004	29° N	43.0'	61° W	18.0'	24	10	-
165	3/16/2004	30° N	52.5'	59° W	40.0'	21	-	-
166	3/17/2004	31° N	59.5'	58° W	5.1'	24 b)	-	-
167	3/18/2004	33° N	8.2'	56° W	29.6'	21	-	-
168	3/19/2004	36° N	17.2'	56° W	24.1'	21	10	9
169	3/20/2004	34° N	48.2'	55° W	45.6'	18	-	-
171	3/21/2004	31° N	0.0'	54° W	27.0'	19	-	-
172	3/21/2004	29° N	46.0'	54° W	9.0'	20	-	-
173	3/22/2004	28° N	12.6'	53° W	46.7'	21	-	-
175	3/24/2004	31° N	44.8'	50° W	45.1'	22	10	10
177	3/25/2004	33° N	55.1'	49° W	35.3'	20	-	-
178	3/26/2004	35° N	59.5'	47° W	6.0'	16	-	-
179	3/27/2004	37° N	37.2'	45° W	22.6'	20	10	4
180	3/27/2004	38° N	59.7'	44° W	0.0'	20	-	-
181	3/28/2004	42° N	0.1'	42° W	0.0'	21	10	9
182	3/31/2004	32° N	10.3'	45° W	29.9'	17	-	-
183	4/1/2004	32° N	36.2'	43° W	34.4'	16	-	
184	4/1/2004	33° N	0.4'	41° W	29.3'	20	-	-
185	4/2/2004	33° N	24.9'	37° W	21.3'	20	10	10
186	4/4/2004	33° N	42.7'	32° W	20.1'	20	-	-
187	4/4/2004	33° N	59.0'	30° W	37.5'	20	-	-
188	4/5/2004	33° N	58.6'	30° W	10.4'	9	-	-
189	4/5/2004	32° N	35.1'	28° W	35.0'	23	-	-
190	4/6/2004	30° N	48.7'	26° W	43.8'	21	-	-
191	4/6/2004	31° N	57.4'	26° W	14.0'	19	-	-
192	4/7/2004	33° N	46.1'	25° W	7.9'	21	-	-
194	4/8/2004	35 °N	31.5'	23 °W	58.9'	20	11	10
195	4/10/2004	37° N	35.1'	22° W	39.4'	20	-	-
196	4/10/2004	38° N	0.0'	20° W	0.1'	20	-	-
197	4/11/2004	37° N	52.2'	17° W	28.2'	22	-	-
198	4/12/2004	37° N	45.6'	15° W	33.4'	20	-	-
199	4/12/2004	37° N	35.3'	13° W	28.6'	23	9	9
201	4/13/2004	37°N	34,65’	10°W	10,87’	18	-	-
Gesamt						**819**	**92**	**72**

[a)] triplets per depth were taken

[b)] measurements at home

5.4.11 Bioassay Experiments

(Matthew Mills, Rebecca Langlois, Kerstin Nachtigal, Peter Fritsche, Eric Achterberg, Angela Milne, Mark Moore)

Introduction

There is long-standing debate as to whether nitrogen or phosphorus is the nutrient that limits phytoplankton productivity in the sea . Nutrient enrichment experiments in oligotrophic waters tend to indicate that N limits the rate of primary productivity in the modern ocean. However, on longer time scales, nitrogen fixation can increase the nitrate inventory of the ocean, thus increasing primary production. In turn, nitrogen fixation may be limited by either P or Fe, two essential nutrients that are in sparse supply in oligotrophic oceans. In previous work, bioassay experiments aboard the Meteor 55 cruise in the tropical North Atlantic showed that phytoplankton productivity and biomass were nitrogen limited while the active diazotrophic (N_2 fixing) community was phosphorus and iron co-limited. Additionally, Saharan dust was a source of both phosphorus and iron, and stimulated nitrogen fixation as measured with $^{15}N_2$ gas. The direct evidence of nitrogen limitation of CO_2 fixation and phytoplankton biomass contradicts a trend in the literature suggesting the North Atlantic phytoplankton community is P limited, while the direct measurements of P&Fe co-limitation of N_2 fixation contradicts evidence suggesting there is enough Fe in the North Atlantic to meet diazotroph needs.

Building on the work conducted during Meteor 55, we carried out similar bioassay experiments investigating the nutrient limitation of CO_2 fixation, chlorophyll a biomass, N_2 fixation, and bacterial productivity during Meteor 60. The more northly cruise track as well the different time of year make for an excellent comparison to the experiments carried out on Meteor 55.

Measurements and sampling

Trace metal clean techniques were used throughout the preparation and execution of the experiments. Surface seawater was collected (~5 m) after dark using a trace metal clean diaphragm pump. Seawater was pumped into 60 l carboys from which it was siphoned into 1.18 L acid-washed polycarbonate bottles. Under a laminar flow hood, nutrients were added alone and in combination to final concentrations of 1.0 µM NH_4^+ + 1.0 µM NO_3^- , 0.2 µM NaH_2PO_4, and 2.0 nM $FeCl_3$. Two types of Saharan dust were also added to bottles to a final concentration of 2 mg L^{-1} (D1: dust from Southern Algeria, D2: atmospherically processed Saharan dust collected in Turkey). The bottles were then sealed and placed in on-deck incubators with circulating surface seawater. For each treatment, parallel incubations for carbon fixation, nitrogen fixation, bacterial production, and chlorophyl *a* biomass, were run in triplicate over 48 h with nitrogen fixation and primary productivity rate measurements made during the final 24 h. Chlorophyll a concentration and bacterial productivity measurements were determined at 48 h. Net nitrogen fixation rates were assessed using the $^{15}N_2$ technique while primary productivity was assessed using the ^{14}C technique. Lastly bacterial productivity was measured using the ^{3}H-thymidine method. Simulated *in situ* incubations were conducted in Perspex flow-through incubators cooled by flowing surface seawater. Light was attenuated to 20% of incident surface values by blue filters.

In addtion to the rate measurements, other variables monitored or sampled for included nutrient

concentrations (NO_3^-, NH_4^+. $PO4^{3-}$, TDN, TDP, Fe^{2+}, DFe), active fluoresence (assessed using fast repitition rate fluorometry), cell abundance and diversity, phosphatase activity and DNA/RNA sampling for the presence and activity of nitrogen fixing organisms. Underway measurements of Fe II and DFe were also taken throughout the cruise, and at several stations (approxomately 15) profiles for the presence and activity of the N_2 fixing enzyme nitrogenase (*nifH)*, as well as measurements of active fluoresence, were taken.

In total eight experiments were conducted (Fig 5.9). Five experiments were considered oligotrophic (undetectable levels of nutrients in the surface waters, low chlorophyll a concentrations). In three experiments, an additional DOC (glucose) treatment was conducted in which DOC was added to all nutrient treatments in addtion to the above described treatment set-up. Bacterial production, active fluoresence, and cell abundance and diversity were measured in those bottles with added DOC.

Finally, an experiment monitoring the dissolution of nutrients from 6 different types of desert dust was conducted. Five of the dust samples were were from Africa (Algeria, Mauritania, Morocco, Namibia, and atmospherically processed Saharan dust collected from Turkey) and a 6^{th} sample from the Gobi desert was also used. Three concentrations of each dust (0.1, 2.0 and 10 mg L-1) were added to 1 L of trace metal clean seawater and samples were taken over eight days to monitor the concentrations of the following nutrients (NH_4^+, NO_3^-, PO_4^{3-}, TDN, Fe^{2+}, DFe).

3. Preliminary resulsts

Initial results show that at the five oligotrophic sites primary production and chlorophyll a production was nitrogen limited (Figure 5.10). Once nitrogen limitation was relieved CO_2 fixation rates and chlorophyll a concentrations increased further with the addition of phosphate. Likewise the bacterial productivity was stimulated by the combined addition of nitrogen and phosphorus. Further additons of Fe did not generally enhance primary production, chlorophyll a concentrations, or bacterial production. The addition of glucose did not stimulate bacterial production on its own, but increased productivity approximately 100x when added to the combined N and P treatments.

In all experiments where surface nutrient concentrations were undetectable the addition of Saharan dust stimulated primary production, chlorophyll a biomass, and bacterial productivity. The dust dissolution experiment showed that the two dusts used in the nutrient limitation experiments, D1 and D2, released both inorganic nitrogen and phosphorus. The dust collected in southern Algeria (D1) was relatively P rich while the atmospherically processed dust collected in Turkey (D2) was rich in N. The other four samples of dust tested showed no measurable increases in N or P during the one week experiment. Both D1 and D2 had increased DFe concentrations after 8 days.

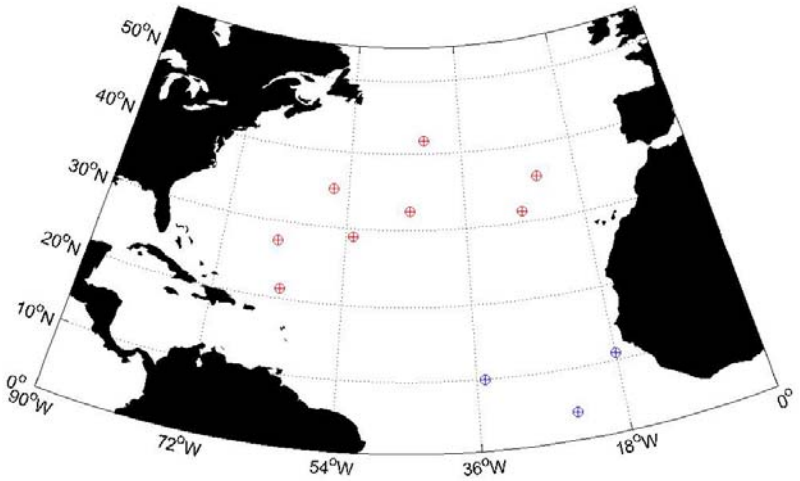

Figure 5.9. Map showing sites of M60/5 (red) and M55 (blue) bioassay experiments.

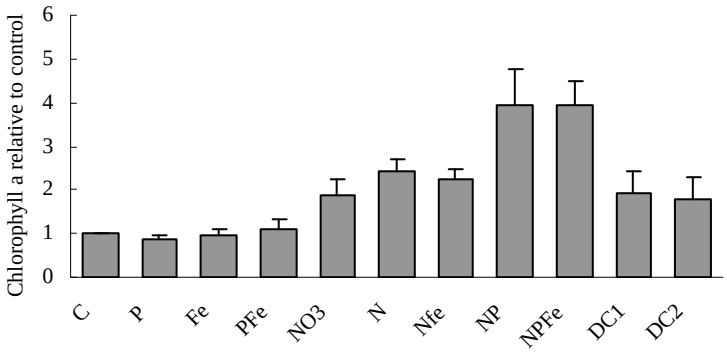

Figure 5.10. Mean chloryphyll a response in at the five sites with undetectable levels of nutrients in the surface waters (oligotrophic). Responses are relative to control.

There was still considerable work to be carried out after M60/5. Samples for the nitrogen fixation rates were to be analyzed in Kiel over the next 6 months, and the DNA/RNA samples analyzed during the next 12 months. Additionally the flow cytometry samples collected for cell abundance and diversity and low level phosphate measurements were to be made during this time.

4. Acknowledgements

Assistasnce was provided by the FS Meteor's technicians for the hookups of water and electricity to the clean container. Additionally, we would like to acknowledge the deck crew for help in securing and moving the incubators used by the bioassay group during the cruise, the deployment of the fish, and the supply of compressed air to the pump used for the collection of trace metal clean sea water.

5.5 Weather situation during the cruise M60/5

(Christoph Joppich)

During the first section of the cruise (en route station 161) the weather was dominated by a weak ridge of the subtropical high, extending westward to the Greater Antilles. Therefore moderate easterly winds were observed during the northwest course. The swell was moderate from easterly directions at first, but it grew up to 4 meters from northerly direction at March 12th due to a storm low development near Cape Hatteras. The next section of the cruise (en route station 168) started under high pressure influence with easterly winds about Bft 5 and decreasing swell from north. At March 17th a new storm low born near Cape Hatteras moved northeast. At the front side of this low Meteor sailed northeast with southerly winds increasing up to Bft 7 at March 18th. After a short period with intermittent high pressure influence another storm low developed northwest of Meteor. An exact route-planning based on interpretation of meteorological prediction model output made it possible to reach all stations in this area with secure distance to the storm centre. The associated cold front passed Meteor's route at March 20th with thunder showers, but maximum winds only reached Bft 6.

In the following section (en route station 173) the remarkable appearance was a very high swell (up to 5 meters) due to the low described above. The observed easterly winds didn't exceed Bft 5. The track to the northernmost point of the cruise (station 181) was dominated by two high pressure centres: The first high remained stationary north of Azores, the second high south of Newfoundland. An air mass boundary between both pressure systems had exactly the course of RV Meteor. At the cold side of this boundary northeast gales occurred for several days, while at the warm (easterly) side only moderate easterly winds (up to Bft 5) were observed. At March 25th Meteor got the gale force side of the front for a short time and observed winds grew up to Bft 8 to 9. But due to ships easterly course the calm side of the air mass boundary was reached soon. Only the high swell (up to 5 meters) with short period affected the ship for a longer time. At the northernmost station near 420N 420W southerly winds did not exceed Bft 5 due to the strong high north of Azores.

The following transit to station 190 brought no significant meteorological appearances. Meteor sailed southward under northerly winds with about 10 knots and a south moving cold front of a Greenland-low could not reach the vessel.

During the last section of the Cruise (en route Lisbon) there was a remarkable low pressure development near 28oN 47oW at April 1st.This low crossed the route of Meteor in the early morning of April 2nd and the centre passed only about 15 miles east of the vessel. In front of this low winds grew up to Bft 9. At the following day this low became stationary near 37oN 34oW and it was still active until April 5th. The observed winds at the track of Meteor in this time lay between 25 and 35 knots accompanied by high swell with short period from northwest. At April 6th south of 33oN the weather became quite calm and sunny due to high pressure southwest of Meteor.

The final track of Meteor was dominated by a nearly stationary high north of Azores and temporary strong winds up to Bft 6 from north to northeast. The observed swell grew up to 3 Meters for a time. But wind and swell calmed down to the end of cruise.

5.6 Station List

Station	Date Start UTC	Time	Latitude	Latitude	Longitude	Longitude	Date	Time	Latitude	Latitude	Longitude	Longitude
	UTC	UTC	Degrees	Minutes	Degrees	Minutes	UTC	UTC	Degrees	Minutes	Degrees	Minutes
			Station Start						Station End			
155	March 10, 2004	18:15	18	34.1	-61	33.6	March 10, 2004	20:45	18	34.4	-61	32.4
156	March 11, 2004	2:36	19	29.6	-61	58.1	March 11, 2004	6:55	19	29.7	-61	58
157	March 11, 2004	14:25	20	47.4	-62	16	March 11, 2004	20:40	20	47.8	-62	15.6
158	March 12, 2004	4:44	22	3.7	-63	13.9	March 12, 2004	9:54	22	3.8	-63	13.8
159	March 12, 2004	17:55	23	17.7	-64	9.6	March 12, 2004	23:05	23	18.9	-64	11
160	March 13, 2004	8:41	24	33.7	-65	6.2	March 13, 2004	12:29	24	33.7	-65	6.8
161	March 13, 2004	21:40	25	47	-66	0	March 14, 2004	2:48	25	47.8	-65	59.8
162	March 14, 2004	14:29	27	2	-64	34.2	March 14, 2004	19:52	27	3.7	-64	36.7
163	March 15, 2004	8:00	28	20.1	-62	58.1	March 15, 2004	11:43	28	20.1	-62	58
164	March 16, 2004	0:37	29	43	-61	18	March 16, 2004	10:44	29	43.6	-61	18.1
165	March 16, 2004	21:39	30	52.5	-59	40	March 17, 2004	3:45	30	52.4	-59	39.7
166	March 17, 2004	14:05	31	59.5	-58	5.1	March 17, 2004	19:06	31	58.7	-58	6.9
167	March 18, 2004	5:43	33	8.2	-56	29.6	March 18, 2004	11:46	33	8.1	-56	29.3
168	March 19, 2004	8:35	36	17.2	-56	24.1	March 19, 2004	14:51	36	17.2	-56	23.9
169	March 20, 2004	1:10	34	48.2	-55	45.6	March 20, 2004	4:49	34	47.8	-55	43.7
170	March 20, 2004	17:06	32	56.9	-55	6.3	March 20, 2004	20:58	32	57	-55	7.4
171	March 21, 2004	8:50	31	0	-54	27	March 21, 2004	11:50	30	59.7	-54	29.3
172	March 21, 2004	20:40	29	46	-54	9	March 22, 2004	0:35	29	46.7	-54	9.9
173	March 22, 2004	10:50	28	12.6	-53	46.7	March 22, 2004	16:46	28	11.6	-53	52
174	March 23, 2004	5:12	29	34	-52	20.1	March 23, 2004	14:15	29	34.2	-52	19.6
175	March 24, 2004	4:06	31	44.8	-50	45.1	March 24, 2004	9:09	31	44.7	-50	45.1
176	March 24, 2004	16:24	32	56	-50	7.9	March 24, 2004	19:52	32	55.8	-50	6.9
177	March 25, 2004	2:09	33	55.1	-49	35.3	March 25, 2004	5:54	33	56.1	-49	36.7
178	March 26, 2004	8:39	35	59.5	-47	6	March 26, 2004	14:06	36	5.6	-47	1.8
179	March 27, 2004	2:20	37	37.2	-45	22.6	March 27, 2004	5:56	37	37.3	-45	21.6
180	March 27, 2004	16:34	38	59.7	-44	0	March 27, 2004	21:22	39	0.1	-43	59.8
181	March 28, 2004	14:48	42	0.1	-42	0	March 28, 2004	20:02	41	58.9	-41	58.9
182	March 31, 2004	12:06	32	10.3	-45	29.9	March 31, 2004	16:12	32	11.3	-45	30.4
183	April 1, 2004	2:31	32	36.2	-43	34.4	April 1, 2004	5:02	32	35.7	-43	34.2
184	April 1, 2004	15:55	33	0.4	-41	29.3	April 1, 2004	20:08	33	1.1	-41	28.5
185	April 2, 2004	21:00	33	24.9	-37	21.3	April 2, 2004	23:39	33	23.7	-37	20.2
186	April 4, 2004	7:30	33	42.7	-32	20.1	April 4, 2004	10:10	33	42.4	-32	21
187	April 4, 2004	18:51	33	59	-30	37.5	April 4, 2004	22:15	33	57.8	-30	37.7
188	April 5, 2004	2:26	33	58.6	-30	10.4	April 5, 2004	3:13	33	57.9	-30	10.3
189	April 5, 2004	14:35	32	35.1	-28	35	April 5, 2004	18:45	32	34.4	-28	35.5
190	April 6, 2004	9:00	30	48.7	-26	43.8	April 6, 2004	13:45	30	48.9	-26	45.3
191	April 6, 2004	21:19	31	57.4	-26	14	April 7, 2004	0:53	31	56.9	-26	15.4
192	April 7, 2004	12:58	33	46.1	-25	7.9	April 7, 2004	18:05	33	45.6	-25	8.2
193	April 8, 2004	5:16	34	46	-23	6	April 8, 2004	8:46	34	46	-23	6.2
194	April 8, 2004	15:10	35	31.5	-23	58.9	April 8, 2004	20:14	35	31.6	-23	58.6
195	April 10, 2004	2:14	37	35.1	-22	39.4	April 10, 2004	5:18	37	36.2	-22	39.5
196	April 10, 2004	20:15	38	0	-20	0.1	April 10, 2004	23:40	38	1.1	-20	1.7
197	April 11, 2004	12:45	37	52.2	-17	28.2	April 11, 2004	18:04	37	52.6	-17	28.2
198	April 12, 2004	3:12	37	45.6	-15	33.4	April 12, 2004	6:29	37	45.7	-15	33.4
199	April 12, 2004	16:34	37	35.3	-13	28.6	April 12, 2004	21:48	37	35.3	-13	28.7
200	April 13, 2004	5:49	37	36.5	-11	49.6	April 13, 2004	11:38	37	36.5	-11	50.2
201	April 13, 2004	19:32	37	34.6	-10	10.3	April 13, 2004	22:34	37	34.7	-10	11.3